



DEVELOPMENT OF LOW COST OPTICAL SENSORS FOR PRODUCE
QUALITY EVALUATION



A Thesis Submitted to the Graduate School of Naresuan University
in Partial Fulfillment of the Requirements
for the Doctor of Philosophy in Chemistry- (Type 1.1)

2023

Copyright by Naresuan University

DEVELOPMENT OF LOW COST OPTICAL SENSORS FOR PRODUCE
QUALITY EVALUATION



A Thesis Submitted to the Graduate School of Naresuan University
in Partial Fulfillment of the Requirements
for the Doctor of Philosophy in Chemistry- (Type 1.1)
2023
Copyright by Naresuan University

Thesis entitled "Development of low cost optical sensors for produce quality evaluation"

By Attawit Praiphui

has been approved by the Graduate School as partial fulfillment of the requirements for the Doctor of Philosophy in Chemistry- (Type 1.1) of Naresuan University

Oral Defense Committee

..... Chair
(Professor Emeritus Nuntavan Bunyaphatsara, Ph.D.)

..... Advisor
(Assistant Professor Filip Kielar, Ph.D.)

..... Co Advisor
(Assistant Professor Uthai Wichai, Ph.D.)

..... Co Advisor
(Professor Metha Rutnakornpituk, Ph.D.)

..... Internal Examiner
(Associate Professor Boonjira Rutnakornpituk, Ph.D.)

Approved

.....
(Associate Professor Krongkarn Chootip, Ph.D.)
Dean of the Graduate School

Title	DEVELOPMENT OF LOW COST OPTICAL SENSORS FOR PRODUCE QUALITY EVALUATION
Author	Attawit Praiphui
Advisor	Assistant Professor Filip Kielar, Ph.D.
Co-Advisor	Assistant Professor Uthai Wichai, Ph.D.
Academic Paper	Professor Metha Rutnakornpituk, Ph.D. Ph.D. Dissertation in Chemistry- (Type 1.1), Naresuan University, 2023
Keywords	NIR spectroscopy, portable spectrometer, Construction of the in-house optical spectrometer, mango, tomato, PLSR, dry matter, total soluble solids, titratable acidity, pH, firmness

ABSTRACT

Near-infrared (NIR) spectroscopy is a powerful tool for non-destructive measurements of various quality parameters. Moreover, the performance of NIR spectroscopy for quality evaluation is dependent on two key components: 1) suitable spectrometers and 2) appropriate calibration models. The aim of this study was 1) to develop predictive models for quality parameters of mangoes and tomatoes using different commercial spectrometers, 2) to construct a prototype of an in-house NIR spectrometer and investigate the possibility to use it as a source of spectral data for the development of calibration models for quality parameters of mangoes and tomatoes. This work focuses on the goal of determining quality parameters of fruits and vegetables: mangoes and tomatoes. Dry matter (DM), total soluble solids (TSS), titratable acidity (TA), pH, and firmness were selected as the key quality parameters in this study. The calibration models were developed using partial least squares regression (PLSR) and the data analysis used both unprocessed data and preprocessed data (e.g. Savitzky-Golay derivative, SNV).

The possibility to perform the prediction of quality parameters of mango and tomato samples was evaluated using different commercial spectrometers (SCIO, Linksquare, Texas Instruments NIRscan Nano, and Neospectra). In case of mango samples, good predictive models were developed for DM, TSS, TA, and pH using the

spectroscopic measurements from SCIO and Linksure operating in both visible and NIR modes. The best model for DM using SCIO spectrometer exhibited a cross validation values of 0.92 and 0.739% for R^2 and RMSE, respectively. The best predictive models for TSS, TA, and pH parameters were developed using Linksure operated in the visible mode. The R^2 values of calibration and cross-validation (brackets) for TSS, TA, and pH were 0.91 (0.75), 0.91 (0.79), and 0.93 (0.81) respectively. The RMSE values of calibration and cross-validation (brackets) for TSS, TA, and pH were 1.03 °Brix (1.76 °Brix), 0.38% (0.58%), and 0.21 (0.35), respectively. Poorly performing predictive models with modest R^2 values were obtained using spectral data from Texas Instruments NIR Scan Nano and Neospectra instruments.

For the work with tomatoes, cherry tomato was chosen for the test of quality parameters. Only three commercial spectrometers (SCIO, Linksure and Texas Instruments) were utilized in this part because of the sampling window of Neospectra is too large to allow the spectroscopic measurements. Good predictive models were developed for predicting DM and firmness using the spectroscopic measurements taken with SCIO and Linksure operating in both visible and NIR modes. The best model for DM was obtained using spectral data from the SCIO spectrometer and has exhibited a cross validation values of 0.89 and 0.27% for R^2 and RMSE, respectively. For the firmness, the best results were obtained using spectral data acquired using the Linksure instrument operating in visible mode. The R^2 values of calibration and cross-validation (brackets) were 0.91 (0.87). The RMSE values of calibration and cross-validation (brackets) for firmness were 0.91 N (0.87 N). The performance of models for predicting quality parameters based on spectral data acquired using the Texas Instruments NIRscan Nano were poor with modest R^2 values exhibiting similar results as for the work carried out with mangoes.

Given the encouraging results obtained with commercial low cost NIR instruments in the first part of this work, we proceeded to the second part where an in-house NIR spectrometer prototype was constructed and evaluated. The performance of an NIR spectrometer depends on three key components: light source, wavelength selector, and detector. The prototype of a potentially low cost portable NIR

spectrometer has been constructed around the Hamamatsu C14384MA-01 sensor. The in-house spectrometer prototype had been made in two version using different light sources. The first version used an NIR LED (SFH 4376, OSRAM) light source while the second version used a tungsten halogen filament bulb (TH). These spectrometers operated in the wavelength range from 650 to 1050 nm. The performance of the spectrometer prototype was then tested by using it to collect spectral data from mangoes and tomatoes for the purpose of developing predictive models for selected quality parameters.

In case of mango samples, good predictive models were obtained for predicting DM, TSS, TA, and pH using both NIR LED and TH light sources. The best models for predicting DM were obtained using the spectrometer version with the TH filament light source. The R^2 values of the test set was 0.82. For the best models for TSS, TA, and pH were obtained using data acquired with the prototype equipped the NIR LED. The R^2 values of the test sets for TSS, TA, and pH were 0.86, 0.92, and 0.86, respectively. Models developed for the prediction of firmness were poor with moderate R^2 values in the case of both spectrometer versions. In conclusion, the in-house spectrometer prototype has been used to collect spectroscopic data from Nam Dok Mai mangoes, which were collected in two different harvesting seasons. Predictive models for mango quality parameters (DM, TSS, TA, pH, firmness) were developed from this spectroscopic data. Models with satisfactory quality ($R^2 > 0.80$ in the test set) were developed for DM, TSS, TA, and pH. The results indicate that the constructed instrument can collect usable spectroscopic data from produce samples.

In the case of tomato samples, predictive models of modest quality were developed for all quality parameters, with R^2 values of the test set below 0.70 in all instances. The performance of predicting DM, TSS, TA, pH, and firmness using both NIR LED and TH filament light sources were significantly worse than predictive models reported in previous publications. On the other hand, the predictive models of in-house spectrometers show better performance in comparison with previous prototype (MOEMS technology) for predicting, TSS, DM, TA, and pH for tomato samples. In conclusion, the potential of low cost NIR spectrometer using new generation of MOEMS technology (C14383MA-01) for rapid and non-destructive

measurement of tomato samples was evaluated. The results showed that the predictive models can be used to predict DM, TSS, and pH. The predictive models with satisfactory quality ($R^2 > 0.50$) have been developed for DM, TSS, and pH. But for the TA and firmness yielded poor prediction performance.



ACKNOWLEDGEMENTS

I would like to express my deep gratitude to my advisor, Assistant Professor.Dr.Filip Kielar, of the Faculty of Science at Naresuan University for the invaluable help and consultant throughout the activity of this research. I am the most grateful for him not only the teaching of research activity but also many other given opportunities in my life. He gives a lot of advice, possibility, encouragement, and enthusiastic to me. I would not have achieved this thesis would not have been completed without all the support from him.

In addition, I am grateful to my co advisors, Assistant Professor.Dr.Uthai Wichai and Professor.Dr. Metha Rutnakornpituk of the Faculty of Science at Naresuan University for the suggestions and all their help.

I would also to acknowledgement to Assistant Professor.Dr. Kyle Vatautas Lopin of the Faculty of Science at Naresuan University all of help for the construction and suggestion of the in-house optical spectrometers.

I also appreciate suggestions from the members of committee, Professor Emeritus Dr. Nuntavan Bunyaphatsara, and Associate Professor.Dr. Boonjira Rutnakornpituk.

I would like to acknowledge the financial support from Thailand Research Fund; grant No. RDG6220018, and the Department of Chemistry, Faculty of science, Naresuan University for support equipment of laboratory facilities and The Staff at Naresuan University for making the processes smoothly.

Finally, I would like to thank all of member in the SC4-401, SC4-504, and SC4-50X including Kielar research group, Uthai Research group, and Metha Research Group, Boonjira Research Group, and Nungrethai suphom for their friendship, technical discussions.

Attawit Praiphui

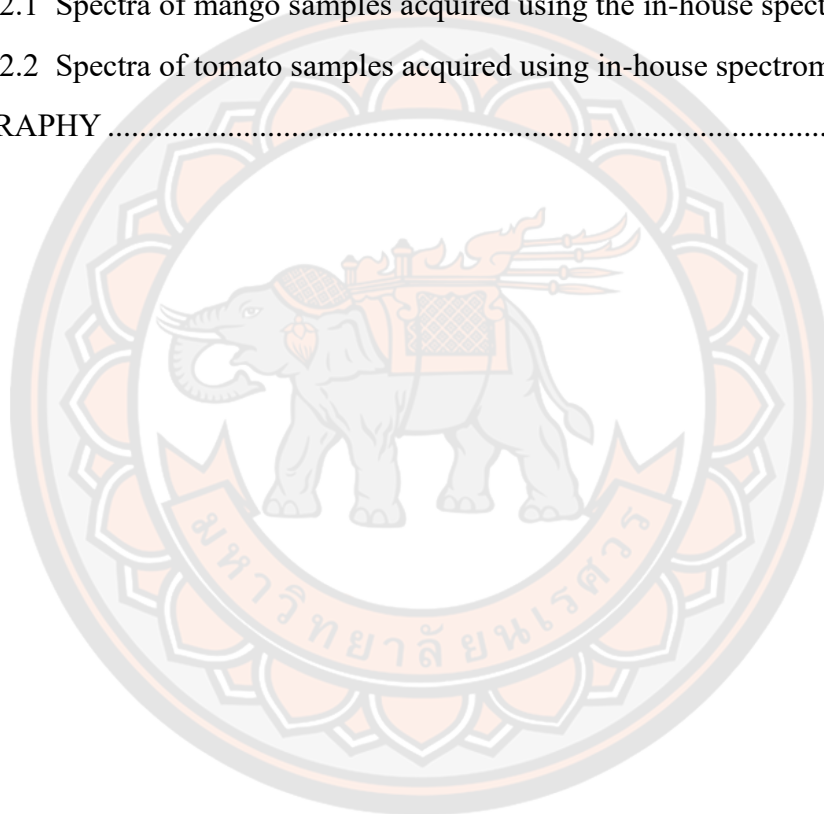
TABLE OF CONTENTS

	Page
ABSTRACT.....	C
ACKNOWLEDGEMENTS.....	G
TABLE OF CONTENTS.....	H
LIST OF TABLES.....	L
LIST OF FIGURES.....	O
CHAPTER I INTRODUCTION.....	1
1.1 Background and Significance of the Study.....	1
1.2 Research Hypothesis.....	1
1.2.1 Development of in-house optical spectrometer.....	2
1.2.1.1 Development of in-house optical spectrometer: Light sources.....	2
1.2.1.2 Development of an in-house optical spectrometer: Detector.....	3
1.2.1.3 Development of in-house optical spectrometer: Wavelength selector.....	4
1.2.2 Testing performance of in-house optical spectrometer for quantitative measurements to predict key quality parameters of mango and tomato.	5
1.2.2.1 Utilization of NIR spectroscopy in nondestructive mango analysis.....	5
1.2.2.2 Utilization of NIR spectroscopy in nondestructive tomato analysis.....	6
1.2.3 Testing performance of in-house optical spectrometer for quantitative measurements to predict other quality parameters from mango and tomato.....	7
1.3 Research Objectives.....	8
1.4 Research Scope.....	8
CHAPTER II LITERATURE REVIEW.....	10
2.1 Utilization of NIR spectroscopy in nondestructive analysis.....	11
2.2 Utilization of NIR spectroscopy in nondestructive mango analysis.....	12

2.3 Utilization of NIR spectroscopy in nondestructive tomato analysis	24
2.4 Theory of Near infrared spectroscopy analysis	31
2.4.1 Introduction of near infrared spectroscopy.....	31
2.4.2 Chemometrics.....	33
2.4.2.1 Data preprocessing.....	33
2.4.2.2 Calibration	34
2.5 NIR spectrometers: affordability and portability	34
2.5.1 Commercial spectrometer details	39
2.5.1.1 SCIO	39
2.5.1.2 Linksquire	43
2.5.1.3 Texas Instruments (TI) – DLP NIRscan Nano.....	44
2.5.1.4 Neospectra	45
2.5.2 The design of NIR spectrometers	46
2.5.2.1 Light source	46
2.5.2.2 Wavelength selection techniques	50
2.5.2.3 Detectors.....	57
CHAPTER III RESEARCH METHODOLOGY	59
3.1 Instrumentals and chemicals in research methodology.....	59
3.1.1 Instrumentals	59
3.1.2 Chemicals	59
3.2 Research plan and Methodology	60
3.2.1 Testing performance of commercial portable spectrometers for quantitative measurements to predict key quality parameters from mango and tomato.	60
3.2.2 Development of in-house optical spectrometer	62
3.2.2.1 Development of in-house optical spectrometer: Light source.....	62
3.2.2.2 Development of in-house optical spectrometer: Wavelength selector.	63
3.2.2.3 Development of in-house optical spectrometer: Light detector ...	64

3.2.3 Testing performance of in-house optical spectrometer for quantitative measurements to predict key quality parameters from mango and tomato.	64
CHAPTER IV RESULT AND DISCUSSION	69
4.1 Testing performance of commercial portable spectrometers for quantitative measurements to predict key quality parameters from mango and tomato.	69
4.1.1 Testing the performance of commercial spectrometers for non-destructive determination of mango quality parameters.	75
4.1.1.1 SCiO	75
4.1.1.2 Linksquare	79
4.1.1.3 Texas Instruments (TI) – DLP NIRscan Nano	83
4.1.1.4 Neospectra	87
4.1.2 Testing the performance of commercial spectrometers for non-destructive determination of tomato.	101
4.1.2.1 SCiO	107
4.1.2.2 Linksquare	118
4.1.2.3 Texas Instruments (TI) – DLP NIRscan Nano	125
4.2 Construction of the in-house optical spectrometer	137
4.2.1 Selection of a sensor for the in-house optical spectrometer	137
4.2.2 Construction of the in-house optical spectrometer	138
4.3 Development of in-house optical spectrometer	141
4.3.1 Development of in-house optical spectrometer with different light source.	141
4.3.2 Testing performance of the in-house optical spectrometer.....	142
4.4 Testing performance of in-house optical spectrometer for quantitative measurements to predict keys quality parameters from mango and tomato. ..	145
4.4.1 Mango samples.....	145
4.4.2 Predictive models for tomato quality parameters.....	174
CHAPTER V CONCLUSION.....	216
REFERENCES	220
APPENDIX.....	225

1. Plots of sample absorbances or reflectances versus wavelength acquired for the purpose of development of models for quality parameters of mangoes and tomatoes acquired using commercial spectrometers.	226
1.1 Plots of spectra of mango samples acquired using commercial spectrometers.	226
1.1 Spectra of tomato samples acquired using commercial spectrometers.	235
2. Spectra of mango and tomato samples acquired with the in-house spectrometer used to develop predictive models for quality parameters.	244
2.1 Spectra of mango samples acquired using the in-house spectrometer.	244
2.2 Spectra of tomato samples acquired using in-house spectrometer.	247
BIOGRAPHY	250



LIST OF TABLES

	Page
Table 1 parameter consumption analysis of mango fruit (<i>Mangifera indica</i> L.).....	13
Table 2 parameter consumption analysis of Tomato (<i>Solanum lycopersicum</i>).	25
Table 3 Summary of the technical parameters of popular NIR spectrometers	36
Table 4 Specifications of F-751-Mango Mango Quality Meter.....	55
Table 5 Numbers of samples based on location of collection for commercial portable spectrometers for mango.....	69
Table 6 Descriptive statistics for quality parameters analyzed in mango samples using commercial spectrometers	74
Table 7 Best R^2 values for cross-validation for mango quality parameters using the SCiO spectrometer.	79
Table 8 Best R^2 values for calibration and cross-validation for mango quality parameters obtained using data acquired with the LS spectrometer operating in the visible and NIR modes.....	82
Table 9 Summary of model parameters for predictive models for mango quality parameters developed using spectral data acquired using the NIRScan Nano spectrometer developed without pretreatment procedure and showing the best cases.	86
Table 10. Summary of model parameters for predictive models for mango quality parameters developed by using spectral data acquired using the Neospectra developed without pretreatment procedure and showing the best cases.	89
Table 11 Best R^2 values for calibration and cross-validation (in brackets) for mango quality parameters obtained by collecting calibration data using the commercial spectrometers.	91
Table 12 Comparison of performance of models for mango quality parameters reported in previous literature and describe in this work.....	98
Table 13 Numbers of samples based on location of collection for commercial portable spectrometers for tomato.	101
Table 14 Descriptive statistics for quality parameters analyzed in tomato samples using commercial spectrometers.....	106

Table 15 Best R ² values for cross-validation for cherry tomato quality parameters using the SCIO spectrometers.....	117
Table 16 Best R ² values for calibration and cross-validation for cherry tomato quality parameters using the LS spectrometers operating of the visible and NIR modes.	122
Table 17 Summary of model parameters for predictive models for tomato quality parameters developed using spectral data acquired using the NIRScan Nano developed without pretreatment procedure and showing the best cases.....	129
Table 18 Best R ² values for calibration and cross-validation (in brackets) for cherry tomato quality parameters obtained by collecting calibration data using the commercial spectrometers	131
Table 19 Comparison of performance models for the quality parameters of cherry tomato reported in previous literature and describe in this work.....	135
Table 20 Repeatability and reproducibility of spectral measurements taken with the in-house developed instrument	145
Table 21 Numbers of samples based on location of collection for in-house optical spectrometers of mango for first and second period times.	146
Table 22 Descriptive statistics for quality parameters analyzed for mango samples collected in the first sampling period.....	147
Table 23 Descriptive statistics for quality parameters analyzed for mango samples collected in the second sampling period.	147
Table 24 Summary of model parameters developed using NIR LED and filament bulb light source from mango samples collected in the first sampling period and predictive model parameters for second period time.	154
Table 25 Descriptive statistics of mango quality parameters for samples collected in both sampling periods.	156
Table 26 Summary of model parameters developed using NIR LED and filament light source from mango samples collected in combine sampling periods	162
Table 27 Summary of model parameters developed using NIR LED and filament bulb light source from mango samples collected in both sampling periods and split into calibration and prediction sets	166
Table 28 Summary of model parameters developed using NIR LED and filament bulb light source from mango samples collected in both sampling periods and split into calibration and prediction sets	167
Table 29 Comparison of performance models for the quality parameters of cherry tomato reported in previous literature and describe in this work.....	172

Table 30 Numbers of samples based on location of collection for in-house optical spectrometers of tomato for first and second period times.....	174
Table 31 Descriptive statistics for quality parameters analyzed in tomato sample for first collection period.	178
Table 32 Descriptive statistics for quality parameters analyzed in tomato samples in the second collection period.....	179
Table 33 Summary of model parameters developed using NIR LED and filament bulb light source from tomato samples collected in the first sampling period and predictive model parameters for the second sampling period.....	186
Table 34 Descriptive statistics for quality parameters analyzed in tomato sample for combine period time.	191
Table 35 Summary of model parameters developed using NIR LED and filament bulb light source from tomato samples collected in combine sampling periods	201
Table 36 Summary of model parameters developed using NIR LED and filament bulb light source from tomato samples collected in both sampling periods and split into calibration and prediction sets	209
Table 37 Summary of model parameters developed using NIR LED and filament bulb light source from mango samples collected in both sampling periods and split into calibration and prediction sets	211
Table 38 Comparison of performance models for the quality parameters of tomato reported in previous literature using F-750 Produce Quality Mater and describe in this work.....	215

LIST OF FIGURES

	Page
Figure 1 Image of the F-751-Mango Mango Quality Meter.....	4
Figure 2 Spectral range for the NIR showing wavelengths and wavenumbers.	10
Figure 3 NIR reflectance spectra of selected fruits.....	11
Figure 4 NIR absorbance spectra of a) ground and b) intact wheat.....	12
Figure 5 Predicted versus measured values of RPI and IQI for the visible region (a), the visible-near infrared region (b) and near-infrared region (c).	18
Figure 6 Prediction results for quality attributes: (a) firmness, (b) total soluble solids (TS) and (c) titratable acidity (TA) (d) ripening index (RPI) using the overall NIRS calibration model to predict values for individual harvest years.	20
Figure 7 Plots of predicted versus measured (a) SSC and (b) DM values of ‘Palmer’ mangoes harvested at different developmental stages measured using a portable F-750 spectrometer.....	21
Figure 8 Prediction models of soluble solids content using near infrared spectra based on (a) flesh, (b) peel and flesh, and (c) adjusted peel and flesh spectra.	23
Figure 9 A summary of models made on variables selected with bootstrapping soft shrinkage (BOSS) approach for SCiO and Zeiss data. PLSR models on SCiO data for batch 1 (A) and batch 2 (B). PLSR models on reduced spectral range Zeiss data for batch 1 (C), batch 2 (D) and batch 3 (E). PLSR models on full spectral range Zeiss data for batch 1 (F), batch 2 (G) and batch 3 (H).	24
Figure 10 Reference data vs. NIRS predicted data for the validation set for (a) SSC (b) TA.....	27
Figure 11 Plots of predicted values of lycopene, total acid, sugar, phenols, and antioxidant activity versus results of standard analyses (RBF-NN model).	29
Figure 12 Short NIR (700-1100 nm) spectra of nectarines, peaches and plums.	32
Figure 13 Three illumination detector configurations of near infrared spectroscopy: A. light source; B. sample; C. sample holder; D. optic fiber; E. detector.....	32
Figure 14 selected popular miniaturized NIR spectrometers a) MicroPHAZIR, b) DLP NIR scan (Texas instruments), c) Neospectra, d) nano FTIR NIR, e) NIRone, f) MicroNIR.....	35
Figure 15 A picture of the SCiO spectrometer. Demonstrating of its dimensions.....	39

Figure 16 The definition of the sample attributes and reference measurements for data collection of the web-based SCiO spectrometer.....	40
Figure 17 Screen shots of the smart phone-based app for the SCiO spectrometer showing the data collection (A), possibility to add samples to a collection (B), scanning process (C), and data review (D)	40
Figure 18 Database of sample attributes shown in the web-based interface for the SCiO spectrometer	41
Figure 19 The spectral data was recorded in the web-based interface for the SCiO spectrometer.....	41
Figure 20 Chemometric model development page in the web-based interface for the SCiO spectrometer.....	42
Figure 21 Model summary view in the web-based interface of the SCiO spectrometer	43
Figure 22 A photograph of the Linksquare spectrometer.....	43
Figure 23 A screen short of the computer-based application for differ spectral modes using Linksquare spectrometer.	44
Figure 24 A photograph of the DLP NIRscan Nano spectrometer	44
Figure 25 A screen shot of the computer-based application for DLP NIRscan Nano spectrometer.....	45
Figure 26 A photograph of the Neospectra instrument	45
Figure 27 A screen shot of the computer based application for Neospectra spectrometer.....	46
Figure 28 Spectral profile of LEDs for fluorescence spectroscopy at different wavelength range	47
Figure 29 Experimental set up illustration of spectroscopy measurement.	49
Figure 30 Illustration of the dispersive spectrometer in diffuse reflectance mode.....	51
Figure 31 Illustration of the FT spectrometer in diffuse reflectance mode.	52
Figure 32 Comparison of the specification of FT-NIR and dispersive spectrometers.	53
Figure 33 (a) Image of the F-751-Mango Mango Quality Meter (b) model validation study.....	54
Figure 34 photo image of MS (C11708MA), 2) Micro (C12666MA and C12880MA), and 3) SMD (C1438MA-01) series.....	56
Figure 35 spectral response of Micro, MS, and SMD series	56

Figure 36 (a) evaluation kit for SMD series (C14989+C15036) (b) evaluation software display example.....	57
Figure 37 A photograph of the popular portable spectrometers (a) SCiO (b) Linksquare (c) Texas Instruments (TI) – DLP NIRscan Nano (d) Neospectra.....	61
Figure 38 Illustration of the different light sources used for in-house built spectrometers (a) Near infrared light emitting diode, NIR LED (b) filament bulb, TH.	63
Figure 39 Image of the Hamamatsu C14384MA-01 sensor.....	64
Figure 40 Determination of firmness values from tensile measurement.....	66
Figure 41 Representative images of front and back sides of a mango sample with marked sampling sites.....	70
Figure 42. Plot of reflectance versus wavelength acquired using the SCiO spectrometer used to develop predictive model for dry matter.....	71
Figure 43. Plot of reflectance versus wavelength for the dry matter dataset obtained using the Linksquare spectrometer with (a) visible (b) NIR light illumination.....	72
Figure 44. Plot of absorbance versus wavelength for the dry matter dataset obtained using the TI NIRscan Nano spectrometer.....	73
Figure 45. percentage of reflectance spectra for the dry matter dataset obtained using the Neospectra spectrometer.....	73
Figure 46 Plots of predicted versus measured mango quality parameters (a) DM (b) TSS (c) TA (d) pH, and (e) Firmness obtained with calibration models based on spectral data acquired using the SCiO spectrometer without pretreatment.....	77
Figure 47 Plot of predicted versus measured quality parameters with the best cases of figure of merit values using the SCiO spectrometer for (a) DM (b) TSS (c) TA (d) pH and (d) Firmness.....	79
Figure 48. Plot of predicted versus measured quality parameters for calibration models made with spectral data acquired using the Linksquare spectrometer operating in the visible mode without preprocessing for predicting (a) DM (b) TSS (c) TA (d) pH and (d) Firmness.....	80
Figure 49 Plot of predicted versus measured quality parameters for calibration models made with spectral data acquired using the Linksquare spectrometer operating in the NIR mode without preprocessing for predicting (a) DM (b) TSS (c) TA (d) pH and (d) Firmness.....	81

Figure 50. Plots of predicted versus measured values of mango quality parameters for calibration models made using data acquired with the LS spectrometer and exhibiting the best figures of for predicting (a) DM (b) TSS (c) TA (d) pH and (d) Firmness.....	83
Figure 51. Plots of predicted versus measured values of mango quality parameters developed using spectral data acquired with the NIRScan Nano spectrometer without preprocessing used for (a) DM (b) TSS (c) TA (d) pH and (e) Firmness	84
Figure 52 Plots of predicted versus measured values of quality parameters for models exhibiting the best figures of merit for spectral data acquired using the NIRScan Nano spectrometer used for predicting (a) DM (b) TSS (c) TA (d) pH and (d) Firmness	85
Figure 53 Plots of predicted versus measured mango quality parameters developed using spectral data acquired with the Neospectra without preprocessing used for (a) DM (b) TSS (c) TA (d) pH and (e) firmness	87
Figure 54 Plots of predicted versus measured values of quality parameters for models exhibiting the best figures of merit for spectral data acquired using Neospectra used for predicting (a) DM (b) TSS (c) TA (d) pH and (e) Firmness.....	89
Figure 55 Plot of reflectance versus wavelength marking important spectral features acquired using (a) SCIO (b) Linksquare with visible mode (c) Linksquare with NIR mode.....	92
Figure 56 (a) Plot of Absorbance versus wavelength spectra using NIRScan Nano (b) Plot of percentage of reflectance spectra using Neospectra for important spectra acquired with mango samples.....	92
Figure 57 Representative images of sampling sides (a) first (b) second (c) third and (d) forth side of a tomato sample used for DM, TSS, TA, and pH analysis.	102
Figure 58 Representative image of sampling area of a tomato sample used for firmness analysis.....	102
Figure 59 Plot of reflectance versus wavelength acquired using the SCIO spectrometer for tomato samples used to develop predictive models for dry matter	103
Figure 60 Plot of reflectance versus wavelength acquired using the Linksquare spectrometer operating in (a) visible (b) NIR modes for tomato samples used to develop predictive models for dry matter	104
Figure 61 Plot of reflectance versus wavelength acquired using the TI NIRScan Nano spectrometer for tomato samples used to develop predictive models for dry matter	105
Figure 62. Plot of predicted versus measured values of tomato quality parameters obtained using spectral data acquired with the SCIO spectrometer used without pretreatment for (a) DM (b) TSS (c) TA, and (d) pH.....	109

Figure 63 Plot of predicted versus measured values of investigated tomato firmness parameters obtained using spectral data acquired with the SCIO spectrometer and used without preprocessing for (a) Firmness (b) Firmness1 (c) Firmness2 (d) Firmness3 (e) Firmness4 and (f) Firmness5	112
Figure 64 Plot of predicted versus measured values of tomato quality parameters for the calibration models with the best figures of merit obtained using spectral data acquired with the SCIO spectrometer for (a) DM (b) TSS (c) TA and (d) pH	114
Figure 65 Plot of predicted versus measured values of tomato firmness parameters for the calibration models with the best figures of merit obtained using spectral data acquired with the SCIO spectrometer for (a) Firmness (b) Firmness1 (c) Firmness2 (d) Firmness3 (e) Firmness4 and (f) Firmness5	116
Figure 66. Plot of predicted versus measured values of tomato quality parameters obtained using spectral data acquired with the Linksquare spectrometer operating in the visible mode without pretreatment for predicting (a) DM (b) TSS (c) TA and (d) pH.....	118
Figure 67. Plot of predicted versus measured values of tomato firmness parameters obtained using spectral data acquired with the Linksquare spectrometer operating in the visible mode without preprocessing for (a) Firmness (b) Firmness1 (c) Firmness2 (d) Firmness3 (e) Firmness4 and (f) Firmness5.....	119
Figure 68. Plots of predicted versus measured values of tomato quality parameters obtained using spectral data acquired with the Linksquare spectrometer operating in the NIR mode without pretreatment for predicting (a) DM (b) TSS (c) TA and (d) pH	120
Figure 69. Plots of predicted versus measured values of tomato firmness parameters obtained using spectral data acquired with the Linksquare spectrometer operating in the NIR mode without preprocessing for (a) Firmness (b) Firmness1 (c) Firmness2 (d) Firmness3 (e) Firmness4 and (f) Firmness5	121
Figure 70 Plots of predicted versus measured values of tomato quality parameters for calibration models exhibiting the best figures of merit made with spectral data acquired with the Linksquare spectrometer for (a) DM (b) TSS (c) TA, and (d) pH	123
Figure 71 Plots of predicted versus measured values of tomato firmness parameters for calibration models exhibiting the best figures of meirt made with spectral data acquired with the Linksquare spectrometer for (a) Firmness (b) Firmness1 (c) Firmness2 (d) Firmness3 (e) Firmness4, and (f) Firmness5	124

Figure 72. Plots of predicted versus measured tomato quality parameters developed using spectral data acquired with the NIRScan Nano without preprocessing used for (a) DM (b) TSS (c) TA, and (d) pH	125
Figure. 73 Plots of predicted versus measured values of (a) Firmness (b) Firmness1 (c) Firmness2 (d) Firmness3 (e) Firmness4 and (f) Firmness5 obtained using spectral data acquired with the NIRScan Nano spectrometer and used without pretreatment	126
Figure 74 Plots of predicted versus measured values of quality parameters of tomatoes for models exhibiting the best figures of merit for spectral data acquired using Texas Instruments NIRScan Nano used for predicting (a) DM, (b) TSS, (c) TA, and (d) pH	127
Figure 75 Plots of predicted versus measured values of tomato firmness parameters for models exhibiting the best figures of merit for spectral data acquired using Texas Instruments NIRScan Nano used for predicting (a) Firmness (b) Firmness1 (c) Firmness2 (d) Firmness3 (e) Firmness4 and (f) Firmness5	128
Figure 76 Image of the Hamamtsu C14384MA-01 sensor.....	138
Figure 77 Images of prototype of in house developed NIR sensor.....	138
Figure 78 Schematic diagram of the control board for the (a) LED illumination (b) filament bulb sources.	140
Figure 79 The intensity spectra of white reference material in the wavelength range from 560 nm to 1150 nm.....	141
Figure 80 Illustration of the different light sources used for inhouse built spectrometer (a) Near infrared light emitting diode, NIR LED (b) filament bulb, TH.	142
Figure 81 The repeatability of spectral measurement, for (a) white (b) dark reference with NIR LED light source, for (c) white (d) dark reference with filament bulb light source	143
Figure 82 The reproducibility of spectral measurement, for (a) white (b) dark reference with NIR LED light source, for (c) white (d) dark reference with filament bulb light source.....	144
Figure 83 Plot of absorbance versus wavelength for spectra acquired using the in-house spectrometer equipped with the (a) LED light source (b) tungsten light source for mango samples used to develop predictive models for firmness of mango samples.	148
Figure 84 Plot of predicted versus measured values of dry matter(a), total soluble solids (b), titratable acidity (c), pH (d), and firmness (e) of mangoes for	

samples collected in the first collection period made with predictive models based on spectral data acquired using the NIR LED light source used without data pretreatment. The plots are showing datapoints for both calibration (blue) and cross validation (red) and the corresponding regression lines..... 150

Figure 85 Plot of predicted versus measured values of dry matter(a), total soluble solids (b), titratable acidity (c), pH (d), and firmness (e) of mangoes for samples collected in the first collection period made with predictive models based on spectral data acquired using the filament light source used without data pretreatment. The plots are showing datapoints for both calibration (blue) and cross validation (red) and the corresponding regression lines..... 151

Figure 86 Plot of predicted versus measured values without pretreatment of (a) dry matter, (b) total soluble solids, (c) titratable acidity, (d) pH, and (e) firmness for samples collected in both collection periods made with predictive models based on spectral data acquired using the NIR LED light source used without data pretreatment. The plots are showing datapoints for both calibration (blue) and cross validation (red) and the corresponding regression lines..... 157

Figure 87 Plot of predicted versus measured values of (a) dry matter, (b) total soluble solids, (c) titratable acidity, (d) pH, and (e) firmness of mangoes for samples collected in both collection periods made with predictive models based on spectral data acquired using the filament light source used without data pretreatment. The plots are showing datapoints for both calibration (blue) and cross validation (red) and the corresponding regression lines..... 159

Figure 88 Plot of best cases of predicted versus measured values of (a) dry matter, (b) total soluble solids, (c) titratable acidity, (d) pH, and (e) firmness of mangoes for samples collected in both collection periods made with predictive models based on spectral data acquired using the NIR LED light source. The plots are showing datapoints for both calibration (blue) and cross validation (red) and the corresponding regression lines..... 160

Figure 89 Plot of best cases of predicted versus measured values of (a) dry matter, (b) total soluble solids, (c) titratable acidity, (d) pH, and (e) firmness of mangoes for samples collected in both collection periods made with predictive models based on spectral data acquired using the filament light source. The plots are showing datapoints for both calibration (blue) and cross validation (red) and the corresponding regression lines..... 161

Figure 90 Plot of predicted versus measured values of dry matter (a), total soluble solids (b), titratable acidity (c), pH (d), and firmness (e) of tomatoes

using NIR LED light source based on data from testing set of samples collected in both collection periods	164
Figure 91 Plot of predicted versus measured values of dry matter (a), total soluble solids (b), titratable acidity (c), pH (d), and firmness (e) of tomatoes using filament bulb light source based on data from testing set of samples collected in both collection periods	165
Figure 92 Plot of absorbance versus wavelength for important spectral features acquired using the in-house spectrometer equipped with the (a) NIR LED (b) Filament light sources for mango samples	168
Figure 93 Representative images of sampling areas (a) first (b) second (c) third, and (d) forth side of a tomato sample for predicting DM, TSS, TA, and pH with in-house spectrometer.	175
Figure 94 Representative image of sampling are of a tomato sample for predicting firmness with in-house spectrometer.	176
Figure 95 Plot of absorbance versus wavelength for spectra acquired using in-house spectrometer equipped with the LED light source for tomato samples used to develop predictive models for dry matter.....	177
Figure 96 Plot of absorbance versus wavelength for spectra acquired using in-house spectrometer equipped with the tungsten light source for tomato samples used to develop predictive models for dry matter	177
Figure 97 Plot of predicted versus measured values of (a) dry matter, (b) total soluble solids, (c) titratable acidity, and (d) pH of tomatoes for samples collected in the first collection period made with predictive models based on spectral data acquired using the NIR LED light source used without data pretreatment. The plots are showing datapoints for both calibration (blue) and cross validation (red) and the corresponding regression lines.....	180
Figure 98 Plot of predicted versus measured values without pretreatment of (a) Firmness, (b) Firmness1, (c) Firmness2 (d) Firmness3, (e) Firmness4, and (f) Firmness5 of tomatoes using NIR LED light source from samples collected in the first collection period showing both datapoints for both calibration (blue) and cross validation (red) and the corresponding regression lines.....	181
Figure 99 Plot of predicted versus measured values of (a) dry matter, (b) total soluble solids, (c) titratable acidity, and (d) pH of tomatoes for samples collected in the first collection period made with predictive models based on spectral data acquired using the filament light source used without data	

pretreatment. The plots are showing datapoints for both calibration (blue) and cross validation (red) and the corresponding regression lines..... 183

Figure 100 Plot of predicted versus measured values of (a) Firmness, (b) Firmness1, (c) Firmness2 (d) Firmness3, (e) Firmness4, and (f) Firmness5 of tomatoes for samples collected in the first collection period made with predictive models based on spectral data acquired using the filament light source used without data pretreatment. The plots are showing datapoints for both calibration (blue) and cross validation (red) and the corresponding regression lines..... 184

Figure 101 Plot of predicted versus measured values of (a) dry matter, (b) total soluble solids, (c) titratable acidity, and (d) pH of tomatoes for samples collected in both collection periods made with predictive models based on spectral data acquired using the NIR LED light source used without data pretreatment. The plots are showing datapoints for both calibration (blue) and cross validation (red) and the corresponding regression lines..... 192

Figure 102 Plot of predicted versus measured values without pretreatment of (a) firmness, (b) firmness1, (c) firmness2 (d) firmness3, (e) firmness4, and (f) firmness5 of tomatoes using NIR LED light source from samples collected in the combine period time showing both datapoints for both calibration (blue) and cross validation (red) and the corresponding regression lines 193

Figure 103 Plot of predicted versus measured values without pretreatment of (a) dry matter, (b) total soluble solids, (c) titratable acidity, and (d) pH of tomatoes using filament bulb light source from samples collected in the combine period time showing both datapoints for both calibration (blue) and cross validation (red) and the corresponding regression lines 195

Figure 104 Plot of predicted versus measured without pretreatment of (a) Firmness, (b) Firmness1, (c) Firmness2 (d) Firmness3, (e) Firmness4, and (f) Firmness5 of tomatoes using filament bulb light source from samples collected in the combine period time showing both datapoints for both calibration (blue) and cross validation (red) and the corresponding regression lines 196

Figure 105 Plot of best cases of predicted versus measured values of (a) dry matter, (b) total soluble solids, (c) titratable acidity, and (d) pH of tomatoes for samples collected in both collection periods made with predictive models based on spectral data acquired using the NIR LED light source. The plots are showing datapoints for both calibration (blue) and cross validation (red) and the corresponding regression lines. 197

Figure 106 Plot of best cases of predicted versus measured values of (a) Firmness, (b) Firmness1, (c) Firmness2 (d) Firmness3, (e) Firmness4, and (f) Firmness5 of tomatoes for samples collected in both collection periods made with predictive models based on spectral data acquired using the NIR LED light source. The plots are showing datapoints for both calibration (blue) and cross validation (red) and the corresponding regression lines.....	198
Figure 107 Plot of best cases of predicted versus measured values of (a) dry matter, (b) total soluble solids, (c) titratable acidity, and (d) pH of tomatoes for samples collected in both collection periods made with predictive models based on spectral data acquired using the filament light. The plots are showing datapoints for both calibration (blue) and cross validation (red) and the corresponding regression lines.	199
Figure 108 Plot of best cases of predicted versus measured values of (a) Firmness, (b) Firmness1, (c) Firmness2 (d) Firmness3, (e) Firmness4, and (f) Firmness5 of tomatoes for samples collected in both collection periods made with predictive models based on spectral data acquired using the filament light source. The plots are showing datapoints for both calibration (blue) and cross validation (red) and the corresponding regression lines.....	200
Figure 109 Plot of predicted versus measured values of dry matter (a), total soluble solids (b), titratable acidity (c), and pH (d) of tomatoes obtained using spectral data measured with NIR LED light source based on data from testing set of samples collected in both collection periods.....	204
Figure 110 Plot of predicted versus measured values of (a) Firmness, (b) Firmness1, (c) Firmness2 (d) Firmness3, (e) Firmness4, and (f) Firmness5 of tomatoes obtained using spectral data measured with NIR LED light source based on data from testing set of samples collected in both collection periods	205
Figure 111 Plot of predicted versus measured values of dry matter (a), total soluble solids (b), titratable acidity (c), pH (d), and firmness (e) of tomatoes obtained using spectral data measured with filament light source based on data from testing set of samples collected in both collection periods	206
Figure 112 Plot of predicted versus measured values of (a) Firmness, (b) Firmness1, (c) Firmness2 (d) Firmness3, (e) Firmness4, and (f) Firmness5 of tomatoes obtained using spectral data measured with filament light source based on data from testing set of samples collected in both collection periods	207
Figure 113 Plot of absorbance versus wavelength for important spectra acquired using in-house spectrometer equipped with the (a) NIR LED (b) Filament light sources used for tomato samples.....	212

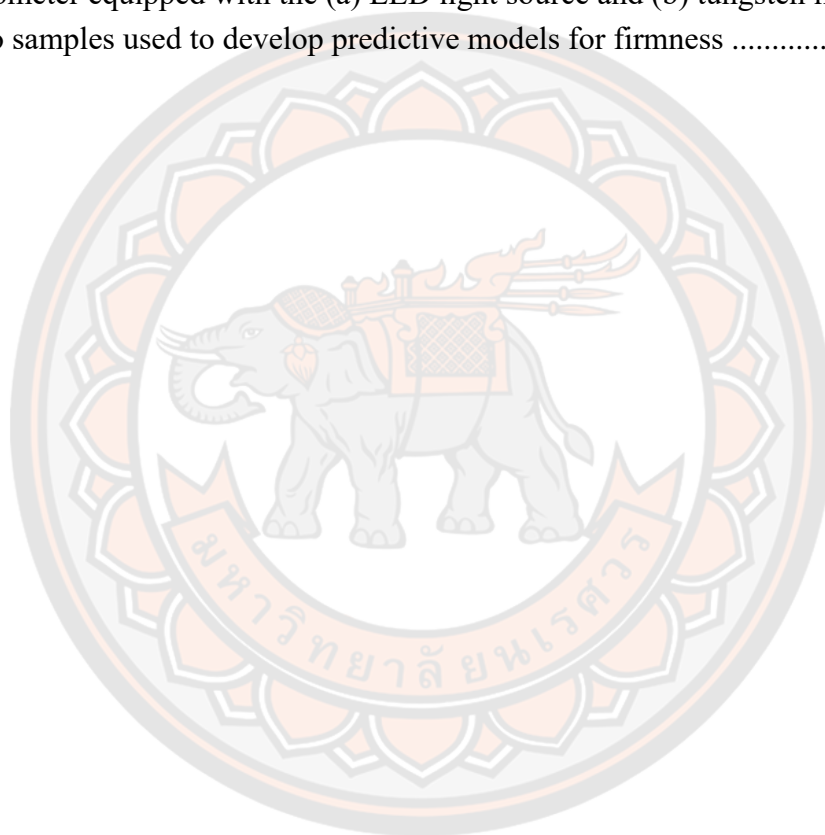
Figure 114 Plot of reflectance versus wavelength acquired using the SCiO spectrometer for samples used to develop predictive model for dry matter	226
Figure 115 Plots of reflectance versus wavelength acquired using the Linksquare spectrometer operated in the (a) visible (b) NIR modes for mango samples used to develop predictive model for dry matter.....	227
Figure 116 Plot of absorbance versus wavelength acquired using the NIRScan Nano spectrometer for mango samples used to develop predictive model for dry matter ..	228
Figure 117 Plot of reflectance versus wavelength acquired using the Neospectra spectrometer for mango samples used to develop predictive model for dry matter ..	228
Figure 118 Plot of reflectance versus wavelength acquired using the SCiO spectrometer for mango samples used to develop predictive model for total soluble solids, titratable acidity, and pH.....	229
Figure 119 Plots of reflectance versus wavelength acquired using the Linksquare spectrometer operated in the (a) visible and (b) NIR modes for mango samples used to develop predictive model for total soluble solids, tirtratable acidity, and pH	230
Figure 120 Plot of absorbance versus wavelength acquired using the NIRScan Naon spectrometer for mango samples used to develop predictive model for total soluble solids, tirtratable acidity, and pH	231
Figure 121 Plot of reflectance versus wavelength acquired using the Neospectra spectrometer for mango samples used to develop predictive model for total soluble solids, tirtratable acidity, and pH	231
Figure 122 Plot of reflectance versus wavelength acquired using the SCiO spectrometer for mango samples used to develop predictive model for firmness.....	232
Figure 123 Plots of reflectance versus wavelength spectra acquired using the Linksquare spectrometer operated in the (a) visible and (b) NIR modes for mango samples used to develop predictive model for firmness	233
Figure 124 Plot of absorbance versus wavelength acquired using the NIRScan Nano spectrometer for mango samples used to develop predictive model for firmness.....	234
Figure 125 Plot of reflectance versus wavelength spectra acquired using the Neospectra spectrometer for samples used to develop predictive model for firmness	234
Figure 126 Plot of reflectance versus wavelength acquired using the SCiO spectrometer for tomato samples used to develop predictive model for dry matter..	235

Figure 127 Plots of reflectance versus wavelength acquired using the Linksquare spectrometer operating in (a) visible and (b) NIR modes for tomato samples used to develop predictive model for dry matter.....	236
Figure 128 Plot of reflectance versus wavelength spectra acquired using the NIRScan Nano spectrometer for tomato samples used to develop predictive model for dry matter	237
Figure 129 Plot of reflectance versus wavelength acquired using the Linksquare spectrometer operating in visible mode for tomato samples used to develop predictive model for total soluble solids, titratable acidity, and pH	238
Figure 130 Plot of reflectance versus wavelength spectra acquired using the Linksquare spectrometer operating in (a) visible (b) NIR modes for tomato samples used to develop predictive model for total soluble solids, titratable acidity, and pH	239
Figure 131 Plot of reflectance versus wavelength spectra acquired using the NIRscan Nano spectrometer for tomato samples used to develop predictive model for total soluble solids, titratable acidity, and pH	240
Figure 132 Plot of reflectance versus wavelength acquired using the SCiO spectrometer for tomato samples used to develop predictive model for firmness measured using research tensile instrument.....	241
Figure 133 Plots of reflectance versus wavelength for spectra acquired using the Linksquare spectrometer operating in (a) visible (b) NIR modes for tomato samples used to develop predictive model for firmness measured using research tensile instrument	242
Figure 134 Plot of reflectance versus wavelength acquired using the TI NIRScan Nano spectrometer for tomato samples used to develop predictive model for firmness measured using research tensile instrument.....	243
Figure 135 Plots of absorbance versus wavelength acquired using the in-house spectrometer equipped with the (a) LED light source and (b) tungsten light source for mango samples used to develop predictive models for dry matter	244
Figure 136 Plots of absorbance versus wavelength acquired using in-house spectrometer equipped with the (a) LED light source and (b) tungsten light source for mango samples used to develop predictive models for total soluble solids, titratable acidity, and pH	245
Figure 137 Plots of absorbance versus wavelength acquired using in-house spectrometer equipped with the (a) LED light source and (b) tungsten light source for mango samples used to develop predictive models for firmness.....	246

Figure 138 Plots of absorbance versus wavelength for spectra acquired using in-house spectrometer equipped with the (a) LED light source and (b) tungsten light source for tomato samples used to develop predictive models for dry matter.....247

Figure 139 Plots of absorbance versus wavelength acquired using in-house spectrometer equipped with the (a) LED light source and (b) tungsten light source for tomato samples used to develop predictive models for total soluble solids, titratable acidity, and pH248

Figure 140 Plots of absorbance versus wavelength acquired using in-house spectrometer equipped with the (a) LED light source and (b) tungsten light source for tomato samples used to develop predictive models for firmness249



CHAPTER I

INTRODUCTION

1.1 Background and Significance of the Study

Agriculture and farming are important human activities. The agricultural sector in Thailand accounts for 9.9% of the GDP and involves 49% of the total labor force. Important factors impacting agricultural products are 1) high costs of inputs (seeds, fertilizers, pesticides etc.), 2) uncertainty in terms of the amount and quality of product produced, and 3) the perishable nature of the products. These factors directly impact agriculture and farming. Nowadays, science provides and develops solutions to enhance and improve the quality of agricultural products. Included among these scientific methods are the tools based on optical spectroscopy.

Optical spectroscopy is a discipline that is focused on the interaction of optical electromagnetic radiation with matter. In many cases, this interaction involves specific transitions between energy levels. This technique has been widely used to characterize samples in terms of quantitative and/or qualitative analysis in agriculture, agrochemical quality control, ripeness parameters determination etc. Optical spectroscopy, for example in the near infrared (NIR) range, can provide the tools for rapid and non-destructive determination of various produce quality parameters. Moreover, the optical measurements can be carried out using small and portable instruments. Development of these instruments and their utilization is of importance for a more widespread utilization of these techniques. Therefore, we are interested in developing optical sensors and testing their performance for produce quality evaluation of agricultural products (e.g. mango and tomato). Furthermore, the results will also be used to develop a proprietary optical instrument.

1.2 Research Hypothesis

Near infrared spectroscopy is a spectroscopic method that uses the near-infrared region of the electromagnetic spectrum (from 780 nm to 2500 nm). It is based on molecular overtone and combination vibration bands in the near infrared region of the spectrum. The NIR spectral data contain information about the absorption of

organic molecules related to vibrations of C-H, O-H, and N-H bonds in specific regions or at specific wavelengths. [1]

Near infrared spectroscopy has received a remarkable measure of interest as a non-destructive analytical technique and it became the tool of choice in several fields. Its typical applications include agriculture-food, pharmaceuticals, natural medicines, soils etc. [2]. NIR spectroscopy is a suitable tool for the determination of internal quality and chemical composition of fruits, vegetables, and agricultural products (e.g. mango and tomato) due to its fast, non-destructive, and facile implementation in field and online analysis. The literature review below represents a limited snapshot of the potential of NIR spectroscopy in agriculture and beyond. The advance of utilization of NIR spectroscopy in Thailand requires the development of new affordable instruments together with suitable models that will enable the real-world deployment of these new instruments.

1.2.1 Development of in-house optical spectrometer

As mentioned above, NIR spectroscopy has received a remarkable measure of interest as a non-destructive analytical technique, and it became the tool of choice in several fields of typical applications including agriculture-food. The key components of popular NIR spectrometers can be divided into three categories 1) light source, 2) wavelength selector, and 3) detector, which determine optical spectrometer properties.

1.2.1.1 Development of in-house optical spectrometer: Light sources

Two different types of NIR light source are used in commercially available spectrometers. These are tungsten halogen (TH) light source and light emitting diodes (LED). The first type, tungsten halogen light source, is a general light source for spectroscopic applications in the visible and NIR range from 300 to 2600 nm. TH is a reliable and inexpensive light source, which provides a stable output. However, it is a thermal radiation source, which produces a significant amount of heat when used for a long time. The second potential type of light source is are light emitting diodes (LEDs). LEDs are efficient enough to be powered by low-voltage batteries or other inexpensive power supplies. Furthermore, LEDs have several advantages for applications in highly miniaturized spectrometers. LEDs feature very low dimensions,

low power consumption, low voltage, and are robust and inexpensive, which is required for working in on site analysis.

Several publications have reported the performance of LED and TH as light sources with optical spectrometers for predicting produce quality parameters. TH light sources have been used in most instances. TH light sources have made it possible to develop predictive models for SSC, DM, and firmness [3-5] with good performance. On the other hand, LEDs have been studied to a limited extent when compared with TH.

Choing. W. and co-workers compared white light emitting diode (White-LED) and tungsten-halogen lamp for predicting the acidity and soluble solids content of intact Sala Mango. The results indicated that the use of both White-LED and tungsten-halogen lamp could be used to successfully to predict the acidity with comparable coefficient of determination ($R^2 = 0.8995-0.9227$) [6].

As mentioned above, previous work comparing the performance of LED and TH as light sources has shown comparable ability in prediction of quality parameters of interest. Therefore, we are interested in utilizing the TH and LED light sources during this project for the development of an in-house optical spectrometer for predicting quality parameters of mangoes and tomatoes.

1.2.1.2 Development of an in-house optical spectrometer: Detector

There are two different classes of detectors that are generally used in miniaturized spectrometers. The first one is based on photovoltaic silicon (Si) diodes, which have suitable sensitivity in the wavelength range of 700-1100 nm. The second are indium gallium arsenide (InGaAs) photodetectors, which are typically suitable in the range 900-1700 nm. Photovoltaic silicon (Si) diodes are suitable for compact and inexpensive instruments operating in Visible and Visible to short wavelength NIR regions. Photovoltaic silicon diodes feature lower S/N However, photovoltaic silicon diodes are significantly cheaper than InGaAs detectors.

As mentioned above, publications reporting predicting quality parameters for mango and tomato usually utilize visible to short near infrared region where the sensitivity of Photovoltaic silicon diodes is suitable.

Therefore, we are interested in utilizing Photovoltaic silicon (Si) diodes as detectors in the developed instruments for predicting quality parameters of mangoes and tomatoes.

1.2.1.3 Development of in-house optical spectrometer: Wavelength selector.

The most essential element of a wavelength selector is the dispersive component as spectroscopy is based on the dispersion of light into its component wavelengths. The dispersion of light can be achieved using a prism or monochromator gratings. Dispersive spectroscopy is widely used in UV, Vis, and NIR applications.

Dispersive Spectrometers are broadly grouped into monochromator and polychromator types. Monochromators use a grating as the wavelength dispersive selector for separating the incident light into a monochromatic spectrum, which is detected in a stepwise manner by a single detector unit. Polychromators have a similar principle as monochromators but are designed with multiple detecting elements to allow simultaneous detection of multiple spectral components. Miniaturized spectrometers commonly fall in the polychromator type.



Figure 1 Image of the F-751-Mango Mango Quality Meter

F-751-Mango Mango Quality Meter is a commercial portable spectrometer for predicting mango quality parameters. This spectrometer has shown strong performance in a validation study with very high accuracy for the prediction of dry matter and %brix. The key component in this spectrometer is the Hamamatsu C11708MA sensors.

The C11708MA is an ultra-compact mini-spectrometer integrating MEMS and image sensor technologies. Therefore, in the second part of this work, we are interested in using the C14384MA-01 sensor from Hamamatsu, which is a new generation of sensor developed from the C17708MA sensor, as a wavelength selector for developing the in-house optical spectrometer

1.2.2 Testing performance of in-house optical spectrometer for quantitative measurements to predict key quality parameters of mango and tomato.

1.2.2.1 Utilization of NIR spectroscopy in nondestructive mango analysis

Mango (*Mangifera indica*) is an important tropical fruit with high demand in the world market. It is called the king of fruits. The taste and texture of the flesh varies across cultivars. The popularity of mango derives from its pleasant taste, color, and texture as well as from its beneficial nutritional value. Mango is an excellent source of fibers, vitamins, and bioactive compounds such as carotenoids, terpenoids, flavonoids, essential oils etc. [7] Moreover, mangoes exhibit a number of pharmacological activities such as antioxidant, anti-inflammatory, and antibacterial properties [7]. The phenotypic changes observed during mango ripening are complex. In most cases the green fruits become more colorful, softer, sweeter, and aromatic. Numerous physical and chemical properties that can be quantified during ripening include size, shape, texture, firmness, external colour, internal colour, concentration of chlorophyll, soluble solids content (SSC) [8], total sugar, pH, starch, sugars, acids, oils, internal ethylene concentration, and/or important active ingredients. The key ripening parameters for mango fruits are firmness, acidity, and soluble solids content. This work focuses on the applications of NIR spectroscopy for the prediction of these key ripening parameters of mango.

Benchtop NIR spectrometers are common in NIR spectroscopy and they can be used for predicting TSS, acidity, and firmness with excellent performance [9]. The distinctive design of benchtop NIR spectrometers results in the superior performance of these instruments. However, these benchtop instruments are large and are costly. Therefore, benchtop instruments are not suitable for onsite analysis. On the other hand, miniaturized spectrometers have been studied to a limited extent when compared with benchtop instruments with high prediction accuracy. For example, Jha,

S. N. et al. determined total soluble solids content for predicting sweetness using Handheld visual spectra analysis. The correlation coefficient for predicting TSS of the model was 0.90 [10]. Cortes V. et al. reported a new ripening index (RPI) for mango. The results showed the possibility to predict RPI with an R_p^2 of 0.831-0.871 [8]. Emanuel, M. et al. published a report on non-destructive determination of quality parameters of mango using a novel handheld near infrared spectrometer for predicting soluble solids (SS), dry matter (DM), titratable acidity (TA), and pulp firmness (PF). The results showed that a handheld spectrometer can be used for predicting SS of internal quality with a strong performance. In contrast, predictive models for DM, TA, and PF exhibited moderate performance [3]. Fauzana N. et al. have evaluated assessing firmness using broadband miniature spectrophotometer (SCIO) [11]. The SCIO showed good performance for predicting mango firmness (R^2 0.74-0.93;).

As mentioned above, handheld spectrometers can be used for predicting some key parameters with high precision. Miniaturized spectrometers have been studied to a limited extent. This revolutionary step into miniaturization required implementing new technological solutions. Systematic studies of miniaturization of NIR spectrometers are necessary to evaluate the accuracy and robustness in analytical sense in various applications.

Therefore, we are interested assembling and testing an in-house optical spectrometer from section 2.1 for quantitative measurements to predict key quality parameters for mango

1.2.2.2 Utilization of NIR spectroscopy in nondestructive tomato analysis

Tomato (*Solanum lycopersicum*) is the edible berry of a plant from the Solanaceae family [12]. Tomato is an important product in the agricultural market. It is the second most consumed vegetable in the world. The world can produce 177.04 metric tons of tomatoes every year. The largest producers of tomatoes are China, India, and United States [13]. The tomato mostly consists of water, soluble and insoluble solids, phenolics, organic acids, vitamins, and sugar. Total acid, sweetness, solidity, and color are the most important factors for consumers [14]. Acidity, sweetness, and, color define the first impression of tomato [15]. Firmness, soluble solid content, and titratable acidity are the main determinants of tomato flavor [16].

Benchtop NIR spectrometers can be used for predicting soluble solids content, lycopene, and beta-carotene with excellent performance [17], but firmness, pH, and titratable acidity were predicted less accurately for tomato samples [15]. The NIR spectrometer was capable to perform quality measurements, although not all parameters were predicted with the same accuracy. Handheld and luggable spectrometers can also be used for predicting key parameters (dry matter and firmness) of internal quality with excellent performance and with good relation of soluble solids content and titratable acidity for non-destructive determination.

Miniaturized spectrometers have been studied to a limited extent as well as for mango. For example, Tilahun. S. et al. reported models with excellent performance for the prediction of lycopene, beta-carotene [18], and soluble solids content[19].

Therefore, this proposal focusses on applications of in-house the optical spectrometer as a miniaturized spectrometer from 2.1 for quantitative measurements to predict these keys quality parameters for tomato.

1.2.3 Testing performance of in-house optical spectrometer for quantitative measurements to predict other quality parameters from mango and tomato.

As mentioned above, mango and tomato contain essential nutrients, for example sugars, volatile compounds, phenols, organic acids, carotenoids, and vitamins. Total organic acids and sugar are the most important for taste. On the other hand, carotenoids and vitamins are particularly important as free radical quenchers for antioxidant activity. Vitamin C and E result in various health benefits including prevention of heart disease, arteriosclerosis, and cancers. This proposal focusses on quantitative measurements of NIR spectroscopy for predicting other quality parameters including antioxidant activities, lycopene content, beta-carotene content, and vitamin C content.

Ding. X. et al. published a study focused on a novel NIR spectroscopic method for rapid analyses of lycopene, total acid, sugar, phenols, and antioxidant activity in dehydrated tomato samples using benchtop instruments [14].

The results have shown that total acid, total sugar, lycopene, total phenolic, and antioxidant activity (TAA-DPPH, TAA-FRAP and TAA_ABTS) were accurately

predicted with R^2 values of 0.965, 0.992, 0.978, 0.992, 0.981, 0.988, and 0.993, respectively.

Therefore, in this part of this project, we are interested in developing and testing the performance of an in-house optical spectrometer for quantitative measurements to predict other quality parameters (e.g. Lycopene, Beta-carotene and vitamin C) from mango and tomato.

The literature reports mentioned above represent literature review of the potential of NIR spectrometers for the prediction of quality parameters of mangoes and tomatoes. These reports indicate that it is possible to measure these parameters using non-destructive measurements. However optical measurements of key quality parameters, such as firmness, soluble solids content, titratable acidity, have resulted in prediction models with moderate performance using miniaturized spectrometers. The objective of this study are: 1) development of in-house optical spectrometer for predicting key quality parameters of mangoes and tomatoes depending on key optical instrument components such as light source, wavelength selector, and detector. 2) to research and develop rapid and non-destructive optical method for predicting key quality parameters of mangoes and tomatoes with different chemometric methods of data analysis. 3) to compare the quantitative performance of chemometric analysis for prediction of various quality parameters.

1.3 Research Objectives

1. Development of in-house optical spectrometer
2. Testing performance of the in-house optical spectrometer for quantitative measurements to predict key quality parameters for mangoes
3. Testing performance of the in-house optical spectrometer for quantitative measurements to predict key quality parameters for tomatoes

1.4 Research Scope

The purpose of this research is, to develop an in-house optical spectrometer and to test the performance of this in-house optical spectrometer in predicting key quality parameters (firmness, soluble solids content, titratable acidity) for mango and tomato samples with different chemometric methods of data analysis. Furthermore, an

additional aim is to compare the quantitative performance of chemometric analysis for prediction of various supplemental quality parameters (vitamin C, lycopene, beta-carotene).



CHAPTER II

LITERATURE REVIEW

Fruits and vegetables provide nutrients for human body. These are useful for preventing non-communicable diseases such as diabetes, cardiovascular disease, and in particular cancer [20]. The development of these diseases can be prevented if people take enough fruits and vegetables. Therefore, consumers have begun to pay more attention to the quality of fruits and vegetables. They are increasingly looking for quality products and rejecting products with any contaminants. However, these qualities vary with ripeness state and cannot be measured easily by the consumer during purchase. Nowadays, most consumers rely on surface firmness, etc. to determine the quality of fruit which is often misleading. Therefore, the demand for easy, rapid, and non-destructive techniques for the quality evaluation is increasing. Near infrared spectroscopy (NIR) is a rapid, precise, and non-destructive technique, which can be well utilized in determination of fruit quality [21].

The Near infrared (NIR) spectroscopy is one of the tools of optical spectroscopy. NIR spectroscopy is a spectrometric method that uses near-infrared region of the electromagnetic spectrum (from 780 to 2500 nm) as shown in Figure 2. There are many applications of this technique in various areas such as agriculture, pharmaceuticals, food and agrochemical quality control, remote monitoring etc. The NIR spectra include broad bands that arise from absorptions of overlapping wavelengths. The absorptions measured by NIR spectroscopy correspond mostly to overtones and combinations of vibrational modes involving the C–H, O–H, and N–H chemical bonds [2].

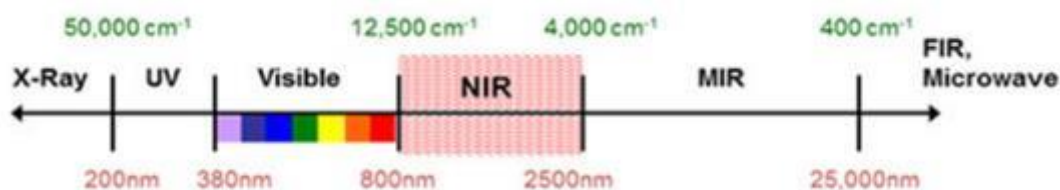


Figure 2 Spectral range for the NIR showing wavelengths and wavenumbers.

2.1 Utilization of NIR spectroscopy in nondestructive analysis

The first applications of NIR were developed in the 1950s by William Herschel. Initially NIRs was used only as an add-on unit to other optical devices primarily used for other wavelengths such as ultraviolet (UV), visible (Vis), or mid-infrared (MIR) spectrometers [2]. NIRs was first used in agricultural applications by Norris to measure moisture in grain [22]. Since then, it has been used for rapid analysis of moisture, protein, and fat content of a wide variety of agricultural and food products [23]. Representative NIR spectra of various fruits can be seen in Figure 3.

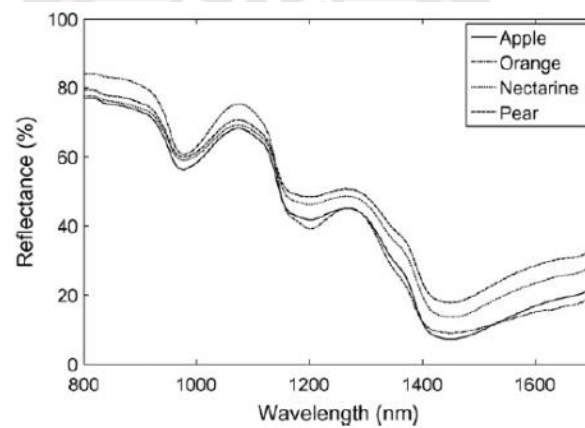


Figure 3 NIR reflectance spectra of selected fruits.

The spectral features in the NIR part relate to vibrational states. However, NIR is different to the mid infrared (MIR) region [23]. The NIR contains overtone and combination bands of the principal vibrations of O-H, N-H, and C-H bonds observed in the MIR. Therefore, in contrast to FT-IR measurements in the MIR region, which contains sharp and resolved peaks, the features in NIR spectra are broad and difficult to interpret. Despite the convoluted appearance of NIR spectra, assignment of several features to specific vibrations is possible and indeed desirable. For example, spectra of fruits are dominated by features belonging to water, O-H overtones at 760, 970, and 1450 nm and a combination band at 1940 nm (Figure 3, Figure 4). [24]

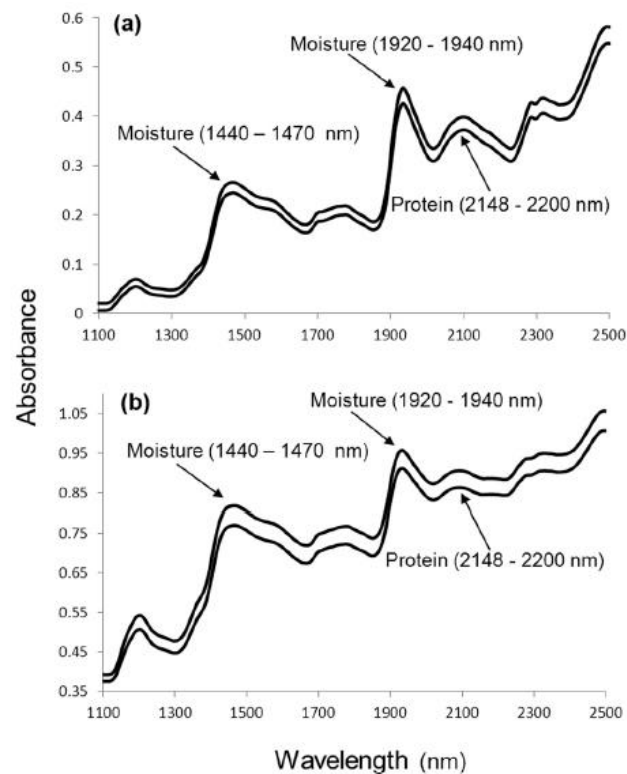


Figure 4 NIR absorbance spectra of a) ground and b) intact wheat.

Despite the possibility of rudimentary qualitative analysis of NIR spectra, the quantitative applications mentioned above require the use of multivariate statistical techniques (chemometrics) to extract useful information from these spectra. Originally multiple linear regression (MLR) has been utilized for this purpose but the development of the computer enabled the use of other methods such as partial least squares regression (PLS) or principal component regression (PCR). [25]

2.2 Utilization of NIR spectroscopy in nondestructive mango analysis

Mango (*Mangifera indica*) is a stone fruit produced by the *Anacardiaceae* family and one of the most important and most widely cultivated fruits of the tropical world. It is called the king of the fruits. Mangoes are generally sweet, however, the taste and texture of the flesh varies across cultivars. The popularity of mango derives from its pleasant taste, color, and texture as well as from its beneficial nutritional value. Mango is an excellent source of fibers, vitamins, and bioactive compounds

such as carotenoids, terpenoids, flavonoids, essential oils etc. The typical content values are shown in Table 1. Moreover, mangoes exhibit many pharmacological activities such as antioxidant, anti-inflammatory, antibacterial properties etc. [26]

Table 1 parameter consumption analysis of mango fruit (*Mangifera indica* L.)

parameter	content
Water (%)	78.9–82.8
Ashes (%)	0.34–0.52
Total lipid (%)	0.30–0.53
Total protein (%)	0.36–0.40
Total carbohydrate (%)	16.20–17.18
Total dietary fiber (%)	0.85–1.06
Energy (kcal)	62.1–190
Ascorbic acid (Vit C), mg/100 g	13.2 – 92.8
Thiamine (Vit B1), mg/100 g	0.01 – 0.04
Riboflavine (vit B2), mg/100 g	0.02 – 0.07
Niacin (vit B3), mg/100 g	0.2 – 1.31
Panthenic acid (Vit B5), mg/100 g	0.16 – 0.24
Pyridoxin (vit B6), mg/100 g	0.05 – 0.16
Vitamin A, µg/100 g	54
Vitamin E (α-tocopherol), mg/100 g	0.79 – 1.02
Vitamin K, µg/100 g	4.2
Calcium (Ca), mg/100 g	7 - 16
Iron (Fe), mg/100 g	0.09 – 0.41
Magnesium (Mg), mg/100 g	8 - 19
Potassium (K), mg/100 g	120 - 211
Zinc (Zn), mg/100 g	0.06 – 0.15
Manganese (Mg), mg/100 g	0.03 – 0.12

In 2000, Schmilovitch, Z. and co-workers have evaluated the determination of mango physiological indices by near-infrared spectrometry [9]. The work has measured the physicochemical properties of mango, cv “Tommy Atkins” and established NIR spectral measurements. The softening of flesh, total soluble solids content, and acidity were studied in this publication. Intact mango was measured in reflectance mode in the wavelength range 1200-2400 nm using a benchtop NIR spectrophotometer (Quantum 1200, manufactured by LTI). The work was conducted on eighty mango fruit samples from a single orchard during a summer harvest season. NIR models were developed based on multiple linear regression (MLR), principal component analysis (PCA), and partial least square (PLS) regression with data preprocessing using first derivative, the logarithms of the reflectance reciprocal, and its second derivative. The best prediction results were obtained using MLR models with second derivative of reciprocal reflectance. The coefficients of determination of TSS, acidity, firmness and, storage period were 0.9276, 0.6085, 0.8226, and 0.9380, respectively. This publication has demonstrated that it is possible to perform non-destructive determination of the maturity factors of mango fruits using benchtop NIR spectrophotometer.

In 2005, Jha, S. N. and co-workers published a study on the determination of sweetness of intact mango using Visual spectral analysis [10]. Total soluble solids (TSS) were determined in this report for predicting sweetness by using visual spectra analysis. The visual spectra analysis was performed by a handheld colorimeter spectrometer (HunterLab miniScan XE plus colorimeter) equipped with a Xenon flash lamp as a light source and a detector operating from 400 to 700 nm in reflectance mode. The work was conducted on 329 mangoes from 3 different orchards. The authors have conducted chemometric analysis using the Unscrambler software. They have split the samples into two sets, one of the sets contained 165 samples for calibration and the other set contained 164 samples for validation purposes. Calibration models made with different wavelength ranges for prediction of total soluble solids content by multiple linear regression (MLR), partial least-squares regression (PLS), and principal component regression (PCR) were prepared. The results showed that the MLR model of original spectra (440-480 nm) was the best. The correlation coefficient for predicting TSS of the calibration models was 0.90.

In 2006, Jha S. N. and co-workers published a report on the determination of firmness and yellowness of mango using visual spectroscopy [27]. The firmness and yellowness were analyzed by a handheld colorimeter spectrometer (HunterLab miniScan XE plus colorimeter) equipped with a Xenon flash lamp as a light source. A detector operating from 400 to 700 nm in reflectance mode was used. A total of 290 fruit samples from four different orchards has been used in this study. The authors have split samples into two sets, each containing 145 samples for calibration and validation purposes, respectively. They developed calibration models using partial least squares regression (PLS1 and PLS2), principal component regression (PCR), and multiple linear regression (MLR) with data collected in reflectance mode in different ranges of wavelengths and tested the resulting models with the validation set. The best results were obtained with the PLS2 model based on data that was preprocessed by smoothing and application of the multiplicative scatter correction (MSC) treated in the spectral wavelength range 530-550 nm. The standard error of calibration, the standard error of prediction, correlation coefficient of calibration, and correlation coefficient of prediction were found to be 5.0-5.45, 4.87-5.76, 0.88-0.90, and 0.95-0.97 for firmness and yellowness index, respectively.

As shown above, visual spectral analysis can be used for predicting TSS, firmness, and yellowness with high correlations between measured and predicted values. The results have also shown that the developed models have a potential for the prediction of TSS, firmness, and yellowness of intact mango. However, the prediction models are not ready for commercial use yet due to more mango varieties and samples are needed.

In 2012, Jha S. N. and co-workers have evaluated the non-destructive prediction of sweetness of mango using NIRs [28]. This work studied a new technology to evaluate the quality of fruits using NIRs. The TSS and pH were determined using portable NIR spectroscopy (Luminar 5030, Brimrose Corp., Maryland, USA)) with reflectance in the wavelength range 1200 to 2200 nm. The instrument is equipped with diffuse reflection optical configuration and an InGaAs detector. The work was conducted on 20 mango fruit samples fruits from 4 different orchards. NIR models were developed based on multiple-linear regression (MLR) and partial least squares (PLS) regression and preprocessing data with baseline correction,

smoothing, multiplicative scatter correction (MSC), and second order derivation. The best calibration model was found using the NIR spectra treated by second order derivative. The multiple correlation coefficients of calibration and validation were 0.782 and 0.762 for TSS and 0.715 and 0.703 for pH respectively.

As reported above, NIRs can be used for predicting TSS and pH with good correlations. However, the results indicated that the developed models can help in designing portable instruments for rapid analysis based on TSS and pH prediction. Furthermore, the developed spectrometer model should have the lowest possible spectral window (wavelength range) for reducing the cost the of instrument.

In 2014, Jha S. N. and co-workers reported the non-destructive prediction of maturity of mango using NIR. The authors studied maturity index (I_m) using physico-chemical characteristic properties and overall acceptability (OA) from nine different orchards. The computed I_m values were determined using 20 equations to determine the maturity index. The best equation for I_m is shown in Equation 1.

$$I_m = \left(n \frac{TSS \times DM}{TA} \right) \quad \text{Equation 1}$$

Where I_m is the maturity index, TSS is total soluble solids (%Brix), DM is dry matter (%), TA is titratable acidity (%), and n is a specific constant.

The NIR spectra were acquired using a portable NIR spectrometer (Luminar 5030, Brimrose Corp., Maryland, USA) with reflectance in the wavelength range 1200 to 2200 nm. The instrument was equipped with a diffuse reflection optical configuration and an InGaAs detector. In total 1180 mango fruit samples were used in this work. Multiple-linear regression (MLR) and partial least squares (PLS) regression were used to predict I_m . The best prediction was achieved with a PLS model calibrated using multiplicative scatter correction (MSC) as data pretreatment in the wavelength range of 1600-1800 nm. The correlation coefficients (R) for calibration and cross-validation of I_m value were 0.74 and 0.68 respectively.

In 2016, Cortes V. and co-workers reported a new internal quality index for mango and its prediction by external visible and near-infrared reflection spectroscopy

[8]. The authors investigated internal quality of intact mango, cv. “Osteen”. The internal quality index (IQI) was correlated with the ripening index (RPI) of the sample. It was developed by combining biochemical properties (total soluble solids, TSS) and physical properties (firmness and color) from mango sample. This work has been conducted with a total of 149 unripe mango samples. The spectral characteristics of the intact mangoes were measured in three different spectral regions (visible region; 400-700nm, visible to near infrared region; 600-1100 nm, and near infrared region; 900-1750nm) in reflectance mode using a multichannel spectrometer platform (AVS-DESKTOP-USB2, Avantes BV, The Netherlands). The spectral characteristics were used to determine the quality indices RPI and IQI using the Unscrambler program. The formulas for the RPI and IQI are shown in Equation 2 and 3.

$$RPI = \ln(100F \times TA \times TSS^{-1}) \quad \text{Equation 2}$$

$$IQI = \ln(100F \times L^* \times h_{ab}^* \times TSS^{-1} \times C_{ab}^{*-1}) \quad \text{Equation 3}$$

Where F is firmness (N), TA is titratable acidity (%), TSS is total soluble solids (%), and L^* , h_{ab}^* , and C_{ab}^{*-1} are the color attributes of flesh color.

Calibration and cross-validation sets of samples were used to predict RPI and IQI using VIS, VIS-NIR, and NIR models. All models have shown high R^2 (0.902-0.934) and R_{cv}^2 (0.831-0.903) values, while RMSEC (0.335-0.509) values were low. The best models have shown the ability to predict RPI using VIS, VIS-NIR, and NIR data with R_p^2 of 0.871, 0.795, and 0.831 and RMSEP of 0.520, 0.548, and 0.613, respectively. The prediction of IQI was achieved with R_p^2 values of 0.838, 0.896, and 0.815 and RMSEP values of 0.537, 0.403, and 0.531 for VIS, VIS-NIR, and NIR data respectively.

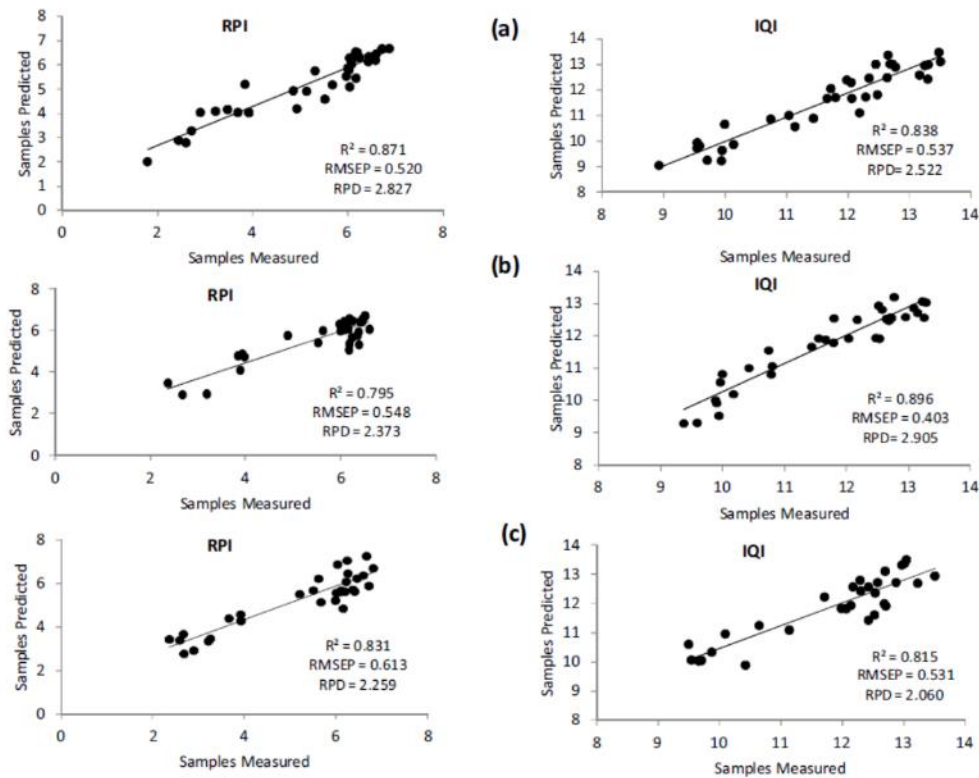


Figure 5 Predicted versus measured values of RPI and IQI for the visible region (a), the visible-near infrared region (b) and near-infrared region (c).

New internal quality parameters of intact mangoes, RPI and IQI, have been defined. Different spectroscopy systems were used to perform measurements in different spectral ranges (VIS, VIS-NIR, and NIR). Models show strong performance for predicting RPI and IQI using full spectral range and the most important wavelengths. Nevertheless, the results obtained external measurements using visible and near-infrared spectroscopy combined with chemometrics can be used for non-destructive determination of internal quality of mangoes.

In 2016, Emanuel M. and co-workers published a report on non-destructive determination of quality parameters in mangoes using a novel handheld near infrared spectrometer [3]. The spectral data were obtained with a handheld ultracompact MicroNIR 1700 spectrometer. The instrument has a linear-variable filter (LVF) directly coupled to a linear Indium gallium arsenide (InGaAS) detector. This system used tungsten filament as a light source. This study was evaluating the potential of

handheld near infrared spectrometer for rapid and non-destructive analysis. Multivariate calibration models were constructed using Partial Least Squares (PLS) regression to determine soluble solids (SS), dry matter (DM), titratable acidity (TA), and pulp firmness (PF). Different spectral pre-processing approaches were tested. The best results were obtained with the SNV method. The Coefficient of determination and root mean square errors of prediction (RMSEP) values were 0.92 and 0.55 % Brix for SS, 0.67 and 0.51% for DM, 0.50 and 0.17% citric acid for TA, and 0.72 and 12.2 N for PF, respectively.

In 2016, Rungpichayapichet P. and co-workers evaluated robust NIRs models for non-destructive prediction of postharvest quality in mango [29]. The TSS, firmness, TA, and RPI were determined using a NIRs (portable VIS/NIR photodiode array spectrometer) in the region of 700-1100 nm. Mango fruit (cv.Nam Dok Mai subcv. Si Thong). A total of 592 fruits from Thailand were used. The prediction models of TSS ($R^2 = 0.9$; SEP = 1.2%), firmness ($R^2 = 0.82$; SEP = 4.22N), TA ($R^2 = 0.74$; SEP = 0.38%), and RPI ($R^2 = 0.8$; SEP = 0.8) have shown good performance. Concurrently, it was found that model robustness can be improved by adding a wider range of data. Classification of mango ripeness was successfully performed with an accuracy of more than 80%. This research can be beneficial for the development of grading and sorting for quality control in industrial handling and marketing of mango.

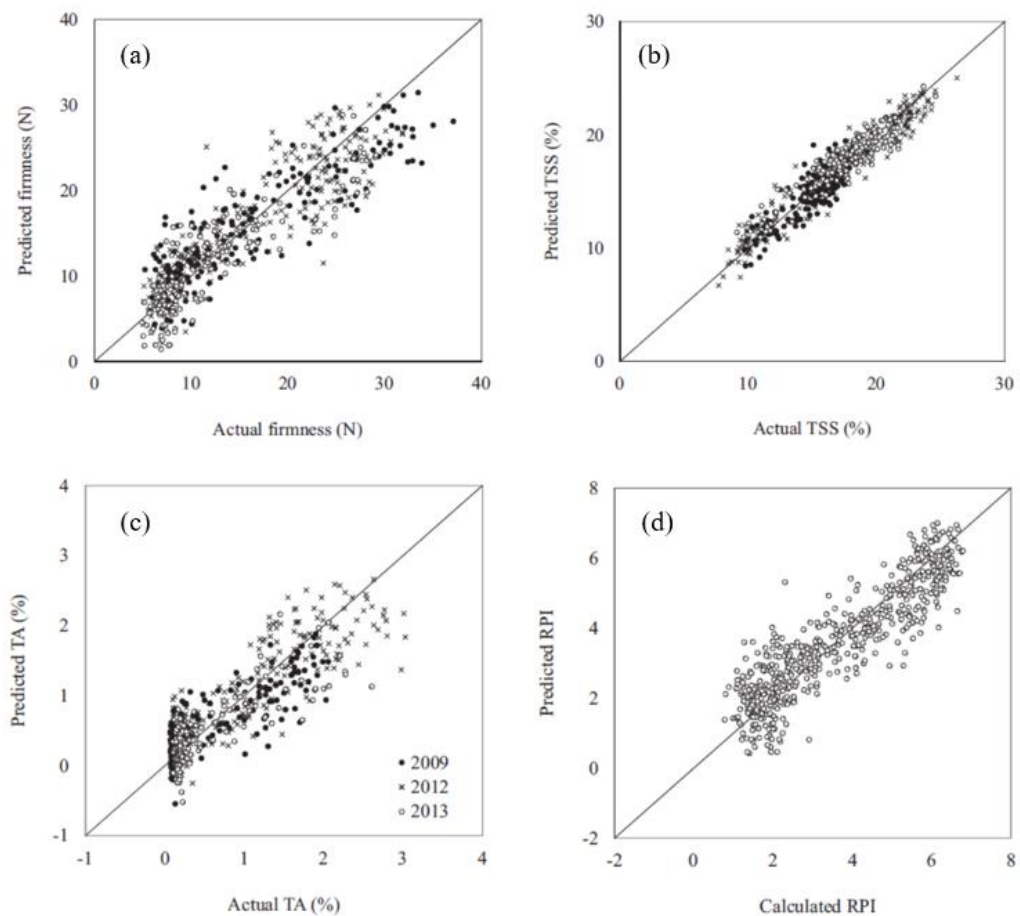


Figure 6 Prediction results for quality attributes: (a) firmness, (b) total soluble solids (TSS) and (c) titratable acidity (TA) (d) ripening index (RPI) using the overall NIRS calibration model to predict values for individual harvest years.

In 2017, Santo. N. and co-workers published the determination of mango maturity indices using a portable near infrared (VIS-NIR) spectrometer [4]. This study has developed calibration models for soluble solids content (SSC) and dry matter (DM) of mango using portable VIS-NIR spectrometer (F-750, Felix Instruments, Washington, USA) operating between 310 to 1100 nm. The light source was a halogen lamp. The spectra were analyzed using partial least square regression (PLSR) with full cross validation. The best result of SSC prediction was achieved with pre-processing using the standard normal variate (SNV), Savitzky-Golay first derivative, and a window of 699–999 nm. The observed RMSE and R^2 values are 1.39% and 0.87,

respectively. In the case of the DM calibration the best result was achieved using the raw spectrum with the window of 699–981 nm. The observed RMSE and R^2 values were 8.81 g kg^{-1} and 0.84, respectively. In contrast, poor calibration models were obtained for firmness.

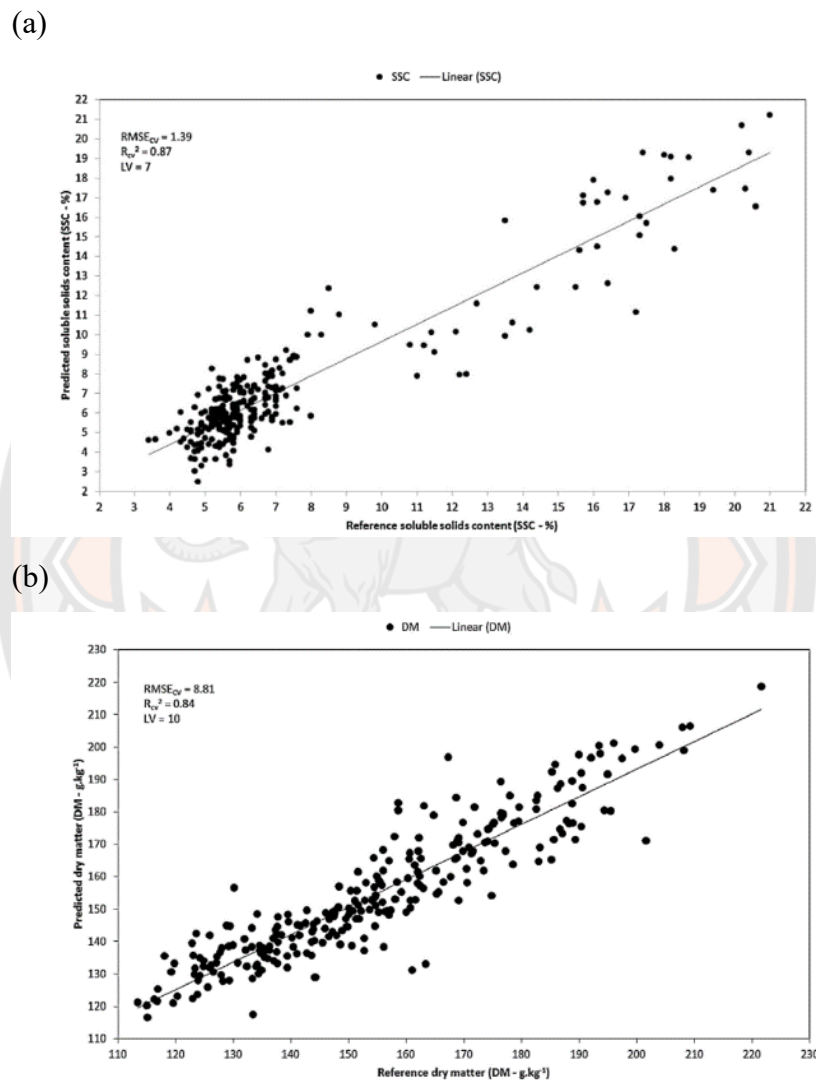


Figure 7 Plots of predicted versus measured (a) SSC and (b) DM values of ‘Palmer’ mangoes harvested at different developmental stages measured using a portable F-750 spectrometer

In 2020, Sun. X. and co-workers evaluated the robustness of NIRs based predictions for intact mangoes to temperature change [5]. They studied a temperature

correction method for reducing the impact of sample temperature change on dry matter content prediction including external parameter orthogonalisation (EPO), generalised least square weighting (GLSW), bias correction, repeatability file, calibration wavelength optimization, and global modelling as data preprocessing approaches. The work was conducted on 2052 samples using three different temperature conditions (cold; 15-18 °C, room temperature; 23-25 °C, high; 30-35 °C). The NIR spectral data were obtained with a handheld NIR spectrometer (F750 handheld NIR spectrometer) from 729 to 975 nm. The light source was a 32W halogen lamp. The authors split the samples into two sets. One of the sets contained 1392 samples for calibration and other set was composed from 660 samples for validation purposes under different temperature conditions. Preprocessing the data using the EPO method resulted in the best model for predicting dry matter content. This approach has shown the highest R^2 (0.82) and lowest RMSEP (1.05%) in comparison with the control method, which gave R^2 and RMSEP values of 0.68 and 1.43%, respectively.

In 2020, Phuangsombut. K. and co-workers published an empirical approach to improve the prediction of soluble solids content in mango using NIRs [30]. This work has been performed with a total of 100 mango fruits (cv. Nam Dokmai) obtained from three different local markets. The NIR spectral data of intact mangoes were measured using a portable NIR spectrometer (FQA-NIR GUN) in the wavelength range of 600-1100 nm. The results demonstrated the effect of peeled and unpeeled samples on NIR spectral data. The authors studied the effect of peel on the performance of NIR analysis for predicting soluble solids content. The results indicated that a partial least squares (PLS) regression model for unpeeled samples had lower accuracy than for peeled samples. The R^2 and RMSE values for the unpeeled samples were 0.84 and 1.50 °Brix, respectively. The R^2 and RMSE values for the peeled samples were 0.88 and 1.27 °Brix, respectively. Improved prediction was achieved applying the empirical approach, which has removed the difference between the flesh and peel. This method has resulted in the highest accuracy ($R^2 = 0.87$; RMSE = 1.36 °Brix).

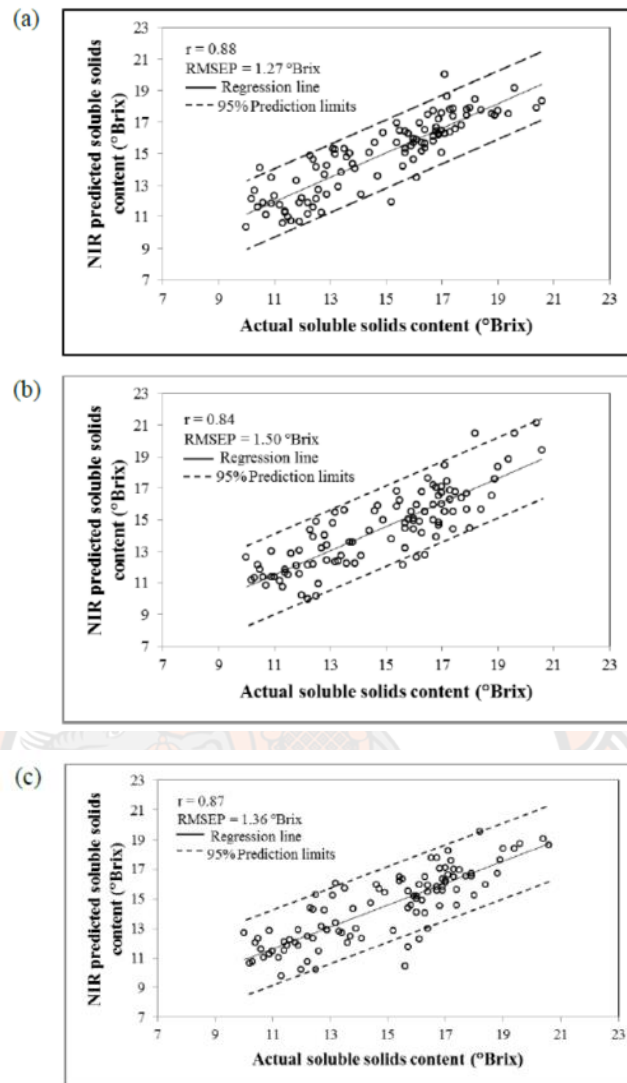


Figure 8 Prediction models of soluble solids content using near infrared spectra based on (a) flesh, (b) peel and flesh, and (c) adjusted peel and flesh spectra.

In 2021, Fauzana. N. and co-workers evaluated assessing firmness in mango using various broadband miniature spectrophotometers [11]. This study has compared a laboratory-based instrument and a miniature spectrophotometer (SCIO) to predict mango fruit firmness. For the SCIO instrument, the light source was a LED coupled with Si photodiode array as a detector. The NIR spectra data were obtained by SCIO pocket molecular scanner from 740 to 1070 nm. The SCIO and laboratory-based instrument showed similar performance predicting mango firmness. The SCIO showed good performance for predicting mango firmness (R^2 0.74-0.93; RMSE 4.8-

8.2 Hz²g^{2/3}). The pocket-sized SCiO NIR sensor can thus be used in optimizing the ripening quality parameters of mango fruit with high accuracy.

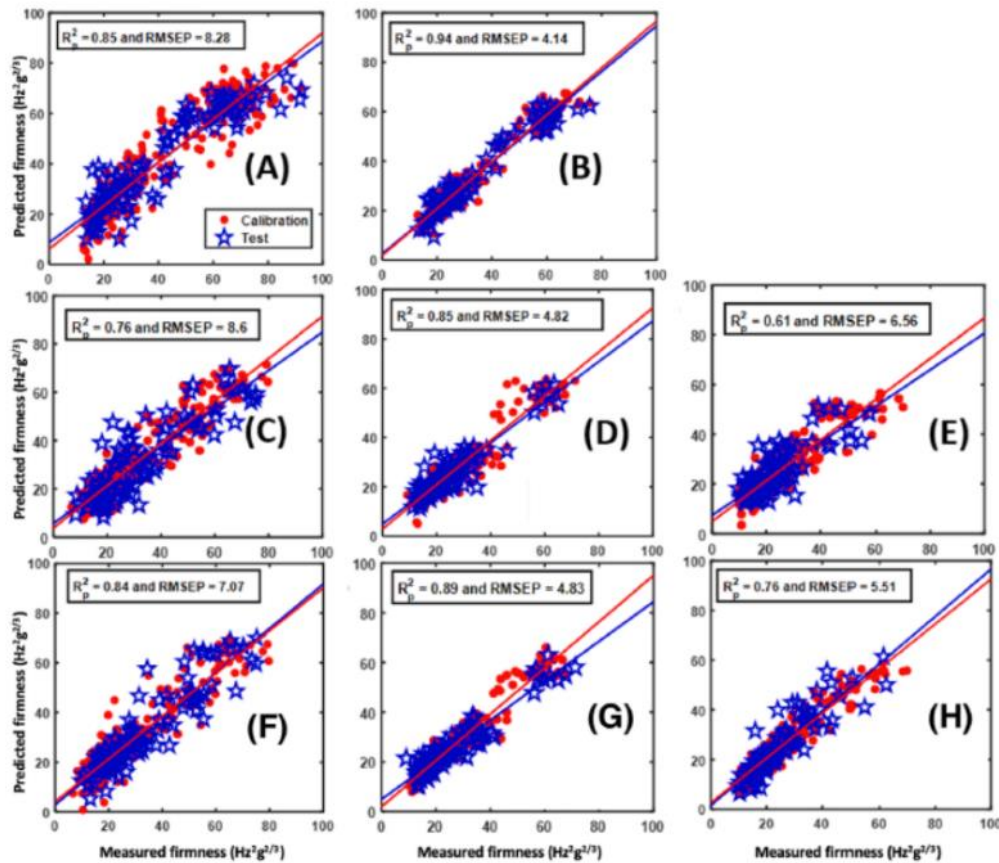


Figure 9 A summary of models made on variables selected with bootstrapping soft shrinkage (BOSS) approach for SCiO and Zeiss data. PLSR models on SCiO data for batch 1 (A) and batch 2 (B). PLSR models on reduced spectral range Zeiss data for batch 1 (C), batch 2 (D) and batch 3 (E). PLSR models on full spectral range Zeiss data for batch 1 (F), batch 2 (G) and batch 3 (H).

2.3 Utilization of NIR spectroscopy in nondestructive tomato analysis

Tomato (*Solanum lycopersicum*) is the edible berry of a plant from the *Solanaceae* family. Tomato is an important product in the agricultural market. It is the second most consumed vegetable in the world. The world can produce 177.04 million metric tons of tomatoes every year. The largest producers of tomatoes are China, India, and United States [13]. Tomato is a source of important nutrients (protein,

lipids, sugar) and bioactive compounds (lycopene, beta-carotene, and ascorbic acid). Importantly, tomatoes are the main source of lycopene and beta-carotene. These carotenoids can act as free-radical scavengers in the body exhibiting antioxidant and anticancer properties etc. [31]. The key components of tomatoes are shown in Table 2.

Table 2 parameter consumption analysis of Tomato (*Solanum lycopersicum*).

parameter	content
Water (%)	94.52
Energy (kcal)	18
Total protein (%)	0.88
Total lipid (%)	0.2
Fiber (%)	1.2
Sugar (%)	2.63
Calcium (Ca), mg/100 g	10
Magnesium (Mg), mg/100 g	11
Phosphorus (P), mg/100 g	24
Potassium (K), mg/100 g	237
Sodium (Na), mg/100 g	5
Ascorbic acid (Vit C), mg/100 g	13.7
Choline, mg/100 g	6.7
Vitamin A, $\mu\text{g}/100\text{ g}$	42
Alpha-carotene, $\mu\text{g}/100\text{ g}$	449
Beta-carotene, $\mu\text{g}/100\text{ g}$	101
lycopene, $\mu\text{g}/100\text{ g}$	2573
Vitamin K, $\mu\text{g}/100\text{ g}$	7.9

In 2005, Pedro. A.M. and co-workers published the first investigation of tomatoes with near infrared spectroscopy entitled “Nondestructive determination of solids and carotenoids in tomato product by near infrared spectroscopy and

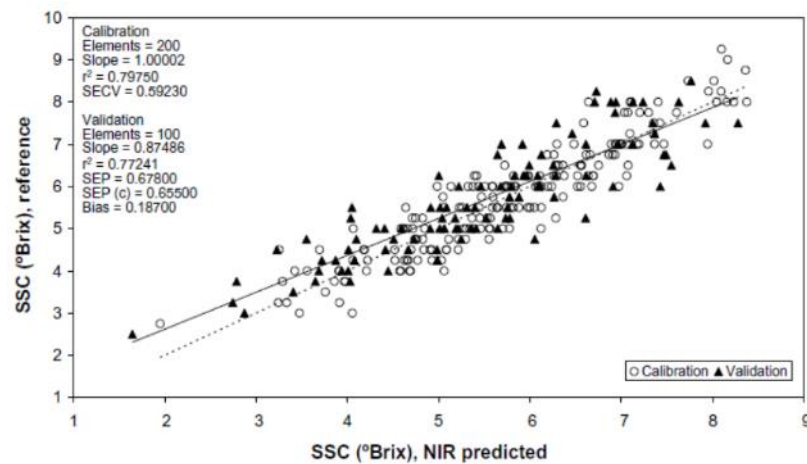
multivariate calibration” [17]. They presented the development of simultaneous and nondestructive method for predicting soluble solids content, lycopene, and beta-carotene in tomatoes by NIRs. The NIR spectra were acquired by a benchtop NIR instrument (Buchi NIRLab N-200 spectrometer). The work was conducted on 42 samples from various markets. NIR models were developed based on partial least square (PLS) regression. For preprocessing data, MSC and secondary derivatives were chosen. The best models presented satisfactory prediction of these parameters. RM-SEC and r values of TSS, lycopene, and beta-carotene were 0.4157, 0.9998, 0.6333, 0.9996, and 0.7296, 0.9981, respectively.

In 2008, Alain. C. and co-workers evaluated the possibility of non-destructive measurement of fresh tomato lycopene content and other physicochemical characteristics using visible-NIR spectroscopy [15]. The authors have measured various quality parameters by non-destructive measurements using vis-NIR reflectance spectroscopy and chemometrics. Lycopene content, color variables (Hunter a, L, b, a/b ratio), tomato color index (TCI), firmness, pH, soluble solids content, titratable acidity, and electrical conductivity were determined using a benchtop NIR instrument (Varian Cary 500 UV-vis-NIR scanning spectrophotometer). The study was conducted with a total of 96 samples. The tomato samples were obtained from three different sources. NIR spectral data were obtained in reflectance mode in the wavelength of 400-1500 nm. The results show that lycopene content was accurately predicted ($r^2 = 0.98$), along with color variables such as Hunter a ($r^2 = 0.98$), L and b ($r^2 = 0.92$). TCI ($r^2 = 0.96$) was predicted with better accuracy than a/b ($r^2 = 0.89$). Firmness prediction ($r^2 = 0.75$) had only modest accuracy. Models for internal quality parameters such as pH, soluble solids content, titratable acidity, and electrical conductivity were less accurate.

In 2009, Flores. K. and co-workers reported a study on the feasibility of NIRs instruments for predicting internal quality in intact tomato [16]. Soluble solids content and titratable acidity were chosen as the two internal quality indices relevant to tomato flavor. This study examined the feasibility of a luggable NIR spectrometer (FNS-6500 scanning monochromator) to be used to calibrate models for the prediction of SSC and TA in tomato. Tomatoes picked in 2006 (N=180), were used for the calibration. Validation was performed with tomatoes picked in 2007 (N=132). The

optical spectra were measured in reflectance mode at 400-2500 nm. The results resulted in coefficient of determination (r^2) for SSC and TA of 0.82 and 0.71, respectively. The regression models were tested with an independent validation sample (N=100). The resulting coefficients of determination (r^2) for SSC and TA were 0.77 and 0.68, respectively.

(a)



(b)

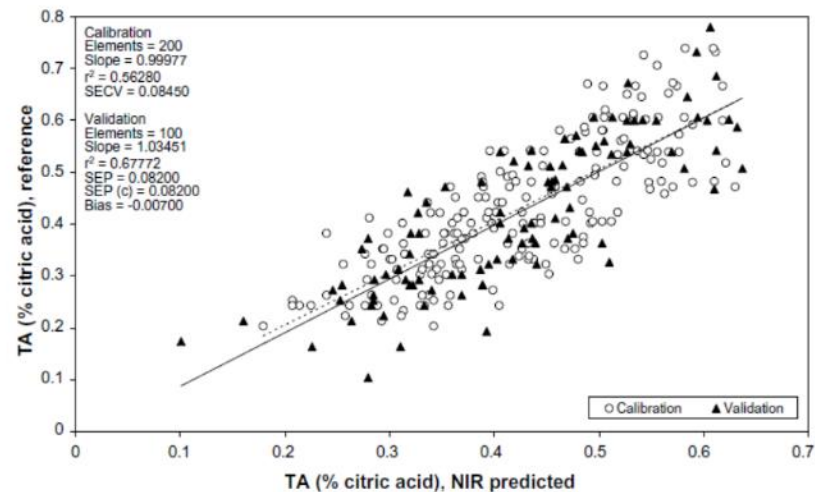


Figure 10 Reference data vs. NIRS predicted data for the validation set for (a) SSC (b) TA.

In 2009, Xie. L. and co-workers published a study focused on rapid determination of ethylene content in tomatoes using visible and short-wave near infrared spectroscopy and wavelength selection [32]. The study was concentrated on visible and short-wave near infrared spectroscopy technique using benchtop FT-NIR instruments for quantitative analysis of ethylene content with three varieties (non-transgenic tomatoes, transgenic tomatoes, and antisense *LeETR1* and *LeETR2* tomatoes) of tomatoes. The results indicated that the determination of ethylene content from tomatoes could be successfully performed by VIS-NIR spectroscopy combined with chemometric methods including PLS and SMLR. The prediction models of PLS and SMLR using selected wavelengths were compared. The results obtained by modeling of PLS using visible region needed less time than those made using the full range of wavelengths.

In 2016, Ding. X. and co-workers published a study focused on a novel NIR spectroscopic method for rapid analyses of lycopene, total acid, sugar, phenols, and antioxidant activity in dehydrated tomato samples [14]. In this work, the authors developed a novel NIR spectroscopic method for rapid analyses of dehydrated tomato samples using a benchtop NIR instrument (U-4100 UV/VIS/NIR spectrometer). The work was conducted on 92 dehydrated tomato samples from different batches, which have been processed with hot air technique at 40°C for 8 h. All of the samples were transformed into tomato powder using high speed pulverizer. The samples were transformed in a plastic container before NIR analysis. The NIR measurements were performed in reflectance mode in the spectral range of 800-2500 nm. Two multivariate calibration models (PLSR and RBF-NN) were applied for rapid non-destructive analysis for the determination of lycopene, total acid, sugar, phenols, and antioxidant activity. The results obtained with the RBF-NN models were better than with the PLSR models. They were also better than a novel NIR spectroscopic method supported by chemometrics.

The results have shown that total acid, total sugar, lycopene, total phenolic content, antioxidant activity (TAA-DPPH, TAA-FRAP and TAA-ABTS) were accurately predicted with R^2 values of 0.965, 0.992, 0.978, 0.992, 0.981, 0.988, and 0.993, respectively.

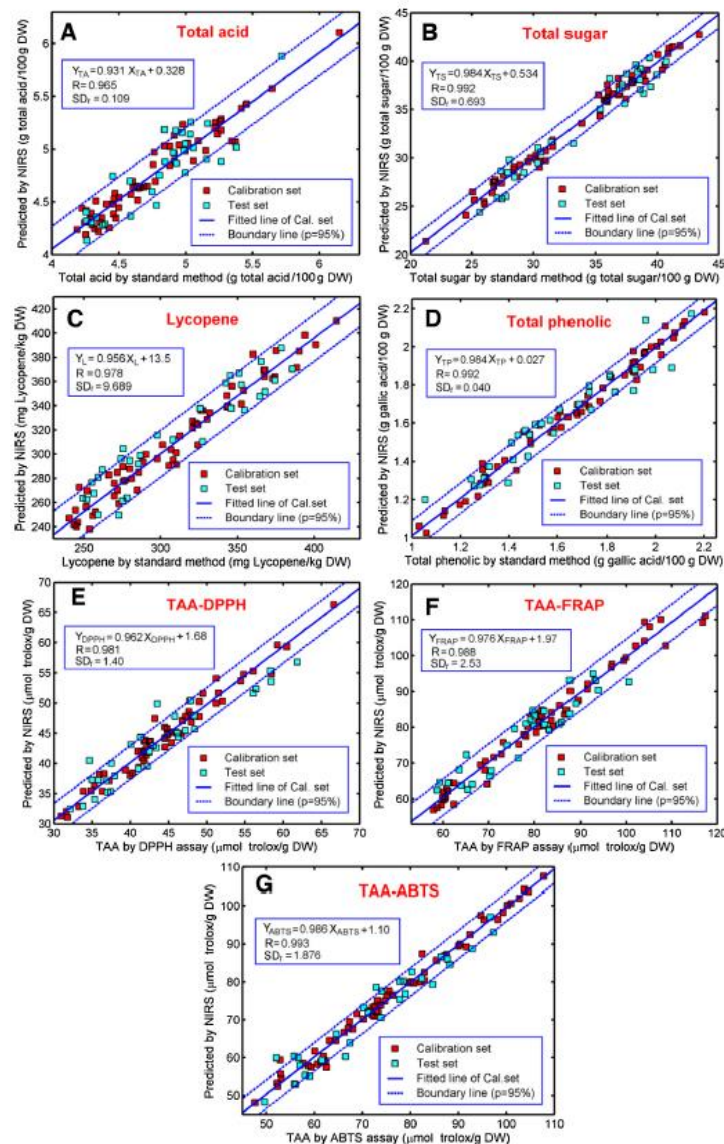


Figure 11 Plots of predicted values of lycopene, total acid, sugar, phenols, and antioxidant activity versus results of standard analyses (RBF-NN model).

In 2016, Audrius. R. and co-workers published a study focused on the determination of quality attributes of tomatoes using near infrared spectroscopy and reference analysis [33]. Dry matter, soluble solids content, fruit skin, and flesh firmness were analyzed by a luggable NIRs (NIR case NCS001A spectrophotometer) in the wavelength range 600-1000 nm. NIR spectroscopic measurements and reference analyses have shown that the determination of tomato fruit and flesh

firmness were similar in performance to determination of dry matter and soluble solids content. High correlation between values predicted by NIR spectroscopy and reference analyses of dry matter, fruit skin, and flesh firmness were observed with R^2 values of 0.9089, 0.9119, and 0.9624, respectively. Regression coefficient between values predicted by NIR spectroscopy and reference analyses of soluble solids content was 0.815.

In 2018, Huang. Y. and co-workers evaluated the assessment of tomato soluble solids content and pH by spatially resolved and conventional Vis/NIR spectroscopy [34]. Spatially resolved spectroscopy (SRS) can help to achieve better interrogation of tissue properties at different depths and it has improved the potential of quality assessment of horticultural products. This research was aimed at the investigation of quality of tomatoes using a portable SRS system, which was compared with the performance of two conventional single-point (SP) spectroscopic instruments. Spectral data were measured in interactance mode with the different spectrometers. The VIS/NIR spectrometer (Vis/SWNIR) has covered the spectral range 400-1100 nm while the NIR spectrometer (NIR) operated in the range 900-1693 nm. The results have shown that SSC and pH prediction was possible with correlation coefficient values in the ranges 0.608-0.791 and 0.688-0.800, respectively. SR predictions of pH ($r_p = 0.819$) were better than with SP Vis/SWNIR ($r_p = 0.743$) and SP Vis/NIR predictions ($r_p = 0.741$). On the other hand, SR predictions of SSC ($r_p = 0.800$) were comparable with the SP Vis/SWNIR prediction ($r_p = 0.810$) but better than SP Vis/SWNIR predictions ($r_p = 0.729$).

In 2018, Tilahun. S. and co-workers reported a study on the prediction of lycopene and beta carotene in tomatoes by a portable chromameter and VIS/NIR spectra [18]. This study has attempted to determine lycopene and beta carotene in intact tomatoes. A total of 244 tomato samples from the same harvest (Kangwon province from south Korea) was used in this study. NIR analyses were obtained with reflectance mode in the wavelength region of 500-1100 nm using portable chromameter and VIS/NIR spectra. Reference analysis has used color variables of lycopene and beta-carotene to determine their content. The results indicated that best calibration equations developed to predict lycopene and beta-carotene content were

based on color values and gave regression coefficient values of 0.97 and 0.85, respectively.

In 2019, Ren. S. and co-workers investigated model development for soluble solids and lycopene contents of cherry tomatoes at different temperatures using near-infrared spectroscopy. External parameter orthogonalization (EPO) was chosen for reducing the effect of temperature change on NIR spectra. The authors have combined the EPO method with chemometrics to predict soluble solids and lycopene content. The work was conducted on 120 samples using a portable spectrometer operating in the wavelength range of 900-1700 nm. The samples were stored at 10, 15, 20, 25, 30, and 35 °C before being used. Regression coefficients for soluble solids content and lycopene for data from mixed temperature measurements without EPO method were 0.8745 and 0.7801, respectively. The use of the EPO method resulted in regression coefficients for soluble solids content and lycopene of 0.8988 and 0.8023, respectively. The results indicated that the EPO method resulted in better prediction than the mixed temperature correction model for data acquired using portable NIR spectrometer. Therefore, the EPO method can be used to reduce the effect of temperature on NIR analysis.

2.4 Theory of Near infrared spectroscopy analysis

2.4.1 Introduction of near infrared spectroscopy

Near infrared spectroscopy is a spectroscopic method that uses the near-infrared region of the electromagnetic spectrum (from 780 nm to 2500 nm). It is based on molecular overtone and combination vibrations in the near infrared region of the electromagnetic spectrum. Overtones and/or combination vibrations of stretching bands are shown in Figure 12. This graph is plotted as $\log(1/R)$ versus wavelength. The absorption spectra in the near infrared region are weaker than in the mid-infrared regions. Moreover, features in the near-infrared spectra are typically very broad and overlap leading to complex spectra. The NIR spectra represent absorptions of C-H, O-H and N-H bonds of organic molecules. These bonds exhibit absorptions in specific regions or at specific wavelengths. For example, 2nd and 1st overtones of OH vibration for moisture have peaks peak around 970 and 1450 nm, respectively. The 1st, 2nd, and 3rd overtones of OH vibrations in organic molecules are around 1445, 1000, 800 nm,

respectively. The 2nd overtone of CH vibration is found around 1190 nm and the 2nd Overtone of N-H vibration is found around 1030 nm respectively [3].

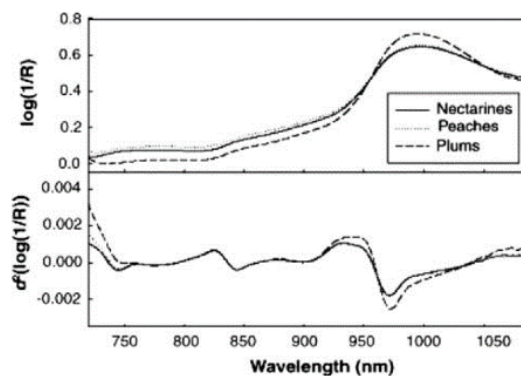


Figure 12 Short NIR (700-1100 nm) spectra of nectarines, peaches and plums.

As mentioned above, NIR spectral data are broad and the weakness of NIR intensity, application of quality evaluation for different fruits needs to be designed according to the fruit size, the thickness of its skin, and the specific attributes to be tested. Dispersive reflectance and transmittance are considered as two main modes of measurement [20]. While the interactance mode is the third, and less utilized mode. The measurement modes of reflectance, transmittance, and interactance are shown in Figure 13

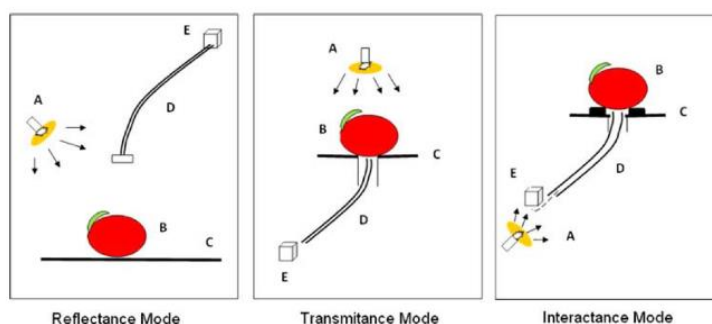


Figure 13 Three illumination detector configurations of near infrared spectroscopy: A. light source; B. sample; C. sample holder; D. optic fiber; E. detector.

The illumination and detector configurations used in these acquisition modes result in different results even for data acquired for the same sample. In the reflectance measurement the NIR beam is reflected by the surface of the sample and then recorded by the detector. This mode of detection is widely used to analyze the internal quality of agricultural produce as it is easy to use without any contact with the sample. In the case of transmittance, where the beam passes through the sample, the beams are sometimes blocked by fruit skin. Marques and co-workers have measured penetration depth of NIR radiation. The results have indicated that NIR radiation penetrates about 7.4 mm into the sample. The interactance mode is a compromise method between reflectance and transmittance. However, the analysis can be difficult and interference from the environment needs to be prevented, which presents a disadvantage for the potential of rapid analysis [20].

2.4.2 Chemometrics

NIR spectra obtained from NIR spectrometers present data from all types of organic molecules in the sample. In addition, the molecular overtone and combination vibration bands lead to complex spectra. Therefore, these spectra contain overlapped information. The lack of efficient data processing methods leads to difficult analysis. For this reason, it is necessary to couple chemometric analysis with NIR data. The general steps of NIR analysis required to develop prediction models are: 1) optimization of the samples' spectral data set, (2) choice of calibration methods to get proper models, and (3) evaluation of the developed prediction models [20].

2.4.2.1 Data preprocessing

As the background of NIR spectra are often complex, several pre-processing methods are applied to optimize the data set after the acquisition of the original data set. These pre-processing methods can help to de-noise and increase spectral resolution of the spectral data and increase accuracy of the chemometric analysis. These procedures are also carried out with the aims of sample set compression, spectral data compression, removal of systematic errors, and data smoothing. For example, smoothing is a data processing method used for de-noising. Derivative, mainly first or second derivative, is employed to increase spectral resolution. Other

methods, like multiplicative scatter correction (MSC), standard normal variate (SNV), orthogonal signal correction (OSC), and net analyte signal also have been developed for the spectral data preprocessing [20].

2.4.2.2 Calibration

Model calibration plays a key role in NIR spectroscopy determination because models directly determine the behavior of the whole system, which is exhibited by both precision of property prediction and the correctness of discrimination. For quantitative analysis, multiple linear regression (MLR), step multiple linear regression (SMLR), principle component regression (PCR), partial least square regression (PLSR), artificial neural network (ANN), and support vector machine regression (SVM) are the most developed methods in fruit quality evaluation [20].

2.5 NIR spectrometers: affordability and portability

Near infrared spectroscopy has received a remarkable measure of interest as a non-destructive analytical technique and it became the working tool in several fields of typical applications including agriculture-food, pharmaceuticals, natural medicines, soils etc. [2]. The main advantages for practical use are: 1) Applicability to a wide variety of samples and 2) rapid and non-destructive analysis. Portable spectroscopy is a tool that is capable of on-site analysis. Nevertheless, several issues connected with the peculiarity of portable spectrometers have become apparent. In contrast to the matured design of a FT-NIR benchtop spectrometer for example the distinctiveness of the NIR spectrometer design (light sources, detectors, optical materials etc.) affects the size and cost [35]. This results in the performance profiles of portable spectrometers that differ from benchtop spectrometers. The most apparent differences are the narrower spectral regions and/or lower spectral resolution with which the compact devices operate. For these reasons, portable spectrometer research focus is directed into thorough systematic evaluation of the applicability limits and analytical performance of such devices and the potential for future advances.

In 2018, Hui. Y. and co-workers published a study focused on quantitative analysis of pharmaceutical formulations and performance comparison of different

handheld near infrared spectrometers [36]. They examined four handheld instruments based on different monochromator principles such as NeoSpectra, NIRONE (Spectral Engines NR-2.0 W), DLP NIRscan, and MicroNIR (Figure 14, Table 3). Consequently, a solid pharmaceutical formulation consisting of two excipients (cellulose and starch) and three APIs (acetylsalicylic acid (ASA), ascorbic acid (ASC) and caffeine (CAF)) have been measured and analyzed with PLS models. The study indicated that the prediction performance of the four instruments performed comparably well with correlations between 0.94 to 0.99. The key ingredient can be predicted with good performance. The results indicated that the LVF spectrometer (MicroNIR) has the most balanced performance. The lowest overall performance with lower prediction capabilities for either ASA or ASC - was shown by the other three interferometer-based instruments (NeoSpectra, NIRONE, and DLP NIRscan).

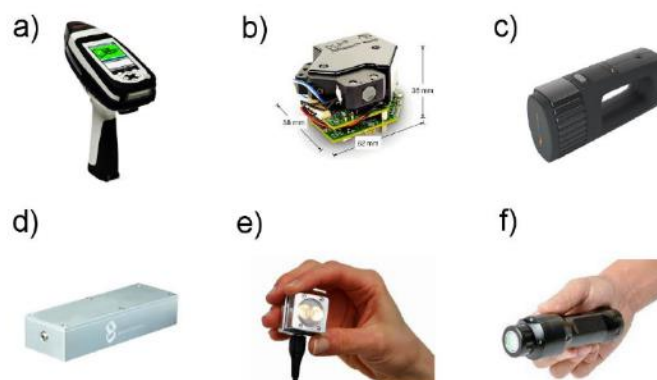


Figure 14 selected popular miniaturized NIR spectrometers a) *MicroPHAZIR*, b) *DLP NIR scan* (Texas instruments), c) *Neospectra*, d) *nano FTIR NIR*, e) *NIRone*, f) *MicroNIR*.

Table 3 Summary of the technical parameters of popular NIR spectrometers

Spectrometer	Key components			Wavelength regions		Spectral resolution (nm)	S/N	Cost (USD)
	Source	Wavelength selector	Detector	(nm)	(cm^{-1})			
MicroNIR Pro	Tungsten halogen	LVF	InGaAs	908 - 1676	11013 - 5967	12.5 (at 1000)	23,000:1	-
ES 1700						25 (at 2000)		
SCiO (Consumer Physics)	LED	Bandpass filter	SI photodiode	740 - 1070	13514 - 9346	N/A	N/A	300
NIRscan (Texas Instruments)	Tungsten halogen	stationary dispersive grating and MEMS DMD	InGaAs	HP: 1350 - 2490 MS: 900-1700	HP: 7407 - 4016 MS: 11,111 - 5882	HP: 12 MS: 10	HP: 30,000:1 MS: 6000:1	999

Spectrometer	Key components		Wavelength regions		Spectral resolution (nm)	S/N	Cost (USD)
	Source	Wavelength selector	Detector (nm)	(cm ⁻¹)			
NIRONE	Tungsten	MEMS	S1.4: 1100 - 1350	9090 - 7407	12 - 16	15,000:1	6490
Sensors	halogen	Fabry–	InGaAs 1350 - 1650	7407 - 6060	13 - 17	–	
(Spectral	(duplicated	Pérot	S1.7 – 1550 - 1950	6451 - 5128	15 - 21	1500:1	
Engines))	interferometer	S2.5: 1750 - 2150	5714 - 4651	16 - 22	[b]	
			InGaAs			(S1.4 – S2.5)	
NeoSpectra-Scanner	Tungsten halogen	MEMS Michelson interferometer	InGaAs 1350 - 2500	7407 - 4000	16 (at 1550)	N/A	5950
nanoFTIR	Tungsten	MEMS	InGaAs 800 - 2600	12,500 - 3846	2.5 (at 1000)	9000:1	22500
NIR (SouthNest Technology)	halogen	Michelson interferometer			6 (at 1600) 13 at 2400)		

In 2019, Bertotto, J and co-workers conducted an evaluation of a handheld near-infrared spectrophotometer for quantitative determination of two active pharmaceutical ingredient (APIs) in a solid pharmaceutical preparation [37]. They examined paracetamol (PCT) and tramadol (TRA) using HPLC compared with benchtop (FOSS) and handheld spectrometer (MicroNIR). The results indicated that the handheld spectrophotometer produces results comparable to those from the benchtop instrument, with high correlation of both calibration and prediction model (R^2 0.98-0.99)

In 2017, Guillemain, A. and co-workers reported performance of NIR handheld spectrometers for the detection of counterfeit tablets [38]. The authors compared two handheld NIR spectrometers (MicroNIR and SCiO) for the task of tablet authentication. The compared instruments differ in operational characteristics as shown in Table X. The results indicated that despite being extremely affordable the SCiO instrument performed better for this application. The results have shown that the SCiO spectrometer had a prediction accuracy higher ($r^2 = 0.96$) than MicroNIR ($r^2 = 0.92$)

In 2019, Wiedemair, V. and co-workers published investigations into the use of handheld near-infrared spectrometers and novel semi-automated data analysis for the determination of protein content in different cultivars of *Panicum miliaceum L* [39]. They compared performance of three different portable NIR spectrometers (microPHAZIR, MicroNIR, and SCiO) and a benchtop spectrometer. The results showed that the benchtop spectrometer was capable of accurately analyzing protein content of millet grains ($R^2 = 0.92-0.94$). The best results achieved for the portable NIR spectrometers were achieved when measuring non-milled samples with SCiO ($R^2 = 0.814-0.867$). While all the evaluated spectrometers performed satisfactorily in this application, protein analysis in grains proved to be more challenging for miniaturized spectrometers, particularly for non-milled samples. The suggested reasons for poorer accuracy may include higher susceptibility to detrimental effects of scattering at the sample surface.

The literature reports mentioned above represent a comparison of potential of portable NIR and benchtop spectrometers as tools for non-destructive analysis. These

reports also support the idea that a more widespread use of this tool is hampered by the cost and at times bulkiness of the bench top instruments.

2.5.1 Commercial spectrometer details

2.5.1.1 SCIO

The SCIO spectrometer is a miniature spectrometer (Figure 15) weighting 35g. The operating wavelength in the range 740 to 1,070 nm. The battery operated instrument is connected to a consumer application with several predefined prediction models costs 300 USD. The instrument together with a license needed for the collection and chemometric analysis of data costs 1,000 USD. This is the license available to us for the purpose of this work.



Figure 15 A picture of the SCIO spectrometer. Demonstrating of its dimensions.

This license gives access to an additional application on a smart phone for data collection as well as accessing the website data storage and analysis environment. Firstly, the website data storage allows the definition of the sample attributes such (e.g., sample number, location number, variant) and reference measurements (e.g., TSS, TA, and pH) as shown in Figure 16.

Sample Attributes + Add Attribute

What characteristics help you identify sample and separate it from other samples? Is it its type, brand, batch ID or lot percentage? Each one of these is an attribute. Each attribute may impact the fingerprint, and help in creating a good model.

Sample Number	Number - Unlimited - unlabelled
Location Number	Number - Unlimited - unlabelled
Variant	String
Temperature	Number - Temperature - Celsius
Humidity	Number - Concentration - %
TSS	Number - Concentration - %
TA	Number - Concentration - %
pH	Number - Unlimited - unlabelled

Scan Attributes

The automatic attributes SCiO adds to each scan upon scanning.

Sampled At	Date
Device S/N	String
Sample Name	Numeric

Figure 16 The definition of the sample attributes and reference measurements for data collection of the web-based SCiO spectrometer.

A data collection access is created using the web-based interface. This can then be accessed via the smart phone-based app (Figure 17A). This allows adding new samples to the data collection (Figure 17B) and performing the spectroscopic measurement (Figure 17C). Finally, the app also allows the review of the data (Figure 17D).

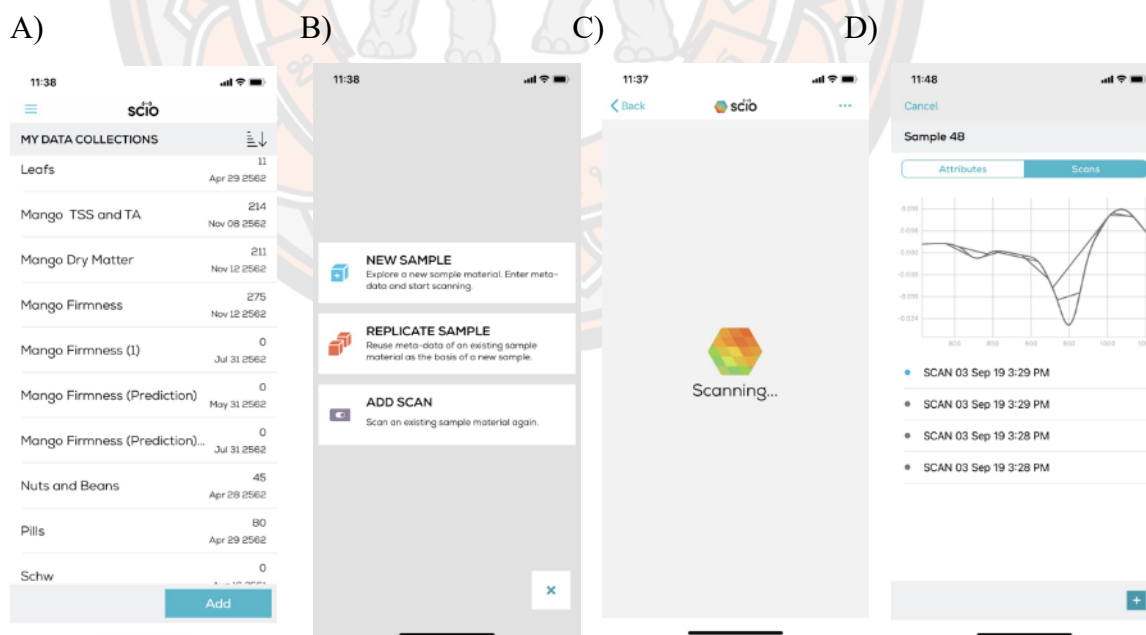
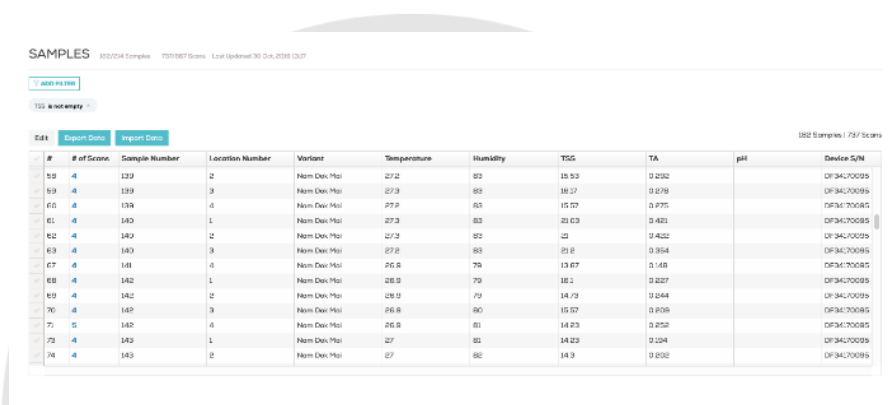


Figure 17 Screen shots of the smart phone-based app for the SCiO spectrometer showing the data collection (A), possibility to add samples to a collection (B), scanning process (C), and data review (D)

When the data acquisition in the phone-based app is finished, it records the attributes of the samples (Figure 19) as well as the spectra (Figure 20) and makes the information available on the web-based interface. The sample attribute and the spectral data demonstration allow for the filtering of samples based on the attribute values (Figure 19). Moreover, the spectral data representation also allows pre-processing processes of spectral data such as spectral derivatives, data smoothing, and standard normal variate (SNV).



The screenshot shows a web-based interface for a 'SAMPLES' database. At the top, it displays '332/214 Samples' and '720/1867 Scans'. Below this are buttons for 'ADD FILTER' and 'TSS is not empty'. A table with 11 columns is shown, containing 14 rows of sample data. The columns are: #, # of Scans, Sample Number, Location Number, Variant, Temperature, Humidity, TSS, TA, pH, and Device SN. The data rows are numbered 69 to 74.

#	# of Scans	Sample Number	Location Number	Variant	Temperature	Humidity	TSS	TA	pH	Device SN
69	4	139	2	Norm Dec-Mal	27.2	83	15.93	0.252		DF34270029
69	4	139	3	Norm Dec-Mal	27.3	85	16.17	0.279		DF34270039
69	4	139	4	Norm Dec-Mal	27.2	83	15.77	0.275		DF34270049
69	4	140	1	Norm Dec-Mal	27.3	83	22.03	0.421		DF34270059
69	4	140	2	Norm Dec-Mal	27.3	82	22	0.422		DF34270069
69	4	140	3	Norm Dec-Mal	27.2	83	21.9	0.364		DF34270079
69	4	141	4	Norm Dec-Mal	26.8	79	13.67	0.148		DF34270085
69	4	142	1	Norm Dec-Mal	26.9	79	16.1	0.227		DF34270095
69	4	142	2	Norm Dec-Mal	26.9	79	14.72	0.244		DF34270105
69	4	142	3	Norm Dec-Mal	26.8	80	15.07	0.206		DF34270115
71	5	143	4	Norm Dec-Mal	26.8	81	14.23	0.252		DF34270125
73	4	143	1	Norm Dec-Mal	27	81	14.23	0.224		DF34270135
74	4	143	2	Norm Dec-Mal	27	82	14.3	0.202		DF34270145

Figure 18 Database of sample attributes shown in the web-based interface for the SciO spectrometer

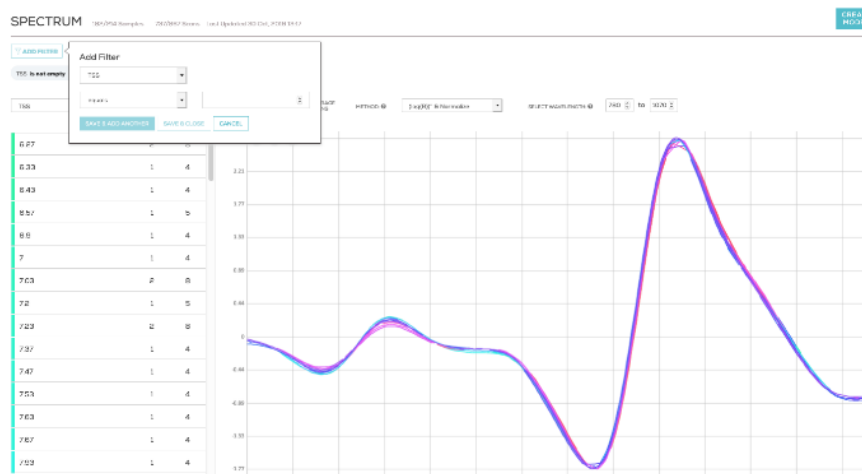


Figure 19 The spectral data was recorded in the web-based interface for the SciO spectrometer

Finally, the spectral data can be utilized via the chemometric development functions using the model creation settings (Figure 20). The model development page allows setting parameters such as data preprocessing, algorithm, number of latent variables (LV), or number of folds. This information is used for model calibration and cross validation (Figure 20). After the model development is performed the results are displayed as a plot between predicted and reference values, summarization of key figures of merit, and other important information (Figure 21).

MODEL CREATION SETTINGS

MODEL NAME: TSS (BR)

TARGETED ATTRIBUTE: TSS

Preprocessing

Lag → Average Score → 2nd Derivative (window: 35, polynomial degree: 2) → Select WL (780nm - 1070nm) → SNV

MINIMAL SCANS PER SAMPLE: 5 Apply when Average Score

Cross Validation

BATCH BY: Sample

NUMBER OF FOLDS: 10

Algorithm

SELECT ALGORITHM: PLSR LIMIT LV: eg. 1,2,4-5

OUTLIER DETECTION: ON OFF

Filters

TSS does not equal is empty

Figure 20 Chemometric model development page in the web-based interface for the SCiO spectrometer



Figure 21 Model summary view in the web-based interface of the SCiO spectrometer

2.5.1.2 Linksquare

The Linksquare is a miniature spectrometer (Figure 22). It operates in the wavelength range from 400 to 1000 nm. The instrument covers visible and near infrared regions of the spectrum. The weight is 57g. It cost 500 USD, which gives access to both a computer-based acquisition application and a smart phone mobile app. The computer-based application allows export and collection of raw spectral data. Thus, standard measurement using spectralon for white and dark reference can be carried out. The instrument can be operated in VIS or NIR acquisition modes (Figure 23). These modes use the same sensor but differ in the light source.



Figure 22 A photograph of the Linksquare spectrometer

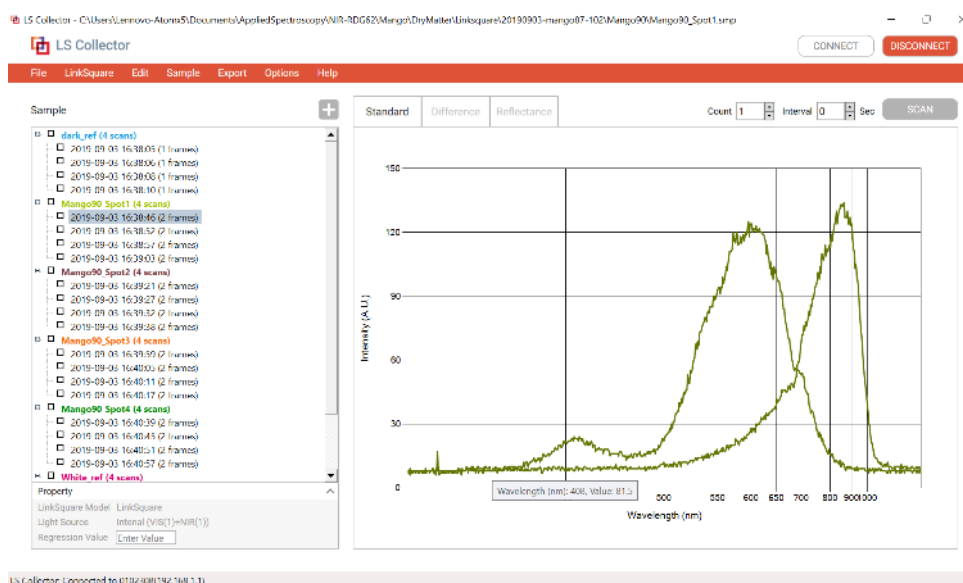


Figure 23 A screen short of the computer-based application for differ spectral modes using Linksquare spectrometer.

2.5.1.3 Texas Instruments (TI) – DLP NIRscan Nano

The NIRscan Nano is a miniature spectrometer (Figure 24). The operating wavelength range is from 900 to 1700 nm. It costs 1,000 USD, which gives access to the computer-based application (Figure 25). The evaluation model is connected via the USB port of a computer. The instrument offers raw spectroscopic data and it makes conversion to reflectance and absorbance using the stored reference values.



Figure 24 A photograph of the DLP NIRscan Nano spectrometer

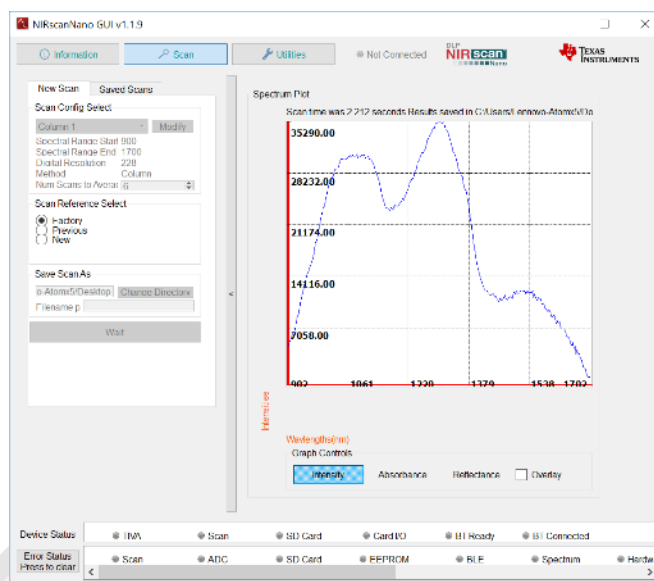


Figure 25 A screen shot of the computer-based application for DLP NIRscan Nano spectrometer

2.5.1.4 Neospectra

The Neospectra is a miniaturized NIR instrument (Figure 26) operating in the wavelength range from 1,300 to 2,500 nm. The evaluation model utilized gives access to a computer-based application and costs 2,400 USD (Figure 27). It is operated via a cable connection to the USB port. Therefore, the standard measurement can use spectralon for white and dark reference.

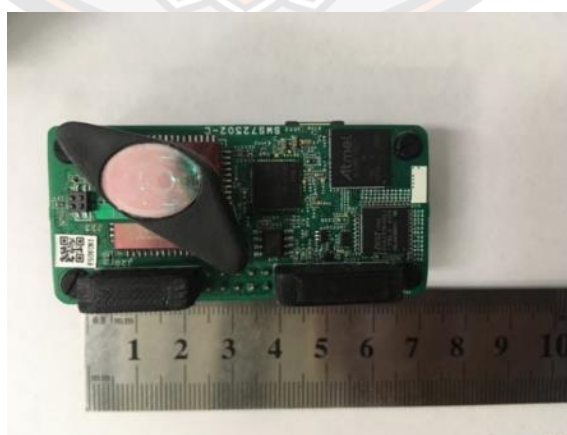


Figure 26 A photograph of the Neospectra instrument

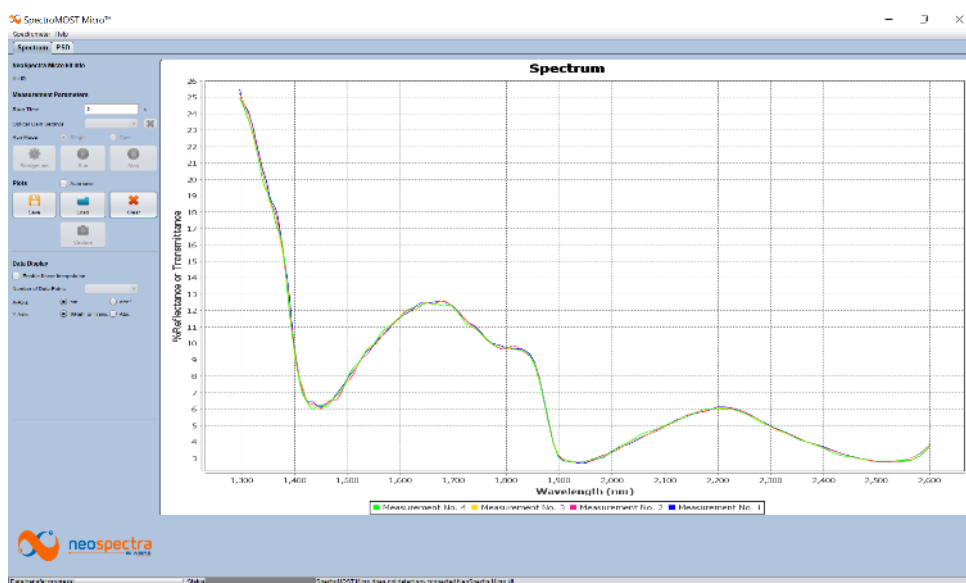


Figure 27 A screen shot of the computer based application for Neospectra spectrometer

2.5.2 The design of NIR spectrometers

2.5.2.1 Light source

Two different types of NIR light source are used in commercially available spectrometers. The first one, is tungsten halogen light source. It is a general light source for visible and NIR range spectroscopic applications. The tungsten halogen light source provides very smooth and stable spectral data, so it is widely used and applied in spectrometric measurements (transmittance/reflectance/absorption) and color measurements. The spectrum of tungsten halogen light source provides illumination from 300 nm to 2600 nm. [40] The tungsten halogen light source is well-known and is used in benchtop instruments. It is a thermal radiation source. This means that light is generated by heating a solid body (the filament) to a very high temperature. Thus, the higher the operating temperature the brighter the emitted. In addition to intensity, the spectral emission profile also depends on temperature of both the filament and the inner wall of the lamp. To stimulate the emission with maximum peak in NIR region, relatively higher temperatures than in case of IR radiation are therefore needed. A thermal emission source is reliable, inexpensive, and gives a stable output. However, for development in miniaturized devices it may need to be

repaired. The thermal stability may become an issue for miniaturized spectrometers. Also, miniaturization of devices reduces the device's thermal capacity, leading to temperature buildup over operation time. Near infrared spectrometers using a tungsten halogen light source including benchtop instruments (nanoFTIR NIR), MicroNIR, NIRscan (Texas Instruments), NIRONE Sensors, and NeoSpectra-Scanner [35] are shown in table 1

The second type of light source are light emitting diodes (LEDs). In principle, current flow recombination of electrons and holes releases excess energy. This excess energy is emitted as photons [40]. LEDs are efficient enough to be powered by low-voltage batteries or inexpensive power supplies. The LED spectral output makes it possible to select an individual diode light source to provide illumination in the desired spectral range

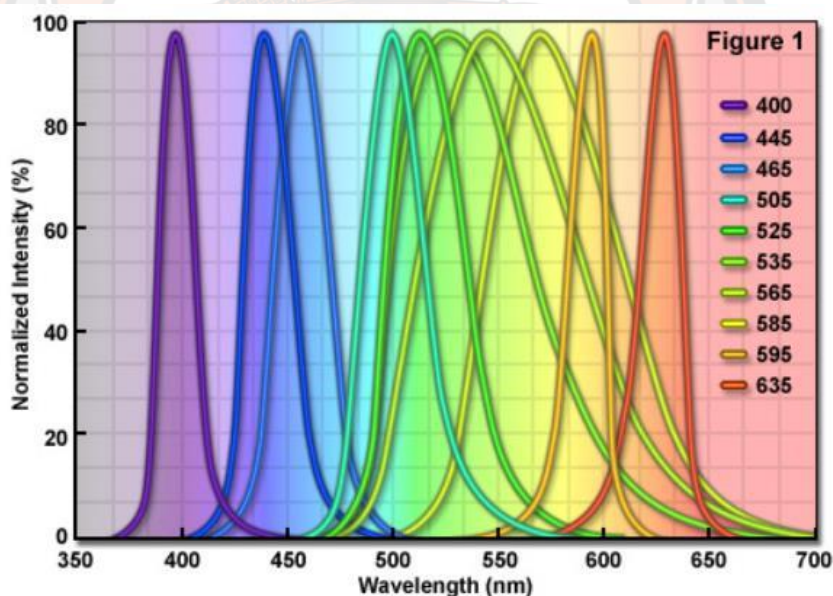


Figure 28 Spectral profile of LEDs for fluorescence spectroscopy at different wavelength range

Furthermore, LEDs have several advantages for application in highly miniaturized spectrometers. LEDs feature very low dimensions, low power consumption, low voltage, robustness, and low cost required for working in onsite

analysis. However, there are significant limitations of LED light sources. The primary one is the narrow emission bandwidth, e.g. gallium arsenide (GaAs) LED has peak emission at 870 nm and only 50 nm of bandwidth. Furthermore, the availability of LEDs emitting in the NIR region remains very limited. Sources covering the Vis/SW-NIR region are, however, available and commercially used in miniaturized spectrometers such as SCIO as shown in Table 3

Santo. N. and co-workers published a report on the determination of mango maturity indices using portable near infrared (VIS-NIR) spectrometer. This study has developed calibration models for soluble solids content (SSC) and dry matter (DM). The light source was a halogen lamp. The models were developed using partial least square regression (PLSR) with full cross validation. The best result of SSC calibration was pre-processed with standard normal variate (SNV), first derivative of Savitzky–Golay in the spectral window of 699–999 nm. The R^2 and RMSE values were 0.87 and 1.39%, respectively. Unprocessed spectral data in the range 699-981 nm was used for the DM model calibration. The R^2 and RMSE values for the model were 0.84 and 8.81 g/kg, respectively. In contrast, poor calibration models were obtained for firmness. [4]

Sun. X. and co-workers have evaluated the robustness of temperature change of NIRs for intact mango. The NIR spectral data were obtained using a handheld NIR spectrometer (F750 handheld NIR spectrometer) in the range from 729 to 975 nm. The light source was a 32W halogen lamp. The best results were achieved using the EPO method for predicting dry matter content. It has shown the highest R^2 and lowest RMSEP (0.82, 1.05%) compared with the control result (0.68, 1.43% respectively). [5]

Fauzana. N. and co-workers have evaluated assessing firmness in mango with several broadband miniature spectrophotometers. This study has compared a laboratory-based instrument and a miniature spectrophotometer (SCIO) in predictions of mango fruit firmness. These systems used LED as light sources coupled with SI photodiode array as a detector. The NIR spectra data were obtained by the SCIO pocket molecular scanner from 740 to 1070 nm. The SCIO showed good performance for predicting mango firmness (R^2 0.74-0.93; RMSE 4.8-8.2 $\text{Hz}^2\text{g}^{2/3}$). The pocket-

sized SCIO NIR sensor was shown to be capable of supporting the optimization of the ripening quality parameters of mango fruit with high accuracy. [11]

As can be seen from the publications mentioned above, most have used tungsten halogen lamp as light source for non-destructive determination of quality parameters. TH light sources have been shown capable of supporting the collection of data for the prediction of SSC, DM, and firmness with good calibration models. On the other hand, LED lamps have been studied to a smaller degree when compared with TH light sources.

In 2017, Choing. W. and co-workers have evaluated white light emitting diode as a potential replacement of tungsten-halogen lamp for a visible spectroscopy system [6]. The authors studied the non-destructive technique based on VIS spectroscopy using LED as lightning for predicting the acidity and soluble solids content of intact Sala Mango. The visible spectral data of mango samples were collected between 400 and 700 nm in reflectance mode using the Jaz spectrometer (Ocean Optics Inc., Florida, U.S.A.). All of the measurements were performed by placing a fiber optic detector with a 600 μm core diameter perpendicularly to the sample surface illuminated with two LED panels positioned at 45° , with respect to the detector, as shown in Figure 29.

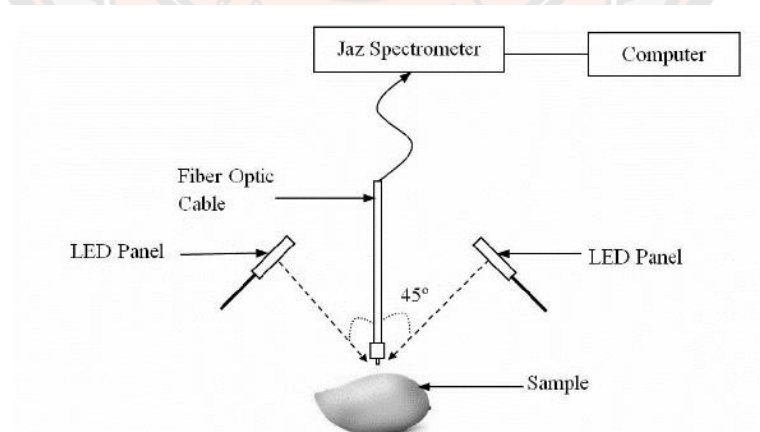


Figure 29 Experimental set up illustration of spectroscopy measurement.

The white LEDs were used in this experiment had different operating conditions (3500K LED, 4500K LED, and 5700K LED) in comparison with a tungsten-halogen lamp. Regression models were measured using multiple linear regression (MLR). The coefficient of determination (r^2) for acidity and SSC obtained with LED lighting operating at various conditions and tungsten-halogen lamp were between 0.8995-0.9227 and 0.6361-0.7276, respectively. The results have shown that determination of mango acidity was successfully performed with VIS spectroscopy, powered by white LED illumination, using MLR with high accuracy. However, worse performance was obtained for models for soluble solid content.

2.5.2.2 Wavelength selection techniques

The most essential element for spectrometer is the wavelength selector, which can be based on various technologies. The first one, is Fourier transform infrared (FT-IR) method of selecting wavelengths is used in benchtop spectrometers. This method is widely used in mid-infrared (MIR) range for determination of chemicals. The second technique is dispersive spectroscopy used in miniaturized spectrometers. The dispersion is based on the dispersion of light into its component wavelengths. The dispersion of light is achieved using a prism or monochromator gratings. Dispersive spectroscopy is the choice in the UV, Vis, and NIR applications.

Principle of Dispersive spectrometers and FT Technique

Dispersive Spectrometers

Polychromatic light is emitted from a light source and diffracted on a grating. The diffraction is dependent on the width of the entrance slit, grooves of the monochromator grating, and incident angle. For the diffracted beam, the wavelengths composing the original light beam are spatially separated. Monochromatic light irradiates the sample through an exit slit. To enable scanning of different wavelengths they sequentially pass through the exit slit to record the intensity spectrum.

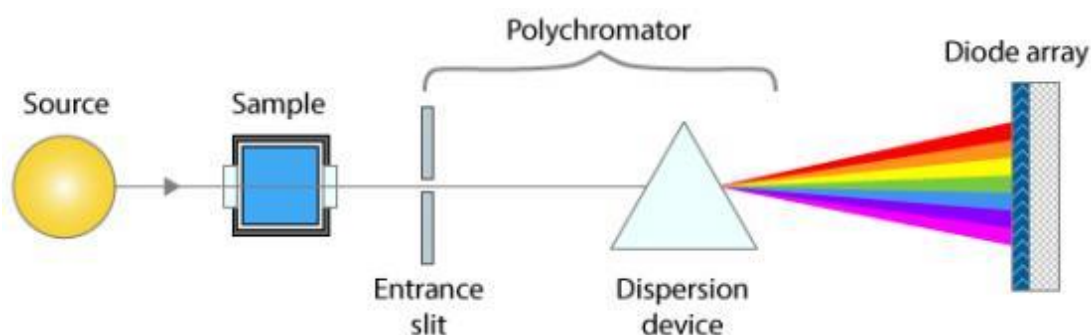


Figure 30 Illustration of the dispersive spectrometer in diffuse reflectance mode.

Alternatively, polychromatic light is used to illuminate the sample and the wavelength separation is achieved with a dispersive element placed between the sample and the detector (Figure 30). This type of arrangement is more common for low-cost spectral detectors and spectrometers.

FT Technique

FT spectrometers contain an interferometer, which is composed of a beam splitter and two mirrors, where one is fixed and another one is moveable. Polychromatic light from a light source is divided into two beams, one beam reaches the fixed mirror while the other beam is reflected from the moving one. Then, the beamlets are combined again at beam splitter. The resulting light intensity depends on phase difference between the two beams. The detected intensity of the polychromatic light is called an interferogram. The interferogram is then transformed by the Fourier transformation to provide the spectrum.

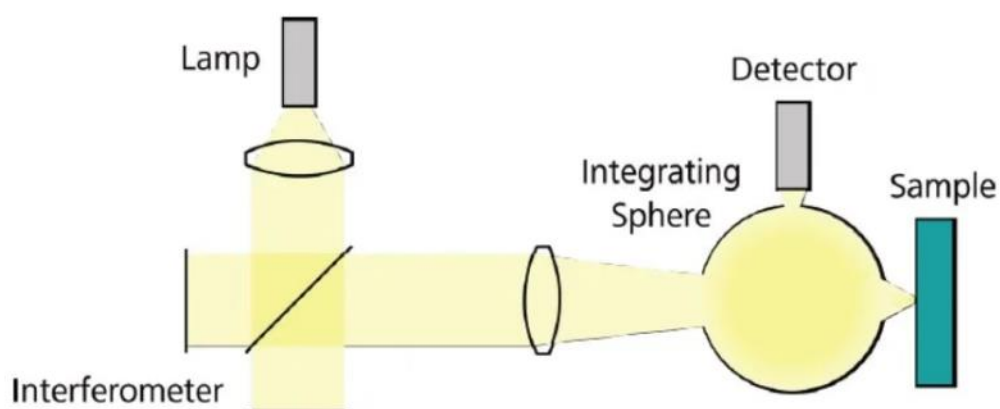


Figure 31 Illustration of the FT spectrometer in diffuse reflectance mode.

FT-NIR system is limited due to optics. It commonly ranges from the MIR range to the visible (800-2500 nm). In contrast, dispersive spectrometers can measure the data down to 400 nm and even below, including visible spectral range. This allows applications in terms of quality parameters from agricultural products. FT-NIR systems provide better spectral resolution than dispersive spectrometers because FT-NIR system has interferometers, which make it possible to adjust the moveable mirror to permit better resolution. However, this results in an expensive spectrometer. In NIR analysis, the spectral features that are analyzed in the NIR range are molecular overtones and combination vibration bands of substances. This results in very broad and overlapped spectra. Therefore, very high spectral resolution is not needed for reliable results.

Attribute	FT-NIR	Predispersive
Source	High intensity	High intensity
Wavelength selection	Interferometer	Grating before sample
Detector	Semiconductor	Semiconductor
Scan time	< 1 s	< 1 s
Resolution	1-64 cm ⁻¹	~ 8 nm (12 cm ⁻¹ @ 2500 nm)
Resistance to vibration	Medium	Good
Accessories	Powder, solid, liquid	Powder, solid, liquid
Wavelength precision	~ 0.01 nm	~ 0.005 nm
Wavelength accuracy	~ 0.05-0.2 nm	~ 0.05 nm

Figure 32 Comparison of the specification of FT-NIR and dispersive spectrometers.

Dispersive spectrometers are broadly grouped into monochromator and polychromator types. Monochromators use a grating as the wavelength dispersive selector for separating the incident light into a monochromatic spectrum. Polychromators have similar principle of monochromators but are designed to allow simultaneous detection of multiple wavelengths. Miniaturized spectroscopy falls under the polychromator type.

F-751-Mango Mango Quality Meter

F-751-Mango Quality Meter is a commercial portable spectrometer for non-destructive determination of mango quality. This enables growers to accurately predict their crop harvest dates, reducing guesswork and minimizing spoilage, while increasing harvest predictability. The prediction models were built with Tommy K, Ataulfo, and other variants not common in Thailand.

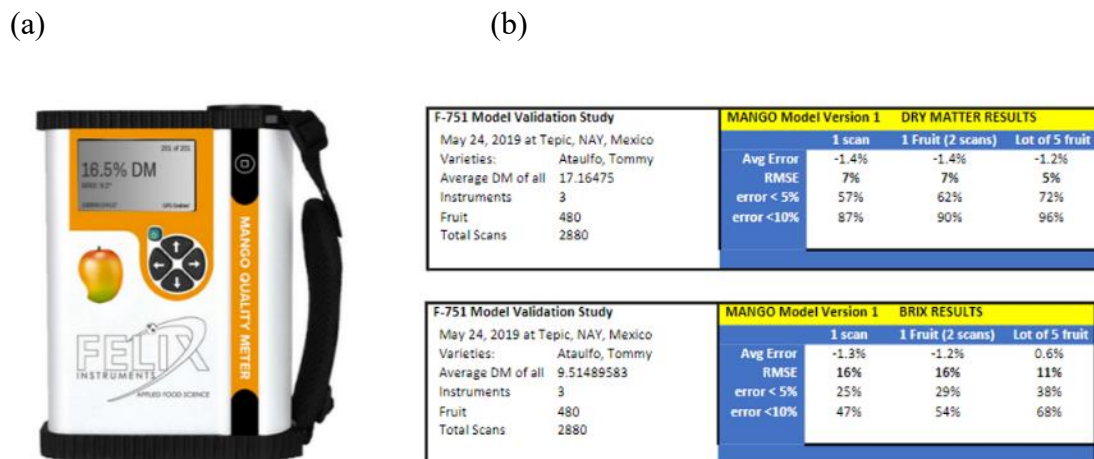


Figure 33 (a) Image of the F-751-Mango Mango Quality Meter (b) model validation study

Figure 33 shows the validation study of F-751-Mango Mango Quality Meter for predicting ripeness indicators. The validation study was conducted with 480 samples and 2880 total scans. The results indicated that percentage of Root Mean Square Error (%RMSE) of Lot of 5 fruits for predicting dry matter and %brix, were 5 and 11%, respectively.

The results show the feasibility of using F-751-Mango Mango Quality Meter to determine quality parameters in the ‘Tommy K, Ataulfo’ mangoes

Table 4 Specifications of F-751-Mango Mango Quality Meter

Spectrometer:	Hamamatsu C11708MA
Range:	640-1050 nm
Spectral Sample Size:	2.3 nm
Spectral Resolution:	20 nm (FWHM) maximum
Light Source:	Halogen Tungsten Lamp with gold reflector
Lens:	Fused silica coated to enhance NIR
Shutter:	White painted reference standard
Display:	Sunlight visible transfective LCD screen with backlight
PC Interface:	Wi-Fi
Data Recorded:	Raw data, reflectance, absorbance, first derivative second derivative, GPS coordinates, Date, Time
Measurement:	Dry matter & Brix
Power Source:	Removable 3400 milliamp hour lithium-ion batteries
Battery Life:	500+ measurements
Body:	Heavy-duty powder coated aluminum body
Dimensions:	7.1" x 4.75"W, 1.75" thick
Weight:	1.05 kg

As mentioned above, F-751-Mango Mango Quality Meter is a commercial portable spectrometer for predicting mango quality parameters. This spectrometer has shown strong performance in a validation study with very high accuracy for the prediction of dry matter and %brix. The key component in this spectrometer is the Hamamatsu C11708MA sensor.

The C11708MA, is an ultra-compact mini-spectrometer integrating MEMS and image sensor technologies. It's based on an advanced MOEMS (micro-opto-electro-mechanical-systems) technology, which combines optical technology including opto-semiconductor devices and optical systems and MEMS technology. A thumb sized ultra-compact spectrometer heads. ultra-compact spectrometer heads can

be divided into three series 1) MS (C11708MA), 2) Micro (C12666MA and C12880MA), and 3) SMD (C1438MA-01) series are showed in Figure 34

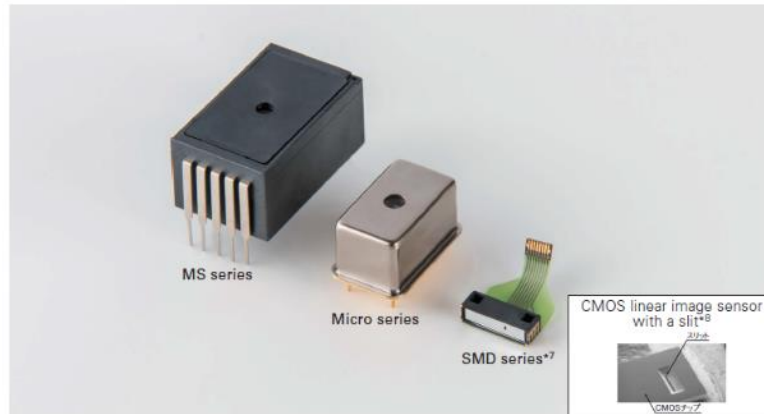


Figure 34 photo image of MS (C11708MA), 2) Micro (C12666MA and C12880MA), and 3) SMD (C1438MA-01) series

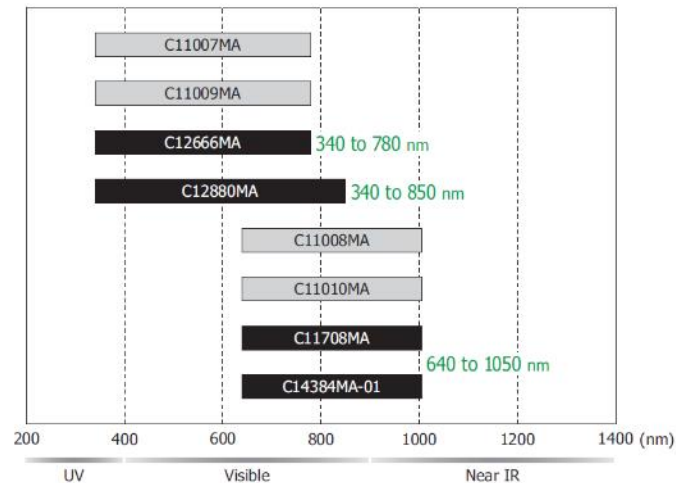


Figure 35 spectral response of Micro, MS, and SMD series

For the work in this project, the C14383MA-01 sensor, which is a new generation relative to the C11708MA, has been chosen. The C14383MA-01 detector has spectral response in wavelength of 640 to 1050 nm. Its suitable for using with sugar content, moisture, fat, taste evaluation, and composition analysis etc. The

C14383MA-01 as a SMD series is highest spectral resolution when compared with Micro and MS series. The product has been downsized through Hamamatsu unique optical design, which helps to further reduce the size of devices.

A circuit board designed to simply evaluate the characteristics of the SMD series (C14989+C15036). The C14383MA-01 is connected to a PC with USB cable. Evaluation software is included.

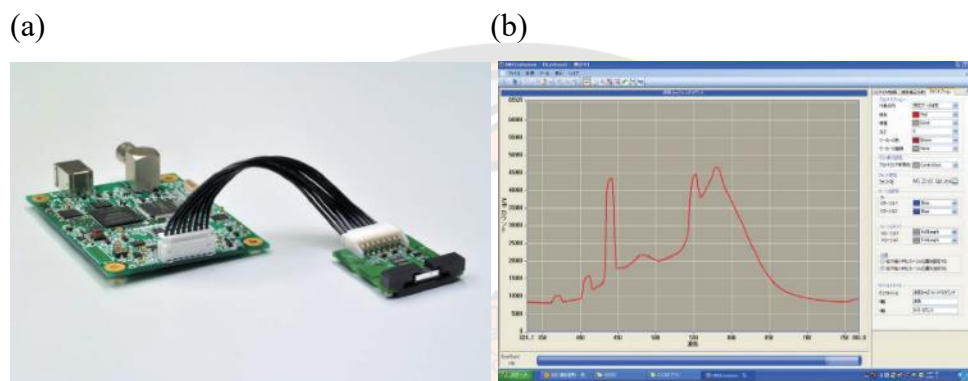


Figure 36 (a) evaluation kit for SMD series (C14989+C15036) (b) evaluation software display example

5.5.2.3 Detectors

Two different classes of detectors are generally used in miniaturized spectrometers. The first one are photovoltaic silicon (Si) diodes. They have suitable sensitivity for wavelengths in the range 700-1100 nm and are suitable for compact and inexpensive devices operating in Visible and Visible to short wavelength NIR regions. Photovoltaic silicon diodes feature lower S/N. Photodiodes are widely used in portable spectrometers and require using wavelength cut-off filters to eliminate the risk of the detector responding to sunlight when measuring mid and long wavelength NIR regions (1050-2500 nm). The second type of detectors are indium gallium arsenide (InGaAs) photodetectors. They are typically suitable for the wavelength range of 900-1700 nm. Comparison of the Si diodes and InGaAs detectors shows that the InGaAs have a more rapid response time, better quantum efficiency, and lower dark current at a given sensor area enabling short scanning times with good S/N. On the other hand the InGaAS detectors are more expensive than Si diodes. Moreover,

InGaAs suitable to detect wavelengths longer than 1700 nm but requires cooling when used for longer time.



CHAPTER III

RESEARCH METHODOLOGY

3.1 Instrumentals and chemicals in research methodology.

3.1.1 Instrumentals

1. The SCIO sensor (Consumer Physics Inc., Tel-Aviv, Israel)
2. The Linksquire sensor (TellSpec Inc., Toronto, ON, Canada)
3. The DLP NIRscan Nano (Texas Instruments)
4. The Neospectra sensor (Neospectra-Module, Si-Ware Systems, Cairo, Egypt)
5. Unscrambler software (Unscrambler 10, Camo, Norway)
6. Penetrometers (Turoli FT011, Froli, Italy)
7. Penetrometers (Turoli FT327, Froli, Italy)
8. Universal testing machine (Instron Model 5965, Norwood USA)
9. Oven (Mettler, Schwabach, Germany)
10. Refractometer (HI 96800, Hanna Instruments, Woonsocket, USA)
11. Automatic burette (Titrator, BrandTech®, Essex, USA).
12. pH meter (HI 98100, Hanna Instruments, Woonsocket, USA).

3.1.2 Chemicals

1. NaOH
2. phenolphthalein
3. Distilled water
4. White reference
5. Dark reference (covering of the Spectralon®, supplier, Country)
6. cheese cloth
7. hand juicer

3.2 Research plan and Methodology

Four main aims of this project are followers.

1. Development of in-house optical spectrometer
2. Testing the performance of in-house optical spectrometer for quantitative measurements to predict key quality parameters from mango.
3. Testing performance of in-house optical spectrometer for quantitative measurements to predict key quality parameters from tomato.
4. Comparison of the quantitative performance of chemometric analysis for prediction of various quality parameters.

3.2.1 Testing performance of commercial portable spectrometers for quantitative measurements to predict key quality parameters from mango and tomato.

As literature report mentioned above, popular portable NIR spectrometers are classified in four spectrometers such as 1) SCIO, 740 to 1,070 nm. 2) Linksquare, 400-1000 nm 3) Texas Instruments (TI), 900-1,700 nm. 4) Neospectra, 1,300-2,500 nm. Therefore, in the first part of this work, we are interested in testing performance of commercial portable spectrometer for predicting key quality parameters from mango and tomato using these commercial spectrometers.

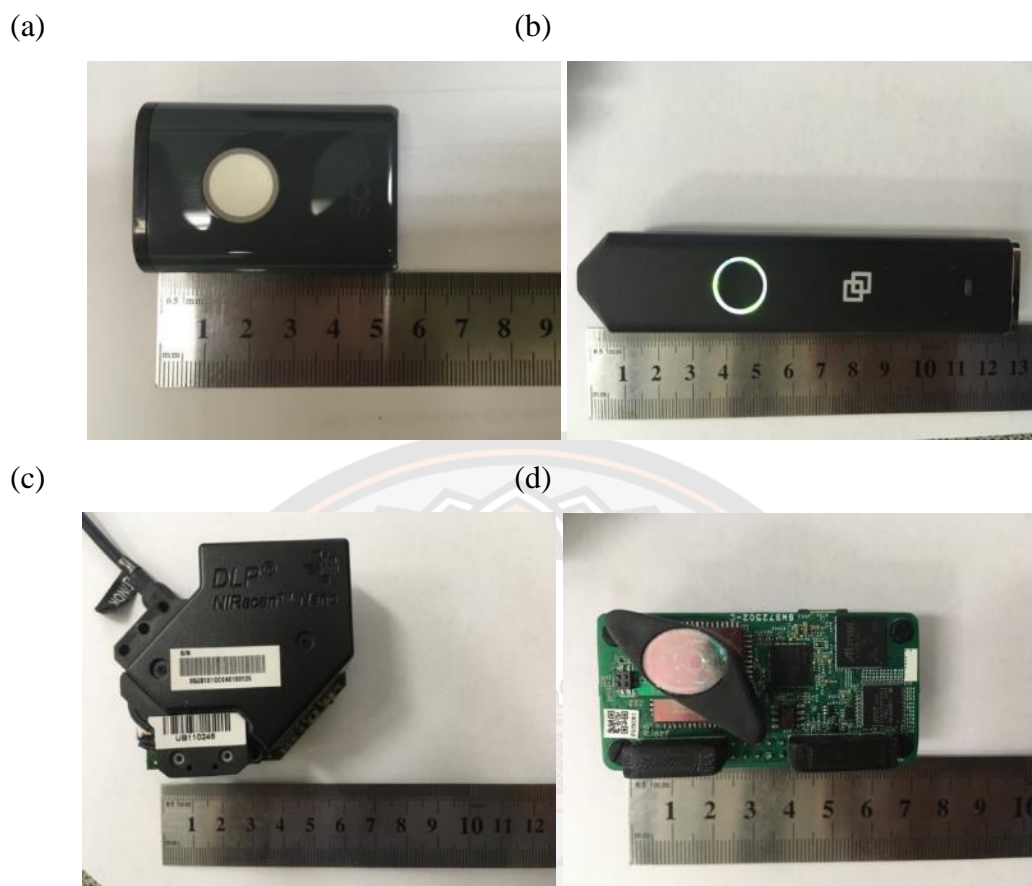


Figure 37 A photograph of the popular portable spectrometers (a) SCIO (b) Linksquare (c) Texas Instruments (TI) – DLP NIRscan Nano (d) Neospectra

The acquisition of NIR spectra of the mango samples was performed with four different commercial NIR spectrometers: SCIO, Linksquare, DLP NIRscan Nano, and Neospectra.

The SCIO sensor (Consumer Physics Inc., Tel-Aviv, Israel), works in the range of 740-1070 nm with a wavelength resolution $<10 \text{ nm}$ and sampling interval of 1 nm. Version 1.0 of SCIO sensor was used in this work. The data analysis and analysis environment were accessed using The SCIO Lab online application produced by same company (Consumer Physics Inc., Tel-Aviv, Israel). There were used on the smartphone for collecting, storing, and analyzing environment of the samples. [41]

The Linksquare sensor (TellSpec Inc., Toronto, ON, Canada), operates in the range 400-1050 nm. The instrument is operated in VIS (400-1000 nm) and NIR

(700-1050 nm) acquisition modes. These modes use the same sensor but differ in the light source. The spectral data were acquired in the reflectance mode with 3 nm spectral resolution. [42]

The DLP NIRscan Nano (Texas Instruments) is a miniature spectrometer operating in the wavelength range 900-1700 nm. The reflectance mode was used in this work with 10 nm spectral resolution. [43]

The Neospectra sensor (Neospectra-Module, Si-Ware Systems, Cairo, Egypt) operates in the wavelength range 1,300-2,500 nm. The spectral resolution was 16 nm. The spectroscopic measurements were operation with reflectance mode. [44]

3.2.2 Development of in-house optical spectrometer

As mentioned above, optical spectroscopy has received a remarkable measure of attention as a non-destructive analytical technique and it became the tool in several fields of typical applications including agriculture and food. The key components of popular NIR spectrometers are light source, wavelength selector, and detector. These key components result in different optical spectrometer properties. Therefore, in the second part of this project, we are interested in developing an in-house optical spectrometer with differences in these key components.

3.2.2.1 Development of in-house optical spectrometer: Light source.

As mentioned above, two different types of NIR sources are used in commercially available spectrometers such as filament bulb (TH) light source and Near infrared light emitting diode (NIR LED). Publications report wide use of filament bulb lamps as a commercial light source for non-destructive determination. TH light sources have been used in works showing prediction of SSC, DM, and firmness with good calibration models. On the other hand, NIR LED lamps have been studied to a lesser extent. The comparison of potential performance between NIR LED and TH for prediction of quality parameters is of interest. Therefore, we are interested in utilizing these different light sources for predicting quality parameters from mango and tomato.

(a)

(b)

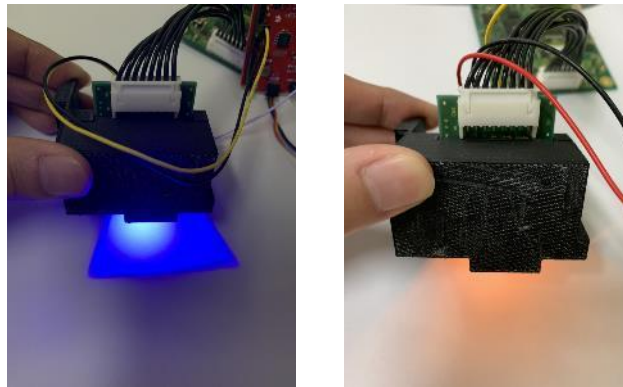


Figure 38 Illustration of the different light sources used for in-house built spectrometers (a) Near infrared light emitting diode, NIR LED (b) filament bulb, TH.

3.2.2.2 Development of in-house optical spectrometer: Wavelength selector.

As mentioned above, the F-751-Mango Mango Quality Meter is an interesting spectrometer for predicting ripeness indicators from mango samples. The key component used in this instrument is the Hamamatsu C11708MA spectral sensor.

This commercially available spectrometer from Felix Instruments can be used to assess quality parameters of mangoes. This provides supporting evidence for the possibility to construct a usable device based on this or similar sensor. The sensor chosen for this project is a new generation of NIR sensors from Hamamatsu, the C14384MA sensor, which operates in the same spectral range as the C11798MA sensor but has a higher sensitivity. The cost of the sensor, at the moment, is 20,000 THB. It should be noted that this is a unit price, which gets reduced to 10,000 THB per piece for volumes above ten sensors. In addition, the first prototype sensor will be made with Hamamatsu made evaluation board C14898. This board costs 40,000 THB. However, in future iterations it would be replaced by significantly cheaper custom-made PCB.

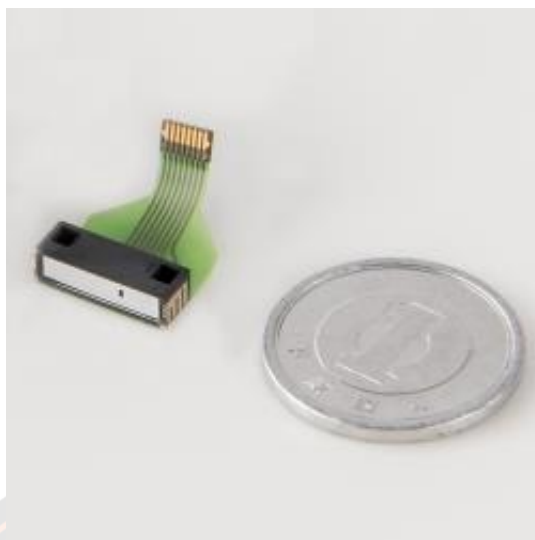


Figure 39 Image of the Hamamatsu C14384MA-01 sensor

3.2.2.3 Development of in-house optical spectrometer: Light detector

As mentioned above, two different classes of detectors are generally used in miniaturized spectrometers. The first one are Photovoltaic silicon (Si) diodes. These detectors have suitable sensitivity for the wavelength range of 700-1100 nm. The second one is indium gallium arsenide (InGaAs) photodetectors. It is typically suitable for the range 900-1700 nm. The Photovoltaic silicon (Si) diodes are suitable for compact and inexpensive devices operating in the Visible and short wavelength of NIR regions. Photovoltaic silicon diodes feature lower S/N, but are cheaper than InGaAs.

Therefore, we are interested in utilizing a Photovoltaic silicon (Si) diode as a detector for predicting quality parameters from mango and tomato.

3.2.3 Testing performance of in-house optical spectrometer for quantitative measurements to predict key quality parameters from mango and tomato.

As mentioned above, optical spectroscopy has received a remarkable measure interest as a non-destructive analytical technique and it became the tool of choice in several fields of applications including agriculture and food, where it is widely used to measure key quality parameters such as firmness, soluble solids content or, titratable acidity. However, while optical spectroscopy can provide a

measurement of these parameters not all quality parameters are predicted with the same accuracy. Therefore, in this part of this project, we are interested in developing the performance of the in-house optical spectrometer for quantitative measurements to predict key quality parameters from mango and tomato.

Sample preparation

The mango (Nam Dok Mai) and tomato (Cherry) were obtained from farmers as well as marketplaces throughout Thailand. Samples were obtained at various stages of ripening. At least 100 produce samples will be obtained and investigated.

Optical analysis

Measurement of optical spectra was performed using the in-house optical spectrometer mentioned in section 6.1. in reflectance mode. The optical spectral data were collected from intact samples. Spectra were acquired from at least four different locations on the surface of the samples with three repeat acquisitions at each location. All of the spectra acquired for an individual fruit sample were averaged to give a single spectrum representative of the sample for the purpose of further analysis.

Reference analysis

Firmness

Firmness measurements were carried out using penetrometers (Turoi FT011 and FT327) and universal testing machine (Instron Model 5965, Norwood USA)

The penetrometer measurements were equipped with a 13 mm steel plunger (Turoi, Froli Italy). The plunger is pressed into the sample fruit flesh until the portion of the plunger marked by a line was completely submerged. The measured values were recorded in pounds (lb) and converted to Newtons (N) using the following equation $1 \text{ lb} = 4.44822 \text{ N}$.

Alternatively, tensile measurements were carried out using 13 mm steel plunger. The operating condition were: 1.5 mm/s, 0.5 mm/s, and 10 mm/s during the pre-testing, testing, and post-testing phases of the measurement, respectively. The firmness value was described below.

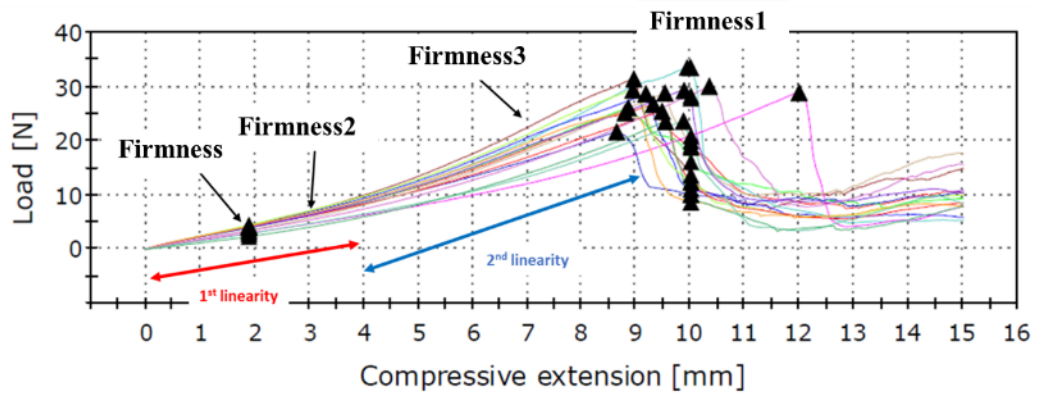


Figure 40 Determination of firmness values from tensile measurement

Firmness was recorded at 1.9 mm, which corresponds to the head inserted of steel plunger.

Firmness1 was recorded at the maximum load value of samples.

Firmness2 was recorded at the first linearity as described above at penetration dept of 3 mm.

Firmness3 was recorded at the second linearity as described above at penetration dept of 7 mm.

Firmness4 was obtained from the tensile instrumentation was the slope of the tensile curve in the second linearity region (from 4 mm to maximum firmness).

$$Firmness4 = \frac{Load_{max} - Load_{4mm}}{Com_{max} - Com_{4mm}} \quad \text{Equation4}$$

Firmness5 was measured as average slope of the curve up to maximum firmness (0 mm to maximum firmness).

$$Firmness5 = \frac{Load_{max} - Load_{0mm}}{Com_{max} - Com_{0mm}} \quad \text{Equation5}$$

Dry matter

The flesh under the location of the spectroscopic measurement was cut out, placed in a clean beaker, weighed and placed in an oven (Mettler, Schwabach, Germany) at 80°C. The sample was left in the oven for 24 h, allowed to cool down to room temperature, and weighed again. The content of dry matter was expressed as ratio of the weight of the dried sample (m_{dry}) and the fresh sample (m_{fresh}) as shown below.

$$\%Dry\ matter = \frac{m_{dry}}{m_{fresh}} \times 100 \quad \text{Equation 6}$$

Total Soluble Solids (TSS), Titratable Acidity (TA), and pH

The flesh from the location of the spectroscopic measurement was cut out. The juice was extracted using a hand juicer lined with two layers of cheese cloth. The extracted juice was used for the determination of all three parameters. TSS was measured using a portable refractometer (HI 96800, Hanna Instruments, Woonsocket, USA) and expressed as ° Brix. TA was measured by titration with 0.1 M NaOH solution using phenolphthalein as the end point indicator using an automatic burette (Titrette, BrandTech®, Essex, USA). The TA was expressed in % of malic acid using Equation X, where V_{NaOH} and V_{sample} are the volumes of 0.1 M NaOH solution used and volume of sample (1 ml), respectively:

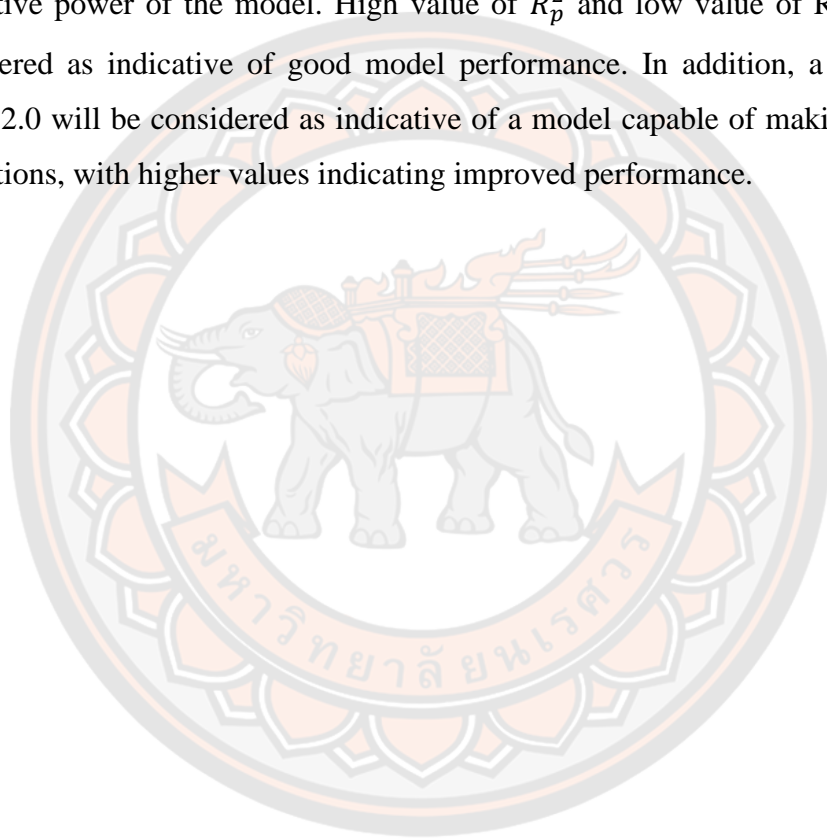
$$\%malic\ acid = \frac{V_{NaOH} \times 0.067 \times 100}{V_{sample}} \quad \text{Equation 7}$$

The pH of the juice was recorded using a handheld pH meter (HI 98100, Hanna Instruments, Woonsocket, USA).

Chemometric analysis

Development and evaluation of prediction models obtained for data from the in-house spectrometer will be carried out using Unscrambler software. Partial least squares (PLS) and multiple linear (MLR) regression will be used and various data pretreatment methods (e.g. standard normal variate, derivatives using Savitzky-Golay

algorithm, multiplicative scatter correction, etc.) will be tested. The models will be evaluated based on their coefficient of determination for calibration (R_c^2), root mean square error of calibration (RMSEC) High value of R_c^2 and low values of RMSEC and LV will be considered as indicative of good models. The predictive potential of the model will then be tested on samples not included in the model development. The coefficient of determination for prediction R_p^2 , root mean square error of prediction RMSEP, and ratio of prediction to deviation (RPD) will be used to judge the predictive power of the model. High value of R_p^2 and low value of RMSEP will be considered as indicative of good model performance. In addition, a value of RPD above 2.0 will be considered as indicative of a model capable of making quantitative predictions, with higher values indicating improved performance.



CHAPTER IV

RESULT AND DISCUSSION

The aim of this work was to evaluate the performance of low cost commercial and in-house built optical spectrometers to predict quality parameters (e.g., DM, firmness, TSS, TA and pH) for mangoes and tomatoes.

4.1 Testing performance of commercial portable spectrometers for quantitative measurements to predict key quality parameters from mango and tomato.

Sample preparation

Mango (Nam Dok Mai) samples were obtained from fresh produce markets (Bangkok, Prachup Khiri Khan, and Phitsanulok) and local retail stores (Macro, Phitsanulok). The number of samples and location of sources are summarized in Table 5.

Table 5 Numbers of samples based on location of collection for commercial portable spectrometers for mango.

Source Location	N
Bangkok	295
Phachuap Khiri Khan	62
Phitsanulok	69
Macro	122
Total	548

Total 548 samples were obtained in this work. Mangoes were washed with water to remove the gum and stored at ambient conditions prior to analysis. Four sampling areas (2x2cm) have been marked on the samples. Two sampling areas were located on each of the two opposite sides of the sample. Spectroscopic measurements were performed on the surface of these areas are show in Figure 41.

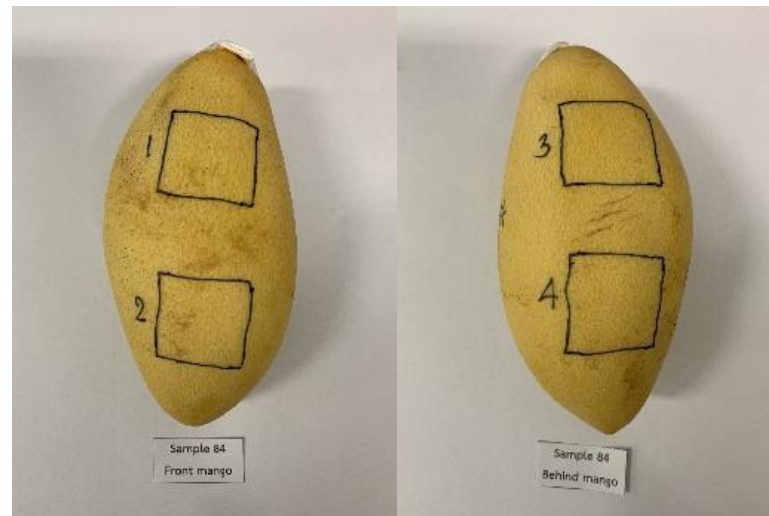


Figure 41 Representative images of front and back sides of a mango sample with marked sampling sites.

Data Acquisition of commercial spectrometers for mango

Spectroscopic measurements from at the marked areas were performed using the four commercial spectrometers (SCIO, Linksquare, TI, and Neospectra). Four spectra were recorded for each location. These spectra were averaged, and the averaged spectra were used for the subsequent chemometric analysis. The spectra obtained by measurements with these spectrometers are shown in Figure 42 to Figure 45. The mango samples were split into three groups for the purpose of reference standard analyses. Samples in the first group were used for firmness analysis. The second group of samples was used for the determination of total soluble solids (TSS), titratable acidity (TA), and pH determination. Finally, the last group of samples was used for dry matter (DM).

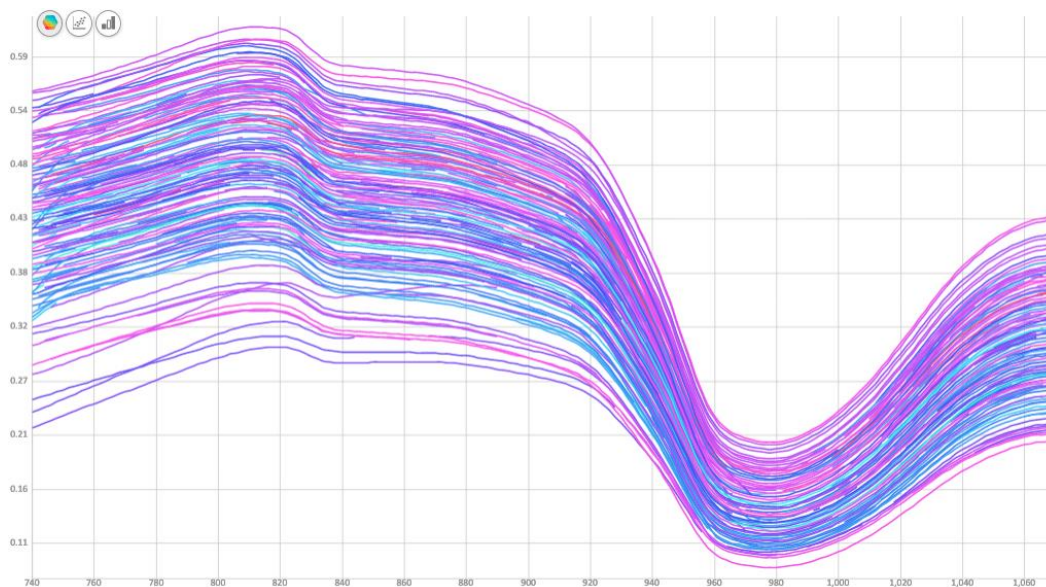
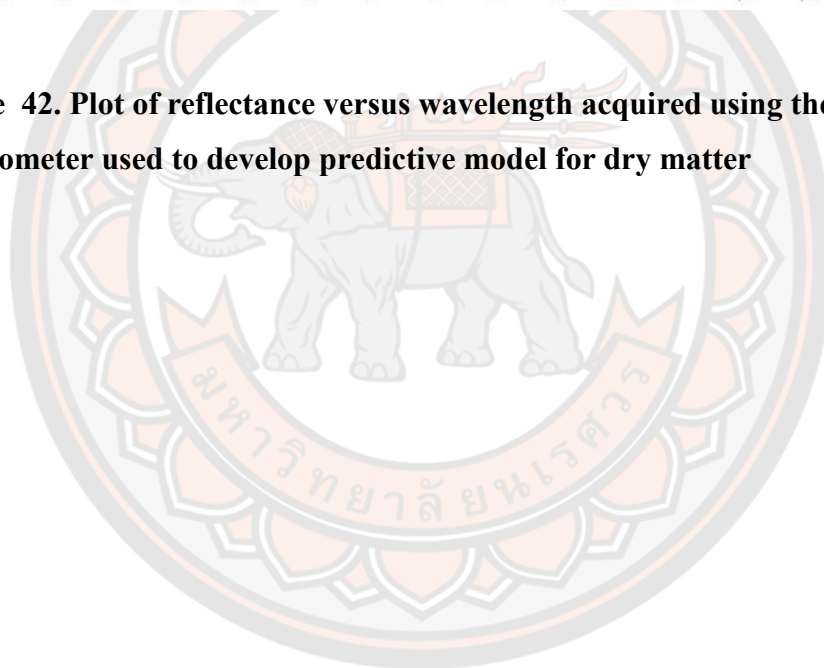
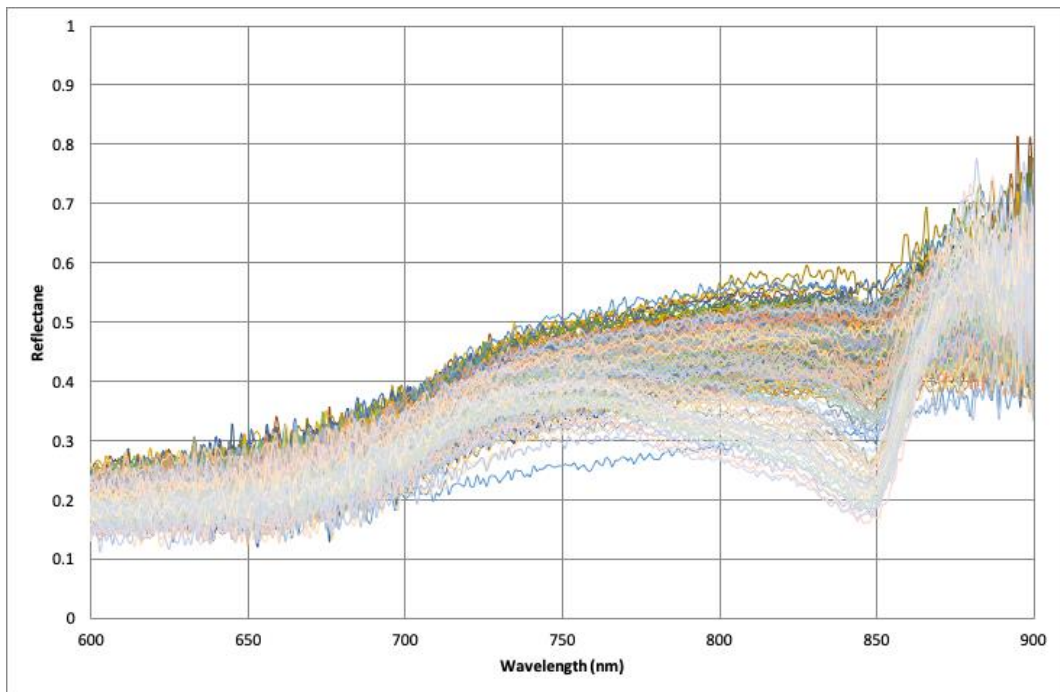


Figure 42. Plot of reflectance versus wavelength acquired using the SCiO spectrometer used to develop predictive model for dry matter



(a)



(b)

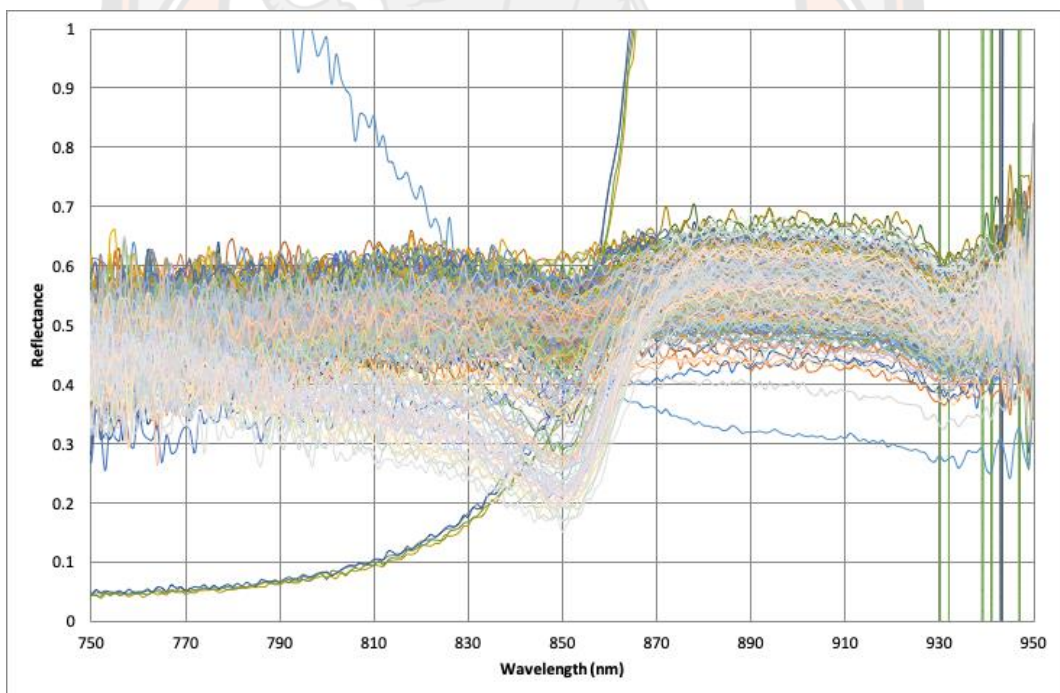


Figure 43. Plot of reflectance versus wavelength for the dry matter dataset obtained using the Linksquare spectrometer with (a) visible (b) NIR light illumination

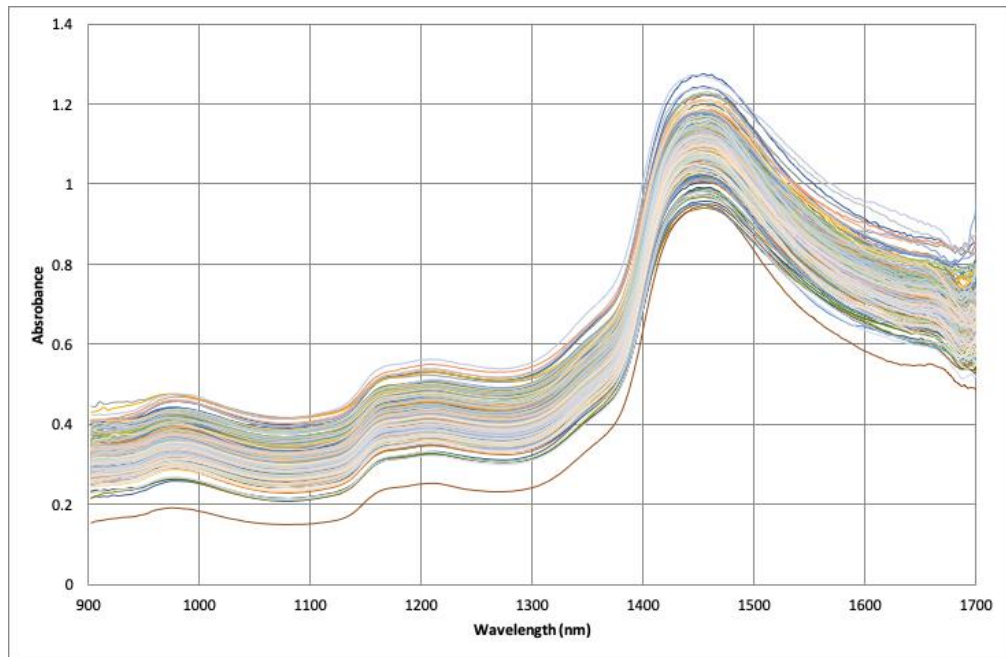


Figure 44. Plot of absorbance versus wavelength for the dry matter dataset obtained using the TI NIRscan Nano spectrometer

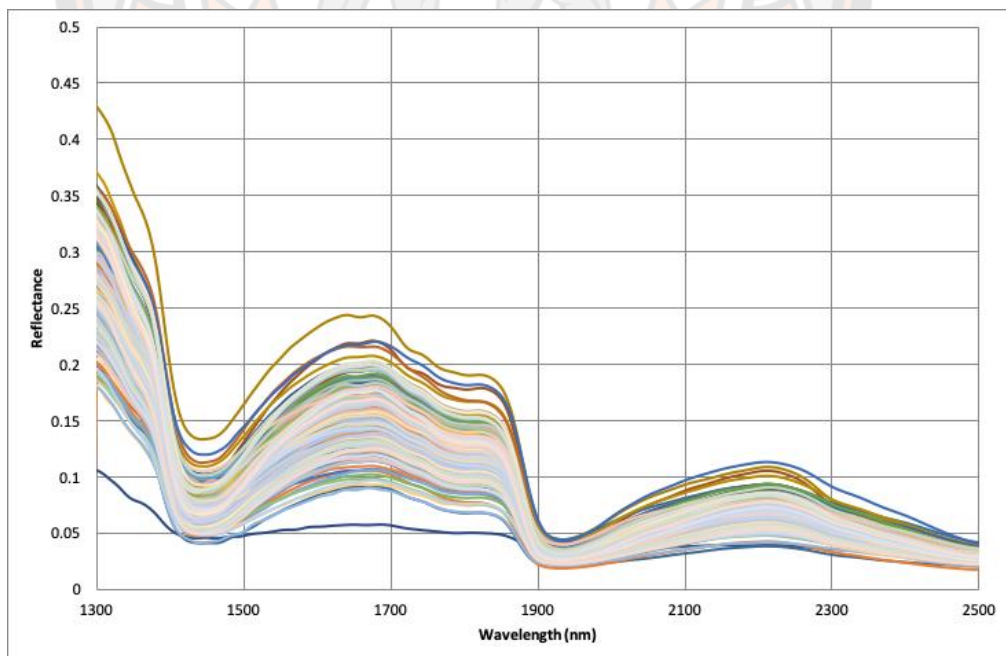


Figure 45. percentage of reflectance spectra for the dry matter dataset obtained using the Neospectra spectrometer.

Reference analysis of commercial spectrometers for non-destructive determination of mango.

Five quality parameters (DM, TSS, TA, pH, and firmness) were investigated for the mango samples using commercial spectrometers. The descriptive statistics for the investigated mango quality parameters are summarized in Table 6.

Table 6 Descriptive statistics for quality parameters analyzed in mango samples using commercial spectrometers

parameter	N	Average	Min	Max	Std
DM (%)	207	16.4	9.7	23.9	2.6
TSS (°Brix)	182	13.9	6.3	21.3	3.5
TA (%)	184	1.04	0.215	5.359	1.1
pH	93	3.57	2.59	5.16	0.8
Firmness (N)	223	9.1	0.4	122.6	12.0

Table 6 shows the range of measurement (minimum and maximum values), average, and standard deviation of the quality parameters in the mango samples. The values of Dry matter, TSS, TA, pH, and firmness were in the range 9.7-23.9%, 6.3-21.3°Brix, 0.215-5.359%, 2.59-5.16, and 19.83-58.50 N, respectively.

4.1.1 Testing the performance of commercial spectrometers for non-destructive determination of mango quality parameters.

4.1.1.1 SCiO

The SCiO spectrometer is a miniature spectroscopic device operating in the spectral range from 740 to 1,070 nm. It is an interesting instrument and therefore, the performance of the SCiO spectrometer for the development of calibration models to be used to predict quality parameters of mango samples. The SCiO spectrometer was purchased with access to an online chemometric interface where the analysis was performed. Figure 46 shows the outcome for the development of the calibration models performed using spectroscopic data obtained with the SCiO spectrometer and utilized without any pretreatment procedure.

The R^2 values for cross validation of calibration models based on spectroscopic data acquired using the SCiO spectrometer and made without pretreatment for predicting DM, TSS, TA, pH, and firmness of mangoes were 0.920, 0.845, 0.439, 0.725, and 0.04, respectively. The RMSE values for DM, TSS, TA, pH, and firmness were 0.739%, 1.354°Brix, 0.789%, 0.414, and 11.948N, respectively (Figure 46).

The calibration models using spectral data from the SCiO instrument exhibit good figures merit for DM and TSS with R^2 values greater than 0.80. The online chemometric tool also allowed the application of various pretreatment procedures. The following four pretreatment procedures were used in this work:

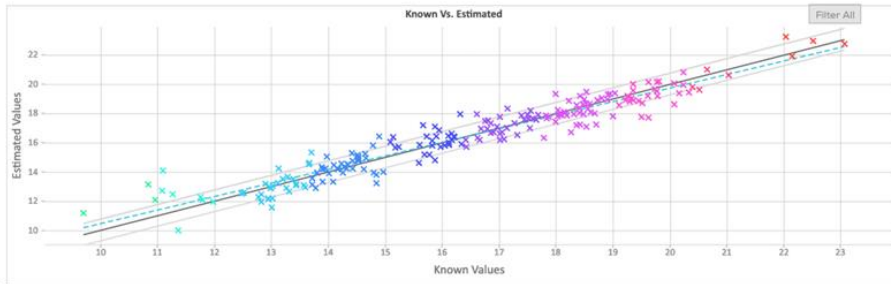
Procedure 1: Scan averaging, wavelength selection (790-1,070 nm), SNV

Procedure 2: Scan averaging, spectrum smoothing and 1st derivative (2nd degree polynomial, Window: 35), wavelength selection (790-1,070 nm), SNV

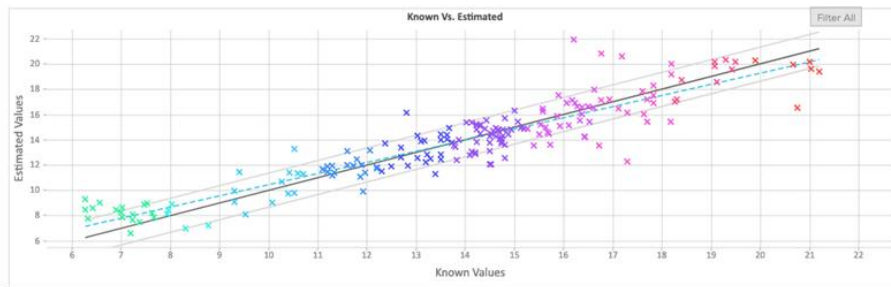
Procedure 3: Scan averaging, spectrum smoothing and 1st derivative (2nd degree polynomial, Window: 35), wavelength selection (790-1,070 nm), average subtraction

Procedure 4: Logarithm, scan averaging, spectrum smoothing and 2nd derivative (2nd degree polynomial, Window: 35), (790-1,070 nm), SNV.

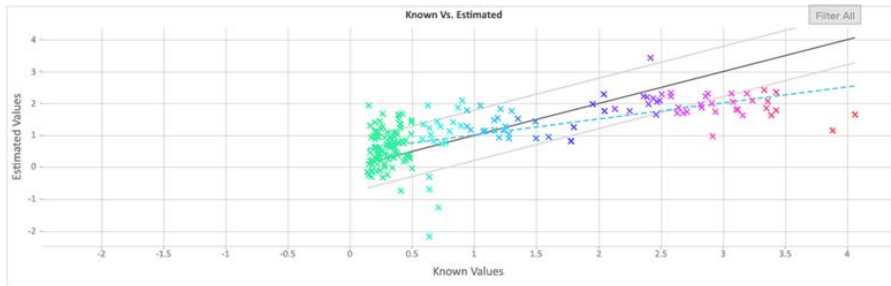
Target: Dry Matter
Performance: RMSE = 0.739 | R2 = 0.92 | SEP = 0.739 | precision = 0 | r2 = 0.921 | slope = 0.932 | (a)



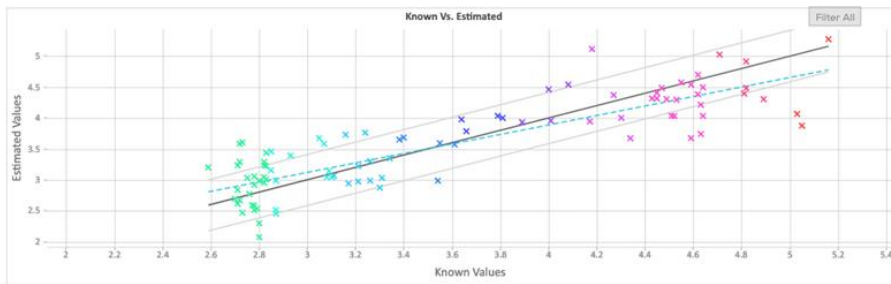
Target: TSS
Performance: RMSE = 1.354 | R2 = 0.845 | SEP = 1.354 | precision = 0 | r2 = 0.847 | slope = 0.881 | (b)



Target: TA
Performance: RMSE = 0.789 | R2 = 0.439 | SEP = 0.789 | precision = 0 | r2 = 0.446 | slope = 0.5 | (c)



Target: pH
Performance: RMSE = 0.414 | R2 = 0.725 | SEP = 0.414 | precision = 0 | r2 = 0.727 | slope = 0.767 | (d)



Target: Firmness
Performance: RMSE = 11.948 | R2 = -0.004 | SEP = 11.948 | precision = 0 | r2 = 0 | slope = 0 | (e)

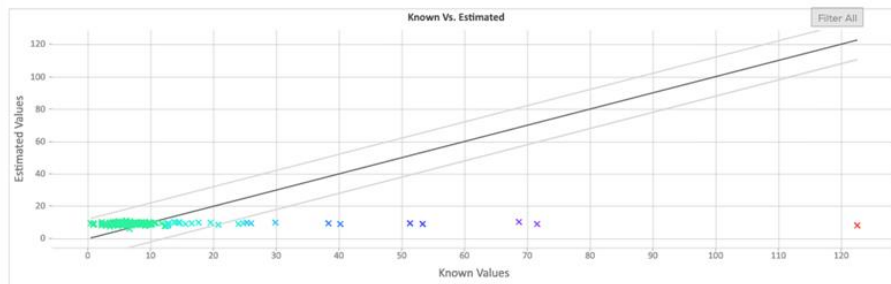
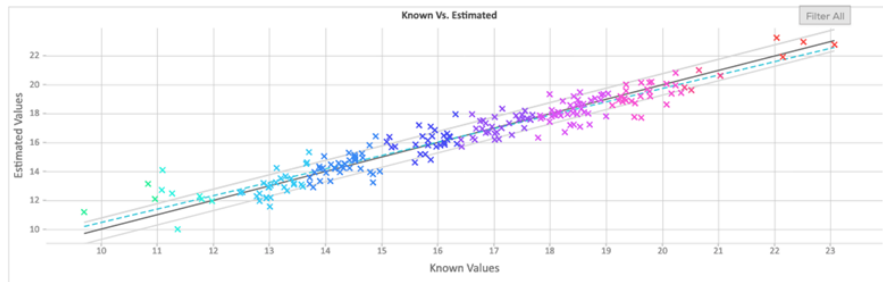


Figure 46 Plots of predicted versus measured mango quality parameters (a) DM (b) TSS (c) TA (d) pH, and (e) Firmness obtained with calibration models based on spectral data acquired using the SCIO spectrometer without pretreatment

Calibration plots for the models with the best performance for each quality parameter are shown in Figure 47. The results indicate that the best R^2 values for cross validation were 0.920, 0.845, 0.497, 0.744, and 0.261 for DM, TSS, TA, pH, and firmness, respectively. The corresponding RMSE values were 0.739%, 1.354 °Brix, 0.747%, 0.400, and 2.695N, for DM, TSS, TA, pH, and firmness, respectively.

It can be seen that in the cases of DM, TSS, and Firmness the best models were obtained using data without preprocessing, with the R^2 values exhibiting decreases when data preprocessing was used. On the other hand, in the case of TA and pH better R^2 values were obtained for calibration modes made after data pretreatment by Procedure 2 and 4, respectively.

Target: Dry Matter
Performance: RMSE = 0.739 | R2 = 0.92 | SEP = 0.739 | precision = 0 | r2 = 0.921 | slope = 0.932 | (a)



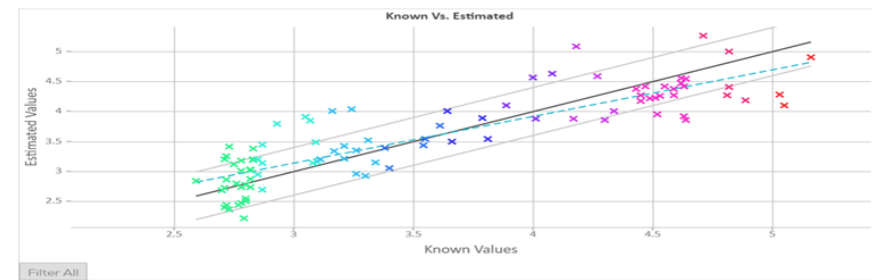
Target: TSS
Performance: RMSE = 1.354 | R2 = 0.845 | SEP = 1.354 | precision = 0 | r2 = 0.847 | slope = 0.881 | (b)



Target: TA
Performance: RMSE = 0.747 | R2 = 0.497 | SEP = 0.747 | precision = 0 | r2 = 0.502 | slope = 0.553 | (c)



Target: pH
Performance: RMSE = 0.4 | R2 = 0.744 | SEP = 0.399 | precision = 0 | r2 = 0.745 | slope = 0.778 | (d)



Target: Firmness
Performance: RMSE = 2.695 | R2 = 0.261 | SEP = 2.695 | precision = 0 | r2 = 0.274 | slope = 0.335 | (e)

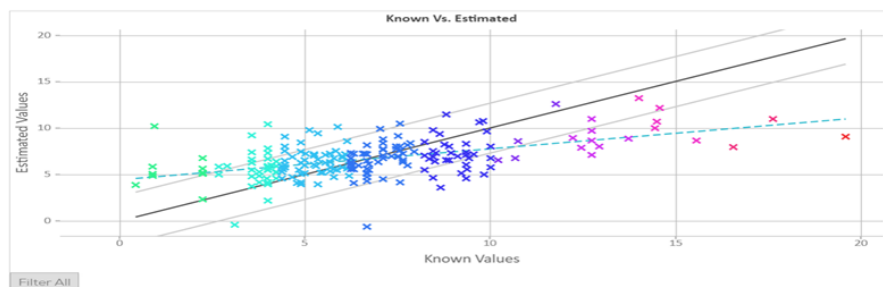


Figure 47 Plot of predicted versus measured quality parameters with the best cases of figure of merit values using the SCiO spectrometer for (a) DM (b) TSS (c) TA (d) pH and (d) Firmness

Table 7 Best R^2 values for cross-validation for mango quality parameters using the SCiO spectrometer.

parameter	pretreatment	Cross validation		
		R^2	RMSE	LV
Dry matter	None	0.920	0.739	12
TSS	None	0.845	1.354	12
TA	Procedure 2	0.497	0.747	8
pH	Procedure 4	0.744	0.400	7
Firmness	None	0.261	2.695	9

Procedure 1: Scan averaging, wavelength selection (790-1,070 nm), SNV;

Procedure 2: Scan averaging, spectrum smoothing and 1st derivative (2nd degree polynomial, Window: 35), wavelength selection (790-1,070 nm), SNV;

Procedure 3: Scan averaging, spectrum smoothing and 1st derivative (2nd degree polynomial, Window: 35), wavelength selection (790-1,070 nm), average subtraction

Procedure 4: Logarithm, scan averaging, spectrum smoothing and 2nd derivative (2nd degree polynomial, Window: 35), (790-1,070 nm), SNV.

4.1.1.2 Linksquare

As mentioned above, Linksquare spectrometer operates in the range from 400 to 1,000 nm. This instrument can be used in two acquisition modes: VIS (400-1000 nm) and NIR (700-1050 nm). These modes use the same sensor but differ in the light source. Figure 48 shows representative plots for calibration models obtained with spectral data used without preprocessing.

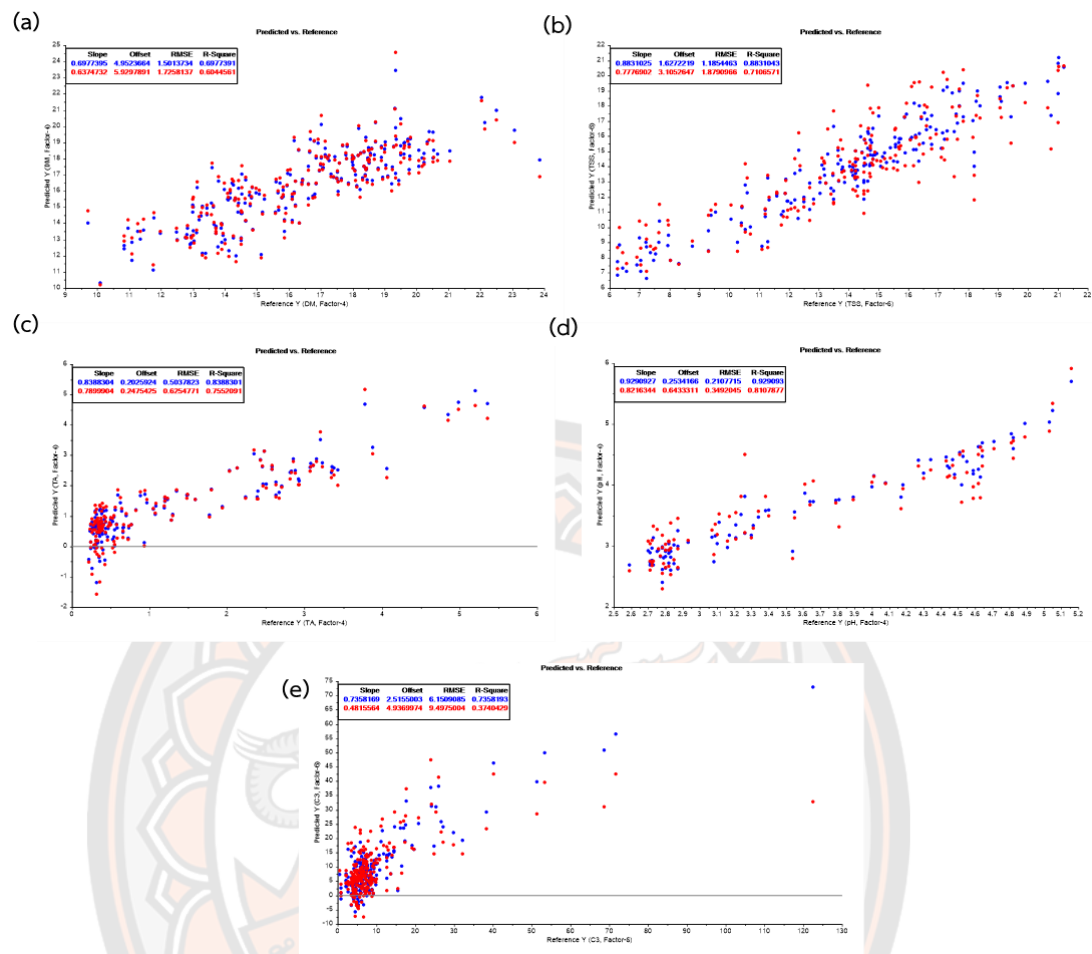


Figure 48. Plot of predicted versus measured quality parameters for calibration models made with spectral data acquired using the Linksquare spectrometer operating in the visible mode without preprocessing for predicting (a) DM (b) TSS (c) TA (d) pH and (e) Firmness

As can be seen in Figure 48, the calibration models based on data acquired using the Linksquare operating in the visible mode exhibit R^2 values for the calibration and cross validation (in brackets) of 0.70 (0.60), 0.88 (0.71), 0.84 (0.76), 0.93 (0.81), and 0.74 (0.37) for DM, TSS, TA, pH, and Firmness, respectively. The RMSE values for calibration and cross validation (in brackets) were 1.50% (1.73%), 1.19 °Brix (1.88 °Brix), 0.50% (0.63%), 0.21 (0.35), and 6.15N (9.50N) for DM, TSS, TA, pH, and Firmness, respectively.

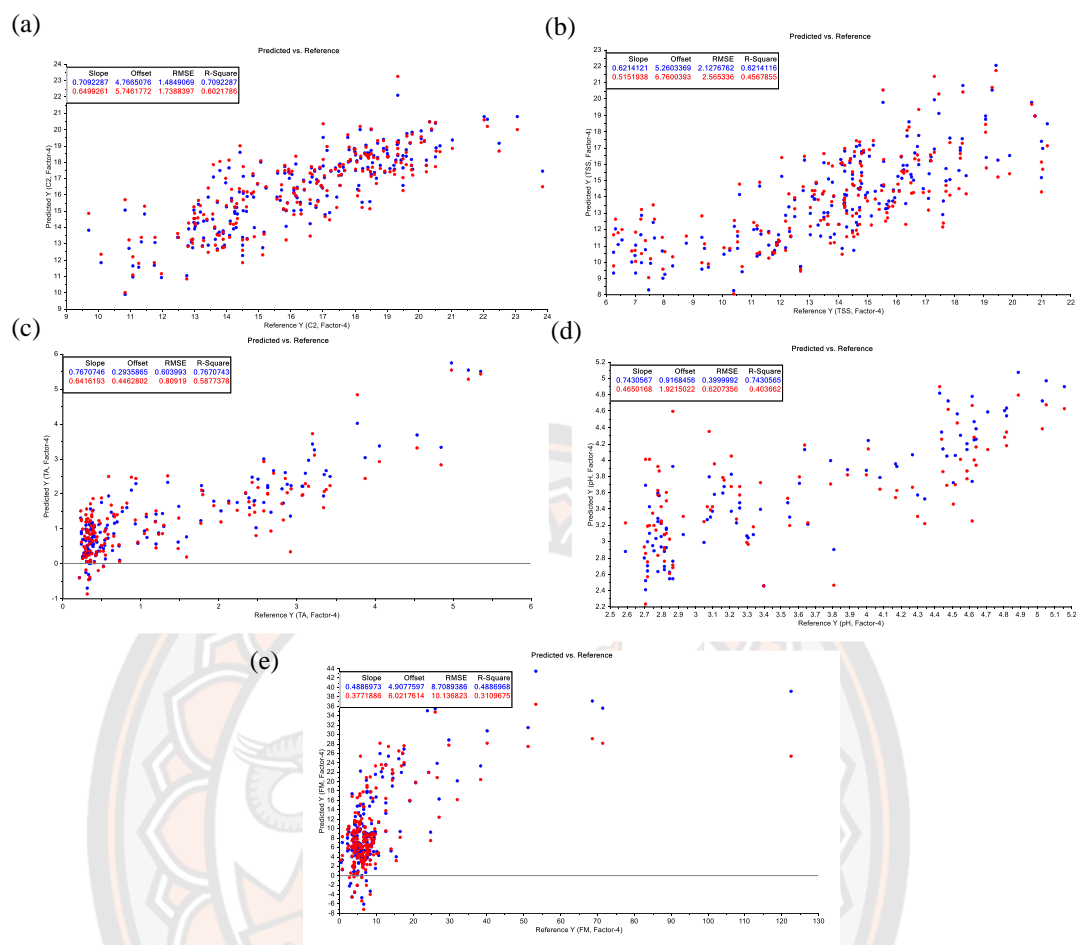


Figure 49 Plot of predicted versus measured quality parameters for calibration models made with spectral data acquired using the Linksquare spectrometer operating in the NIR mode without preprocessing for predicting (a) DM (b) TSS (c) TA (d) pH and (d) Firmness

As can be seen in Figure 49, the calibration models based on data acquired using the Linksquare spectrometer operating in the NIR mode exhibit R^2 values for the calibration and cross validation (in brackets) of 0.71 (0.60), 0.62 (0.46), 0.77 (0.59), 0.74 (0.40) and 0.49 (0.31) for DM, TSS, TA, pH, and Firmness, respectively. The RMSE values for calibration and cross validation (in brackets) were 1.48% (1.74%), 2.13 °Brix (2.57 °Brix), 0.60% (0.81%), 0.40 (0.62), and 8.71N (10.13N) for DM, TSS, TA, pH, and Firmness, respectively.

The models developed by using data acquired with the LS spectrometer operating in the visible mode and used without preprocessing exhibit good figures of merit with high R^2 values for TSS, TA, and pH in calibration and cross validation.

Unfortunately, the models developed by using data acquired with the LS spectrometer operating in the NIR mode and made without data preprocessing exhibit fairly significant drop in the R^2 values for calibration and cross validation in comparison to the models based on data acquired in the visible mode.

The best cases for predicting quality parameters using LS spectrometer for the visible and NIR modes were shown in Table 8.

Table 8 Best R^2 values for calibration and cross-validation for mango quality parameters obtained using data acquired with the LS spectrometer operating in the visible and NIR modes.

Parameter	Mode	Pre- processing	Calibration		Cross validation		LV
			R^2	RMSE	R^2	RMSE	
Dry matter	visible	Procedure 5	0.81	1.19	0.64	1.65	3
TSS	visible	Procedure 5	0.91	1.03	0.75	1.76	4
TA	visible	Procedure 5	0.91	0.38	0.79	0.58	3
pH	visible	None	0.93	0.21	0.81	0.35	4
Firmness	visible	None	0.74	6.15	0.37	9.50	6

Procedure 1: Spectrum smoothing and 1st derivative (2nd degree polynomial, Window: 3);

Procedure 2: Spectrum smoothing and 1st derivative (2nd degree polynomial, Window: 21);

Procedure 3: Spectrum smoothing and 2nd derivative (2nd degree polynomial, Window: 3);

Procedure 4: Spectrum smoothing and 2nd derivative (2nd degree polynomial, Window: 21);

Procedure 5: SNV

The results indicate good performance of the developed models for calibration and cross validation for the DM, TSS, TA, and pH. The R^2 values for the calibration and cross validation (in brackets) were 0.81 (0.64), 0.91 (0.75), 0.91 (0.79), and 0.93 (0.81) for DM, TSS, TA, and pH respectively.

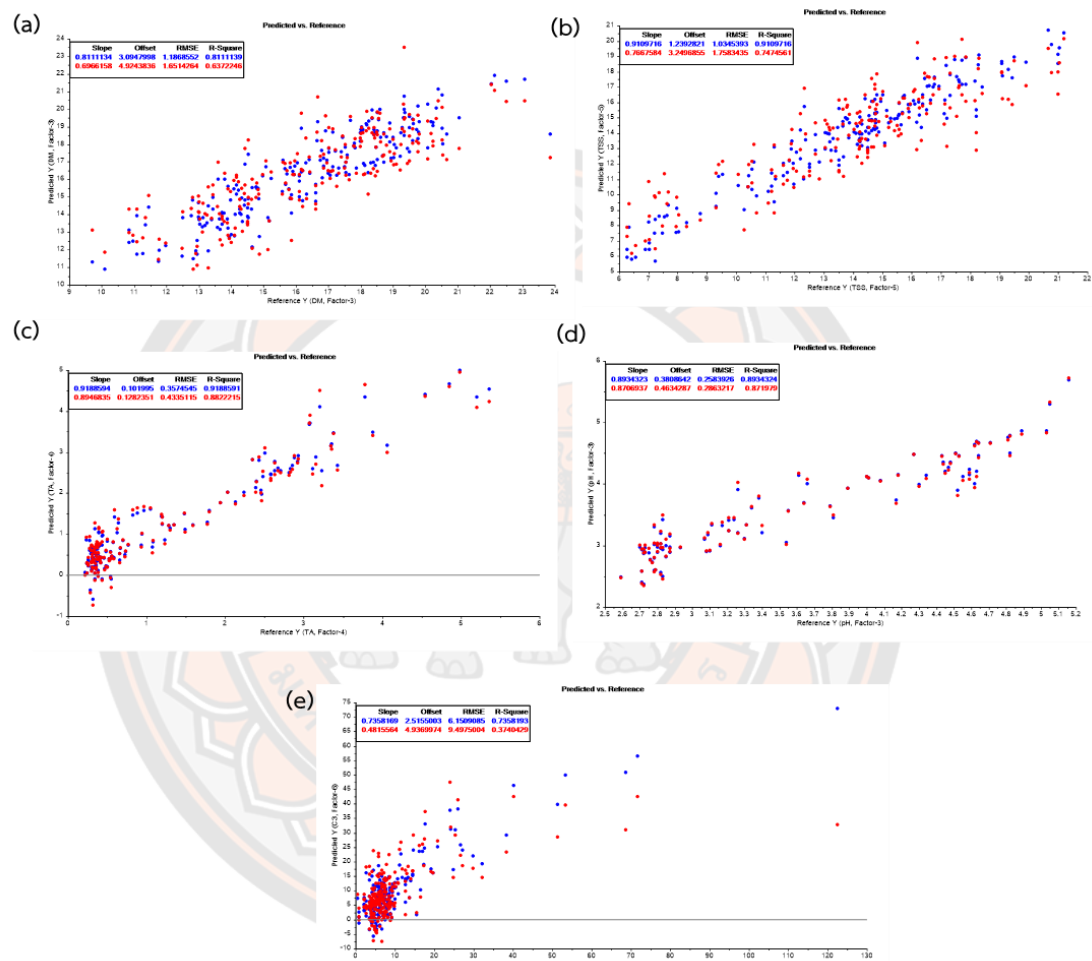


Figure 50. Plots of predicted versus measured values of mango quality parameters for calibration models made using data acquired with the LS spectrometer and exhibiting the best figures of for predicting (a) DM (b) TSS (c) TA (d) pH and (d) Firmness

4.1.1.3 Texas Instruments (TI) – DLP NIRscan Nano

The NIRscan Nano spectrometer operates in the range from 900 to 1,700 nm. Figure 51 shows the plots of the calibration models for the determination of mango

quality parameters using spectral data acquired with the NIRScan Nano spectrometer. The spectral data was used without preprocessing.

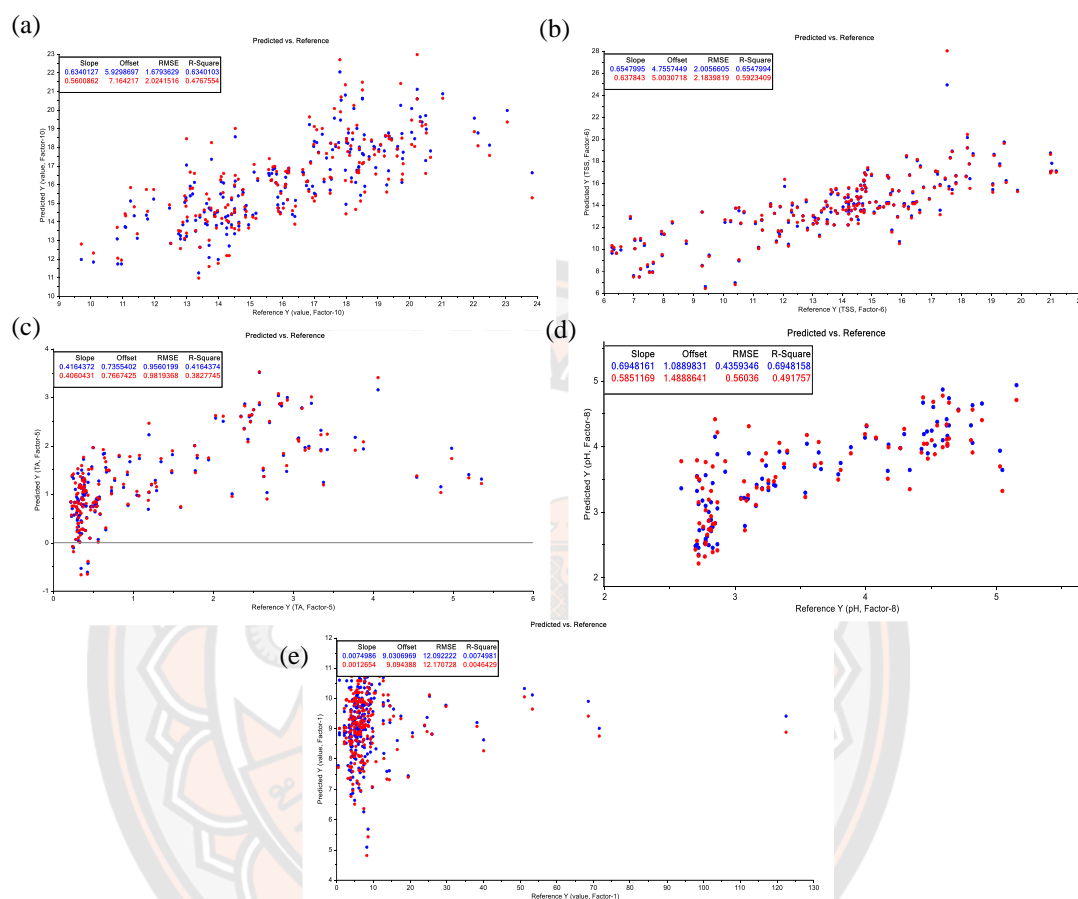


Figure 51. Plots of predicted versus measured values of mango quality parameters developed using spectral data acquired with the NIRScan Nano spectrometer without preprocessing used for (a) DM (b) TSS (c) TA (d) pH and (e) Firmness

As can be seen in Figure 51, the models obtained with spectral data acquired with the Texas Instruments NIRScan Nano exhibited R^2 values for calibration and cross validation (in brackets) of 0.63 (0.48), 0.65 (0.59), 0.42 (0.38), 0.69 (0.49), and 0.007 (0.005) for DM, TSS, TA, pH, and Firmness, respectively. The RMSE values for the calibration and cross validation (in brackets) were 1.68% (2.02%), 2.01 °Brix

(2.18 °Brix), 0.96% (0.98%), 0.44 (0.56), and 12.09N (12.17N) for DM, TSS, TA, pH, and Firmness, respectively.

The models developed using spectral data acquired with the NIRScan Nano spectrometer without preprocessing exhibit moderate figures of merit for TSS, TA, and pH with modest R^2 values for calibration and cross validation.

The best cases of models developed for predicting quality parameters of mangoes using spectral data acquired with the NIRScan Nano spectrometer are shown in Table 9.

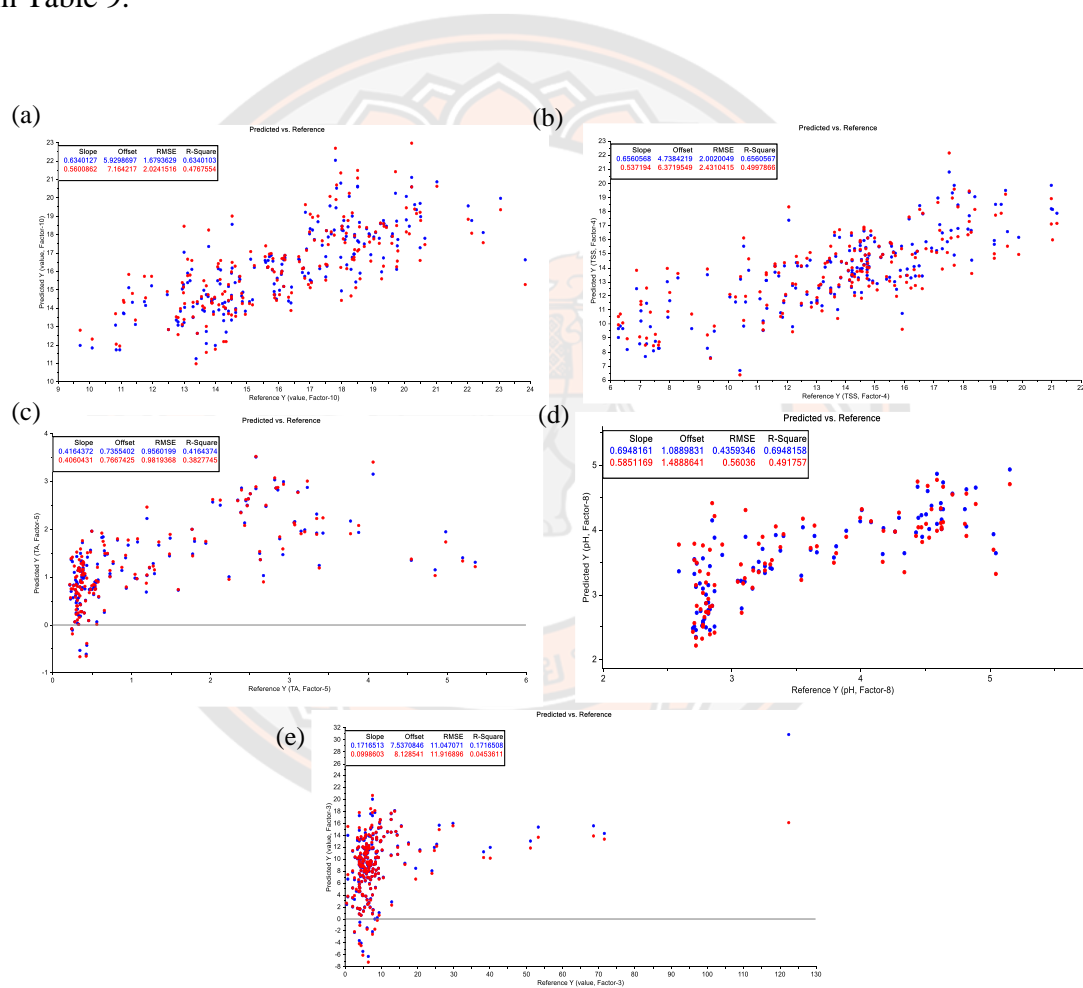


Figure 52 Plots of predicted versus measured values of quality parameters for models exhibiting the best figures of merit for spectral data acquired using the NIRScan Nano spectrometer used for predicting (a) DM (b) TSS (c) TA (d) pH and (e) Firmness

The results indicate that moderate performance of the models in calibration and cross validation has been achieved for DM, TSS, TA, and pH. The R^2 values for calibration and cross validation (in brackets) are 0.63 (0.48), 0.66 (0.50), 0.42 (0.38), 0.69 (0.49), and 0.172 (0.045) for DM, TSS, TA, pH, and firmness respectively. The corresponding RMSE values for the calibration and cross validation (in brackets) were 1.68% (2.02%), 1.99 °Brix (2.43 °Brix), 0.96% (0.98%), 0.44 (0.56), and 11.05N (11.92N) for DM, TSS, TA, pH, and Firmness, respectively.

Table 9 Summary of model parameters for predictive models for mango quality parameters developed using spectral data acquired using the NIRScan Nano spectrometer developed without pretreatment procedure and showing the best cases.

Parameter	Preprocessing	Calibration		Cross validation		LV
		R^2	RMSE	R^2	RMSE	
Dry Matter	None	0.63	1.68	0.48	2.02	10
TSS	None	0.65	2.01	0.59	2.18	6
	Procedure 1	0.66	1.99	0.50	2.43	4
TA	None	0.42	0.96	0.38	0.98	5
pH	None	0.69	0.44	0.49	0.56	8
Firmness	None	0.007	12.09	0.005	12.17	1
	Procedure 2	0.172	11.05	0.045	11.92	3

Procedure 1: Spectrum smoothing and 1st derivative (2nd degree polynomial, Window: 3);

Procedure 2: Spectrum smoothing and 1st derivative (2nd degree polynomial, Window: 21);

Procedure 3: Spectrum smoothing and 2nd derivative (2nd degree polynomial, Window: 3);

Procedure 4: Spectrum smoothing and 2nd derivative (2nd degree polynomial, Window: 21);

Procedure 5: SNV

The results indicate that the performance of calibration models for predicting quality parameters of mango were moderate with R^2 values for the DM, TSS, TA, and pH being approximately 0.50. Moreover, the performance of models for the prediction of firmness was poor with very low R^2 values.

4.1.1.4 Neospectra

The Neospectra spectrometer operates in the range from 1,300 to 2,500 nm. Figure 53 shows the plots of the calibration models for the determination of mango quality parameters using spectral data acquired with the Neospectra spectrometer. The spectral data was used without preprocessing.

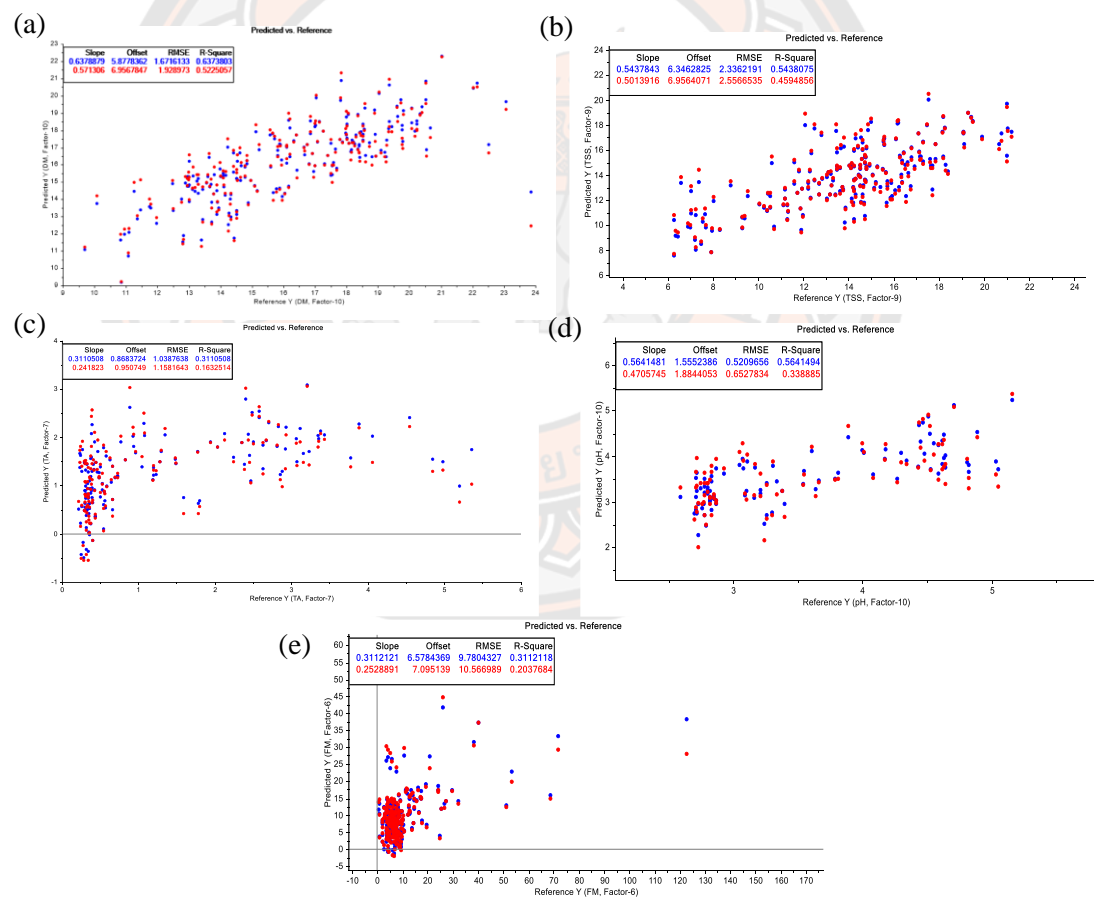


Figure 53 Plots of predicted versus measured mango quality parameters developed using spectral data acquired with the Neospectra without preprocessing used for (a) DM (b) TSS (c) TA (d) pH and (e) firmness

As can be seen in Figure 53, the calibration models obtained with spectral data acquired using the Neospectra spectrometer exhibited R^2 values for calibration and cross validation (in brackets) of 0.64 (0.52), 0.54 (0.46), 0.31 (0.16), 0.56 (0.34), and 0.31 (0.20) for DM, TSS, TA, pH, and firmness, respectively. The RMSE values for the calibration and cross validation (in brackets) were 1.67% (1.93%), 2.34 °Brix (2.56 °Brix), 1.04% (1.16%), 0.52 (0.34), and 9.78N (10.59N) for DM, TSS, TA, pH, and firmness, respectively.

The models developed using spectral data acquired with the Neospectra without preprocessing exhibit moderate figures of merit with relatively modest R^2 values for TSS, TA, and pH for both calibration and cross validation.

The best cases of for predicting mango quality parameters using data acquired with Neospectra are shown in Figure 54 and Table 10.

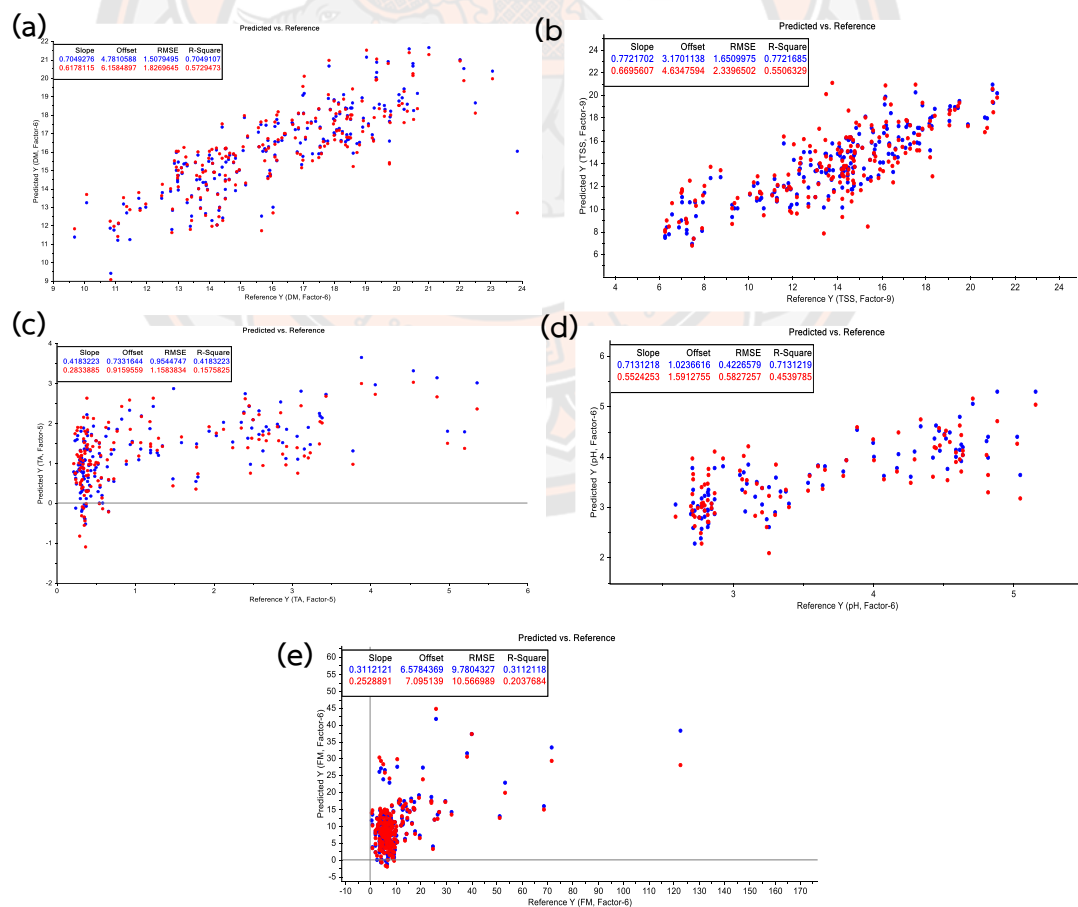


Figure 54 Plots of predicted versus measured values of quality parameters for models exhibiting the best figures of merit for spectral data acquired using Neospectra used for predicting (a) DM (b) TSS (c) TA (d) pH and (e) Firmness

The results indicate that moderately performing calibration models were obtained for DM, TSS, TA, and pH. These models exhibit R^2 values for calibration and cross validation (in brackets) of 0.70 (0.57), 0.77 (0.55), 0.42 (0.16), 0.71 (0.45), and 0.33 (0.18) for DM, TSS, TA, pH, and firmness respectively. The RMSE values for the calibration and cross validation (in brackets) were 1.51% (1.83%), 1.65 °Brix (2.34 °Brix), 0.95% (1.16%), 0.42 (0.45), and 9.62N (10.77N) for DM, TSS, TA, pH, and Firmness, respectively.

Table 10. Summary of model parameters for predictive models for mango quality parameters developed by using spectral data acquired using the Neospectra developed without pretreatment procedure and showing the best cases.

parameter	preprocessing	Calibration		Cross validation		LV
		R^2	RMSE	R^2	RMSE	
Dry Matter	None	0.64	1.67	0.52	1.93	10
	Procedure 1	0.70	1.51	0.57	1.83	4
TSS	None	0.54	2.34	0.46	2.56	9
	Procedure 1	0.77	1.65	0.55	2.34	9
TA	None	0.31	1.04	0.16	1.16	7
	Procedure 3	0.42	0.95	0.16	1.16	5
pH	None	0.56	0.52	0.34	0.65	10
	Procedure 1	0.71	0.42	0.45	0.58	6
Firmness	None	0.31	9.78	0.20	10.59	6
	Procedure 4	0.33	9.62	0.18	10.77	6

Procedure 1: Spectrum smoothing and 1st derivative (2nd degree polynomial, Window: 3);

Procedure 2: Spectrum smoothing and 1st derivative (2nd degree polynomial, Window: 21);

Procedure 3: Spectrum smoothing and 2nd derivative (2nd degree polynomial, Window: 3);

Procedure 4: Spectrum smoothing and 2nd derivative (2nd degree polynomial, Window: 21);

Procedure 5: SNV

The results indicate that the performance of the calibration models for predicting mango quality parameters was good with R^2 values for DM, TSS, and pH at about 0.70. On the other hand, the predictive models for TA and firmness were poor with very low R^2 values.

Best R^2 values by commercial spectrometers

The possibility to predict mango quality parameters using commercial spectrometers (SCIO, Linksquare, Texas Instruments NIRScan nano, and Neospectra) has been investigated. Calibration models showing good performance were obtained using SCIO, Linksquare operating in visible mode, and Linksquare operating in NIR mode (Table 11).

In the case of SCIO (740-1070 nm), the best model for DM exhibits cross validation values of 0.92 and 0.739% for R^2 and RMSE, respectively. The best model case for TSS exhibits cross validation values of 0.845 and 1.354 °Brix for R^2 and RMSE, respectively. On the other hand, the best model for pH had an R^2 value of 0.744 and an RMSE value of 0.400. Unfortunately, the models for firmness and TA were poor, with low R^2 and high RMSE values.

In case of Linksquare (400-1000 nm), the best models for investigation mango quality parameters with high R^2 and low RMSE were obtained using the instrument operating in the visible mode (400-1000). In comparison, the results of calibration and cross validation obtained by using the instrument operating in the NIR mode (700-1050 nm) exhibit significant drops in the R^2 values.

Moreover, the calibration models developed using data acquired with the TI and Neospectra spectrometers exhibited poor performance for all of quality parameters.

Table 11 Best R² values for calibration and cross-validation (in brackets) for mango quality parameters obtained by collecting calibration data using the commercial spectrometers.

	SCiO	Linksquare (visible)	Linksquare (NIR)	NIRscan nano	Neospectra
Dry Matter	0.92	0.81 (0.64)	0.86 (0.62)	0.63 (0.48)	0.70 (0.57)
TSS	0.84	0.91 (0.75)	0.76 (0.50)	0.66 (0.50)	0.77 (0.55)
TA	0.50	0.91 (0.79)	0.85 (0.51)	0.42 (0.38)	0.42 (0.20)
pH	0.74	0.93 (0.81)	0.86 (0.44)	0.69 (0.49)	0.71 (0.45)
Firmness	0.26	0.74 (0.37)	0.49 (0.31)	0.17 (0.045)	0.33 (0.18)

Spectral characteristics of mango and reference measurements

In general, fruits contain around 80-90% of water and different compounds such as starch, carbohydrates, chlorophyll, organic acids, and other organic molecules. [26] Therefore, the NIR spectral data show wide and complex bands as the results of hydrogen bonding interactions with these molecules. The water band is usually present at approximately 970 nm. This band is related to the second overtone of the O-H stretch of water molecules . [3]

Starch and sugars found in mangoes and tomatoes normally exhibit strong water absorptions at 970 nm. Features at approximately 910 nm to 920 nm are related to the 2nd overtone of the O-H stretch. The absorption band at 750 nm is usually related to the 4th overtone of the C-H stretching vibration. [45, 46]

Organic acids generally show bands related to the O-H group. The bands are related to second and third overtone at around 1000 nm and 800 nm, respectively. [47]

Chlorophylls are responsible for green colors in young fruits. The strong bands related to chlorophyll content can be observed at approximately 670 nm to 680

nm. Moreover, the ripening process of the fruit is related to the change of contents of chlorophyll, carotenoids, and anthocyanins. [8]

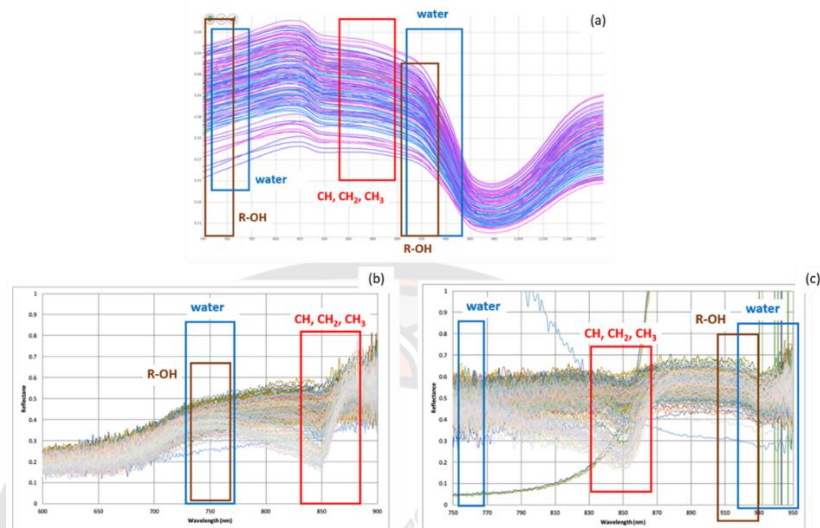


Figure 55 Plot of reflectance versus wavelength marking important spectral features acquired using (a) SCIO (b) Linksquare with visible mode (c) Linksquare with NIR mode

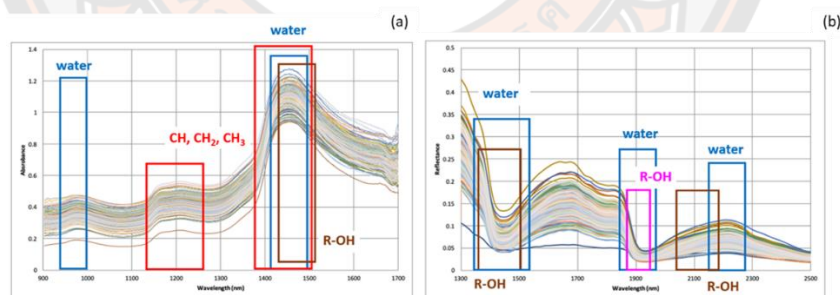


Figure 56 (a) Plot of Absorbance versus wavelength spectra using NIRScan Nano (b) Plot of percentage of reflectance spectra using Neospectra for important spectra acquired with mango samples

Dry matter (DM)

The DM content is a measurement of the residual mass of an object after being completely dried. Thus, DM refers to the material remaining after removal of

water, while the moisture content reflects the amount of water present in a sample. The water content of mangoes is usually high at the harvest time and decreases during the ripening process. [48]

Figures 55 and 56 show plots of reflectance versus wavelength acquired using the SCiO, LS, NIRScan nano, and Neospectra spectrometers. These plots show how the variability of water content results in spectral variability in the regions of 930 and 950 nm for Linksquare, and SCiO spectrometers, respectively. Furthermore, the features at 1450, 1900, and 2250 nm present in the spectra acquired with the NIRScan Nano and Neospectra instruments are related to water absorption as well. Spectral features at these wavelengths make it possible to characterize the DM content of mangoes.

The results show that the SCiO and Linksquare spectrometers operating in visible and NIR modes exhibit strong performance with high R^2 and low RMSE values. The cross validation R^2 for model predicting DM obtained using the SCiO instrument was 0.92. The ability of spectral data obtained using the SCiO instrument to result in good predictive model for DM is likely related to the responsiveness of the 950 nm feature to DM. In the case of the Linksquare spectrometer operating in the visible range the resulting models for predicting DM have shown R^2 values of calibration and cross-validation (in brackets) of 0.81 (0.64) and 0.86 (0.62). The ability of spectral data obtained using the Linksquare instrument to result in good predictive models for DM is likely related to the responsiveness of the 930 nm feature to DM. The spectral features at 1450, 1900, and 2250 nm accessible by the DLP NIRscan Nano and Neospectra instruments gave models with moderate performance showing R^2 values below 0.70.

Table 12 provides a comparison of the performance of predictive models for DM from two previous reports and this work. The first report was published by Neto and coworkers in 2017 [4]. This work was performed using the portable F750 spectrometer operating in the Vis-NIR range 310-1100 nm. The model for prediction of DM obtained in this work exhibited R_c^2 value of 0.84, which is below the performance of the predictive models reported herein obtained from spectral data acquired with the SCiO and Linksquare (VIS mode) spectrometers. The reported model performance is comparable to the results obtained herein for the Linksquare

spectrometer operating in the NIR mode. The second publication was reported by the same group in 2019 [49]. In addition, the authors have carried out the work using the same instrument. The results indicate that the resulting models had R_c^2 value of 0.70 for predicting DM, which is below the performance of the predictive models reported herein based on data acquired using the SCiO and Linksquare (VIS and NIR mode) spectrometers.

Total soluble solids content (TSS)

The TSS content is defined as the amount of soluble solid materials present in samples including sugars and soluble minerals. The TSS values can change because of the conversion of complex carbohydrates into simple sugars. Usually, the TSS values increase during the ripening process. [48]

As mentioned above, Figure 55-56 shows plots of reflectance versus wavelength obtained using SCiO, LS, NIRScan nano, and Neospectra spectrometers. These plots show that strong variability is present in the spectral regions around 750 and 800 nm for Linksquare and SCiO, respectively, which can be attributed to varying starch content. Thus, data from these wavelengths make it possible to characterize the TSS content.

The best R^2 values for predicting TSS shown in Table 11 indicate that Linksquare operating in visible and NIR modes provides data leading to well performing calibration models with high R^2 values and low RMSE values. The cross validation R^2 value for model based on data acquired with the SCiO spectrometer for predicting TSS was 0.84. The ability of spectral data obtained using the SCiO instrument to result in good predictive models for TSS is likely related to the responsiveness of the 800 nm feature to TSS. The Linksquare instrument operating in the visible mode provided spectral data leading to calibration models with R^2 values for calibration and cross-validation (in brackets) for TSS of 0.91 (0.75). The ability of this spectral data to result in good calibration models for TSS is likely related to the responsiveness of the feature at 750 nm acquired by Linksquare, related to the 4th overtone of the C-H stretch, to TSS and starch content.

Results from four publications reporting the predictive models for total soluble solids (TSS) or soluble solid content (SSC) are shown in Table 12. The first

one was published by Jha and coworkers in 2012 [28]. This work was conducted with the portable Luminar 5030 spectrometer operating in the wavelength range 1200-2200 nm. The model for prediction TSS obtained in this work had an R_c^2 value of 0.56, which is significantly worse than the results obtained in this work. Secondly, Rungpichayapichet and coworkers have published two reports in 2016 and 2017 [29, 50]. In their first work, they studied the performance of HandySpect Field 1000 spectrometer operating in the range 700-1100 nm. The results indicated that the models for the prediction of TSS could be obtained with R_c^2 and R_p^2 values of 0.80-0.90, which is comparable to the results obtained herein for the SCiO and Linksquare (VIS mode). In their second work, the authors also used the HandySpect Field 1000. However, the R_c^2 values obtained in this work were in the range 0.40-0.50, which is significantly worse than the results obtained herein. Finally, a publication from Neto and coworkers was reported in 2017 [4]. This work was conducted with the F-750 spectrometer. The reported model for the prediction of TSS and exhibits R_c^2 of 0.87, which is comparable to the results obtained herein for SCiO and Linksquare (VIS mode).

Titratable acidity (TA) and pH

TA and pH are two interrelated concepts in food analysis that analyze sample acidity. TA and pH are attributed to the conversion of citric acid and ascorbic acid to sugars and other compounds. Usually, the acidity of mangoes decreases during the ripening process. Concomitantly, the TA decreases and the pH increases. [48]

Figure 55-56 show plots of reflectance versus wavelength acquired using the SCiO, LS, NIRScan nano, and Neospectra spectrometers. These plots show that the variability of sugar and acidity content in mangoes correlates with spectral changes in the regions of 750 and 930 nm. The results above show that only Linksquare operating in visible and NIR modes provides spectral data leading to models with strong performance characterized by high R^2 and low RMSE values.

The R^2 values of calibration and cross-validation (in brackets) for predicting TA using Linksquare operating in visible and NIR modes were 0.91 (0.79) and 0.85 (0.51), respectively. The R^2 values of calibration and cross-validation (in brackets) for predicting pH using Linksquare operating in visible and NIR modes were 0.93 (0.81),

and 0.86 (0.44), respectively. The ability of the spectral data obtained from using the Linksquare instrument is a good predictive models for TA and pH and it is likely that the responsiveness of the 750 nm feature related to the 4th overtone of the C-H stretch, and the feature at 930 nm, related to the 2nd overtone of O-H stretch in sugars, to TA and pH.

Three previous reports for predicting the performance of TA and pH are shown in Table 12. Rungpichayapichet and coworkers have published two reports for predicting TA in 2016 and 2017 [29, 50]. They have conducted measurements with the HandySpect Field 1000 spectrometer operating in the range 700-1100 nm. The model developed for the prediction of TA was obtained with R_c^2 and R_p^2 values of about 0.74-0.85, which is below performance of the models obtained here in for the LS operating with VIS mode. Jha and coworkers have published work containing models for pH prediction in 2012 [28]. The models exhibited an R_c^2 value of 0.49, which is significantly worse than the results obtained herein.

Firmness

Firmness describes the crispness of fruit. One of the easiest ways to measure firmness is by applying pressure. There are several instruments available to test firmness called pressure testers and penetrometers. The trend of decreasing firmness values during ripening is attributed to cell wall decomposition through the digestion by pectinesterase, polygalacturonase, and other enzymes. This process leads to decreases in firmness values during the ripening process. As shown above, all of the commercial spectrometers studied herein provided data that resulted in models with poor predictive performance for mango firmness. [48]

Finally, four publications report model development for predicting firmness values. Rungpichayapichet and coworkers have published two reports in 2016 and 2017 as mentioned above [29, 50]. The first work has shown models with R_c^2 values of 0.82-0.90 for predicting firmness. The R_p^2 values for these models were 0.70-0.90. The second work has obtained R_c^2 values of 0.77-0.81 for predicting firmness. Mishra and coworkers have reported work based on data measured with the portable spectrometer F-750 operating in the Vis-NIR range 310-1100 nm in 2020 [51].

Models for the predicting firmness were obtained and R_c^2 and R_p^2 values were 0.62-0.75, and 0.67-0.75, respectively. The last publication reporting evaluation of the firmness models was reported by Kasim and coworkers in 2021 [11]. They conducted their work with the SCiO spectrometer. Models for prediction firmness were obtained with R_p^2 values of 0.77-0.94. All four publications report models with significantly better performance than that of the models in this work.

Overall, except of predictive models for firmness, good performance was achieved for models for mango quality parameters.



Table 12 Comparison of performance of models for mango quality parameters reported in previous literature and describe in this work

Reference	Instrument	Wavelength (nm)	DM		TSS/SSC		TA		pH		Firmness	
			R_c^2 (R_p^2)	N.D.	R_c^2 (R_p^2)	0.56	R_c^2 (R_p^2)	N.D.	0.49	R_c^2 (R_p^2)	N.D.	R_c^2 (R_p^2)
Jha et al., 2012 [28]	Luminar 5030	1200-2200	N.D.	N.D.	0.56	N.D.	N.D.	0.49	N.D.	N.D.	N.D.	N.D.
Rungpichayapichet, Mahayothee, Nagle, Khuwijitjaru, & Müller, 2016 [29]	HandySpec Field1000	700-1100	N.D.	N.D.	0.80-0.90 (0.8-0.9)	0.74-0.85 (0.74-0.83)	N.D.	N.D.	N.D.	0.82-0.90 (0.71-0.90)	N.D.	N.D.
João Paixão dos Santos Neto et al., 2017 [4]	F750	310-1100	0.84*	0.87*	N.D.	N.D.	N.D.	N.D.	N.D.	N.D.	N.D.	N.D.
Rungpichayapichet, Nagle, Yuwanbun, Khuwijitjaru, Mahayothee, &	UHD285	450-998	N.D.	0.40-0.50	0.69-0.81	N.D.	N.D.	N.D.	0.77-0.81	N.D.	N.D.	N.D.



4.1.2 Testing the performance of commercial spectrometers for non-destructive determination of tomato.

Sample preparation

The tomato (cherry tomato) samples were obtained from fresh produce markets (Phitsanulok, Kamphaeng Phet and Phetchabun) and local retail stores in Phitsanulok (Central plaza, Macro). The number of samples and source locations are summarized in Table 13.

Table 13 Numbers of samples based on location of collection for commercial portable spectrometers for tomato.

Source Location	N
Phitsanulok	60
Kamphaeng Phet	10
Phetchabun	291
Central plaza	10
Macro	66
Total	480

Total 480 samples were obtained in this work. Tomatoes were washed with water to remove the gum and make them clean. After cleaning, the samples were stored at ambient conditions. Four sampling areas (1x1cm) on the surface of the samples were used for DM, TSS, TA, and pH analyses. A single sampling area was used for firmness analysis. Spectroscopic measurements were performed on the surface of these areas as shown in Figure 57-58.

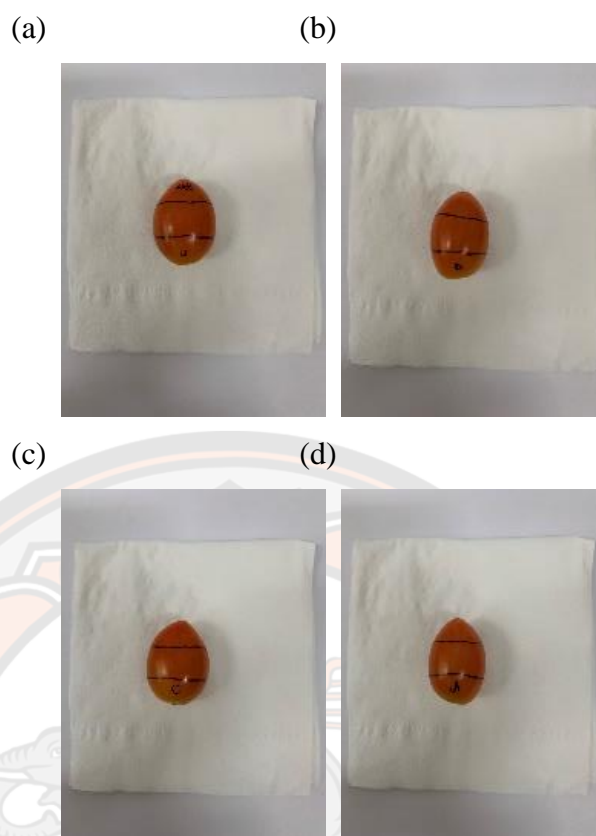


Figure 57 Representative images of sampling sides (a) first (b) second (c) third and (d) fourth side of a tomato sample used for DM, TSS, TA, and pH analysis.



Figure 58 Representative image of sampling area of a tomato sample used for firmness analysis.

Data Acquisition of commercial spectrometers for tomato.

Spectroscopic measurements at the selected areas were performed using three commercial spectrometers (SCIO, Linksquare, and NIRScan Nano). The sampling interface of the Neospectra spectrometer is too large to allow measurements on cherry tomatoes. Sixteen spectra were recorded and averaged for each sample for the determination of DM, TSS, TA, and pH. Four spectra were measured and averaged for each sample for firmness determination. The averaged spectra were subsequently used to perform the chemometric analysis. The reference standard analyses were split into three groups. Samples in the first group were used for dry matter (DM) determination. The second group was used for total soluble solids (TSS), titratable acidity (TA), and pH analysis. Finally, the last group was used for firmness analysis including Firmness, Firmness1, Firmness2, Firmness3, Firmness4, and Firmness5. Spectroscopic measurements performed with these spectrometers on cherry tomato samples are shown in Figure 59 to Figure 61.

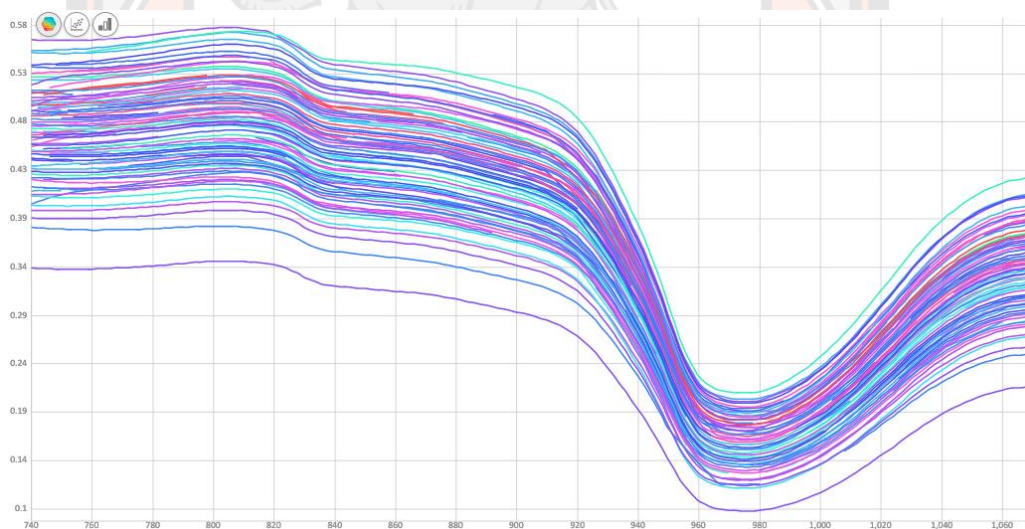
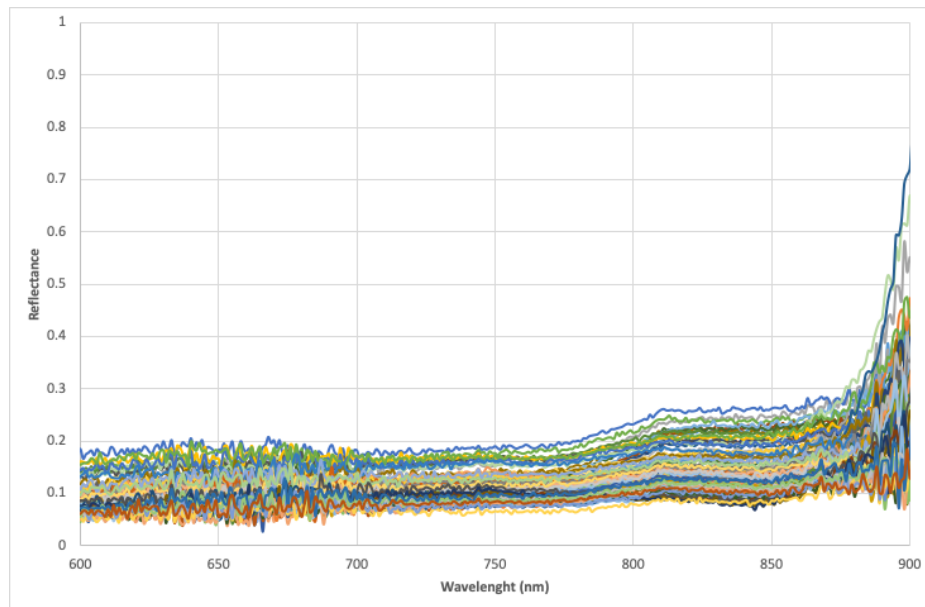


Figure 59 Plot of reflectance versus wavelength acquired using the SCIO spectrometer for tomato samples used to develop predictive models for dry matter

(a)



(b)

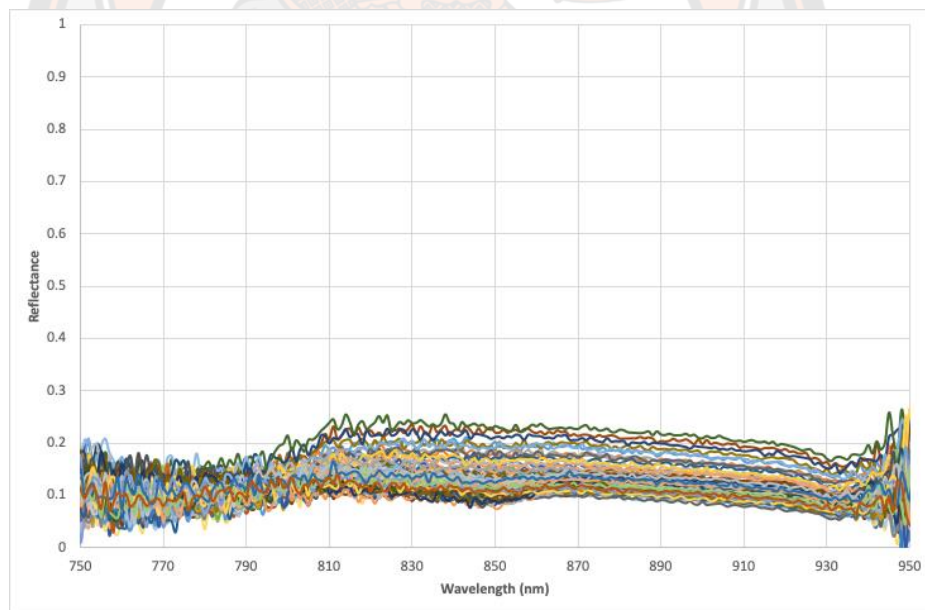


Figure 60 Plot of reflectance versus wavelength acquired using the Linksquare spectrometer operating in (a) visible (b) NIR modes for tomato samples used to develop predictive models for dry matter

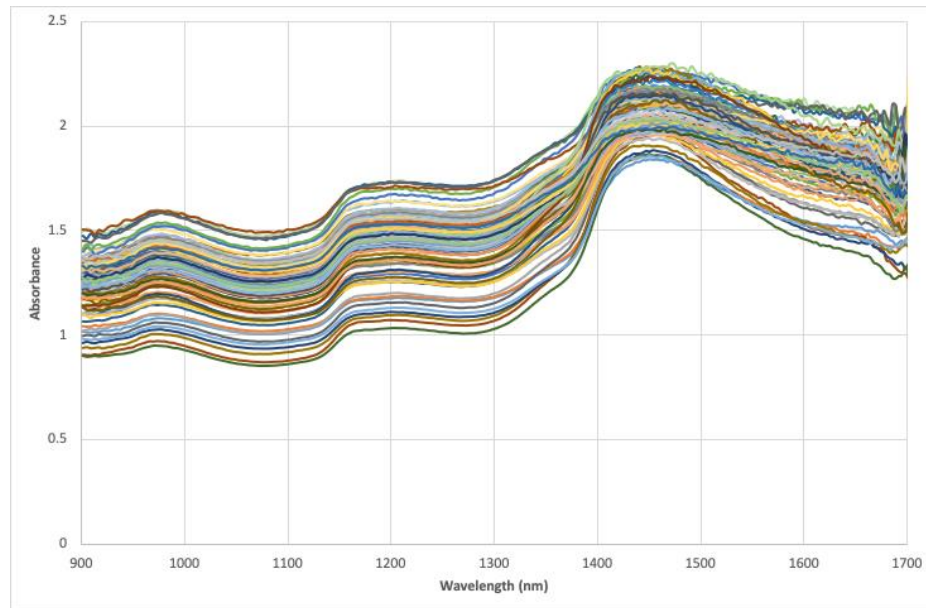


Figure 61 Plot of reflectance versus wavelength acquired using the TI NIRScan Nano spectrometer for tomato samples used to develop predictive models for dry matter

Reference analysis of cherry tomato quality parameters

Five quality parameters (DM, TSS, TA, pH, and firmness) were investigated for cherry tomato samples. The descriptive statistics for cherry tomato quality parameters are shown in Table 14. Table 14 shows average, minimum, maximum, and standard deviation values of the quality parameters of the tomato samples.

The average values of DM, TSS, TA, and pH were 5.2%, 4.2°Brix, 0.61%, and 4.21, respectively. The average firmness values for Firmness, Firmness1, Firmness2, Firmness3, Firmness4, and Firmness5 parameters were 5.64N, 32.53N, 8.28N, 17.46N, 2.39N/mm, and 2.48N/mm, respectively.

Table 14 Descriptive statistics for quality parameters analyzed in tomato samples using commercial spectrometers

parameter	N	Average	Std
DM (%)	100	5.2	0.6
TSS (°Brix)	100	4.2	0.48
TA (%)	100	0.61	0.20
pH	100	4.21	0.18
Firmness (N)	100	5.64	1.73
Firmness1 (N)	100	32.53	8.52
Firmness2 (N)	100	8.28	2.60
Firmness3 (N)	100	17.46	5.51
Firmness4 (N/mm)	100	2.39	0.68
Firmness5 (N/mm)	100	2.48	0.71

The firmness of tomatoes is influenced by several factors, including thickness, epidermal cell shape, and internal structures. Tomato firmness under tensile measurements is a mechanical property relevant to the characterization of processed tomatoes and related to ripening rate. For the work with tomatoes, firmness analysis can be divided into six firmness parameters including Firmness, Firmness1, Firmness2, Firmness3, Firmness4, and Firmness5.

Firmness was recorded at plunger insertion depth of 1.9 mm, which corresponds to the insertion of the head the steel plunger. It expresses the firmness of the tomato skin under reversible conditions.

Firmness1 was recorded at the maximum load value of the samples. It expresses the maximum firmness capacity of the tomato samples.

Firmness2 was recorded at the first linear region, as described above, at penetration depth of 3 mm. It expresses the firmness of the tomato skin and tomato upon entry into irreversible condition.

Firmness3 was recorded at the second linear region, as described above, at penetration depth of 7 mm. It expresses the firmness of the tomato skin and tomato upon entry into irreversible condition.

Firmness4 was obtained from the tensile instrumentation as the slope of the tensile curve in the second linearity region (from 4 mm to maximum firmness).

$$Firmness4 = \frac{Load_{max} - Load_{4mm}}{Com_{max} - Com_{4mm}}$$

It expresses the relation between load values in second linearity region and compressive extension of samples.

Firmness5 was measured as average slope of the curve up to maximum firmness (0 mm to maximum firmness).

$$Firmness5 = \frac{Load_{max} - Load_{0mm}}{Com_{max} - Com_{0mm}}$$

It expresses the relation between maximum load values and compressive extension of samples.

Data analysis

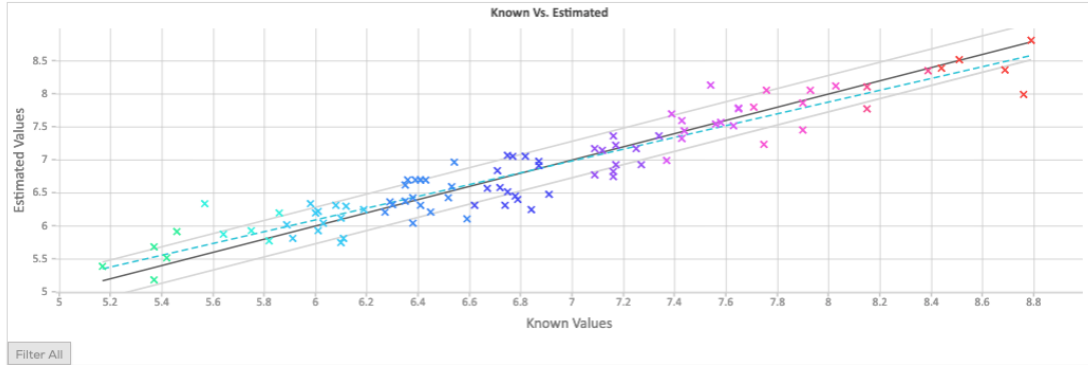
4.1.2.1 SCIO

The results indicate that possibility to utilize spectroscopic data acquired using the SCIO spectrometer to predict quality parameters of cherry tomato samples. Figure 62 shows the outcome for the development of the predictive models using spectroscopic data without preprocessing.

(a)

Target: Dry Matter

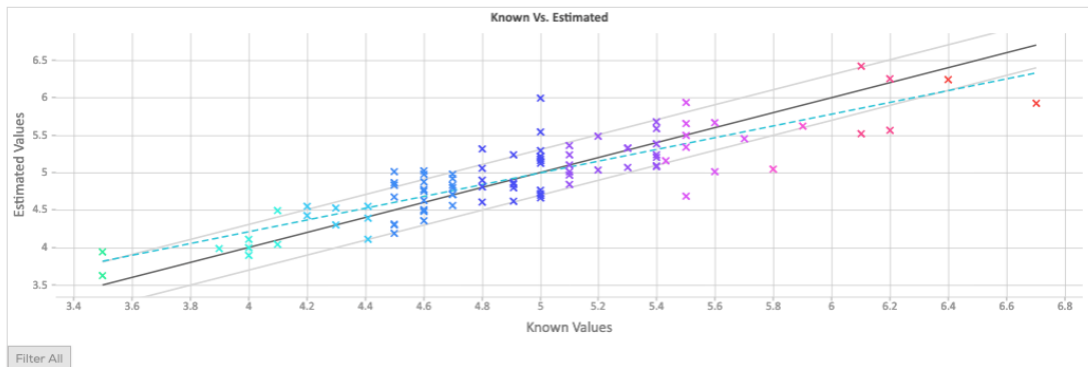
Performance: RMSE = 0.275 | R2 = 0.892 | SEP = 0.275 | precision = 0 | r2 = 0.892 | slope = 0.893 |



(b)

Target: TSS

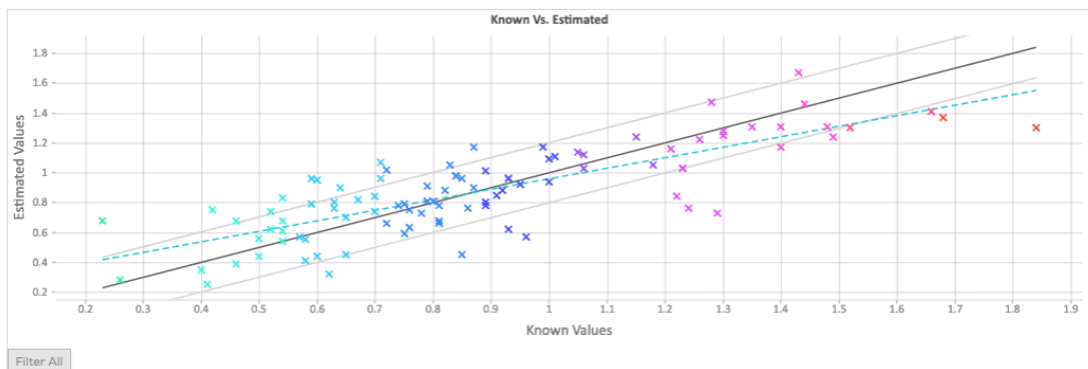
Performance: RMSE = 0.303 | R2 = 0.735 | SEP = 0.303 | precision = 0 | r2 = 0.738 | slope = 0.786 |



(c)

Target: TA

Performance: RMSE = 0.201 | R2 = 0.635 | SEP = 0.201 | precision = 0 | r2 = 0.642 | slope = 0.705 |



(d)

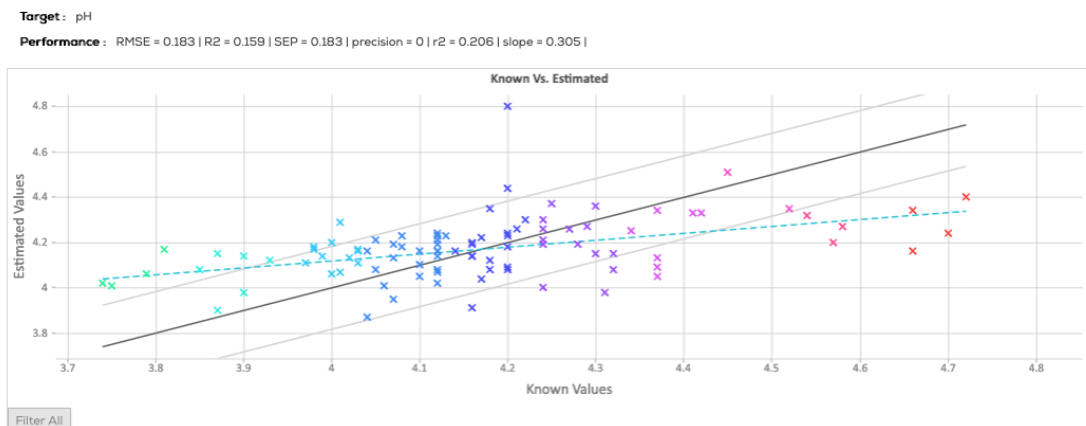


Figure 62. Plot of predicted versus measured values of tomato quality parameters obtained using spectral data acquired with the SCIO spectrometer used without pretreatment for (a) DM (b) TSS (c) TA, and (d) pH

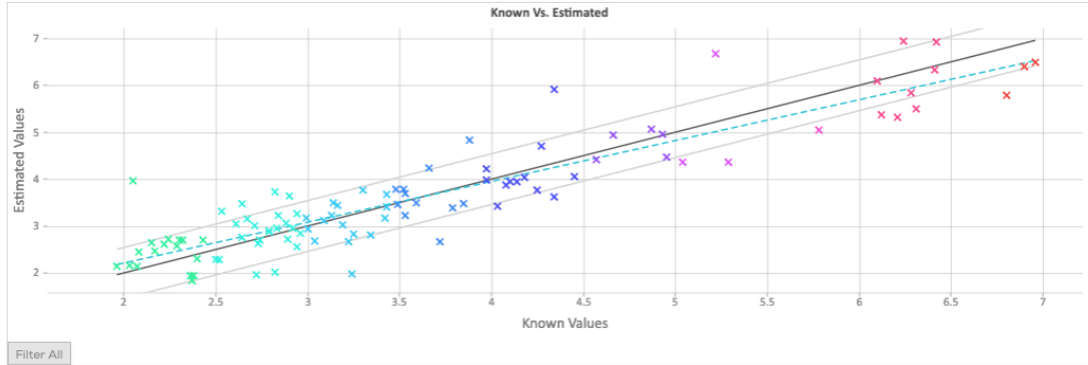
As can be seen in Figure 62, the results show that the R^2 values for cross validation were 0.892, 0.735, 0.635, and 0.159 for DM, TSS, TA, and pH, respectively. The RMSE values were 0.275%, 0.303 °Brix, 0.201%, and 0.183 for DM, TSS, TA, and pH, respectively.

The models developed with spectral data acquired with the SCIO spectrometer without preprocessing exhibit good performance with R^2 over 0.80 values for DM. For TSS and TA moderate R^2 values have been obtained. Finally, the calibration model for pH exhibits poor performance.

(a)

Target: Firmness

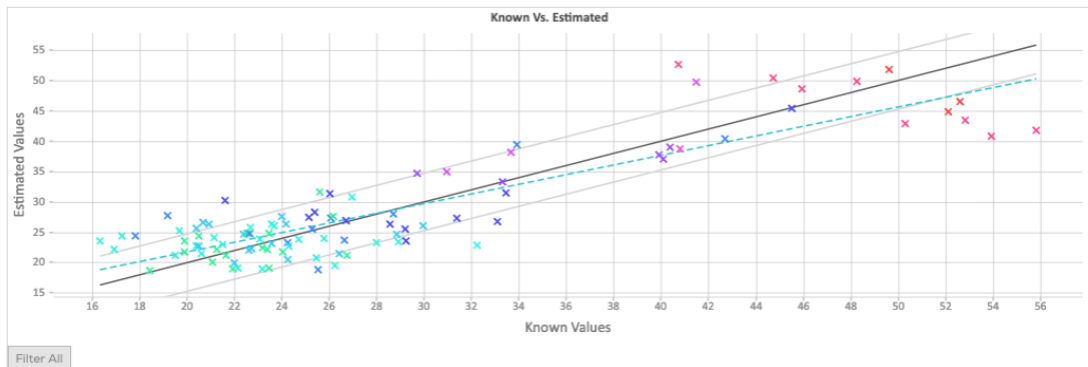
Performance: RMSE = 0.545 | R2 = 0.821 | SEP = 0.545 | precision = 0 | r2 = 0.823 | slope = 0.869 |



(b)

Target: Firmness1

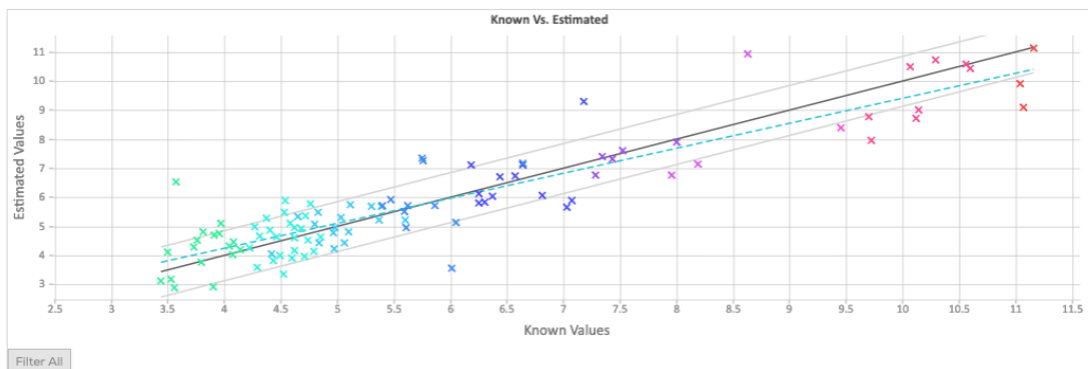
Performance: RMSE = 4.701 | R2 = 0.76 | SEP = 4.701 | precision = 0 | r2 = 0.761 | slope = 0.796 |



(c)

Target: Firmness2

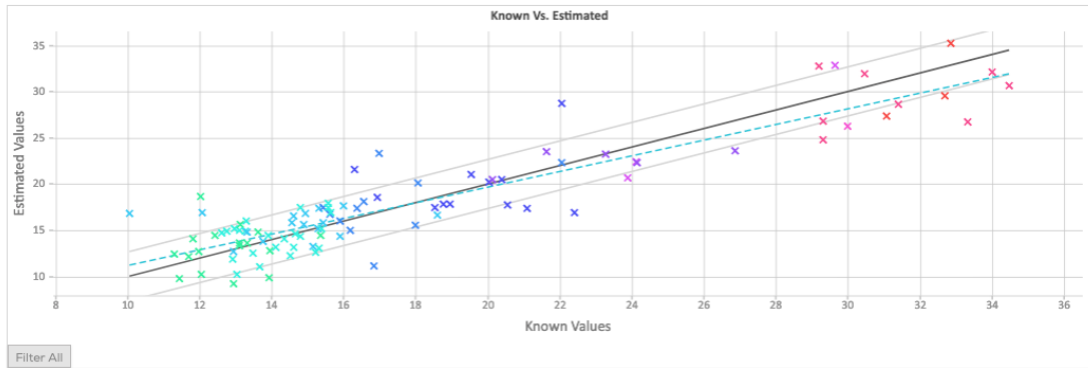
Performance: RMSE = 0.861 | R2 = 0.82 | SEP = 0.86 | precision = 0 | r2 = 0.822 | slope = 0.862 |



(d)

Target: Firmness3

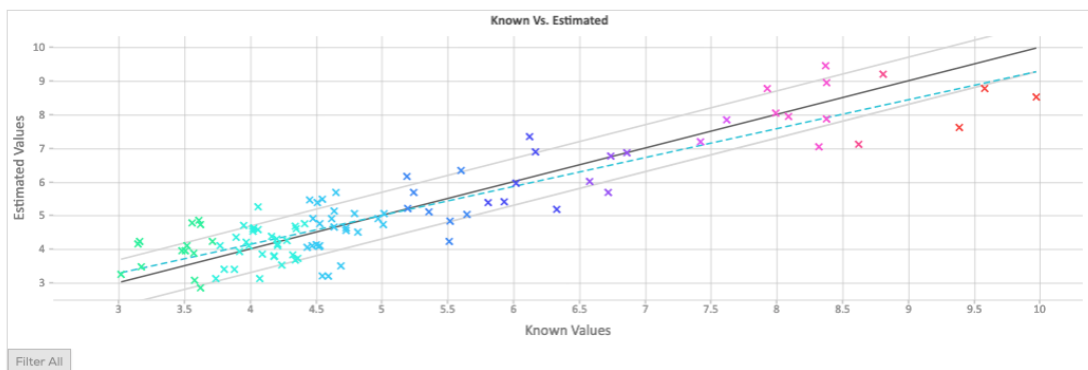
Performance: RMSE = 2.653 | R2 = 0.816 | SEP = 2.653 | precision = 0 | r2 = 0.817 | slope = 0.848 |



(e)

Target: Firmness4

Performance: RMSE = 0.696 | R2 = 0.814 | SEP = 0.696 | precision = 0 | r2 = 0.816 | slope = 0.859 |



(f)

Target: Firmness5

Performance: RMSE = 0.407 | R2 = 0.814 | SEP = 0.407 | precision = 0 | r2 = 0.816 | slope = 0.852 |

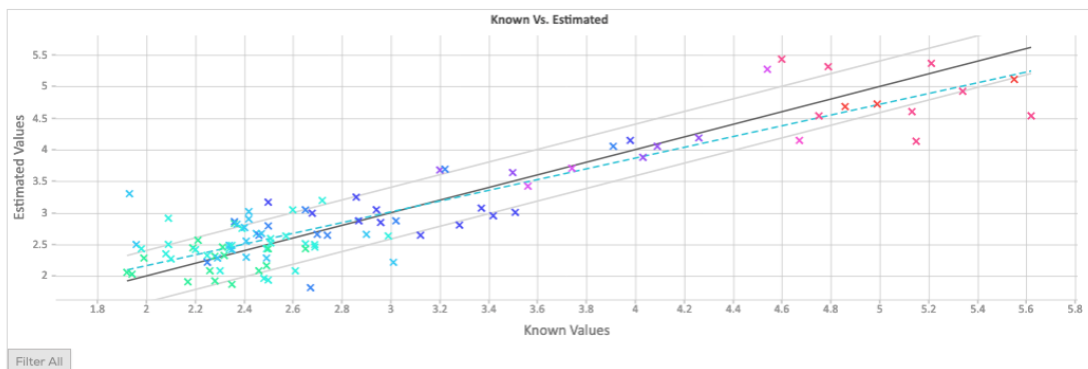
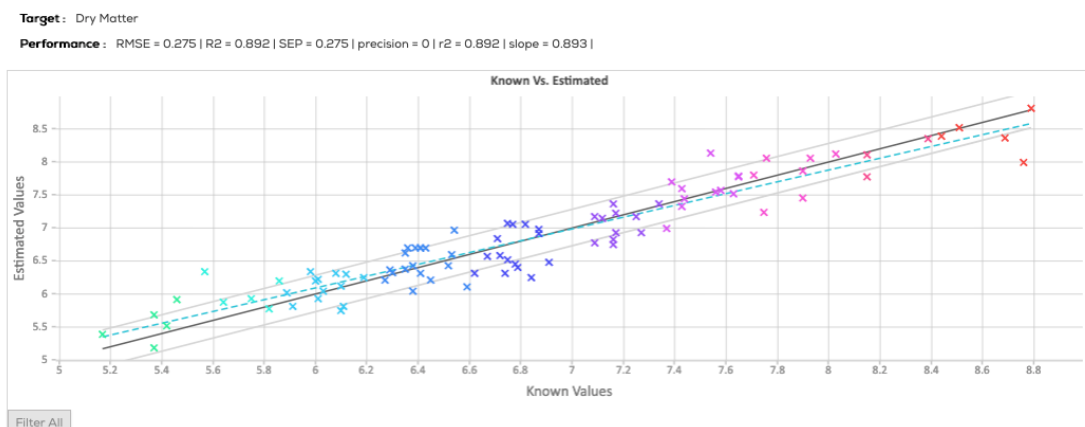


Figure 63 Plot of predicted versus measured values of investigated tomato firmness parameters obtained using spectral data acquired with the SCIO spectrometer and used without preprocessing for (a) Firmness (b) Firmness1 (c) Firmness2 (d) Firmness3 (e) Firmness4 and (f) Firmness5

Figure 63 shows the R^2 values for the cross validation of calibration models for the investigated tomato firmness parameters. The R^2 values are 0.821, 0.760, 0.820, 0.816, 0.814, and 0.814 for firmness, firmness1, firmness2, firmness3, firmness4, and firmness5, respectively. The RMSE values were 0.545N, 4.701N, 0.861N, 2.653N, 0.696N/mm, and 0.407N/mm for Firmness, Firmness1, Firmness2, Firmness3, Firmness4, and Firmness5, respectively.

The calibration models for tomato firmness parameters developed without preprocessing using spectral data acquired with the SCIO spectrometer exhibit very good figures of merit. The R^2 value for firmness 1 is 0.760 while the values for the other parameters are above 0.80.

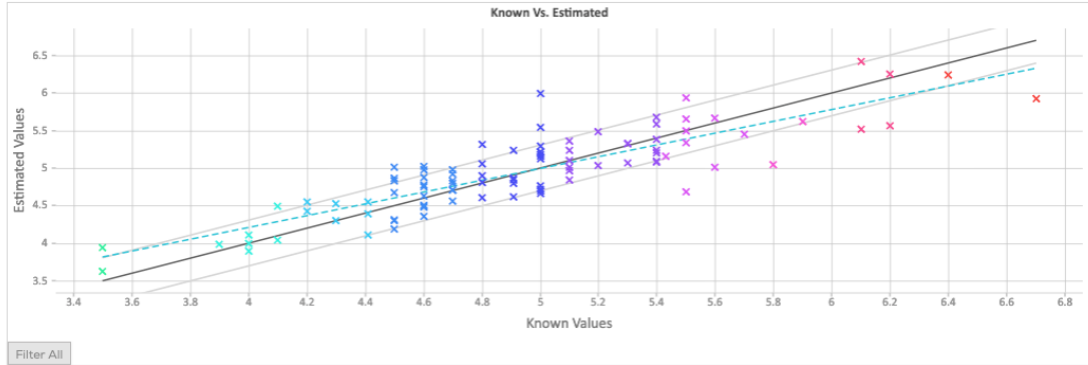
(a)



(b)

Target : TSS

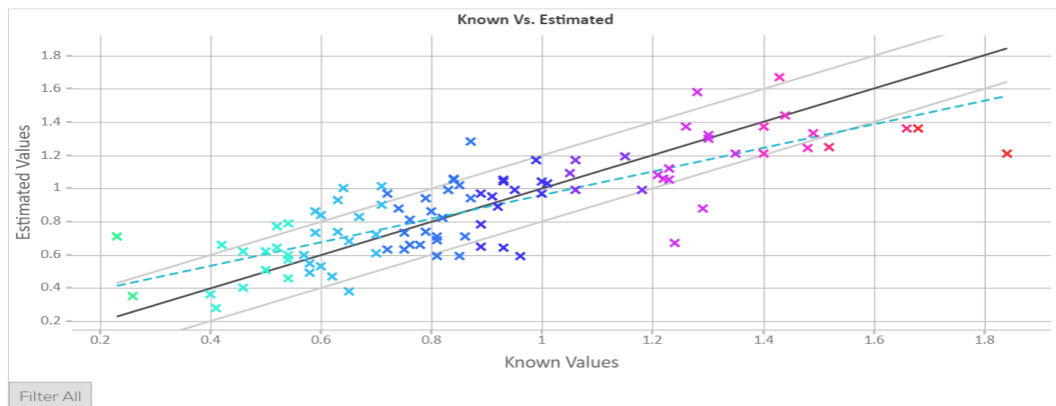
Performance : RMSE = 0.303 | R2 = 0.735 | SEP = 0.303 | precision = 0 | r2 = 0.738 | slope = 0.786 |



(c)

Target : TA

Performance : RMSE = 0.198 | R2 = 0.644 | SEP = 0.198 | precision = 0 | r2 = 0.65 | slope = 0.709 |



(d)

Target : pH

Performance : RMSE = 0.176 | R2 = 0.215 | SEP = 0.176 | precision = 0 | r2 = 0.229 | slope = 0.286 |

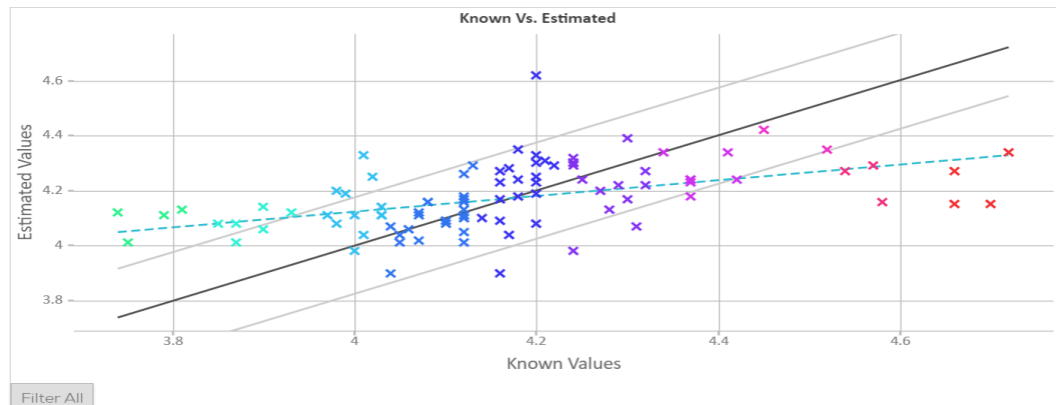
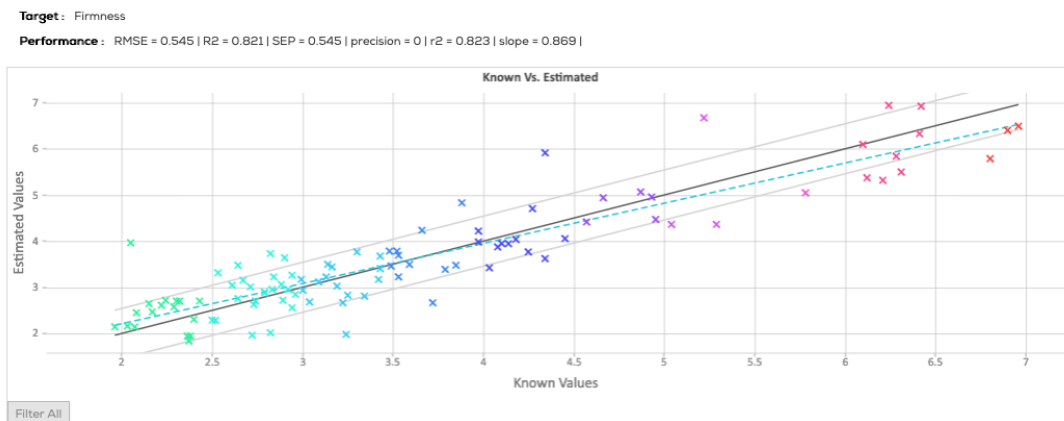


Figure 64 Plot of predicted versus measured values of tomato quality parameters for the calibration models with the best figures of merit obtained using spectral data acquired with the SCIO spectrometer for (a) DM (b) TSS (c) TA and (d) pH

(a)



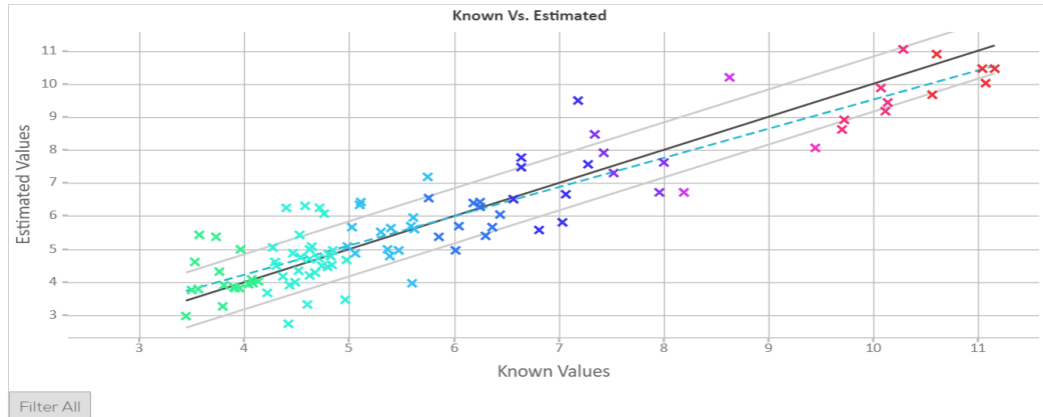
(b)



(c)

Target: Firmness2

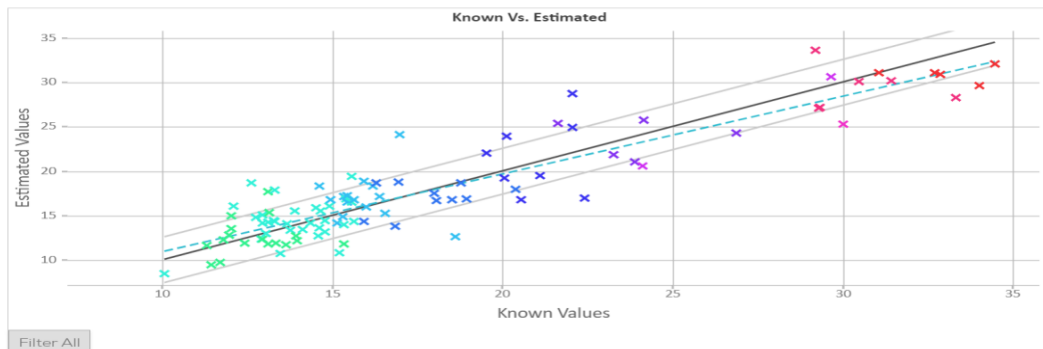
Performance: RMSE = 0.839 | R2 = 0.828 | SEP = 0.839 | precision = 0 | r2 = 0.832 | slope = 0.885 |



(d)

Target: Firmness3

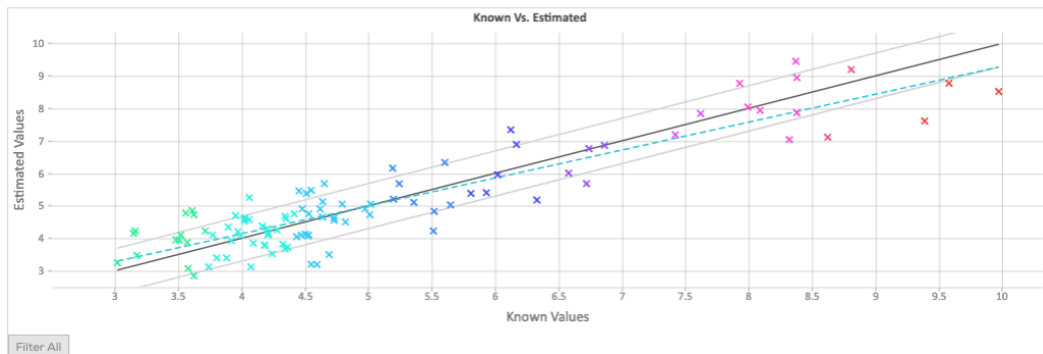
Performance: RMSE = 2.576 | R2 = 0.826 | SEP = 2.576 | precision = 0 | r2 = 0.829 | slope = 0.873 |



(e)

Target: Firmness4

Performance: RMSE = 0.696 | R2 = 0.814 | SEP = 0.696 | precision = 0 | r2 = 0.816 | slope = 0.859 |



(f)

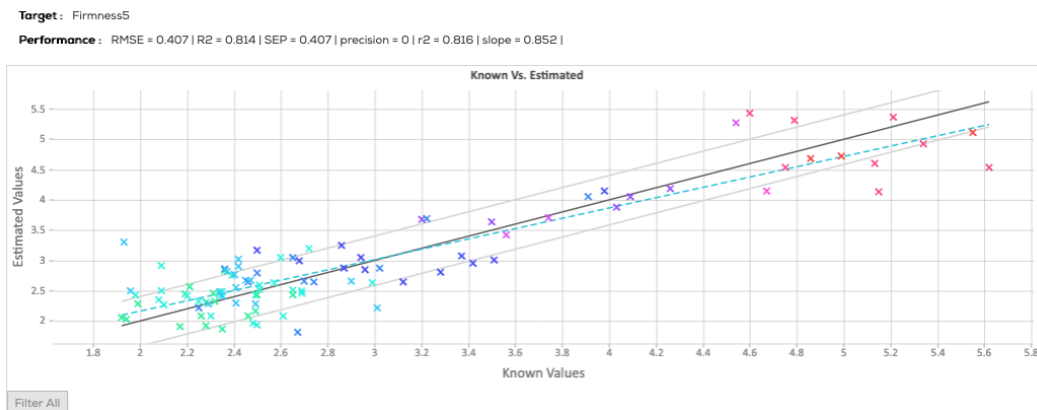


Figure 65 Plot of predicted versus measured values of tomato firmness parameters for the calibration models with the best figures of merit obtained using spectral data acquired with the SCIO spectrometer for (a) Firmness (b) Firmness1 (c) Firmness2 (d) Firmness3 (e) Firmness4 and (f) Firmness5

The figures of merit for the calibration models for tomato quality parameters with the best performance are shown in table 15. The results show that the best cross validation R^2 values are 0.892, 0.735, 0.644, and 0.215 for DM, TSS, TA, and pH respectively. The corresponding RMSE values for these models were 0.275%, 0.303 °Brix, 0.198%, and 0.176 for DM, TSS, TA, and pH, respectively. Unfortunately, in the case of DM and TSS, the R^2 values exhibit a significant drop when data preprocessing is used. On the other hand, slightly better models for TA and pH were obtained using pretreatment Procedure 1 and 2, respectively.

The best models for the investigated firmness parameters have cross validation R^2 values of 0.821, 0.760, 0.828, 0.826, 0.814, and 0.814 for firmness, firmness1, firmness2, firmness3, firmness4, and firmness5, respectively. The respective RMSE values were 0.545N, 4.701N, 0.839N, 2.575N, 0.696N/mm, and 0.407N/mm for firmness, firmness1, firmness2, firmness3, firmness4, and firmness5, respectively. The best models for firmness, firmness1, firmness4, and firmness5 were obtained without pretreatment while the best models for firmness2 and firmness 5 were pretreatment obtained with pretreatment Procedure 4.

Table 15 Best R² values for cross-validation for cherry tomato quality parameters using the SCIO spectrometers

parameter	pretreatment	Cross validation		
		R ²	RMSE	LV
Dry matter	None	0.892	0.275	8
TSS	None	0.735	0.303	14
TA	Procedure 1	0.644	0.198	8
pH	Procedure 2	0.215	0.176	6
Firmness	None	0.821	0.545	10
Firmness1	None	0.760	4.701	10
Firmness2	Procedure 4	0.828	0.839	9
Firmness3	Procedure 4	0.826	2.575	8
Firmness4	None	0.814	0.696	12
Firmness5	None	0.814	0.407	12

Procedure 1: Scan averaging, wavelength selection (790-1,070 nm), SNV;

Procedure 2: Scan averaging, spectrum smoothing and 1st derivative (2nd degree polynomial, Window: 35), wavelength selection (790-1,070 nm), SNV;

Procedure 3: Scan averaging, spectrum smoothing and 1st derivative (2nd degree polynomial, Window: 35), wavelength selection (790-1,070 nm), average subtraction;

Procedure 4: Logarithm, scan averaging, spectrum smoothing and 2nd derivative (2nd degree polynomial, Window: 35), (790-1,070 nm), SNV.

4.1.2.2 Linksquare

Figures 66 and 67 show the plots obtained for calibration models for tomato quality parameters obtained using spectral data acquired with the Linksquare spectrometer operating in the visible mode and used without preprocessing.

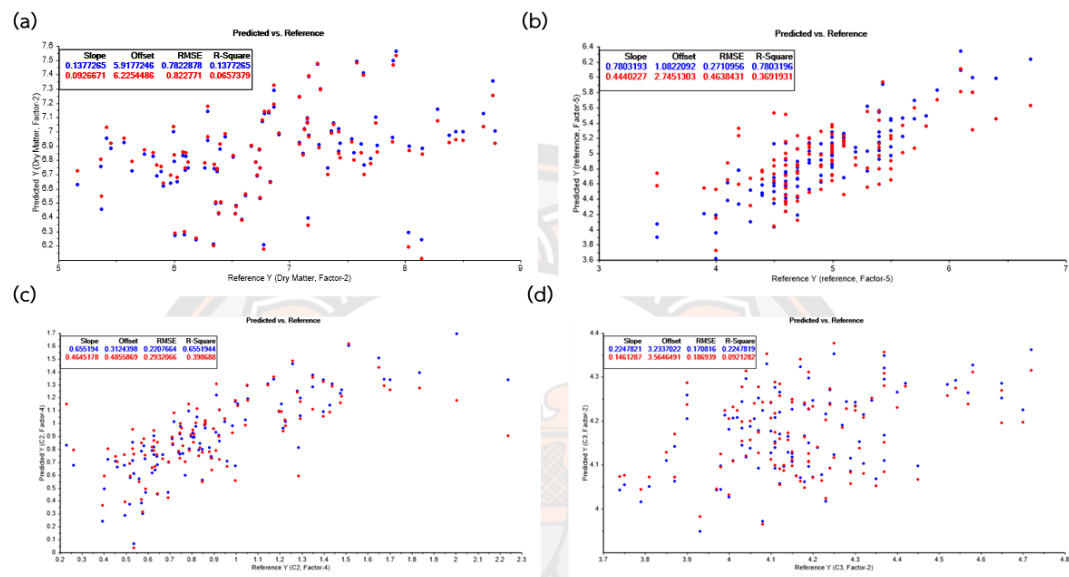


Figure 66. Plot of predicted versus measured values of tomato quality parameters obtained using spectral data acquired with the Linksquare spectrometer operating in the visible mode without pretreatment for predicting (a) DM (b) TSS (c) TA and (d) pH

The results indicate that the R^2 values for calibration and cross validation (in brackets) for the calibration models were 0.14 (0.07), 0.78 (0.37), 0.66 (0.40), and 0.22 (0.09) for DM, TSS, TA, and pH respectively. The respective RMSE values for calibration and cross validation (in brackets) were 0.78% (0.82%), 0.27 °Brix (0.46 °Brix), 0.22% (0.29%) and 0.17 (0.19) for DM, TSS, TA, and pH respectively. The obtained calibration models exhibit moderate performance for TSS and TA. The models for DM and pH are poor with low R^2 and high RMSE values.

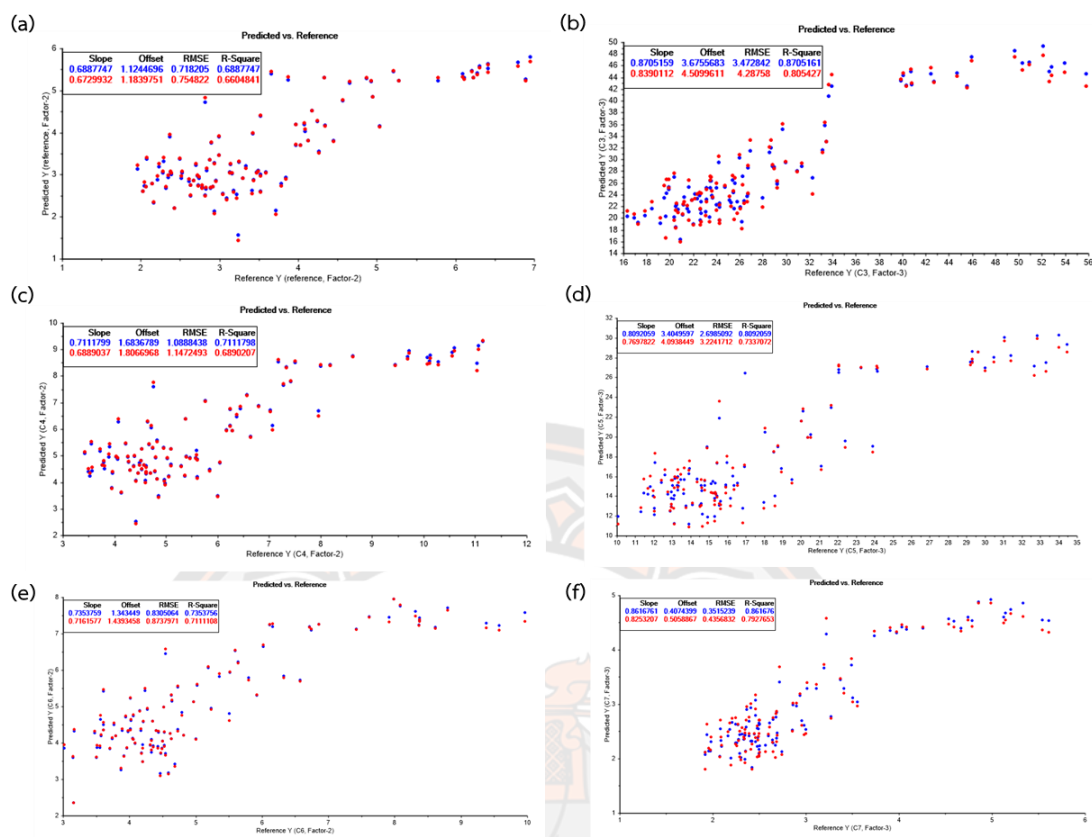


Figure 67. Plot of predicted versus measured values of tomato firmness parameters obtained using spectral data acquired with the Linksquare spectrometer operating in the visible mode without preprocessing for (a) Firmness (b) Firmness1 (c) Firmness2 (d) Firmness3 (e) Firmness4 and (f) Firmness5

Figure 67 shows the plots of calibration models for the investigated tomato firmness parameters obtained using spectral data acquired with the Linksquare spectrometer operating in the visible mode and made without pretreatment. The R^2 values of the obtained calibration models for calibration and cross validation (in brackets) are 0.69 (0.66), 0.87 (0.81), 0.71 (0.69), 0.81 (0.73), 0.74 (0.71), and 0.86 (0.79) for Firmness, Firmness1, Firmness2, Firmness3, Firmness4, and Firmness5, respectively. The RMSE values for the calibration and cross validation (in brackets) were 0.72N (0.75N), 3.48N (4.29N), 1.09N (1.15N), 2.70N (3.22N), 0.83N/mm (0.87N/mm), and 0.35N/mm (0.44N/mm) for Firmness, Firmness1, Firmness2,

Firmness3, Firmness4, and Firmness5, respectively. All calibration models show good performance for the investigated tomato firmness parameters.

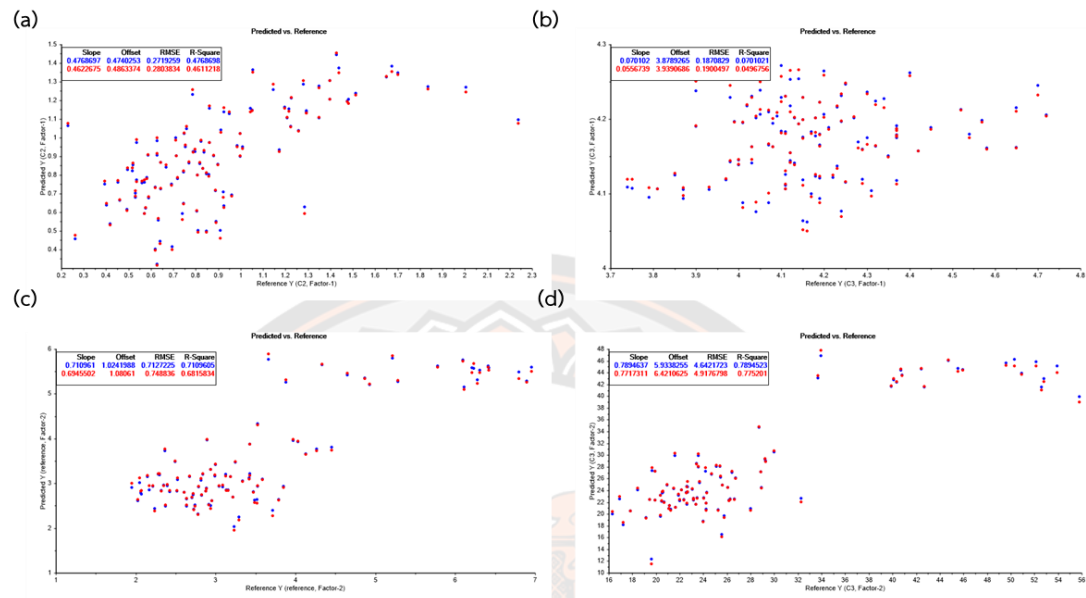


Figure 68. Plots of predicted versus measured values of tomato quality parameters obtained using spectral data acquired with the Linksquare spectrometer operating in the NIR mode without pretreatment for predicting (a) DM (b) TSS (c) TA and (d) pH

Figure 68 shows the plots for calibration models for tomato quality parameters obtained with spectral data acquired with the Linksquare spectrometer operating in the NIR mode without pretreatment. The results indicate that the R^2 values for calibration and cross validation (in brackets) are 0.18 (0.08), 0.06 (0.04), 0.48 (0.46), and 0.07 (0.05) for DM, TSS, TA, and pH respectively. The respective RMSE values for calibration and cross validation (in brackets) were 0.76% (0.82%), 0.56 °Brix (0.57 °Brix), 0.27% (0.28%) and 0.19 (0.19) for DM, TSS, TA, and pH respectively. The results exhibit models with moderate performance for TA and pH while the models for DM and TSS were poor with low R^2 values and high RMSE values.

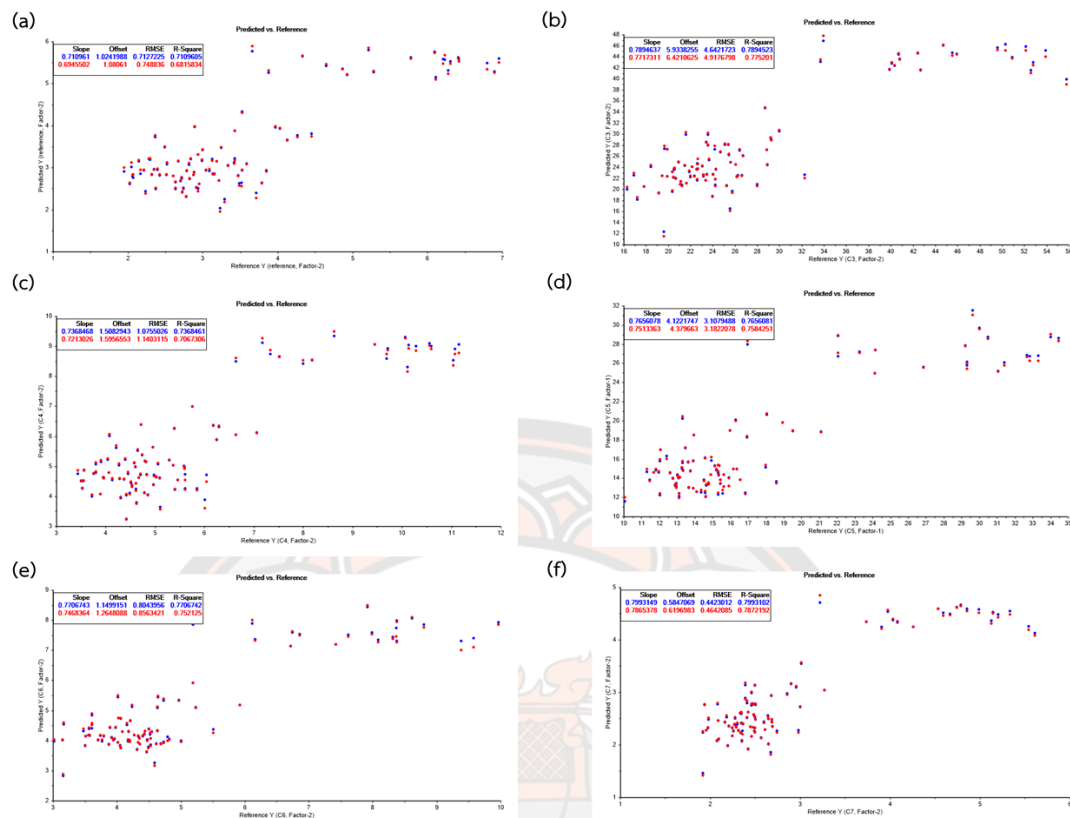


Figure 69. Plots of predicted versus measured values of tomato firmness parameters obtained using spectral data acquired with the Linksquare spectrometer operating in the NIR mode without preprocessing for (a) Firmness (b) Firmness1 (c) Firmness2 (d) Firmness3 (e) Firmness4 and (f) Firmness5

Figure 69 shows the plots for calibration models for the investigated tomato firmness parameters obtained with spectral data acquired with the Linksquare spectrometer operating in the NIR mode and made without pretreatment. The results indicated that the R^2 values for calibration and cross validation (in brackets) are 0.71 (0.68), 0.79 (0.78), 0.74 (0.71), 0.77 (0.76), 0.77 (0.75), and 0.80 (0.79) for Firmness, Firmness1, Firmness2, Firmness3, Firmness4, and Firmness5, respectively. The respective RMSE values for calibration and cross validation (in brackets) are 0.71N (0.75N), 4.64N (4.92N), 1.08N (1.14N), 3.11N (3.18N), 0.80N/mm (0.86N/mm), and 0.44N/mm (0.46N/mm) for Firmness, Firmness1, Firmness2, Firmness3, Firmness4,

and Firmness5, respectively. The results exhibit good performance predicted for all of firmness parameters.

The calibration models developed with data acquired with the Linksquare spectrometer operating in both visible and NIR modes and used without preprocessing gave models with good figures of merit for firmness analysis for firmness, Firmness1, Firmness2, Firmness3, Firmness4, and Firmness 5 exhibiting high R^2 values and low RMSE values for calibration and cross validation. Models for TSS and TA exhibited moderate performance. Finally, the results for DM and pH were unsatisfactory.

Unfortunately, the model developments with preprocessed data acquired with the Linksquare spectrometer operating in the NIR mode exhibit fairly significant drop in the R^2 values for calibration and cross validation.

The best cases for predicting quality parameters using Linksquare spectrometer for the visible and NIR mode were shown in Table 16.

Table 16 Best R^2 values for calibration and cross-validation for cherry tomato quality parameters using the LS spectrometers operating of the visible and NIR modes.

parameter	mode	Preprocessing	Calibration		Cross validation		LV
			R^2	RMSE	R^2	RMSE	
Dry matter	visible	Procedure 4	0.55	0.56	0.08	0.82	3
TSS	visible	None	0.78	0.27	0.37	0.46	5
TA	visible	None	0.66	0.22	0.40	0.29	4
pH	NIR	Procedure 1	0.69	0.11	0.14	0.18	3
Firmness	visible	Procedure 5	0.75	0.64	0.74	0.66	1
Firmness1	visible	Procedure 5	0.91	2.81	0.87	3.50	2
Firmness2	visible	Procedure 3	0.80	0.91	0.63	1.25	2
Firmness3	visible	Procedure 3	0.86	2.31	0.63	3.77	3
Firmness4	visible	Procedure 3	0.87	0.59	0.64	0.98	3
Firmness5	visible	Procedure 5	0.90	0.29	0.86	0.36	2

Procedure 1: Spectrum smoothing and 1st derivative (2nd degree polynomial, Window: 3);

Procedure 2: Spectrum smoothing and 1st derivative (2nd degree polynomial, Window: 21);

Procedure 3: Spectrum smoothing and 2nd derivative (2nd degree polynomial, Window: 3);

Procedure 4: Spectrum smoothing and 2nd derivative (2nd degree polynomial, Window: 21);

Procedure 5: SNV

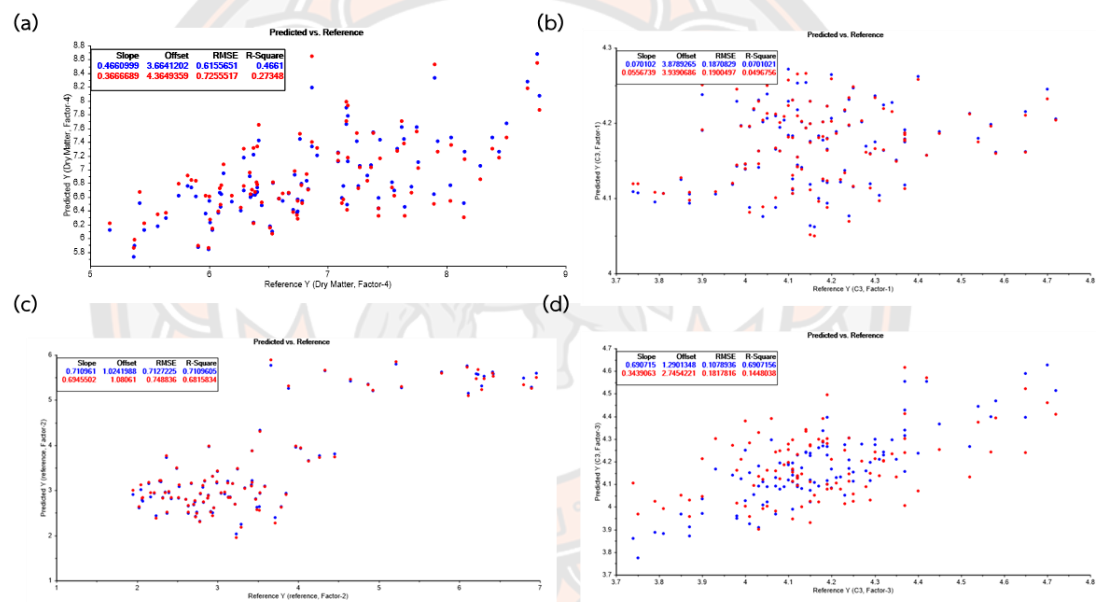


Figure 70 Plots of predicted versus measured values of tomato quality parameters for calibration models exhibiting the best figures of merit made with spectral data acquired with the Linksquare spectrometer for (a) DM (b) TSS (c) TA, and (d) pH

Figure 70 shows that good performing calibration models for calibration and cross validation were obtained for TSS and TA. These R^2 values for these models in calibration and cross validation are 0.78 (0.37), and 0.66 (0.40) for TSS and TA,

respectively. The models for DM and pH were unsatisfactory with R^2 values below 0.20.

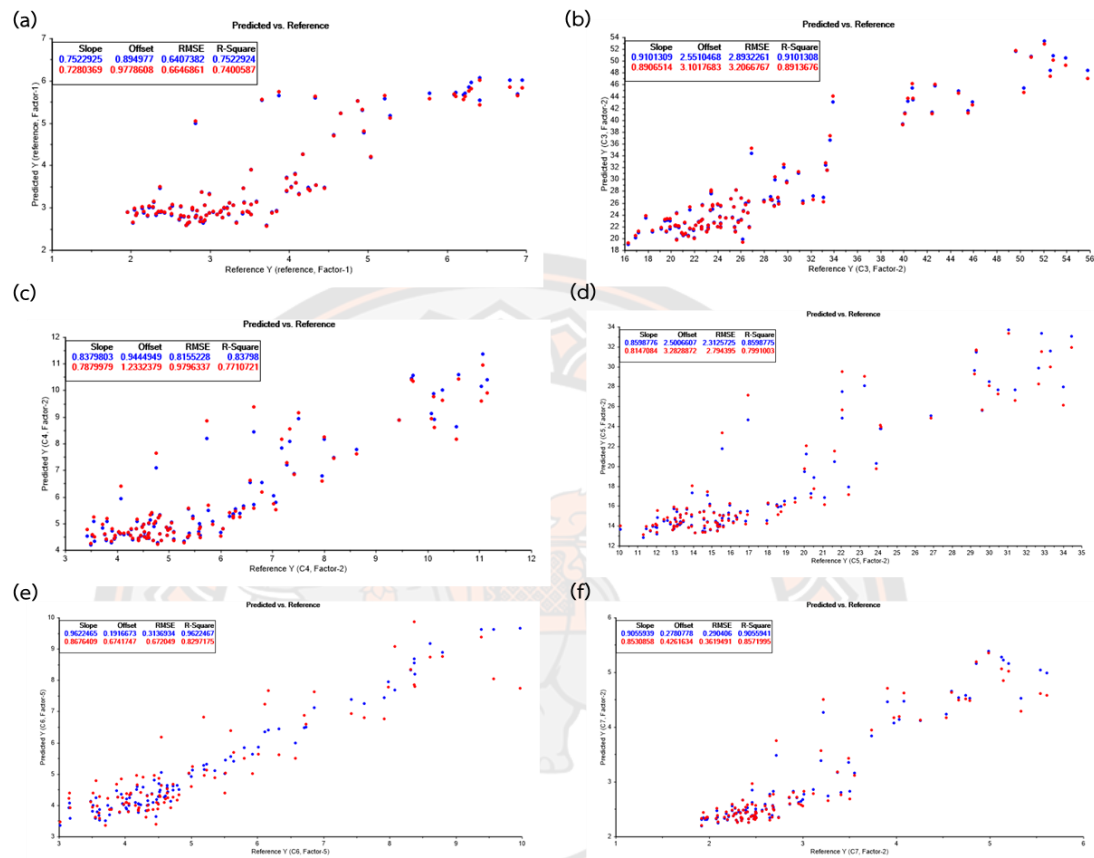


Figure 71 Plots of predicted versus measured values of tomato firmness parameters for calibration models exhibiting the best figures of merit made with spectral data acquired with the Linksquare spectrometer for (a) Firmness (b) Firmness1 (c) Firmness2 (d) Firmness3 (e) Firmness4, and (f) Firmness5

Figure 71 shows the plots of predicted versus measured values of tomato firmness parameters for calibration models with the best figures of merit obtained using data acquired with the Linksquare spectrometer. The results indicate that good performance for calibration and cross validation was obtained for all parameters of the firmness analysis. These R^2 values for the calibration and cross validation were 0.75 (0.74), 0.91 (0.87), 0.80 (0.63), 0.86 (0.63), 0.87 (0.64), and 0.90 (0.86) for Firmness, Firmness1, Firmness2, Firmness3, Firmness4, and Firmness 5, respectively.

4.1.2.3 Texas Instruments (TI) – DLP NIRscan Nano

Figures 72 and 73 show the plots of predicted versus measured values of tomato quality parameters obtained using calibration models made with spectral data acquired with the DLP NIRScan Nano spectrometer without data preprocessing.

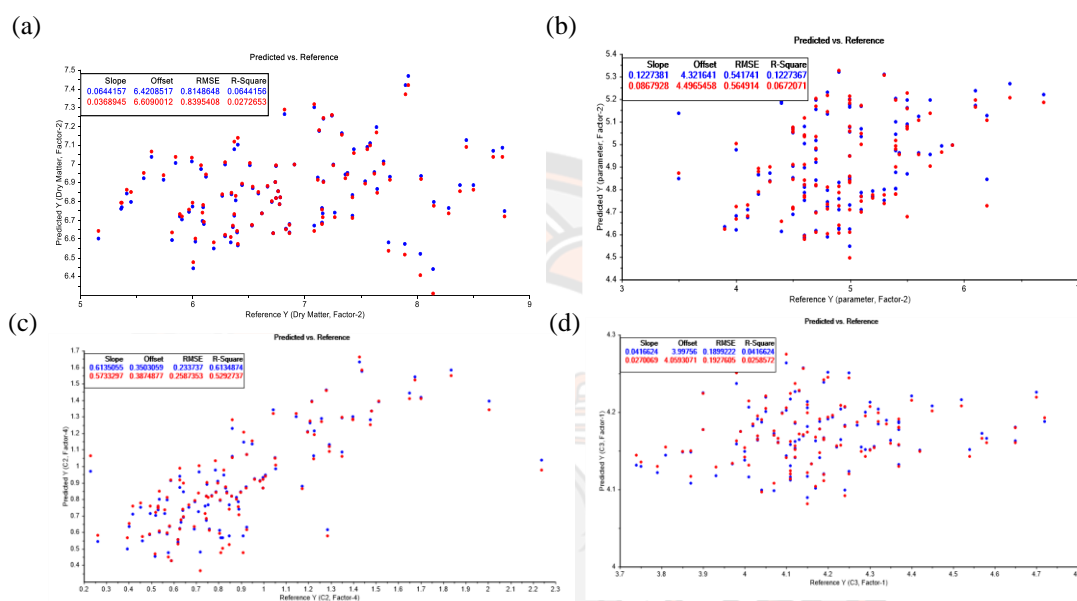


Figure 72. Plots of predicted versus measured tomato quality parameters developed using spectral data acquired with the NIRScan Nano without preprocessing used for (a) DM (b) TSS (c) TA, and (d) pH

The results indicate that the R^2 values for calibration and cross validation (in brackets) were 0.06 (0.03), 0.12 (0.07), 0.61 (0.53), and 0.04 (0.03) for DM, TSS, TA, and pH respectively. The RMSE values for the calibration and cross validation (in brackets) were 0.81% (0.84%), 0.54 °Brix (0.57 °Brix), 0.23% (0.26%) and 0.19 (0.19) for DM, TSS, TA, and pH respectively. The results exhibit moderate performance for TA. Poor calibration models were obtained for DM, TSS, and pH with low R^2 and high RMSE values.

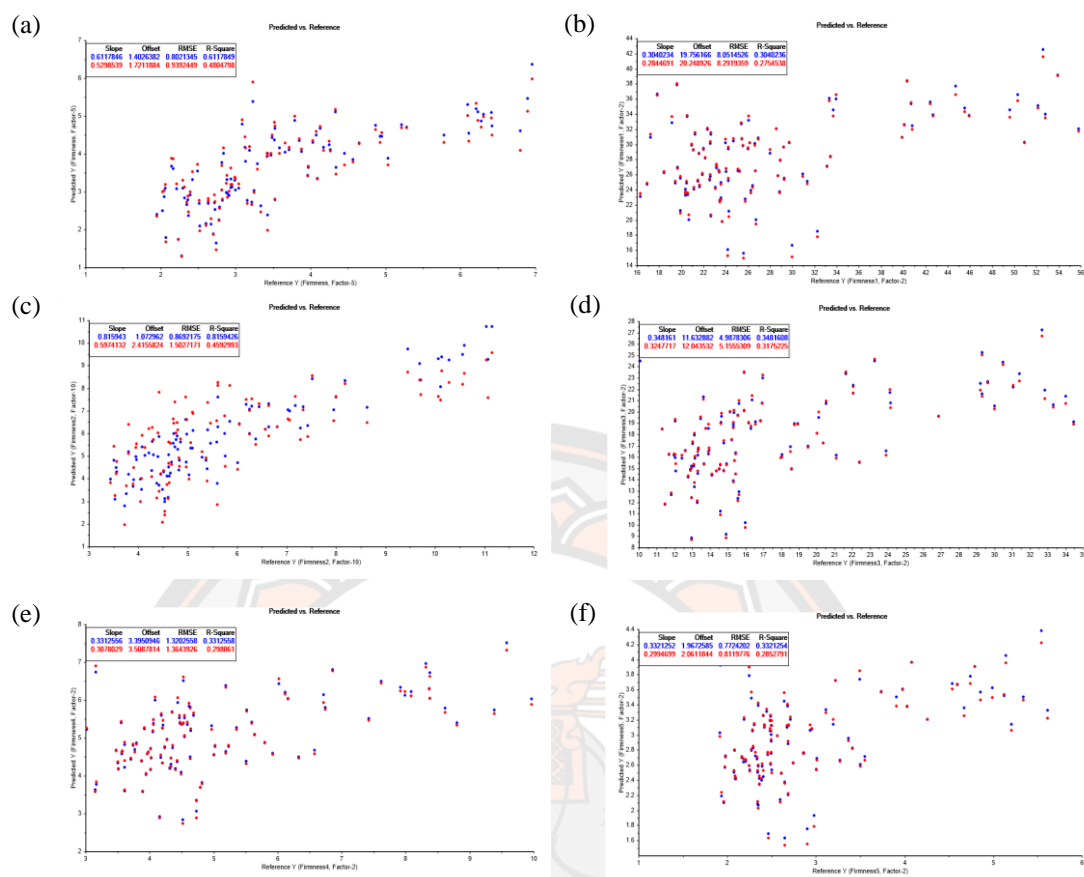


Figure. 73 Plots of predicted versus measured values of (a) Firmness (b) Firmness1 (c) Firmness2 (d) Firmness3 (e) Firmness4 and (f) Firmness5 obtained using spectral data acquired with the NIRScan Nano spectrometer and used without pretreatment

Figure 73 shows the plots of predicted versus measured values of tomato firmness parameters obtained with calibration models made using spectral data acquired with the NIRScan Nano spectrometer without data preprocessing. The results indicate that the R^2 values for calibration and cross validation (in brackets) are 0.61 (0.48), 0.30 (0.28), 0.81 (0.46), 0.35 (0.32), 0.33 (0.30), and 0.33 (0.28) for Firmness, Firmness1, Firmness2, Firmness3, Firmness4, and Firmness5, respectively. The RMSE values for calibration and cross validation (in brackets) were 0.80N (0.94N), 8.05N (8.29N), 0.87N (1.50N), 4.99N (5.16N), 0.33N/mm (0.33N/mm), and

0.33N/mm (0.28N/mm) for Firmness, Firmness1, Firmness2, Firmness3, Firmness4, and Firmness5, respectively.

The results exhibit moderate performance predicted for all of firmness parameters. On the otherhand shows the figures of merit for calibration models for the prediction of the various versions of Firmness parameters obtained using spectral data acquired with the Texas Instruments NIRScan Nano after utilization of data pretreatment procedures.

The best cases of calibration models for predicting quality parameters of tomatoes using data acquired with NIRScan Nano are shown in Table 17.

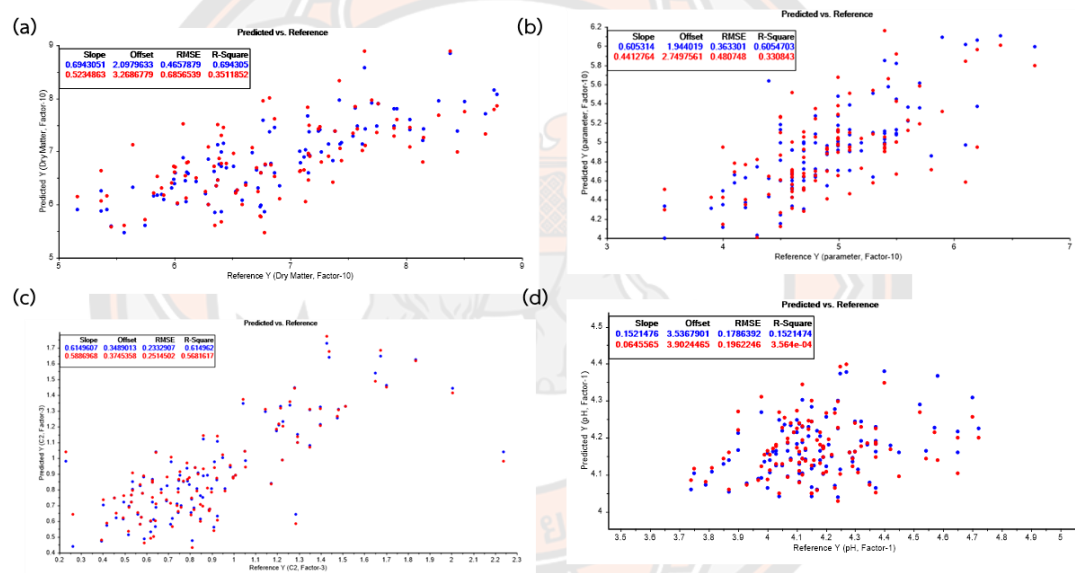


Figure 74 Plots of predicted versus measured values of quality parameters of tomatoes for models exhibiting the best figures of merit for spectral data acquired using Texas Instruments NIRScan Nano used for predicting (a) DM, (b) TSS, (c) TA, and (d) pH

Figure 74 shows the plots of best cases of predicted versus measured quality parameters for calibration models with the best figures of merit acquired using the NIRScan Nano. The results indicate that moderate performance of the calibration models has been achieved for DM, TSS, TA, and pH. These models exhibit R^2 values for calibration and cross validation (in brackets) of 0.69 (0.35), 0.60 (0.33), 0.61

(0.57), and 0.15 (0.00) of DM, TSS, TA, and pH, respectively. The RMSE values for calibration and cross validation (in brackets) were 0.46% (0.68%), 0.36 °Brix (0.48 °Brix), 0.23% (0.25%) and 0.18 (0.20) for DM, TSS, TA, and pH respectively.

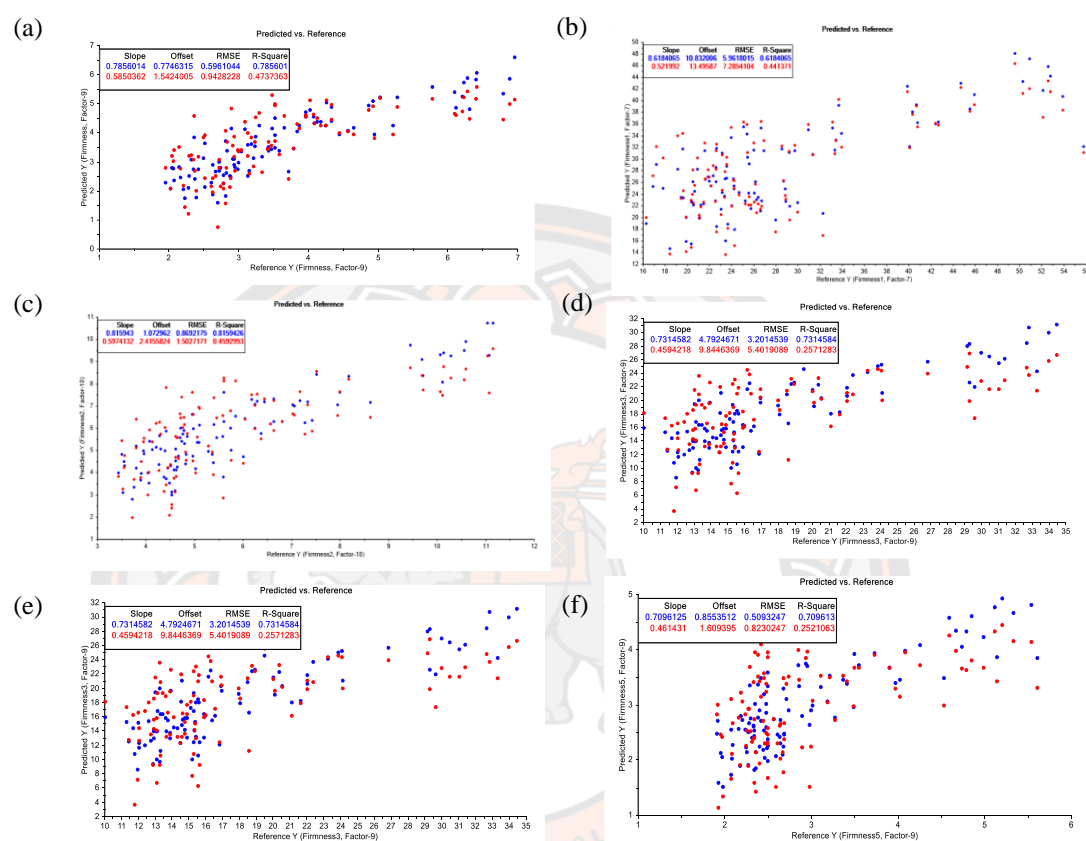


Figure 75 Plots of predicted versus measured values of tomato firmness parameters for models exhibiting the best figures of merit for spectral data acquired using Texas Instruments NIRScan Nano used for predicting (a) Firmness (b) Firmness1 (c) Firmness2 (d) Firmness3 (e) Firmness4 and (f) Firmness5

Figure 75 shows the plots of best cases of predicted versus measured quality parameters for calibration models with the best figures of merit acquired using the Texas Instruments NIRScan Nano. The results indicate that good performing calibration models have been obtained for firmness analysis. These models exhibit R^2 values for the calibration and cross validation of 0.79 (0.47), 0.62 (0.44), 0.81 (0.46),

0.73 (0.26), 0.73 (0.26), and 0.71 (0.25) for Firmness, Firmness1, Firmness2, Firmness3, Firmness4, and Firmness5, respectively. The RMSE values for the calibration and cross validation (in brackets) were 0.60N (0.96N), 5.96N (7.29N), 0.87N (1.50N), 3.20N (5.40N), 3.20N/mm (5.40N/mm), and 0.51N/mm (0.82N/mm) for Firmness, Firmness1, Firmness2, Firmness3, Firmness4, and Firmness5, respectively.

Table 17 Summary of model parameters for predictive models for tomato quality parameters developed using spectral data acquired using the NIRScan Nano developed without pretreatment procedure and showing the best cases.

parameter	preprocessing	Calibration		Cross validation		LV
		R ²	RMSE	R ²	RMSE	
Dry	None	0.06	0.81	0.03	0.84	2
Matter	Procedure 2	0.69	0.46	0.35	0.68	10
TSS	None	0.12	0.54	0.07	0.57	2
	Procedure 2	0.60	0.36	0.33	0.48	10
TA	None	0.61	0.23	0.53	0.26	4
	Procedure 4	0.61	0.23	0.57	0.25	3
pH	None	0.04	0.19	0.03	0.19	1
	Procedure 1	0.15	0.18	0.00	0.20	1
Firmness	None	0.61	0.80	0.48	0.94	5
	Procedure 5	0.79	0.60	0.47	0.94	9
Firmness1	None	0.30	8.05	0.28	8.29	2
	Procedure 2	0.62	5.96	0.44	7.29	7
Firmness2	None	0.81	0.87	0.46	1.50	10
	Procedure 5	0.73	3.20	0.26	5.40	9
Firmness3	None	0.35	4.99	0.32	5.16	2
	Procedure 5	0.73	3.20	0.26	5.40	9
Firmness4	None	0.33	1.32	0.30	1.36	2
	Procedure 5	0.73	3.20	0.26	5.40	9

parameter	preprocessing	Calibration		Cross validation		LV
		R ²	RMSE	R ²	RMSE	
Firmness5	None	0.33	0.77	0.28	0.81	2
	Procedure 5	0.71	0.51	0.25	0.82	9

Procedure 1: Spectrum smoothing and 1st derivative (2nd degree polynomial, Window: 3);

Procedure 2: Spectrum smoothing and 1st derivative (2nd degree polynomial, Window: 21);

Procedure 3: Spectrum smoothing and 2nd derivative (2nd degree polynomial, Window: 3);

Procedure 4: Spectrum smoothing and 2nd derivative (2nd degree polynomial, Window: 21);

Procedure 5: SNV

Best R² values for commercial spectrometers

SCIO, Linksquare, and NIRScan Nano spectrometers were utilized in this work for the development of calibration model for tomato quality parameters (Table 18). In the case of the Neospectra instrument, the sample holder is too large to allow the measurement of the spectroscopic data. The results indicate that the models developed using SCIO for predicting DM and firmness had good performance. The best model for DM has an R² of 0.89 and an RMSE of 0.27 %. The best models show for the firmness parameters had R² values of 0.82, 0.76, 0.82, 0.83, 0.81, and 0.81 for of firmness, firmness1, firmness2, firmness3, firmness4, and firmness 5, respectively. The models for TSS and TA had moderate R² values of 0.74 and 0.64, respectively. Finally, the models for pH based on data acquired with the SCIO spectrometer were poor, with low R² and high RMSE values.

For the Linksquare spectrometer, good predictive models with strong performance exhibiting high R² and low RMSE values were obtained for the instrument operating in both the visible and the NIR modes. The R² values of the models, in calibration and cross validation, made using data acquired in the NIR mode (700-1050 nm) exhibit fairly significant drop in comparison with the models made

using data acquired in the visible mode. The results indicate that excellent performance for calibration and cross validation was achieved for firmness analysis. The models have R^2 values for calibration and cross validation of 0.75 (0.74), 0.91 (0.87), 0.80 (0.63), 0.86 (0.63), 0.87 (0.64), and 0.90 (0.86) of firmness, firmness1, firmness2, firmness3, firmness4, and firmness5, respectively. The models for TSS and TA exhibited moderate performance with R^2 values of 0.78 (0.37), and 0.66 (0.40) for calibration and cross validation. The models for DM and pH were unsatisfactory with R^2 values below 0.20.

Moreover, the model development of the calibration and cross validation using TI spectrometers were poor for predicting all of quality parameters.

Table 18 Best R^2 values for calibration and cross-validation (in brackets) for cherry tomato quality parameters obtained by collecting calibration data using the commercial spectrometers

	SCiO	Linksquare (visible)	Linksquare (NIR)	NIRscan nano
Dry Matter	0.89	0.55 (0.08)	0.18 (0.08)	0.26 (0.11)
TSS	0.74	0.78 (0.37)	0.35 (0.04)	0.60 (0.33)
TA	0.64	0.66 (0.40)	0.48 (0.46)	0.61 (0.57)
pH	0.22	0.36 (0.01)	0.69 (0.14)	0.07 (0.04)
Firmness	0.82	0.75 (0.74)	0.71 (0.68)	0.79 (0.46)
Firmness1	0.76	0.91 (0.87)	0.79 (0.78)	0.62 (0.44)
Firmness2	0.82	0.80 (0.63)	0.74 (0.71)	0.81 (0.46)
Firmness3	0.83	0.86 (0.63)	0.77 (0.76)	0.73 (0.32)
Firmness4	0.81	0.87 (0.64)	0.81 (0.80)	0.73 (0.27)
Firmness5	0.81	0.90 (0.86)	0.85 (0.84)	0.71 (0.28)

Spectral characteristics of cherry tomato and reference measurements

1. Dry matter

As mentioned above, at the wavelengths of 930, 950, 1450, 1900, and 2250 nm are significant wavelengths for predicting DM content. Figure 55 and Figure 56

show a plot of reflectance versus wavelength spectra acquired with the SCIO, Linksquare, and NIRScan Nano spectrometers. These plots indicate the strong pronounced variability of the spectra in the spectral regions related to water vibrations at 930 and 950 nm for Linksquare and SCIO spectrometers, respectively. Similarly, features 1450 and 1900 related to water vibrations can be found in data acquired with the NIRScan Nano spectrometer. These wavelengths can thus be used to characterize DM content.

The results summarizing the R^2 values of calibration models for DM (Table 18) indicate that the SCIO spectrometer provides data resulting in models with good performance having high R^2 and low RMSE values. The best R^2 value for cross validation obtained for a calibration model for DM based on data from the SCIO spectrometer DM was 0.89. The spectral data show importance of the area around 950 nm where strong variability of absorbance is observed leading to the possibility to predict DM. Calibration models developed using data acquired with the Linksquare and NIRScan Nano spectrometers exhibit moderate performance for predicting DM with the R^2 values below 0.70.

Table 19 provides a comparison for the results of the predicting tomato DM using NIR. One previous report was published by Goisser and coworkers in 2020. This work was performed with two spectrometers including the portable F750 and SCIO spectrometers operating in the ranges 310-1100 nm and 740-1070 nm, respectively. The models for predicting DM reported in this work exhibited R_c^2 and R_{cv}^2 (bracket) values of 0.94 (0.93) and 0.97 for F750 and SCICO, respectively. These results are better than those achieved with the models in this work.

2. Total soluble solids content (TSS), Titratable acidity (TA) and pH

As mentioned above, the wavelengths of 750, 800, and 930 nm are important for predicting sugar, starch, and acidity contents. Unfortunately, the results obtained from using all commercial spectrometers were moderate with R^2 values below 0.70 for the prediction of the TSS, TA, and pH contents.

Four publications reporting on predictive models for total soluble solids (TSS) or soluble solid content (SSC) are shown in Table 19. The first work was published by Lei and co-workers in 2018. This work was conducted using a portable

instrument operating in the range 950-1650 nm. The models for prediction TSS had R_c^2 and R_p^2 (bracket) values of 0.998 (0.859). The second work was reported by Ren and co-workers in 2019. They studied the performance of a portable spectrometer operating in the range 900-1700 nm. The R_p^2 value for predicting TSS reported in this work was 0.899. The third publication was reported by Huanhuan and co-workers. An on-line NIR spectrometer operating at 900-1700 nm was used in this work. The reported R_p^2 value for predicting TSS was 0.9053. The last publication was published by Goisser in 2020 as mentioned above. The models for prediction TSS reported in this work had R_c^2 and R_{cv}^2 (bracket) values for F-750 of 0.93 (0.92). The R_p^2 for SCIO was 0.97. All of the published reports show better performance than that of the models in this work.

Goisser and coworkers in 2020 reported on predicting TA for cherry tomato samples. The models for prediction TA and was obtained with R_c^2 and R_{cv}^2 (bracket) values for F-750 of 0.51 (0.49) The R_p^2 for model develop using SCIO was 0.66, which is comparable to the results obtained here in this work.

Lei and coworkers in 2018 reported on predicting pH for cherry tomato. The models for the prediction TA had R_c^2 and R_p^2 (bracket) values of 0.992 (0.810), which is significantly better than that for the models in this work.

3. Firmness

As mentioned above, at the wavelengths of 750 and 920 nm are wavelength with significance for predicting firmness content due to their relationship to the starch content.

The best R^2 values for predicting firmness (Table 18) obtained from this work indicated that SCIO and Linksquire operating with visible and NIR modes provide spectroscopic data resulting in calibration models with strong performance having high R^2 and low RMSE values. The cross validation R^2 values for calibration models developed using spectral data acquired with the SCIO spectrometer for predicting firmness to firmness₅ were in the range 0.76-0.82. The spectral region around the important wavelength of 920 nm exhibited pronounced variable absorbance for the samples as it is related to the 2nd overtone of the O-H stretch of

starch. Calibration models developed using data from the Linksquare spectrometer operating in the visible mode show R^2 values in calibration and cross-validation (in brackets) for predicting firmness to firmness₅ in the range 0.75-0.91 (0.63-0.87). The spectral region around the important wavelength of 750 nm exhibits pronounced variability as it is related to the 4th overtone of C-H stretch of starch, giving it potential for predicting firmness values.

Two reports on predicting firmness analysis for cherry tomato samples were published in 2018 and 2020, as mentioned above. In the first report, the models for prediction of firmness show R_c^2 and R_p^2 (bracket) values of 0.989 (0.961), which is significantly better than that of the models in this work. The second publication, reported by Goisser and co-workers, reports models for prediction firmness and has obtained R_c^2 and R_{cv}^2 (bracket) values for F-750 of 0.49 (0.47). The R_p^2 for data from SCIO was 0.46, which is significantly worse than the results obtained herein.

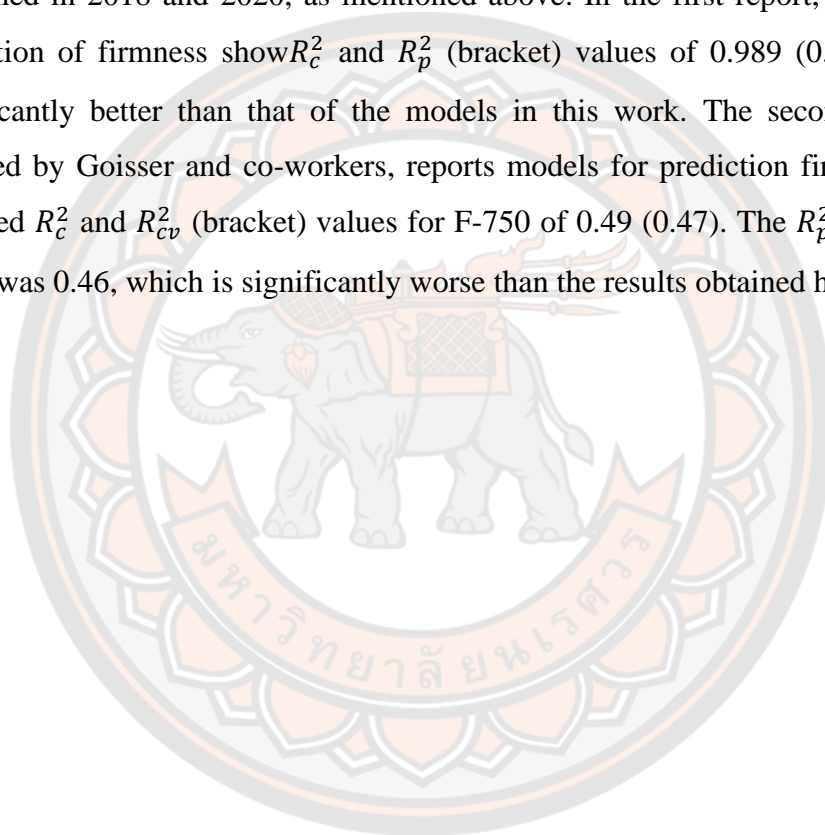
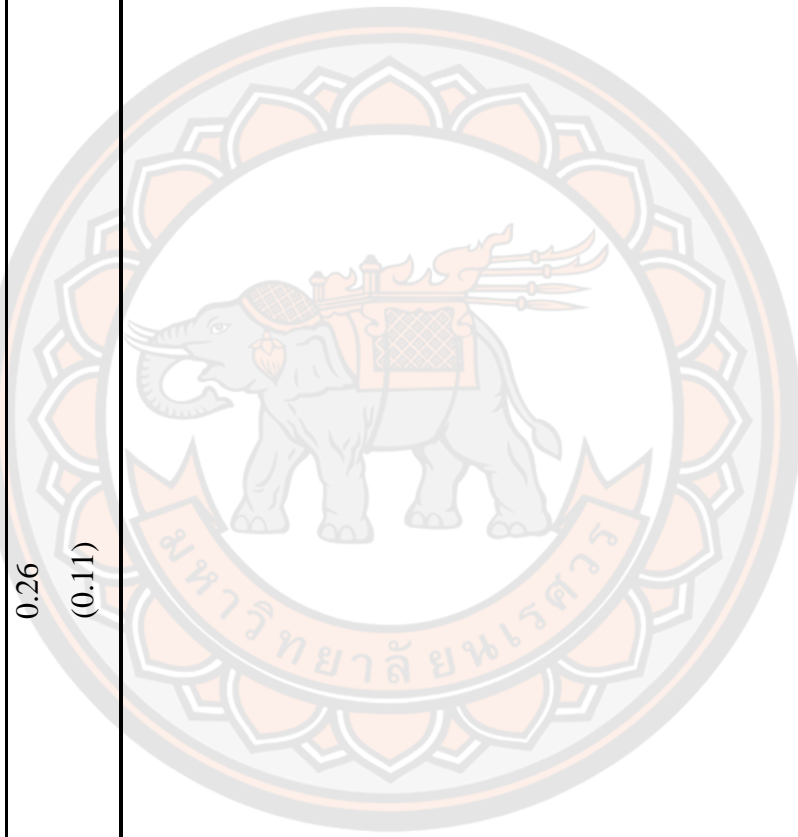


Table 19 Comparison of performance models for the quality parameters of cherry tomato reported in previous literature and describe in this work

Reference	Instrument	Wavelength (nm)	DM		TSS/SSC		TA		pH		Firmness	
			R_c^2	(R_p^2)	R_c^2	(R_p^2)	R_c^2	(R_p^2)	R_c^2	(R_p^2)	R_c^2	(R_p^2)
Lei, F., and co-workers in 2018	Portable NIRs	950-1650	-	-	0.998	-	-	0.992	0.989	(0.961)		
Ren, C., and co-workers in 2019	Portable NIRs	700-1650	-	-	ND	(0.899)	-	-	-	-		
Huanhuan, L., and co-worker in 2020	Online NIRs	900-1700	-	-	ND	(0.9053)	-	-	-	-		
Goisser and co-workers in 2020	F-750	477-1059	0.94	(0.93*)	0.93	(0.92*)	0.51	-	0.49	(0.47)		
							(0.49*)					
	SCIO	740-1070	ND	(0.97)	ND	(0.97)	ND	(0.66)	-	ND	(0.46)	
This work	SCIO	740-1070	0.89		0.74		0.64	0.22	0.76	0.82		
	Linksqre	400-1000	0.55		0.78	(0.37)	0.66	(0.40)	0.36	(0.01)	0.75	0.91(0.63-0.87)
	Linksqre	700-1050	(0.08)		0.35	(0.04)	0.48	(0.46)	0.69	(0.14)	0.71	0.85(0.68-0.84)
	TI	900-1700	0.18	(0.08)	0.60	(0.33)	0.61	(0.57)	0.07	(0.04)	0.62	0.81(0.27-0.46)

Reference	Instrument	Wavelength (nm)	DM $R_c^2 (R_p^2)$	TSS/SSC $R_c^2 (R_p^2)$	TA $R_c^2 (R_p^2)$	pH $R_c^2 (R_p^2)$	Firmness $R_c^2 (R_p^2)$
			0.26 (0.11)				



4.2 Construction of the in-house optical spectrometer

As mentioned above, two of the tested commercial spectrometers exhibited good performance for predicting quality parameters in mango and to a lesser extent in tomato. These instruments were the SCIO (740-1070 nm) spectrometer and the Linksquare spectrometer operating in the visible mode (400-1000). Spectroscopic data from these instruments resulted in calibration models with high R^2 values and low RMSE values. In contrast, spectroscopic data acquired using the NIRscan Nano and Neospectra instruments operating at higher wavelengths resulted in models with unsatisfactory performance. Therefore, it was decided that the inhouse optical spectrometer will be based on a sensor operating within the range of 400-1070 nm.

4.2.1 Selection of a sensor for the in-house optical spectrometer

As mentioned above, the F-751-Mango Quality Meter is an interesting spectrometer for predicting ripeness indicators from mango sample, which is commercially available. The key component used in this instrument is the Hamamatsu C11708MA spectral sensor, which operates in the spectral range of 600-1100 nm. This commercially available spectrometer from Felix Instruments can be used to assess quality parameters of mangoes. This provides supporting evidence for the possibility to construct a usable device based on this or similar sensor.

The sensor chosen for this project is a new generation of NIR sensors from Hamamatsu, the C14384MA sensor, which operates in the same spectral range as the C11798MA sensor but has a higher sensitivity. Both sensors are based on photovoltaic silicon diode technology. The cost of the sensor, at the moment, is 20,000 THB. It should be noted that this is a unit price, which gets reduced to 10,000 THB per piece for volumes above ten sensors. In addition, the first prototype sensor will be made with Hamamatsu made evaluation board C14898. This board costs 40,000 THB. However, in future iterations it would be replaced by significantly cheaper custom-made printed circuit board (PCB).

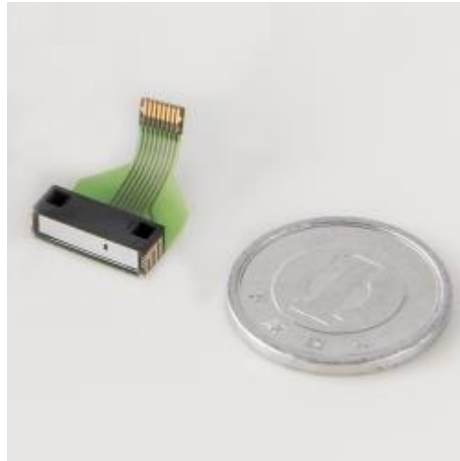


Figure 76 Image of the Hamamatsu C14384MA-01 sensor

4.2.2 Construction of the in-house optical spectrometer

As mentioned above, this sensor has been chosen as it operates in the desired range 640 nm to 1,050 nm. Furthermore, we are interested in 1) LED and TH as light sources, 2) Hamamatsu C14384MA-01 for wavelength selector, and 3) Photovoltaic silicon (Si) diode as a detector for predicting quality parameters for mango and tomato samples. Images of the prototype of the in house developed NIR sensor are shown below.

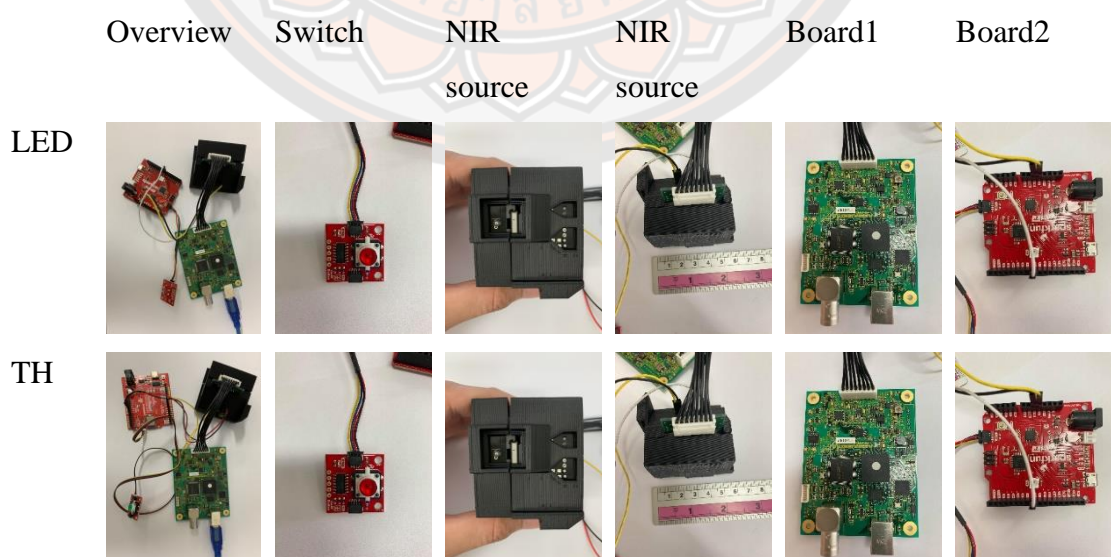


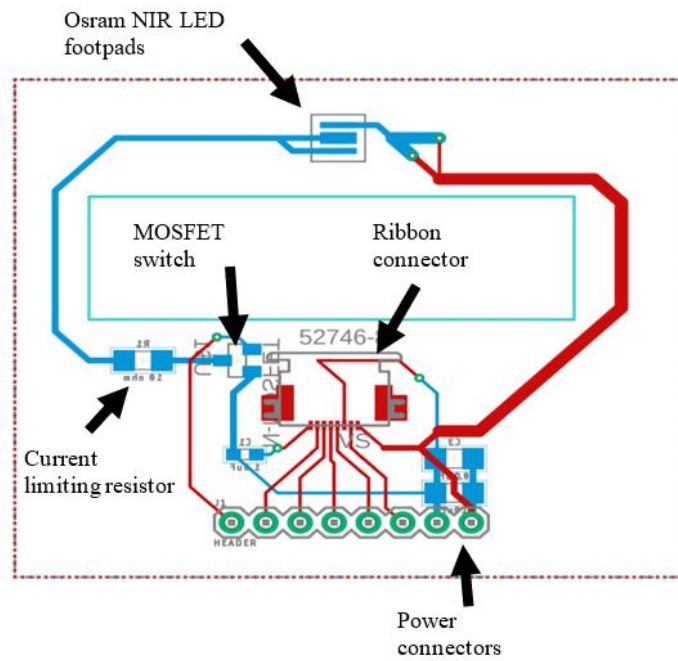
Figure 77 Images of prototype of in house developed NIR sensor

The prototype spectrometer has been made in two versions using two different light sources such as NIR LED (SFH 4376, OSRAM) and tungsten halogen bulb. Suitability of these two light sources is one of the key parameters that will be evaluated in the early part of the utilization of this prototype. The IR LED is a new product that uses a blue LED to excite a phosphorescent surface layer that emits at 600-1050 nm with a very flat spectrum profile. The board designed with the NIR LED source is shown below (Figure 78). The filament board was also designed with the LED replaced with the filament through holes and the current resistor removed (Figure 78). The filament is connected to the PCB using through hole (DIP) technology, while the Osram LED is applied using surface mount technology (SMT) which is much more difficult to build using a soldering iron and a reflow air gun. Both light sources are controlled with an on / off switch implemented with N-channel MOSFET to control the flow of current to the ground. The switch is controlled by a pin on a microcontroller connected to a manual switch the user can use to toggle the light source on or off. The manual switch is connected to the microcontroller by a Qwiic connector, which allows for fast prototype design. The microcontroller simply polls the status of the manual button and changes the level of the digital pin controlling the N-channel MOSFET switch. The Osram LED also has a current control resistor in series to keep the current at ~ 200 mA. We are using a 5V power supply and the LED has a turn on voltage of ~ 3V so that the current is calculated by ohms law as $I = V / R$ ($I = (5V-3V) / 10 \text{ ohms} = 200 \text{ mA}$).

$$\text{current} = \frac{5V - 3V}{10 \text{ ohms}} = 0.2 \text{ A} = 200 \text{ mA}$$

As we are using the evaluation board to control the C14384MA we just make a cutout in the PCB to push the sensor and holder through. In the future if we want to use the sensor alone and make our own control board, we need to connect the sensors cable to the PCB. The current boards incorporate this connector so that we can begin testing right away if we choose to. Images of the sensor equipped with either the LED or filament light sources can be seen in Figure 77.

(a)



(b)

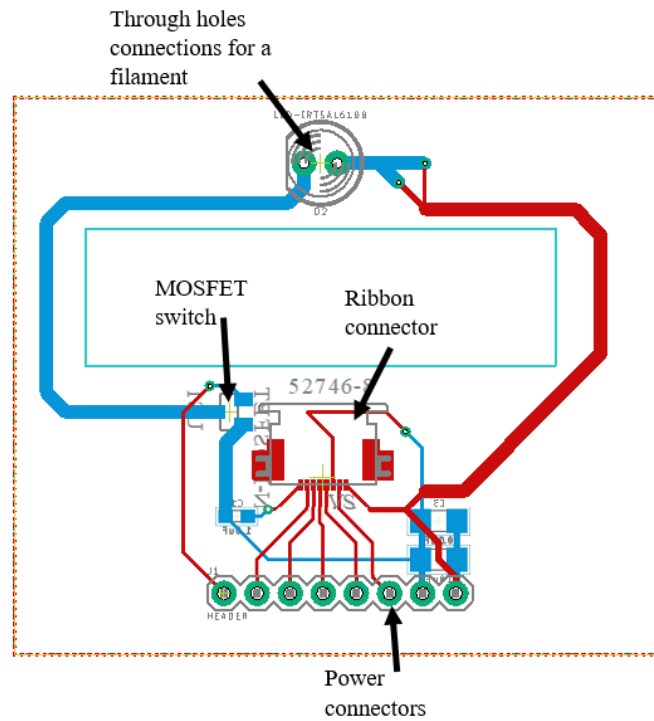


Figure 78 Schematic diagram of the control board for the (a) LED illumination (b) filament bulb sources.

4.3 Development of in-house optical spectrometer

4.3.1 Development of in-house optical spectrometer with different light source.

As mentioned above, two different types of NIR sources are used in commercially available spectrometers such as tungsten halogen (TH) light source and light emitting diode (LED). Publications report wide use of tungsten halogen lamps as commercial light sources for non-destructive determination. TH light sources have been used in works showing prediction of SSC, DM, and firmness with good calibration models. On the other hand, LED lamps have been studied to a lesser extent. Figure 79 shows reflected intensity spectra of white reference (Spectralon®) obtained with the TH and LED lamp.

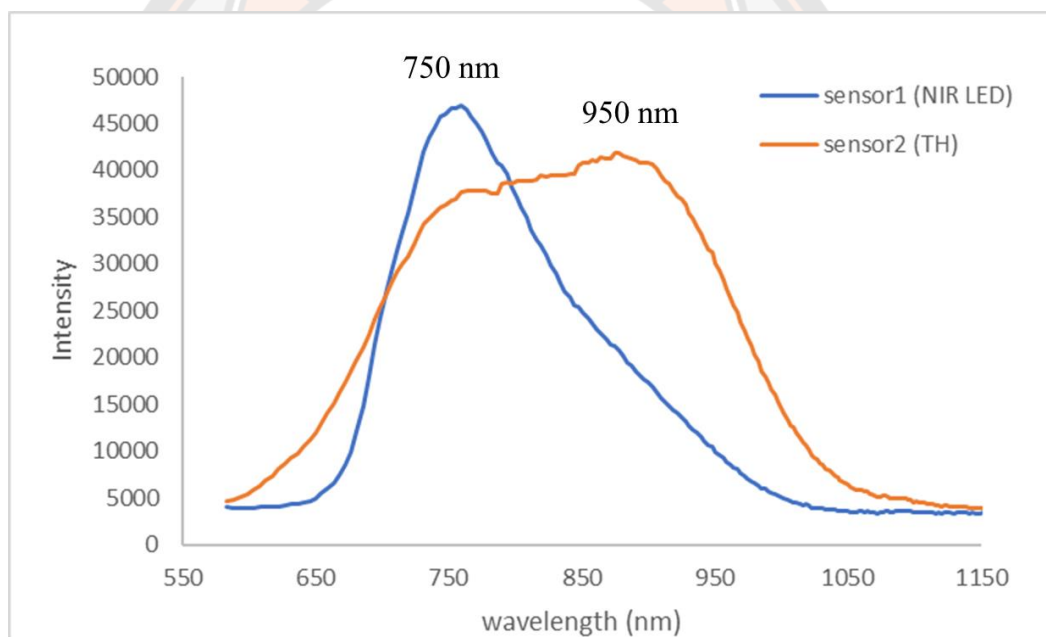


Figure 79 The intensity spectra of white reference material in the wavelength range from 560 nm to 1150 nm.

Figure 79. shows the comparison of the reflected intensity spectra of white reference for LED and TH lamp. The results indicate that the LED lamp provides strong intensity of illumination in the range 700-900 nm. These wavelengths are normally absorbed by the water band (950 nm), third overtone for O-H str of starches and sugars (720 nm), and fourth overtone of C-H str of starch and sugars (750 nm).

The TH lamp provides strong intensity of illumination in the range 600-1000 nm. These wavelengths are normally absorbed by the water band (950 nm), third overtone of O-H str (910 nm), and second overtone of O-H str (920 nm) for starch and sugars, respectively, and third overtone for O-H str of starch and sugars (720 nm), and fourth overtone of C-H str of starch and sugars (750 nm).

Therefore, we decided to utilize both light sources to collect spectral information to be used for predicting quality parameters for mango and tomato.

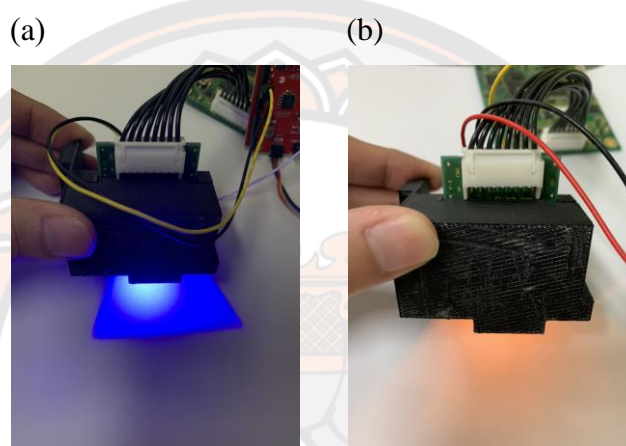


Figure 80 Illustration of the different light sources used for inhouse built spectrometer (a) Near infrared light emitting diode, NIR LED (b) filament bulb, TH.

4.3.2 Testing performance of the in-house optical spectrometer

Repeatability and reproducibility

The repeatability and reproducibility of the spectral measurements taken with the new in-house spectrometers were evaluated by repeated measurements of white and dark reference spectra in one day (repeatability) and over a five-day period (reproducibility) are show in Figure 81 and Figure 82.

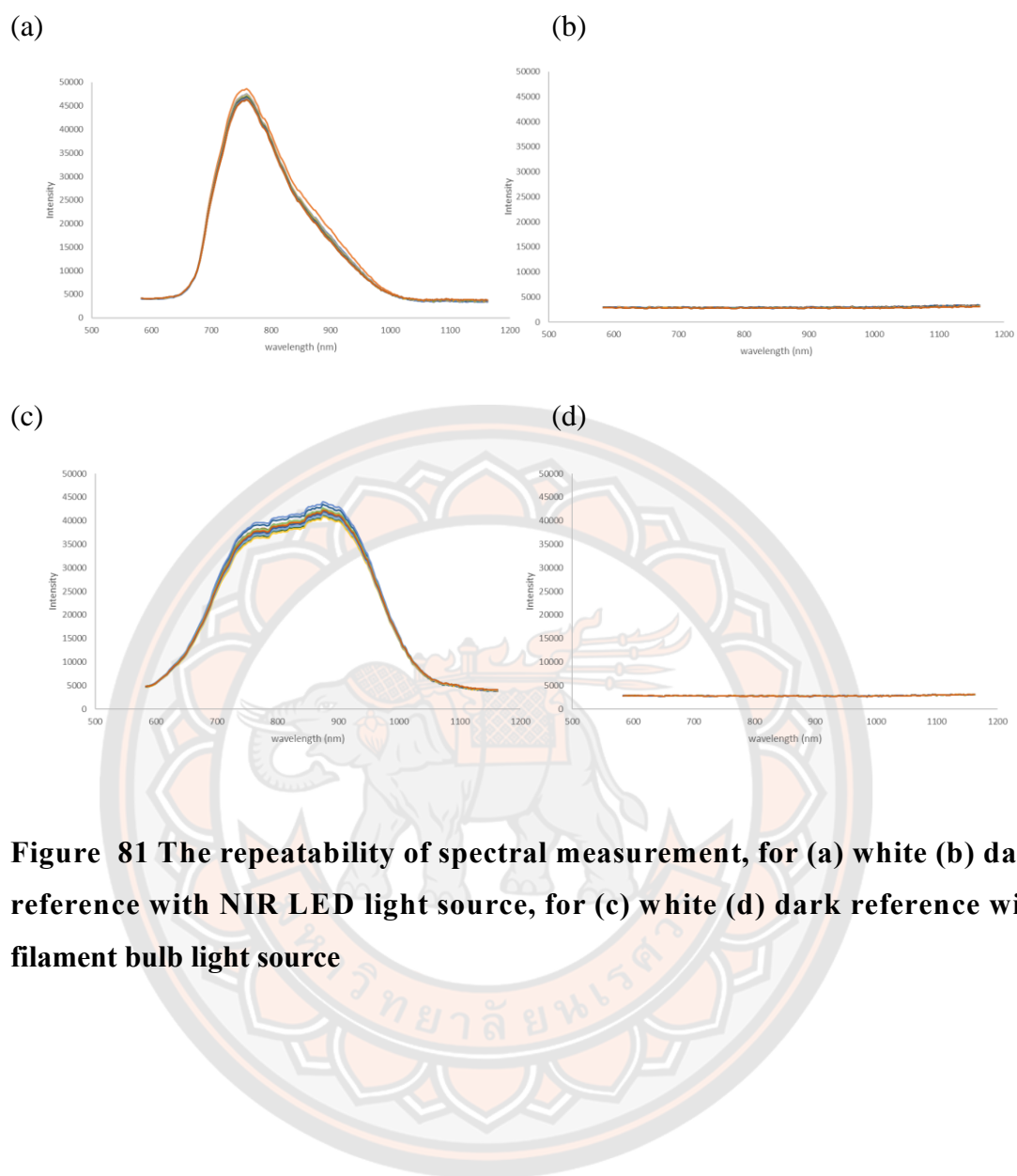


Figure 81 The repeatability of spectral measurement, for (a) white (b) dark reference with NIR LED light source, for (c) white (d) dark reference with filament bulb light source

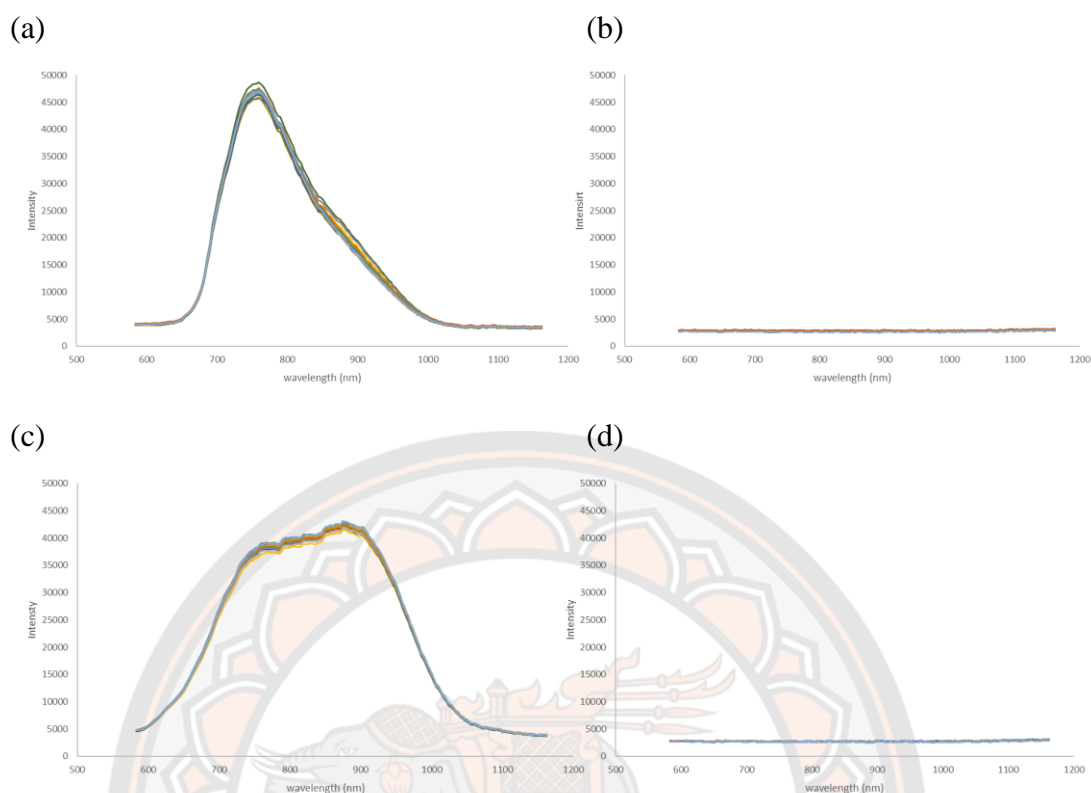


Figure 82 The reproducibility of spectral measurement, for (a) white (b) dark reference with NIR LED light source, for (c) white (d) dark reference with filament bulb light source

The %RSD values at each wavelength have been calculated. The minimum, maximum, and average of %RSD values for entire spectral range are shown in Table 20. The results show that the minimum, maximum and average of %RSD values for both repeatability and reproducibility measurements are below 5%, which indicates good performance of the developed instrument.

Table 20 Repeatability and reproducibility of spectral measurements taken with the in-house developed instrument

Light source	Background type	Repeatability (%RSD)			Reproducibility (%RSD)		
		Max	Min	Avr	Max	Min	Avr
NIR LED	White	3.82	0.60	2.23	4.68	1.20	2.80
	Dark	3.54	1.43	2.48	4.40	3.18	3.78
TH	White	2.22	0.98	1.77	1.72	0.93	1.27
	Dark	0.74	0.36	0.56	3.38	2.47	2.89

4.4 Testing performance of in-house optical spectrometer for quantitative measurements to predict keys quality parameters from mango and tomato.

4.4.1 Mango samples

Sample preparation

As mentioned above, the mango (Nam Dok Mai) samples were obtained from fresh produce market (Phitsanulok, Pichit, Phachuap Khiri Khan) and local retail stores (Tesco lotus, Macro). The number of samples and location of sources are summarized in Table 21.

Table 21 Numbers of samples based on location of collection for in-house optical spectrometers of mango for first and second period times.

Period time	Source Location	N
First period time	Phitsanulok	200
	Pichit	85
	Tesco lotus	15
	Total of first period time	300
Second period time	Phachuap Khiri Khan	100
	Phitsanulok	57
	Tesco lotus	115
	Macro	36
	Total of first period time	308
Total		608

Total 608 samples were obtained in this work. Mangoes were washed with water to remove the gum and clean. After cleaning, the samples were stored at ambient conditions. Four sampling areas (2x2cm) have been marked on the samples. Two sampling areas on each of the two opposite sides of the sample. Spectroscopic measurements were performed on the surface of these areas as shown in Figure 41.

Reference analysis

The mango samples were obtained in two different collection periods. 300 samples were collected in the first and 308 samples in the second sampling period to develop calibration models for five quality parameters (DM, TSS, TA, pH, and firmness). In case of firmness analysis, we focused only maximum load value of the sample. For other firmness measurements, the reference data are slightly different for the different ripening states. The descriptive statistics for the quality parameters can be found in Table 22 and Table 23, respectively.

Table 22 Descriptive statistics for quality parameters analyzed for mango samples collected in the first sampling period.

parameter	N	Average	Min	Max	Std
DM (%)	100	14.43	11.14	17.93	1.54
TSS (°Brix)	100	12.72	6.90	17.00	2.57
TA (%)	100	0.75	0.12	2.77	0.80
pH	100	4.17	2.86	6.65	0.98
Firmness (N)	100	11.78	0.80	56.30	11.84

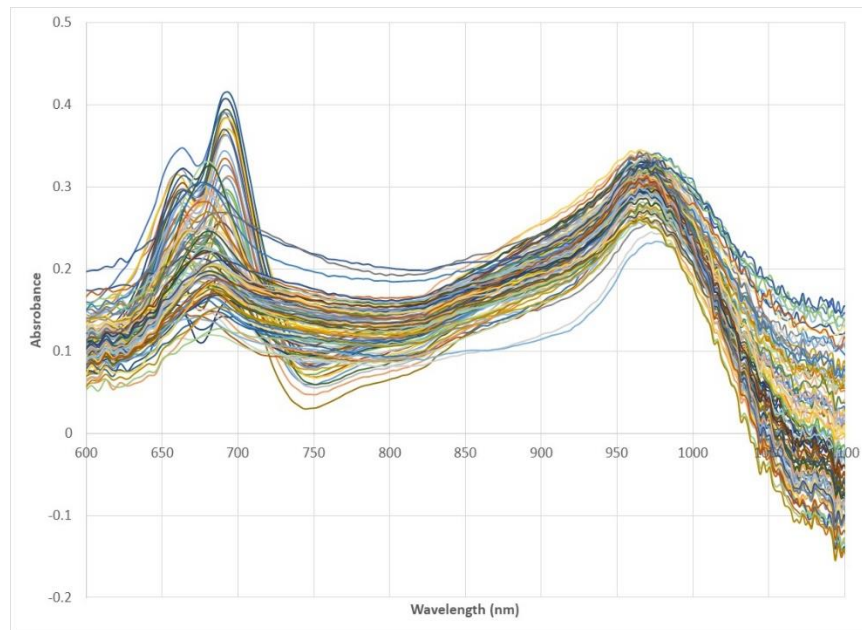
Table 23 Descriptive statistics for quality parameters analyzed for mango samples collected in the second sampling period.

parameter	N	Average	Min	Max	Std
DM (%)	103	13.73	9.68	18.69	2.09
TSS (°Brix)	105	12.65	7.70	21.30	3.15
TA (%)	105	1.15	0.09	4.60	1.46
pH	105	4.48	2.73	6.94	1.26
Firmness (N)	100	6.40	3.71	41.08	4.81

Tables 22 and 23 show the range of measurement (minimum and maximum values), average, and standard deviation of the quality parameters of the mango samples.

The observed values of Dry matter, TSS, TA, pH, and firmness were in the range 11.14-17.93%, 6.90-17.00°Brix, 0.12-2.77%, 2.86-6.65, and 0.80-56.30N for first sampling period, respectively (Table 22). In the second sampling period the values of Dry matter, TSS, TA, pH, and firmness were in the range 9.68-18.69%, 7.70-21.30 °Brix, 0.09-4.60%, 2.73-6.94, and 3.71-41.08N, respectively (Table 23).

(a)



(b)

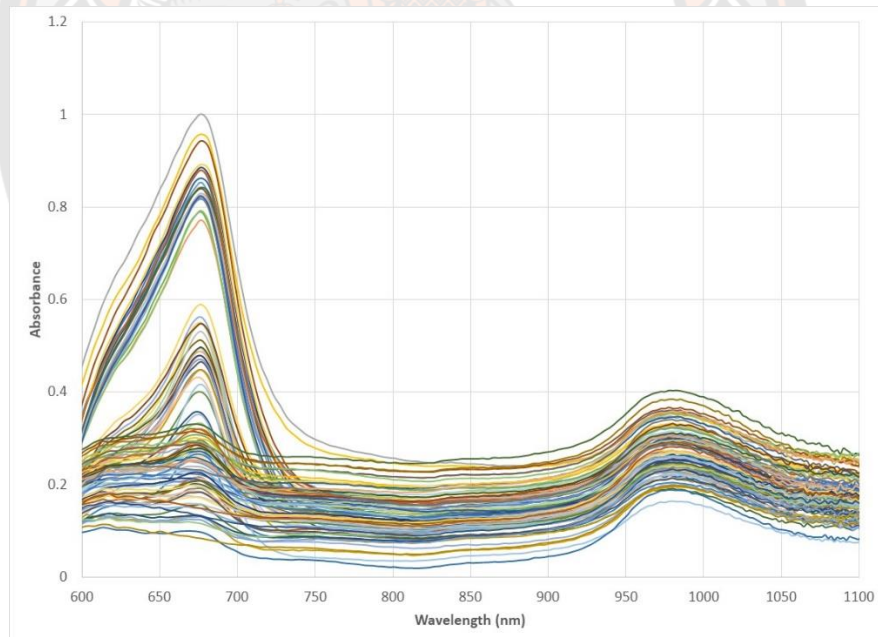


Figure 83 Plot of absorbance versus wavelength for spectra acquired using the in-house spectrometer equipped with the (a) LED light source (b) tungsten light source for mango samples used to develop predictive models for firmness of mango samples.

Data Acquisition of inhouse spectrometers for mango samples

Spectroscopic measurements collected from the sampling areas were performed using the two versions (LED and TH) of the inhouse instrument. Four spectra were recorded for each location. The spectra were averaged and used for conducting the chemometric analysis. The samples were split into three groups for the purpose of the reference analyses. Samples in the first group were used for dry matter (DM) determination. The second group was used for the determination of total soluble solids (TSS), titratable acidity (TA), and pH. Finally, the last group was used for firmness analysis. Spectroscopic measurements obtained with the two versions of the spectrometer prototype are shown on these figure (Figure 83)

Figure 83a shows pronounced variability of the original spectral data at approximately 650, 750, and 970 nm. Figure 83b shows pronounced variability at approximately 670 and 970 nm. The spectral region of 650 to 680 nm corresponds to the absorption of chlorophyll. The features at 750 and 970 nm correspond to the 4th overtone of the C-H stretching vibration of starch or/and sugar, and 2nd overtone of water, respectively.

Data analysis

Figures 84 and 85 demonstrate the models developed for DM, TSS, TA, pH, and firmness using spectral data acquired with both the NIR LED and filament bulb light sources. Eight data preprocessing approaches were applied as mentioned above and the resulting figures of merit are summarized in Appendix Table 48 to Appendix Table 52.

As can be seen in table 24, the results indicate that the R^2 values for calibration and cross-validation (in brackets) for models developed using spectral data acquired with the NIR LED light source and used without pretreatment for DM, TSS, TA, pH, and firmness are 0.70 (0.52), 0.93 (0.84), 0.93 (0.91), 0.93 (0.84), and 0.56 (0.39), respectively. The RMSE values for DM, TSS, TA, pH, and firmness were 0.84% (1.07%), 0.66 °Brix (1.04 °Brix), 0.21% (0.24%), 0.26 (0.39), and 20.09N (23.75N), respectively.

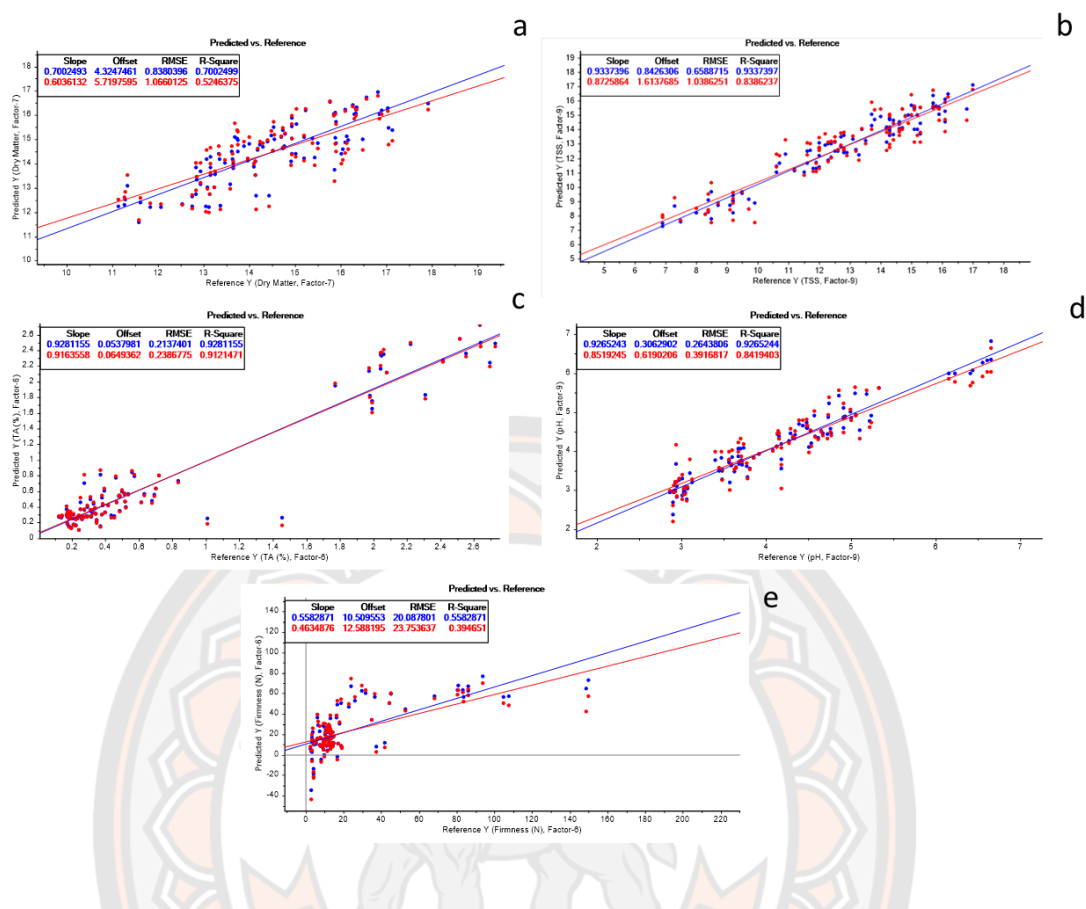


Figure 84 Plot of predicted versus measured values of dry matter(a), total soluble solids (b), titratable acidity (c), pH (d), and firmness (e) of mangoes for samples collected in the first collection period made with predictive models based on spectral data acquired using the NIR LED light source used without data pretreatment. The plots are showing datapoints for both calibration (blue) and cross validation (red) and the corresponding regression lines.

The best R^2 values obtained for the first collection period are shown in Table 24. The R^2 values for calibration and cross-validation (in brackets) for models developed using spectral data acquired with the NIR LED source for DM, TSS, TA, pH, and firmness are 0.81 (0.58), 0.93 (0.84), 0.93 (0.91), 0.93 (0.87), and 0.56 (0.39), respectively. The RMSE values for DM, TSS, TA, pH, and firmness were 0.84% (1.07%), 0.66 °Brix (1.04 °Brix), 0.23% (0.25%), 0.26 (0.39), and 12.52N (20.68N), respectively. These models have been obtained,

for DM and TA after smoothing Savitzky-Golay algorithm and a window of 3 datapoints, for TSS, pH, and firmness without pretreatment.

Moreover, the best performing models obtained from data collected in the first sampling period were used to make predictions for samples collected in the second sampling period (Table 24). The results indicate that the prediction R^2 values for DM, TSS, TA, pH, and firmness for NIR LED are 0.22, 0.16, 0.78, 0.36, and non-detected, respectively. The RMSE values of prediction models for DM, TSS, TA, pH, and firmness were 0.67%, 0.69 °Brix, 1.00%, 0.85, and 23.96N, respectively.

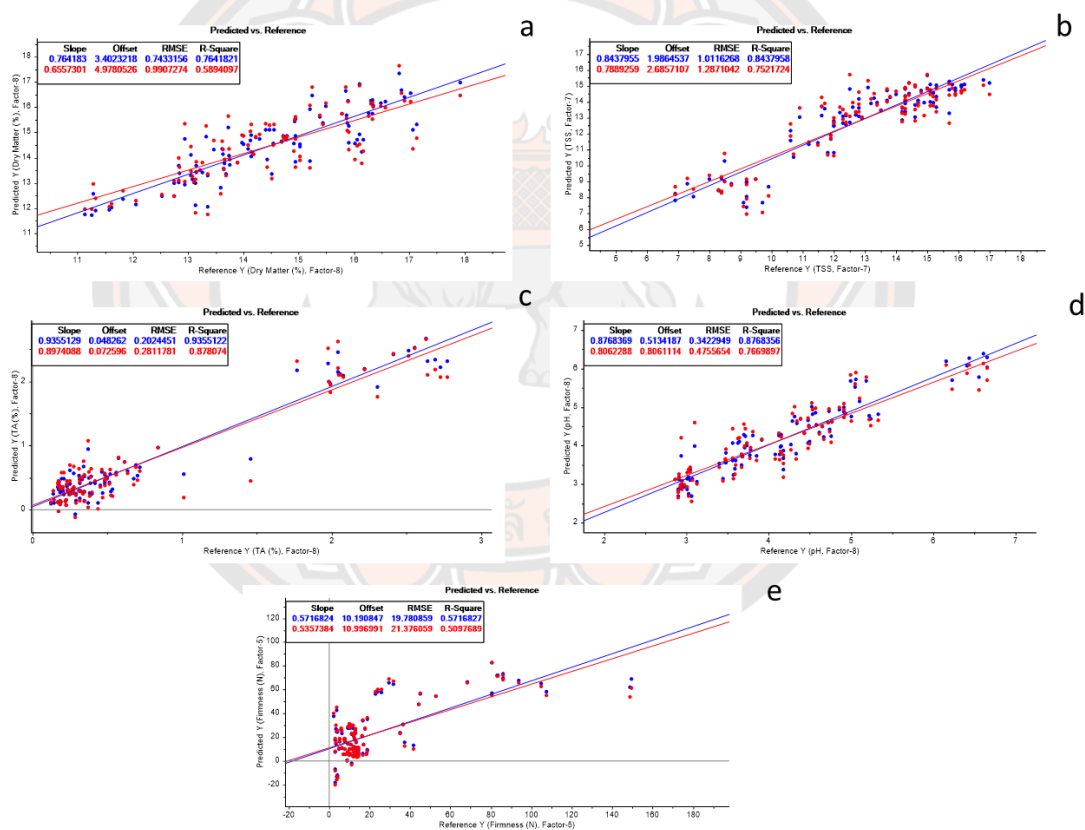


Figure 85 Plot of predicted versus measured values of dry matter(a), total soluble solids (b), titratable acidity (c), pH (d), and firmness (e) of mangoes for samples collected in the first collection period made with predictive models based on spectral data acquired using the filament light source used without data pretreatment. The plots are showing datapoints for both

calibration (blue) and cross validation (red) and the corresponding regression lines.

The results obtained from using spectral data acquired with the filament bulb light source without pretreatment (Figure 85, Table 24) indicate that the R^2 values for calibration and cross-validation (in brackets) for the calibration models for DM, TSS, TA, pH, and firmness are 0.76 (0.59), 0.84 (0.75), 0.94 (0.88), 0.88 (0.77), and 0.57 (0.51) respectively. The RMSE values for DM, TSS, TA, pH, and firmness were 0.74% (0.99%), 1.01 °Brix (1.29 °Brix), 0.20% (0.28%), 0.34 (0.48), and 19.78N (21.38N), respectively.

The best R^2 values for models made with mango samples from the first collection period using spectral data acquired with the filament bulb light source are shown in Table 24. The R^2 values for calibration and cross-validation (in brackets) for models developed with spectral data acquired using the filament bulb light source for DM, TSS, TA, pH, and firmness were 0.82 (0.59), 0.88 (0.81), 0.95 (0.90), 0.88 (0.77), and 0.70 (0.49) respectively. The RMSE values for DM, TSS, TA, pH, and firmness were 0.66% (0.99%), 0.88 °Brix (1.11 °Brix), 0.19% (0.25%), 0.34 (0.48), and 16.64N (21.84N), respectively. The model for pH was obtained without pretreatment. The models for DM and TSS were obtained after SNV pretreatment. The model for TA was obtained after smoothing with a window 3 datapoints. The model for firmness was obtained after conversion to absorbance and smoothing with using a polynomial function with 3 averaging points.

Moreover, the best performing models obtained using data from mango samples collected in the first sampling period were applied to predict parameter values for mango samples collected in the second sampling period time (Table 24) The results indicate that the R^2 values for the predictions of parameter values for samples from the second collection period made with data acquired using the filament bulb light source for DM, TSS, TA, pH, and firmness are 0.47, 0.15, 0.72, 0.56, and non-detected, respectively. The RMSE values of predictive models for DM, TSS, TA, pH, and firmness were 1.52%, 2.89 °Brix, 0.69%, 0.85, and 23.96N, respectively.

The predictions of the parameters of interest for mango samples from the second collection period made with models calibrated on data acquired with mango samples in the first collection period result in R^2 values below 0.50, except for the prediction of TA. The moderate predictive performance of the models based on mango samples collected in the first collection period is likely due to lack robustness given the number of samples and limited sampling time frame. To address the issue, a new sample set was created by combining the samples from the first and the second collection periods. The descriptive statistics for quality parameters of combined sample set can be found in Table 25.

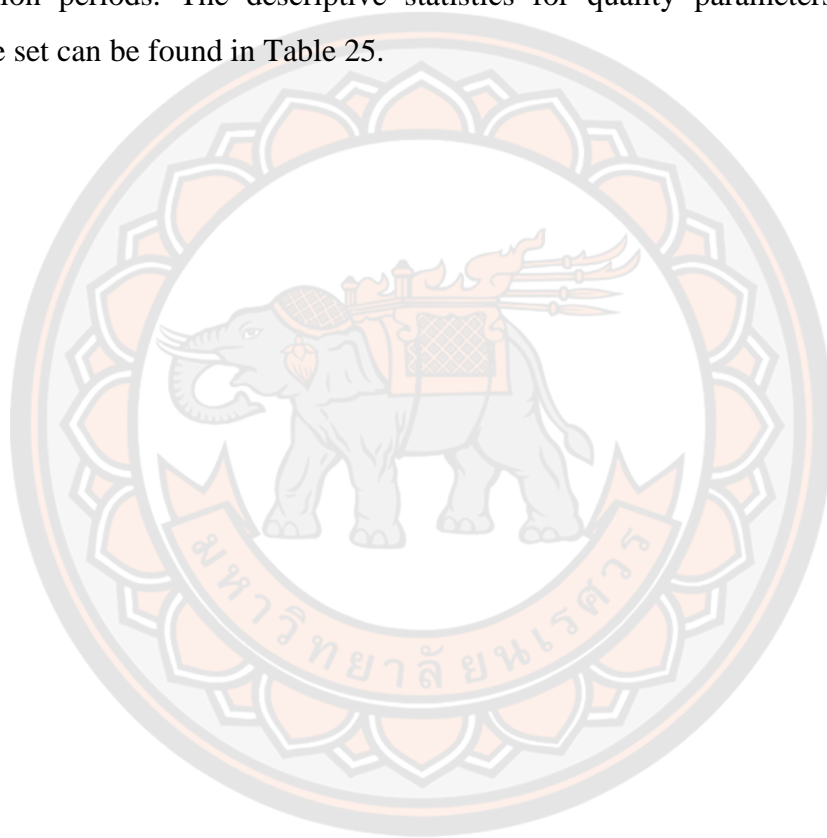


Table 24 Summary of model parameters developed using NIR LED and filament bulb light source from mango samples collected in the first sampling period and predictive model parameters for second period time.

Parameter	Light source	Treatment	Calibration		Cross Validation		Prediction	
			R ²	RMSE	R ²	RMSE	R ²	RMSE
Dry Matter	NIR LED	None	0.70	0.84	0.52	1.07		
	SGD (3)		0.81	0.66	0.58	1.00	0.22	1.83
	SGD* (3)		0.76	0.75	0.65	0.91		
TH	None		0.76	0.74	0.59	0.99		
	SNV		0.82	0.66	0.59	0.99	0.47	1.52
	SNV*		0.78	0.72	0.72	0.82		
TSS	NIR LED	None	0.93	0.66	0.84	1.04	0.16	2.88
	None*		0.88	0.87	0.85	1.01		
	TH	None	0.84	1.01	0.75	1.29		
TA	NIR LED	None	0.93	0.21	0.91	0.24	0.78	0.67
	SGD (3)		0.92	0.23	0.91	0.25		
	SGD* (3)		0.92	0.22	0.91	0.24		

Parameter	Light source	Treatment	Calibration		Cross Validation		Prediction	
			R ²	RMSE	R ²	RMSE	R ²	RMSE
pH	TH	None	0.94	0.20	0.88	0.28	0.72	0.77
		Abs	0.95	0.19	0.90	0.25	0.78	0.69
		Abs*	0.92	0.23	0.90	0.26		
pH	NIR LED	None	0.93	0.26	0.84	0.39	0.36	1.00
		None*	0.91	0.29	0.87	0.36		
		None	0.88	0.34	0.77	0.48	0.56	0.85
Firmness	NIR LED	None	0.80	0.43	0.75	0.49		
		Abs and SNV	0.56	20.09	0.39	23.75		
		Abs and SNV*	0.83	12.52	0.54	20.68	NA	20.12
Firmness	TH	None	0.76	14.75	0.65	17.97		
		None	0.57	19.78	0.51	21.38		
		Abs and 1 st SGD (3)	0.70	16.64	0.49	21.84	NA	23.96
		Abs and 1 st SGD* (3)	0.67	17.24	0.55	20.48		

*Model made after selection of significantly contributing variables

SGD – Savitzky-Golay derivative

Table 25 Descriptive statistics of mango quality parameters for samples collected in both sampling periods.

parameter	N	Average	Min	Max	Std
DM	203	14.07	9.68	18.69	1.86
TSS	205	12.68	6.90	21.30	2.88
TA	205	0.95	0.08	4.59	1.20
pH	205	4.33	2.73	6.94	1.14
Firmness	200	9.09	0.80	56.30	9.41

Table 25 shows the range of values (minimum and maximum values), average, and standard deviation of the quality parameters for the mango samples in the combined dataset. The Dry matter, TSS, TA, pH, and firmness ranged from 9.68-18.69%, 6.90-21.30 °Brix, 0.08-4.59%, 2.73-6.94, and 0.80-56.30N, respectively.

Figure 86-87 show the models developed for DM, TSS, TA, pH, and firmness using NIR LED and filament bulb light sources. Eight data preprocessing procedures were applied as mentioned above.

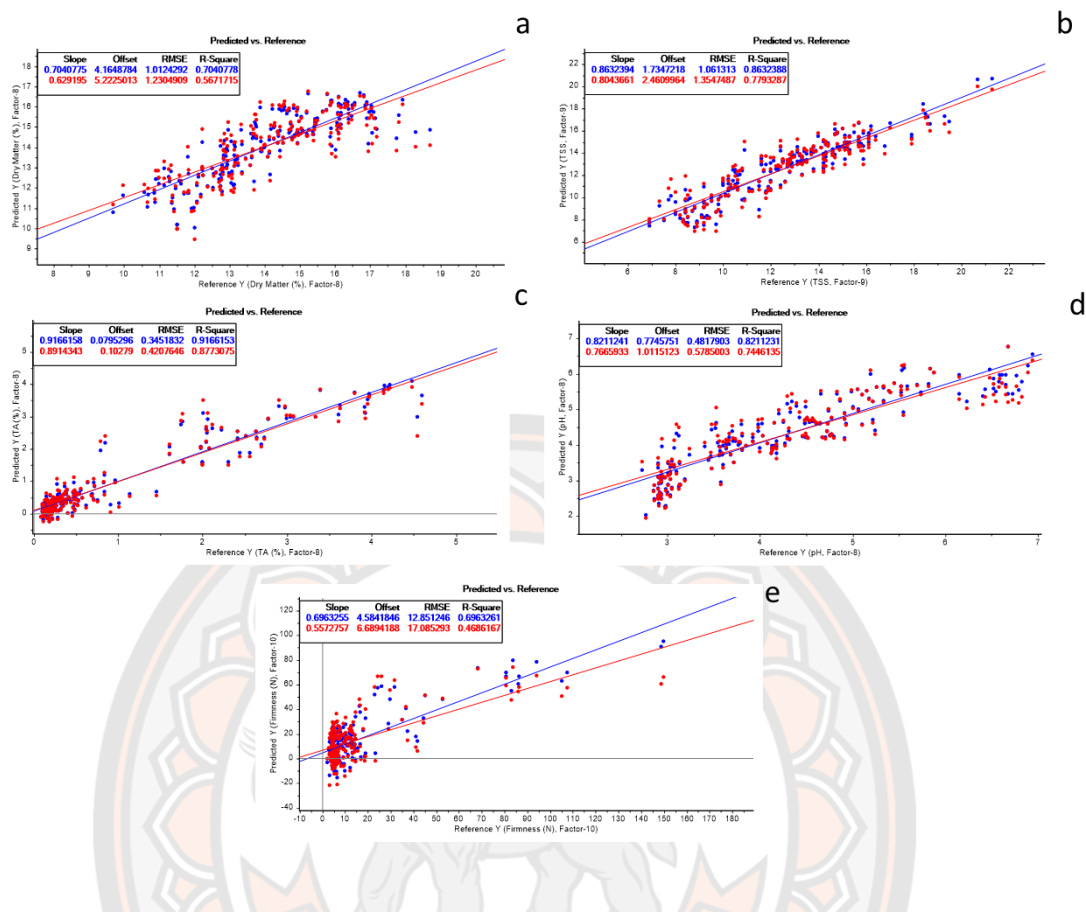


Figure 86 Plot of predicted versus measured values without pretreatment of (a) dry matter, (b) total soluble solids, (c) titratable acidity, (d) pH, and (e) firmness for samples collected in both collection periods made with predictive models based on spectral data acquired using the NIR LED light source used without data pretreatment. The plots are showing datapoints for both calibration (blue) and cross validation (red) and the corresponding regression lines.

As can be seen in Figure 86 and Table 26, the models made with data from mangoes collected in both sampling periods without pretreatment of spectral data collected with NIR LED light source exhibited R^2 values for calibration and cross-validation (in brackets) for DM, TSS, TA, pH, of 0.70 (0.57), 0.86 (0.78), 0.92 (0.88), 0.82 (0.74), and 0.70 (0.47) respectively. The RMSE values for DM, TSS, TA, pH, and firmness were 1.01% (0.57%), 1.06 °Brix (1.35 °Brix), 0.35% (0.42%), 0.48 (0.58), and 12.85N (17.09N), respectively.

The best R^2 values for data collected from the combined period dataset for spectral measurements made with the NIR LED light source are shown in Figure 88 and Table 26. The corresponding R^2 values for calibration and cross-validation (in brackets) for DM, TSS, TA, pH, and firmness for NIR LED were 0.75 (0.53), 0.88 (0.80), 0.93 (0.89), 0.88 (0.79), and 0.83 (0.61), respectively. The RMSE values for DM, TSS, TA, pH, and firmness were 0.93% (1.27%), 1.01 °Brix (1.30 °Brix), 0.31% (0.40%), 0.39 (0.52), and 9.74N (14.70N), respectively. The best models for DM and TSS were obtained using the 2nd derivative with spectrum smoothing with a window of 21 datapoints and absorbance pretreatment. The best model for TA was obtained after using conversion to absorbance. The best model for pH was obtained after conversion of spectral data to absorbance and 1st derivative pretreatment. The best model for firmness was obtained after conversion of spectral data to absorbance and SNV pretreatment.

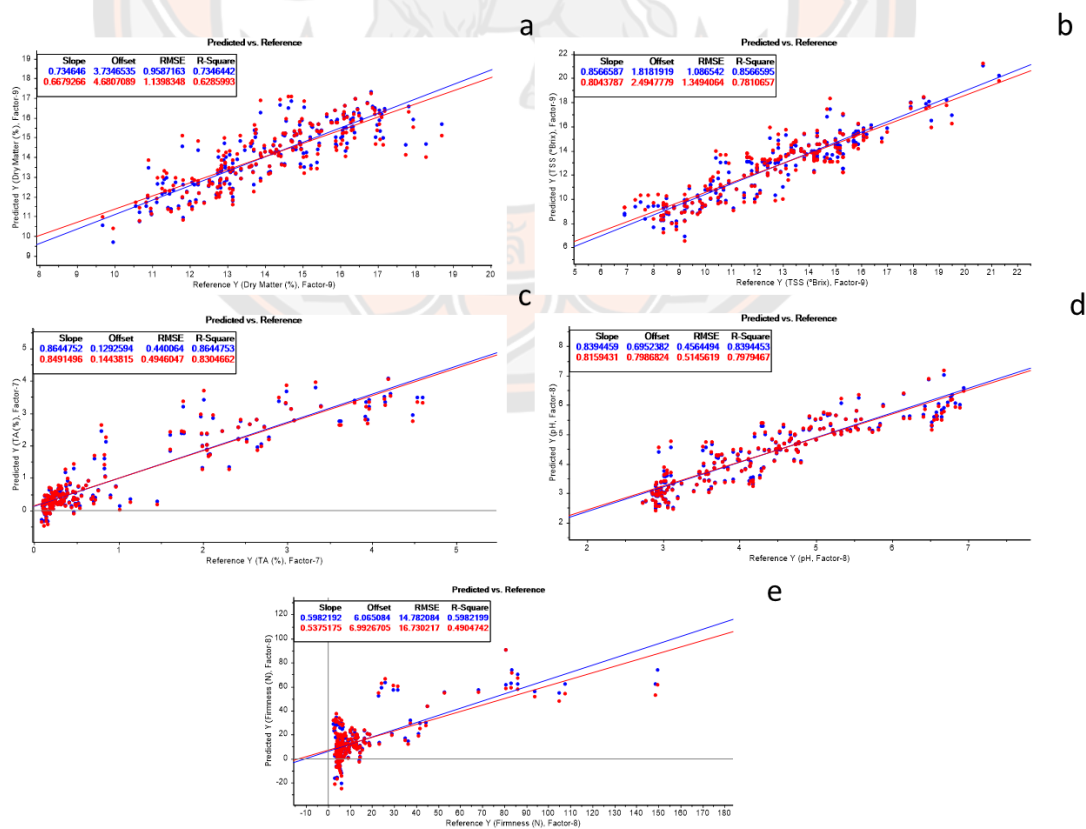


Figure 87 Plot of predicted versus measured values of (a) dry matter, (b) total soluble solids, (c) titratable acidity, (d) pH, and (e) firmness of mangoes for samples collected in both collection periods made with predictive models based on spectral data acquired using the filament light source used without data pretreatment. The plots are showing datapoints for both calibration (blue) and cross validation (red) and the corresponding regression lines.

As can be seen in Figure 87 and Table 26, the models made with data from mangoes collected in both sampling periods without pretreatment of spectral data collected with filament light source exhibited R^2 values for calibration and cross-validation (in brackets) of 0.73 (0.63), 0.86 (0.78), 0.86 (0.83), 0.82 (0.74), and 0.60 (0.49) respectively. The RMSE values for DM, TSS, TA, pH, and firmness were 0.96% (1.14%), 1.09 °Brix (1.35 °Brix), 0.44% (0.49%), 0.46 (0.51), and 14.78N (16.73N), respectively.

The best R^2 values for models based on data from both collection periods for spectral measurements made with the filament light source are shown in Figure 89 and Table 26. The corresponding R^2 values for calibration and cross-validation (in brackets) for DM, TSS, TA, pH, and firmness for NIR LED are 0.79 (0.65), 0.85 (0.80), 0.92 (0.86), 0.86 (0.81), and 0.60 (0.50) respectively. The RMSE values for DM, TSS, TA, pH, and firmness were 0.86% (1.10%), 1.07 °Brix (1.32 °Brix), 0.33% (0.45%), 0.42 (0.50), and 14.72N (16.63N), respectively. The best model for DM was obtained after 2nd derivative pretreatment with spectrum smoothing with a window of 21 datapoints. The best models for TSS and firmness were obtained after 1st derivative pretreatment with spectrum smoothing with a window 21 datapoints. The best model for TA was obtained after 1st derivative pretreatment with spectrum smoothing with a window 3 datapoints. The best model for pH was obtained after SNV pretreatment.

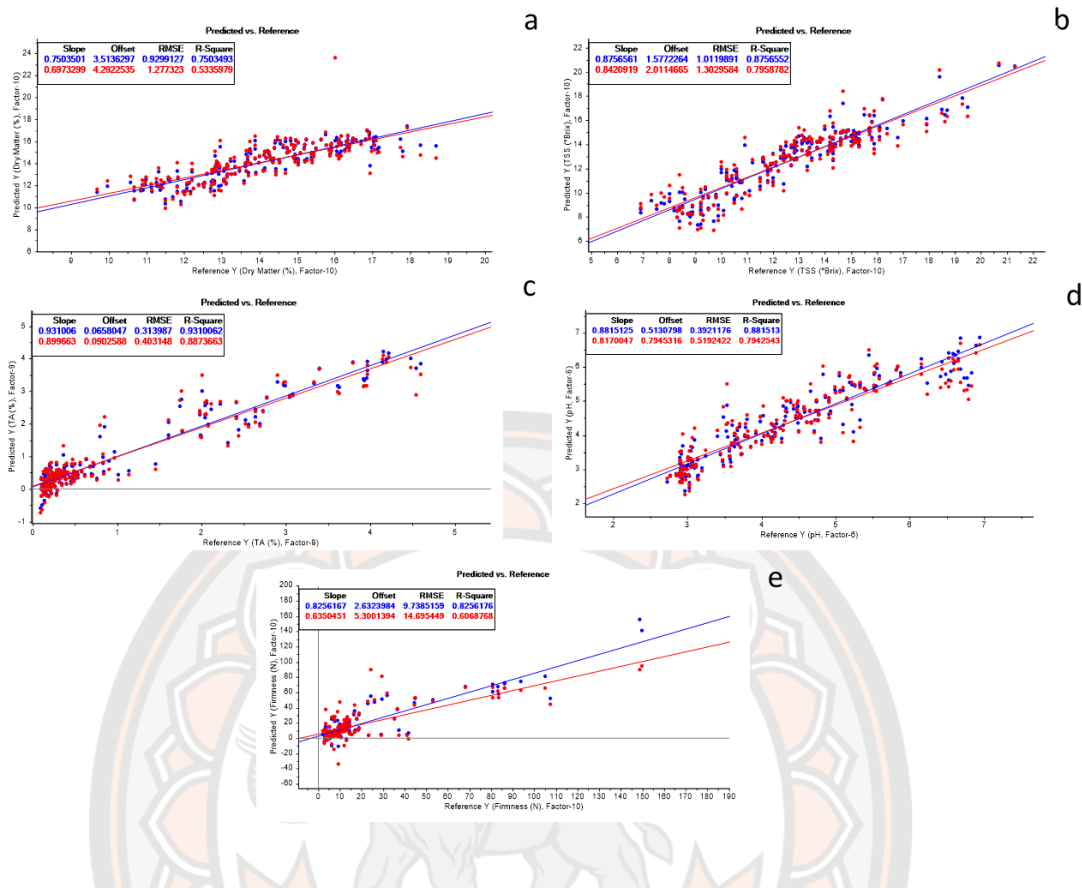


Figure 88 Plot of best cases of predicted versus measured values of (a) dry matter, (b) total soluble solids, (c) titratable acidity, (d) pH, and (e) firmness of mangoes for samples collected in both collection periods made with predictive models based on spectral data acquired using the NIR LED light source. The plots are showing datapoints for both calibration (blue) and cross validation (red) and the corresponding regression lines.

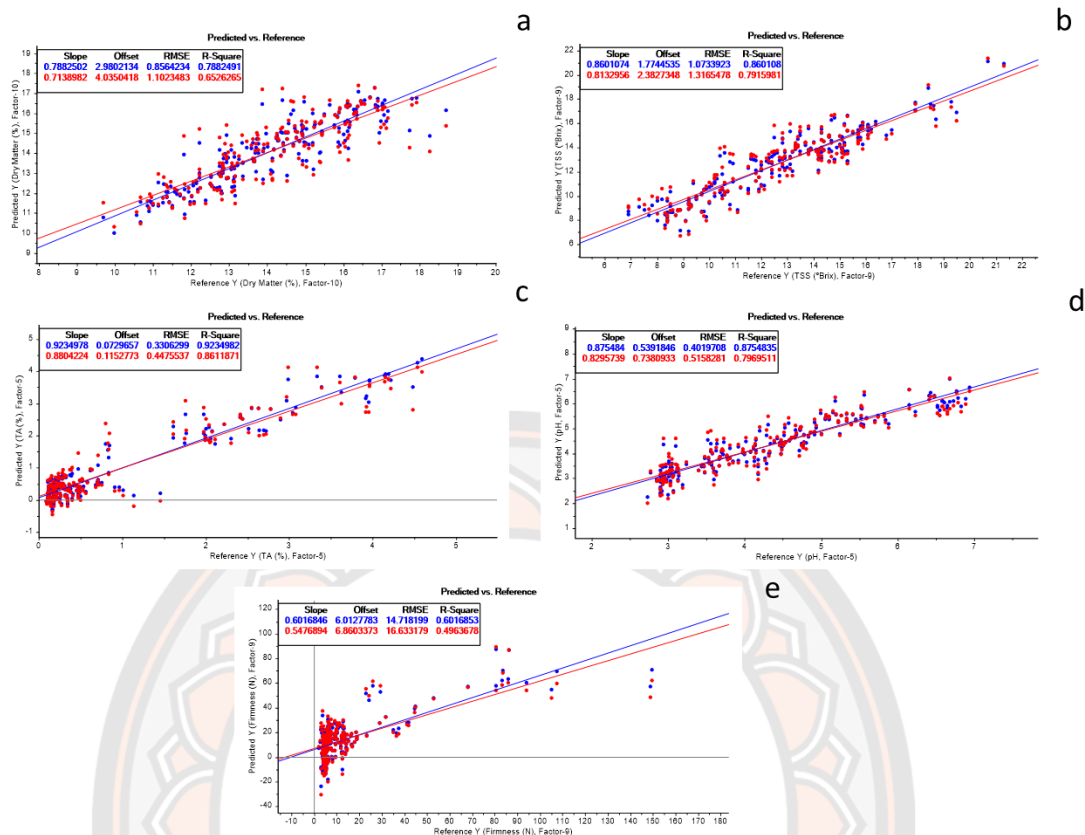


Figure 89 Plot of best cases of predicted versus measured values of (a) dry matter, (b) total soluble solids, (c) titratable acidity, (d) pH, and (e) firmness of mangoes for samples collected in both collection periods made with predictive models based on spectral data acquired using the filament light source. The plots are showing datapoints for both calibration (blue) and cross validation (red) and the corresponding regression lines.

Table 26 Summary of model parameters developed using NIR LED and filament light source from mango samples collected in combine sampling periods

Parameter	Light source	Treatment	Calibration		Cross validation		
			R ²	RMSE	R ²	RMSE	
DM	NIR	None	0.70	1.01	0.57	1.23	
		Abs and 2 nd SGD (21)	0.75	0.93	0.53	1.27	
		Abs and 2 nd SGD* (21)	0.73	0.96	0.67	1.08	
	TH	None	0.73	0.96	0.63	1.14	
		2 nd SGD (21)	0.79	0.86	0.65	1.10	
		2 nd SGD* (21)	0.76	0.92	0.70	1.02	
TSS	NIR	None	0.86	1.06	0.78	1.35	
		Abs and 2 nd SGD (21)	0.88	1.01	0.80	1.30	
		Abs and 2 nd SGD* (21)	0.86	1.09	0.82	1.21	
	TH	None	0.86	1.09	0.78	1.35	
		Abs	0.86	1.07	0.79	1.32	
		Abs*	0.86	1.06	0.82	1.21	
TA	NIR	None	0.92	0.35	0.88	0.42	
		LED	Abs	0.93	0.31	0.89	0.40
			Abs*	0.88	0.41	0.87	0.44
	TH	None	0.86	0.44	0.83	0.49	
		Abs and 1 st SGD (3)	0.92	0.33	0.86	0.45	
		Abs and 1 st SGD* (3)	0.92	0.35	0.90	0.38	
pH	NIR	None	0.82	0.48	0.74	0.58	
		LED	Abs and 1 st SGD (3)	0.88	0.39	0.79	0.52
			Abs and 1 st SGD* (3)	0.86	0.43	0.83	0.48
	TH	None	0.84	0.46	0.80	0.51	
		SNV	0.86	0.42	0.81	0.50	

Parameter	Light source	Treatment	Calibration		Cross validation	
			R ²	RMSE	R ²	RMSE
		SNV*	0.80	0.43	0.75	0.49
Firmness	NIR	None	0.70	12.85	0.47	17.09
		Abs and SNV	0.83	9.74	0.61	14.70
	Abs and SNV*	0.79	10.66	0.70	12.78	
	TH	None	0.60	14.78	0.49	16.73
		Abs and 1 st SGD (21)	0.60	14.72	0.50	16.63
		Abs and 1 st SGD* (21)	0.52	16.08	0.46	17.15

*Model made after selection of significantly contributing variables

SGD – Savitzky-Golay derivative

Furthermore, the data from the combined data set covering the two sampling periods were divided to calibration and test sets. Calibration models were developed using the calibration set and they were subsequently applied for prediction of the quality parameters of the samples in the test set. The performance of the predictions are shown in Figure 90 and Figure 91.

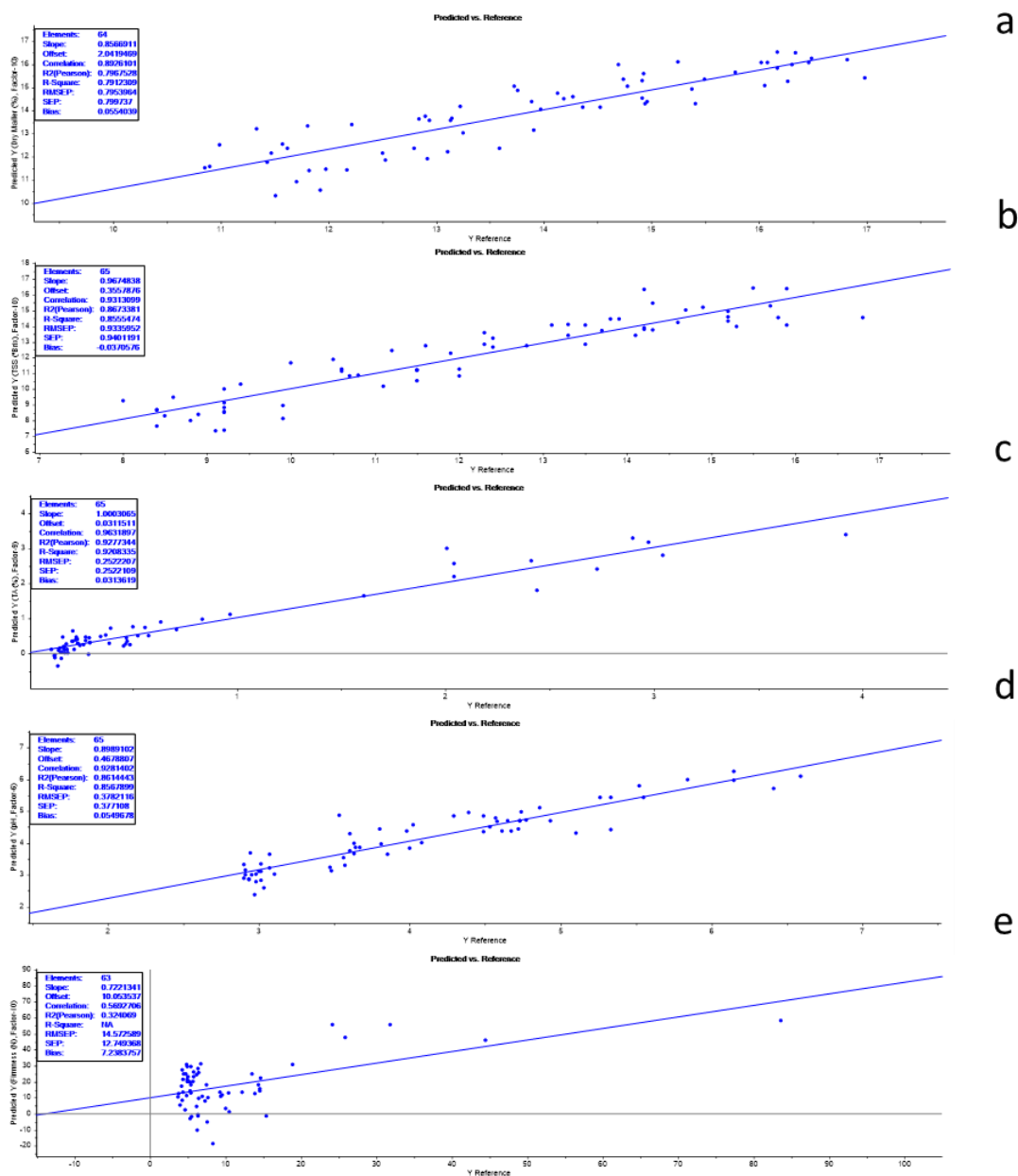


Figure 90 Plot of predicted versus measured values of dry matter (a), total soluble solids (b), titratable acidity (c), pH (d), and firmness (e) of tomatoes using NIR LED light source based on data from testing set of samples collected in both collection periods

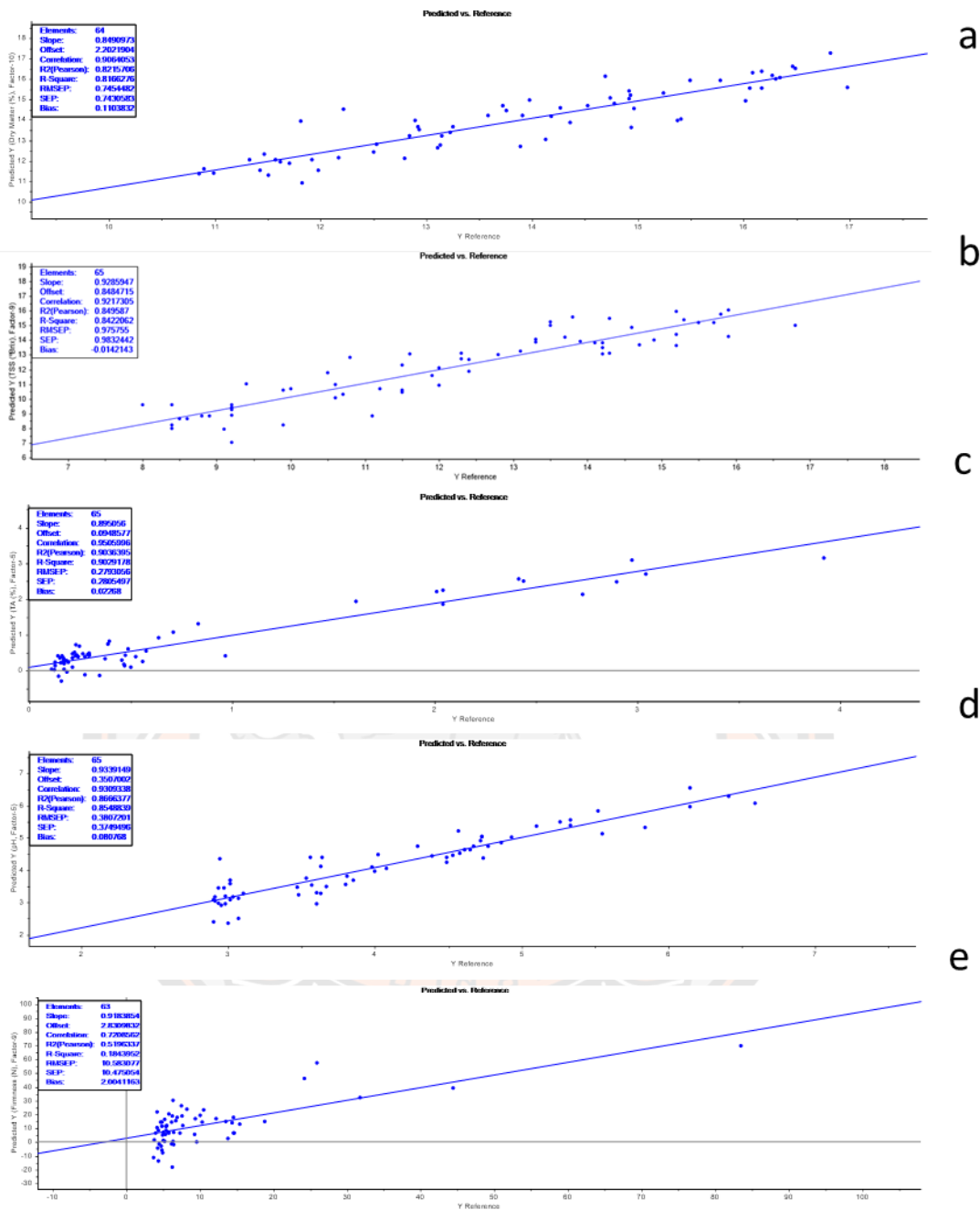


Figure 91 Plot of predicted versus measured values of dry matter (a), total soluble solids (b), titratable acidity (c), pH (d), and firmness (e) of tomatoes using filament bulb light source based on data from testing set of samples collected in both collection periods

Table 27 Summary of model parameters developed using NIR LED and filament bulb light source from mango samples collected in both sampling periods and split into calibration and prediction sets

Parameter	Light source	Analyte mode	Treatment	Calibration		Cross Validation		Test set	
				R ²	RMSE	R ²	RMSE	R ²	RMSE
Dry matter	NIR LED	Absorbance	2 nd SGD (21)	0.75	0.93	0.53	1.27	0.79	0.80
	TH	Reflectance	2 nd SGD (21)	0.79	0.86	0.65	1.10	0.82	0.75
TSS	NIR LED	Absorbance	2 nd SGD (21)	0.88	1.01	0.80	1.30	0.86	0.93
	TH	Absorbance	None	0.86	1.07	0.79	1.32	0.84	0.98
TA	NIR LED	Absorbance	None	0.93	0.31	0.89	0.40	0.92	0.25
	TH	Absorbance	1 st SGD (3)	0.92	0.33	0.86	0.45	0.90	0.28
pH	NIR LED	Absorbance	1 st SGD (3)	0.88	0.39	0.79	0.52	0.86	0.38
	TH	Absorbance	1 st SGD (3)	0.88	0.40	0.80	0.52	0.85	0.38
firmness	NIR LED	Absorbance	SNV	0.83	9.74	0.61	14.70	NA	14.57
	TH	Reflectance	1 st SGD (21)	0.60	14.72	0.50	16.63	0.18	10.58

SGD – Savitzky-Golay derivative

Table 28 Summary of model parameters developed using NIR LED and filament bulb light source from mango samples collected in both sampling periods and split into calibration and prediction sets

Parameter	Light source	Treatment	Test set	
			R ²	RMSE
DM	TH	2 nd SGD (21)	0.82	0.75
TSS	NIR LED	Abs and 2 nd SGD (21)	0.86	0.93
TA	NIR LED	Abs	0.92	0.25
pH	NIR LED	Abs and 1 st SGD (3)	0.86	0.38
firmness	TH	1 st SGD (21)	0.18	10.58

SGD – Savitzky-Golay derivative

Furthermore, the quality parameters are summarized in Table 27. The results indicate that the R² values of the test set for DM, TSS, TA, pH and firmness obtained with spectral measurements using NIR LED light sources were 0.79, 0.86, 0.92, 0.86, and non-detected, respectively. The RMSE values for DM, TSS, TA, pH, and firmness using NIR LED were 0.80%, 0.93 °Brix, 0.25%, 0.38, and 14.52N, respectively.

The R² values of the test set for DM, TSS, TA, pH and firmness for measurements made with filament bulb were 0.82, 0.84, 0.90, 0.85, and 0.18, respectively. The RMSE values for DM, TSS, TA, pH, and firmness using filament bulb were 0.75%, 0.98 °Brix, 0.28%, 0.38, and 10.58N, respectively.

The best model performance in the test using spectral data acquired with the filament bulb is observed for DM and firmness, while spectral data acquired with the NIR LED gave best models for predictions of TSS, TA, and pH. The R² values for DM, TSS, TA, pH and firmness were 0.82, 0.86, 0.92, 0.86, and 0.18, respectively. The RMSE values for DM, TSS, TA, pH, and firmness were 0.75%, 0.93 °Brix, 0.25%, 0.38, and 10.58N, respectively. The models developed for DM, TSS, TA, and pH show acceptable performance for mango quality prediction with R² values

above 0.80. Unfortunately, the predictive models of firmness analysis were of moderate quality with R^2 value for 0.63.

Spectral characteristics of mango and reference measurements

Figure 92a shows pronounced variability in the original spectral data acquired using the NIR LED light source at approximately 650, 750, and 950 nm while Figure 92b shows pronounced variability for data acquired with the filament light bulb at approximately 670 and 970 nm. The spectral region of 650 to 680 nm corresponds to the absorption of chlorophyll. The features at 750 and 950 nm correspond to the 4th overtone of the C-H stretching vibration of starch or/and sugar, and 2nd overtone of water, respectively.

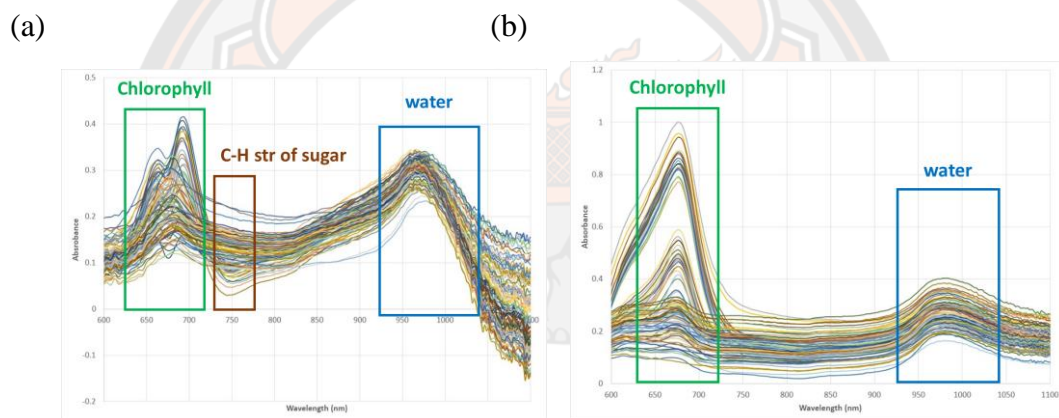


Figure 92 Plot of absorbance versus wavelength for important spectral features acquired using the in-house spectrometer equipped with the (a) NIR LED (b) Filament light sources for mango samples

1. DM

As mentioned above, the spectral features around the wavelength of 950 nm are significant for predicting DM content. Figure 92 shows plot of absorbance versus wavelength for spectra acquired using the NIR LED and TH light sources in the in-house spectrometer. The NIR LED and TH light sources provide spectra with clearly detectable water signal at about 950 nm.

The results for the best cases of R^2 values for predicting DM (Table 29) indicated that the R^2 values of calibration and cross-validation (in brackets) for

predicting DM for NIR LED and TH light sources were 0.75 (0.53) and 0.79 (0.65), respectively. The R^2 values of prediction for the test set for the NIR LED and TH light sources were 0.79 and 0.82, respectively.

Table 29 provides a comparison for the results of the performance of DM. Two publication reports are shown in the Table 29. The first report was published by Neto and coworkers in 2017 [4]. This work was conducted with the portable F750 spectrometer operating in the Vis-NIR range 310-1100 nm. The models for predicting DM exhibited R_c^2 of 0.84, which is better than the performance of the predictive models reported herein for both NIR LED and TH versions of the spectrometers. The second publication was reported by the same group in 2019 [49]. The authors have carried out using the same instrument. The resulting models had R_c^2 of 0.70 for predicting DM, which is below the performance of the predictive models reported here in for both NIR LED and TH versions of the spectrometer.

The comparison of performance between inhouse built spectrometer and commercial spectrometers for evaluating DM in mango samples indicates that models made with both the NIR LED and TH versions of the spectrometer are below the performance of predictive models made with data acquired with SCiO and Linksquare operating with NIR and visible modes.

2. TSS

Figure 92 shows plots of absorbance versus wavelength acquired using NIR LED and TH versions of the spectrometer. The spectra acquired with NIR LED irradiation exhibit strongly variable absorbance around 750 nm. Spectral features in the region are related to the 4th overtone of C-H stretching and can be used for predicting sugar contents. Spectra acquired with TH illumination show only moderate variation of absorbance around 750 nm.

The results for the best cases of R^2 values for predicting TSS (Table 27) indicated that the R^2 values of calibration and cross-validation (in brackets) for predicting TSS with NIR LED and TH illumination were 0.88 (0.80) and 0.86 (0.79), respectively. The R^2 values for prediction for the test set of NIR LED and TH were 0.86 and 0.84, respectively. The R^2 values for calibration, cross-validation, and

prediction are higher for NIR LED illumination in comparison with the TH illumination.

Four published papers, which report predictive models for total soluble solids (TSS) or soluble solid content (SSC) are shown in Table 29. The first one was published by Jha and coworkers in 2012 [28]. Models for prediction TSS were obtained with R_c^2 of 0.56, which is significantly worse than the results obtained in this work. Subsequently, Rungpichayapichet and coworkers have published two reports in 2016 and 2017 [29, 50]. The results in the first work provided models for the prediction of TSS with R_c^2 and R_p^2 of 0.80-0.90, which is slightly below the performance of the results obtained here in. In the second work, the R_c^2 was 0.40-0.50, which is significantly worse than the results obtained herein. Finally, a publication from Neto and coworkers was reported in 2017 [4]. The models for prediction of TSS in this work exhibited R_c^2 of 0.87, which is slightly below the results obtained herein for both NIR LED and TH versions of the inhouse spectrometer.

The comparison of performance between the inhouse built spectrometer and commercial spectrometers investigated in this work show that both NIR LED and TH versions of the inhouse spectrometer give models with better performance of predictive models in comparison with SCiO and Linksquare operating in NIR and visible modes.

3. TA and pH

Figure 92 shows the plot of absorbance versus wavelength obtained using the NIR LED and TH versions of the inhouse spectrometer. The spectra acquired with NIR LED irradiation exhibit strongly variable absorbance around 750 nm. Spectral features in the region are related to the 4th overtone of C-H stretching and can be used for predicting sugar contents. Spectra acquired with TH illumination show only moderate variation of absorbance around 750 nm, which is similar to the situation described for estimating TSS content.

The best cases of R^2 values for predicting TA (Table 27) indicated that the R^2 values of calibration and cross-validation (in brackets) for predicting TA based on data acquired with NIR LED and TH irradiation were 0.93 (0.89) and 0.92 (0.86), respectively. The R^2 values of prediction for the test set in the case of NIR LED and

TH irradiation were 0.92 and 0.90, respectively. The models for predicting pH based on NIR LED and TH irradiation, show that R^2 values for calibration and cross-validation (in brackets) of 0.88 (0.79) and 0.88 (0.80), respectively. The R^2 values of prediction for the test set based on NIR LED and TH irradiation were 0.86 and 0.85, respectively. The performance of models based on data acquired with both NIR LED and TH irradiation are comparable with the R^2 values of calibration, cross-validation, and prediction of the test set. The performance of these models is significantly better than the performance of models for predicting TA and pH obtained in the above-described experiments with commercial spectrometers.

4. Firmness

As mentioned above, the spectral region around 750 nm is significant for predicting firmness based on the starch content. The results for the best cases of R^2 values for predicting Firmness (Table 27) indicate that the R^2 values of calibration and cross-validation (in brackets) obtained with NIR LED and TH irradiation were 0.83 (0.61) and 0.60 (0.50), respectively. Unfortunately, the R^2 values of prediction for the test set of NIR LED and TH were poor with the R^2 values below 0.20.

Reference	Instrument	Wavelength (nm)	DM $R_c^2 (R_p^2)$	TSS/SSC $R_c^2 (R_p^2)$	TA $R_c^2 (R_p^2)$	pH $R_c^2 (R_p^2)$	Firmness $R_c^2 (R_p^2)$
Mishra et al., 2020 [51]	F750	310-1130	N.D.	N.D.	N.D.	N.D.	0.62-0.75 (0.67-0.75)
Kasim, Schouten, Woltering, & Boer, 2021 [11]	Mishra, SCIO	740-1070	N.D.	N.D.	N.D.	N.D.	N.D. (0.77- 0.94)
This work for commercial spectrometers	for SCIO Linksquare Linksquare Neospectra TI	740-1070 400-1000 700-1050 1300-2500 900-1700	0.92 0.81 (0.64) 0.86 (0.62) 0.63 (0.48) 0.70 (0.57)	0.84 0.91 (0.75) 0.76 (0.50) 0.66 (0.50) 0.77 (0.55)	0.50 0.91 (0.79) 0.85 (0.51) 0.42 (0.38) 0.42 (0.20)	0.74 0.93 (0.81) 0.86 (0.44) 0.69 (0.49) 0.71 (0.45)	0.26 0.74 (0.37) 0.49 (0.31) 0.17 (0.05) 0.33 (0.18)
This work of in-house spectrometers	NIR LED TH	640-1050 640-1050	0.75 (0.53) 0.79 (0.65)	0.88 (0.80) 0.86 (0.79)	0.93 (0.89) 0.92 (0.86)	0.88 (0.79) 0.88 (0.80)	0.83 (0.61) 0.60 (0.50)

4.4.2 Predictive models for tomato quality parameters

Sample preparation

As mentioned above, the tomato (Tor tomato) samples were obtained from fresh produce markets (Phitsanulok, Phetchabun) and local supermarkets (Lotus, Macro, Tops). The number of samples and location sources were summarized in Table 30.

Table 30 Numbers of samples based on location of collection for in-house optical spectrometers of tomato for first and second period times.

Collection period	Source Location	N
First period	collection Phitsanulok	200
	Pichit	85
	Tesco lotus	15
	Total of first period time	300
Second period	colection Phachuap Khiri Khan	100
	Phitsanulok	57
	Tesco lotus	115
	Macro	36
	Total of first period time	308
Total		608

In total 608 tomato samples were collected in this work. Tomatoes were washed with water to remove the gum and clean. After cleaning, the samples were stored at ambient conditions. In the case of DM, TSS, TA and pH four sampling areas (2x2cm) were used on the surface of the samples. In the case of firmness analysis only one sampling area on the surface of the samples was used. Spectroscopic measurements were performed on the surface of these areas as shown in Figure 93 and Figure 94.

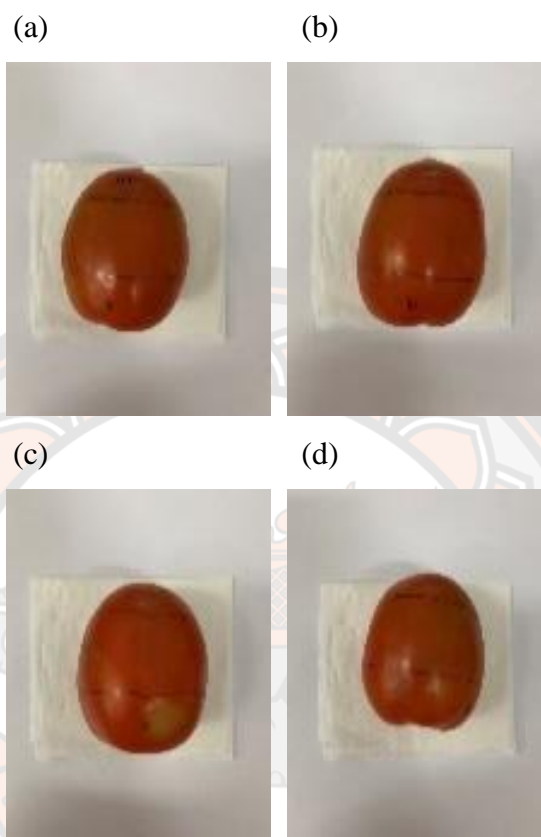


Figure 93 Representative images of sampling areas (a) first (b) second (c) third, and (d) forth side of a tomato sample for predicting DM, TSS, TA, and pH with in-house spectrometer.



Figure 94 Representative image of sampling are of a tomato sample for predicting firmness with in-house spectrometer.

Data Acquisition of inhouse spectrometers for tomato samples

Spectroscopic measurements from the marked areas were performed using two versions of the in-house spectrometer prototype (LED and filament). Four spectra were record for each location. Sixteen spectra acquired from all locations on the tomato sample were averaged and used for the calibration of predictive models for DM, TSS, TA, and pH. Four spectra collected from a single spot were averaged for firmness analysis. The samples were split into three groups for the standard reference analyses. Samples in the first group were used for DM analysis. The second group of samples was used for TSS, TA, and pH. Finally, the last group used for firmness analysis including Firmness, Firmness1, Firmness2, Firmness3, Firmness4, and Firmness5. Spectroscopic measurements conducted with the two versions of the inhouse spectrometer are shown in Figure 95 and Figure 96.

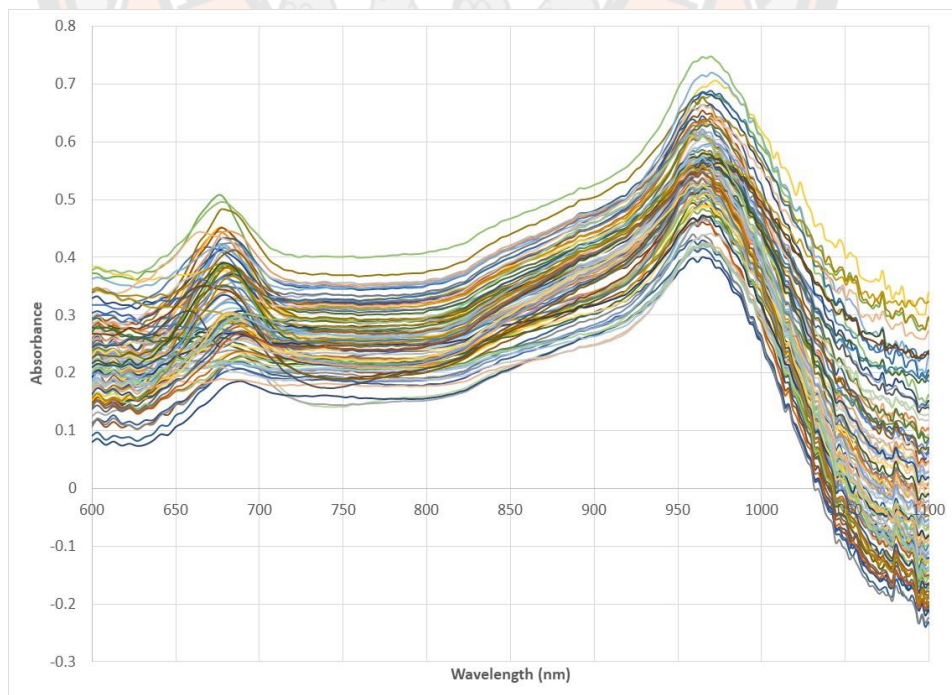


Figure 95 Plot of absorbance versus wavelength for spectra acquired using in-house spectrometer equipped with the LED light source for tomato samples used to develop predictive models for dry matter

Figure 95 shows the absorbance spectra for the tomato samples recorded by the spectrometer equipped with the LED light source spectrometer and used for the development of predictive models for dry matter. The sensor is operating in the range 640 to 1050 nm. The spectral data clearly show the water signal around 970. The spectra also show strong pronounced variability at 670, 710, and 750 nm for chlorophyll content, O-H str of starches and sugars, and C-H str of starches and sugars, respectively.

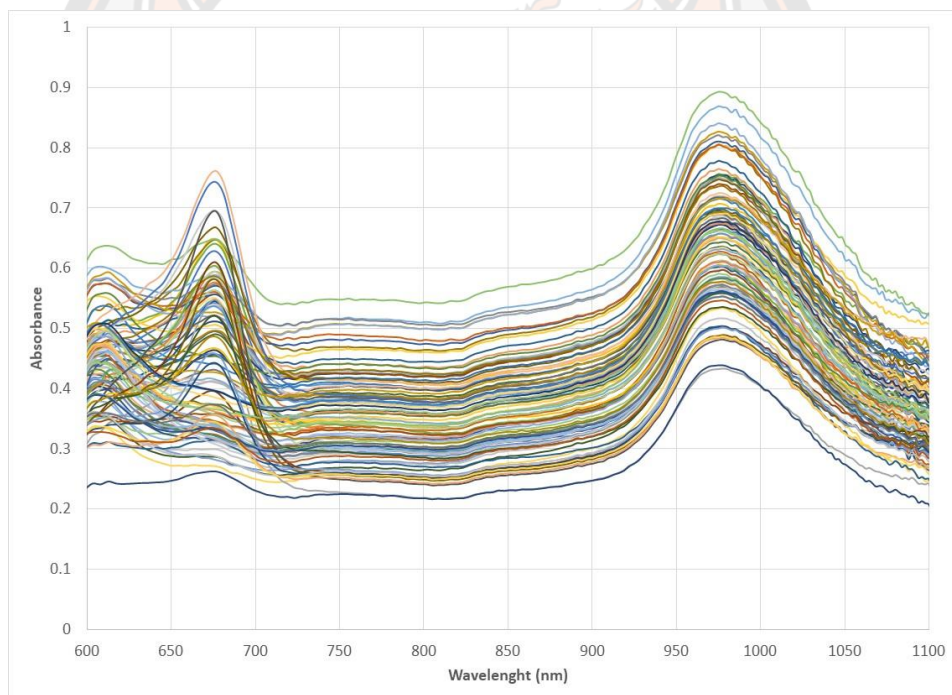


Figure 96 Plot of absorbance versus wavelength for spectra acquired using in-house spectrometer equipped with the tungsten light source for tomato samples used to develop predictive models for dry matter

Figure 96 shows the absorbance spectra for the tomato samples recorded by the spectrometer equipped with the TH light source spectrometer and used for the

development of predictive models for dry matter. The sensor is operating in the range 640 to 1050 nm. The spectral data clearly show the chlorophyll and water signals around 670 and 970 nm, respectively.

Reference analysis

The tomato samples were obtained in two different sampling period. One hundred samples in the first and second collection period were used to develop models for five quality parameters (DM, TSS, TA, pH, and firmness). The descriptive statistics for quality parameters from the first and second collection period can be found in Table 31 and Table 32, respectively.

Table 31 Descriptive statistics for quality parameters analyzed in tomato sample for first collection period.

Parameter	N	Average	Min	Max	Std
DM (%)	100	5.2156	4.0869	7.8026	0.65
TSS (°Brix)	100	4.2	3.2	5.3	0.48
TA (%)	100	0.607	0.320	1.200	0.20
pH	100	4.21	3.85	4.75	0.18
Firmness (N)	100	5.64	2.87	10.67	1.73
Firmness1 (N)	100	32.53	19.83	58.50	8.52
Firmness2 (N)	100	8.28	4.29	15.62	2.60
Firmness3 (N)	100	17.46	8.86	30.54	5.51
Firmness4 (N/mm)	100	2.39	1.50	4.24	0.68
Firmness5 (N/mm)	100	2.48	1.49	4.47	0.71

Table 32 Descriptive statistics for quality parameters analyzed in tomato samples in the second collection period.

parameter	N	Average	Min	Max	Std
DM (%)	100	5.1356	3.6823	7.0378	0.72
TSS (°Brix)	100	4.5	3.0	6.0	0.61
TA (%)	100	0.758	0.299	1.659	0.24
pH	100	4.18	3.63	4.80	0.28
Firmness (N)	100	5.78	2.47	12.35	2.41
Firmness1 (N)	100	33.22	14.56	59.47	11.07
Firmness2 (N)	100	8.62	3.72	18.60	3.62
Firmness3 (N)	100	18.92	8.33	40.13	7.61
Firmness4 (N/mm)	100	2.51	0.97	4.66	0.82
Firmness5 (N/mm)	100	2.60	1.03	5.10	0.90

Table 31 and 32 shows the range of measurement (minimum and maximum values), average, and standard deviation of the quality parameters in the tomato sample.

The values for Dry matter, TSS, TA, pH, Firmness, Firmness1, Firmness2, Firmness3, Firmness4, and Firmness5 were in the range 4.0869-7.8026 %, 3.2-5.3 °Brix, 0.320-1.200 %, 3.85-4.75, 2.87-10.67 N, 19.83-58.50 N, 4.29-15.62 N, 8.86-30.54 N, 1.50-4.24 N/mm, and 1.49-4.47 N/mm for first collection, respectively (Table 31). The values of Dry matter, TSS, TA, pH, Firmness, Firmness1, Firmness2, Firmness3, Firmness4, and Firmness5 for samples analyzed in the second collection period were 3.6823-7.0378 %, 3.0-6.0 °Brix, 0.299-1.659 %, 3.63-4.80, and 2.47-12.35 N, 14.56-59.47 N, 3.72-18.60 N, 8.33-40.13 N, 0.97-4.66 N/mm, and 1.03-5.10 N/mm, respectively (Table 32).

Data analysis

Figure 97 and Figure 98 show the plots of predicted versus measured values of DM, TSS, TA, pH, and firmness obtained using calibration models based on spectral data acquired using the in-house spectrometer prototype equipped with the NIR LED light source.

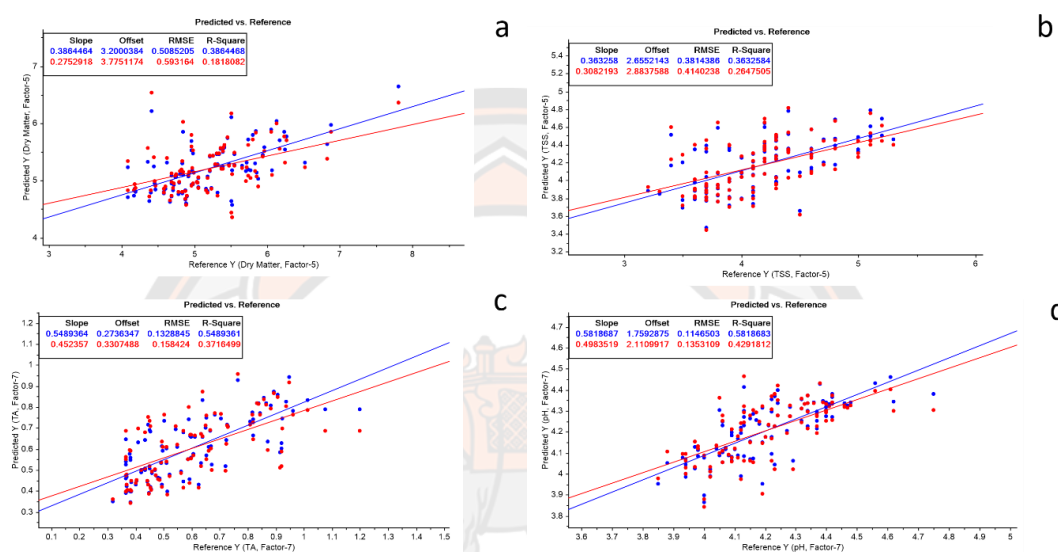


Figure 97 Plot of predicted versus measured values of (a) dry matter, (b) total soluble solids, (c) titratable acidity, and (d) pH of tomatoes for samples collected in the first collection period made with predictive models based on spectral data acquired using the NIR LED light source used without data pretreatment. The plots are showing datapoints for both calibration (blue) and cross validation (red) and the corresponding regression lines.

As can be seen in Table 33, the results indicate that the R^2 values for calibration and cross-validation (in brackets) for models developed using spectral data acquired using the spectrometer equipped with NIR LED light source without pretreatment for DM, TSS, TA, pH, Firmness, Firmness1, Firmness2, Firmness3, Firmness4, and Firmness5 were 0.39 (0.18), 0.36 (0.26), 0.55 (0.37), 0.58 (0.43), 0.83 (0.76), 0.69 (0.57), 0.83 (0.78), 0.83 (0.78), 0.79 (0.61), and 0.78 (0.68), respectively. The RMSE values for DM, TSS, TA, pH,

Firmness, Firmness1, Firmness2, Firmness3, Firmness4, and Firmness5 were 0.51% (0.59%), 0.38 °Brix (0.41 °Brix), 0.13% (0.16%), 0.11 (0.14), and 0.70N (0.85N), 4.73N (5.60N), 1.05N (1.22N), 2.26N (2.63N), 0.31N/mm (0.42N/mm), 0.33N/mm (0.40N/mm), respectively.

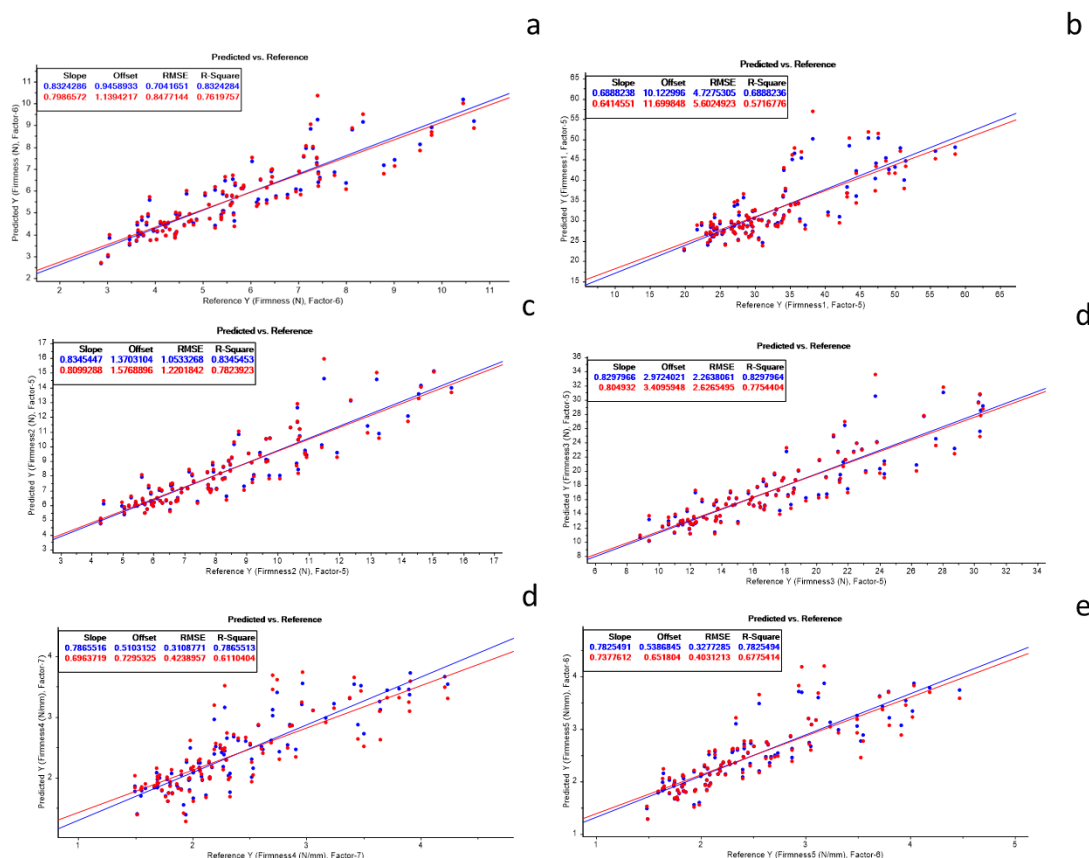


Figure 98 Plot of predicted versus measured values without pretreatment of (a) Firmness, (b) Firmness1, (c) Firmness2 (d) Firmness3, (e) Firmness4, and (f) Firmness5 of tomatoes using NIR LED light source from samples collected in the first collection period showing both datapoints for both calibration (blue) and cross validation (red) and the corresponding regression lines.

The best R^2 values for models developed using tomato samples collected in the first sampling period are shown in Table 33. The R^2 values for calibration and cross-validation (in brackets) for models developed with spectral data acquired using the NIR LED light source for DM, TSS, TA, pH, Firmness,

Firmness1, Firmness2, Firmness3, Firmness4, and Firmness5 were 0.66 (0.33), 0.60 (0.29), 0.62 (0.47), 0.60 (0.40), 0.84 (0.78), 0.72 (0.59), 0.86 (0.81), 0.85 (0.80), 0.78 (0.63), and 0.84 (0.70), respectively. The RMSE values for DM, TSS, TA, pH, firmness, Firmness1, Firmness2, Firmness3, Firmness4, and Firmness5 were 0.38% (0.54%), 0.30 °Brix (0.41 °Brix), 0.12% (0.15%), 0.11 (0.14), and 0.68N (0.82N), 4.48N (5.50N), 0.96N (1.15N), 2.14N (2.50N), 0.31N/mm (0.41N/mm), 0.28N/mm (0.39N/mm), respectively. The best models for DM, pH, and Firmness2 were developed after conversion of spectral data to absorbance. The best models for TSS and TA were obtained after spectral data conversion to absorbance and 2nd derivative with spectrum smoothing and a window of 21 datapoints. The best values for firmness1 and firmness5 were obtained after spectral data conversion to absorbance and SNV pretreatment procedure. The best model for firmness3 was obtained after smoothing pretreatment procedure with spectrum smoothing and a window 3 datapoints. The best model for firmness4 was obtained after SNV pretreatment procedure. The best model for firmness was obtained using spectral data without pretreatment.

Moreover, the best performing models obtained from data collected in the first sampling period were used to make predictions for samples collected in the second sampling (Table 33). The results indicated that the prediction R² values DM, TSS, TA, pH, Firmness, Firmness1, Firmness2, Firmness3, Firmness4, and Firmness5 for NIR LED were non-detected, non-detected, non-detected, non-detected, 0.68, non-detected, 0.65, non-detected, non-detected, and non-detected and non-detected, respectively. The RMSE values for DM, TSS, TA, pH, Firmness, Firmness1, Firmness2, Firmness3, Firmness4, and Firmness5 were 0.81%, 3.39 °Brix, 0.81%, 1.30, 1.36N, 26.36N, 2.12N, 10.61N, 4.57N/mm, and 2.68N/mm, respectively.

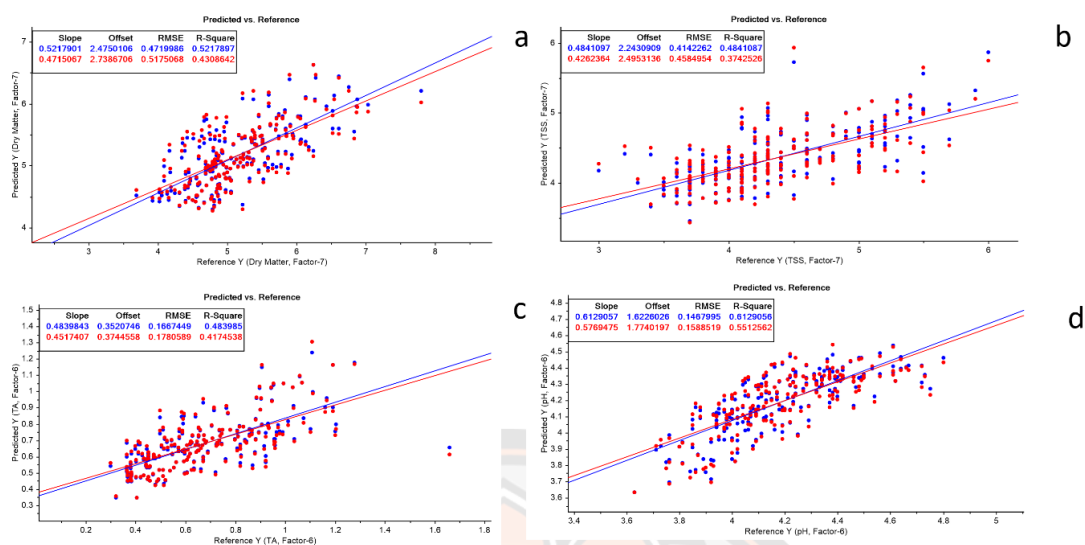


Figure 99 Plot of predicted versus measured values of (a) dry matter, (b) total soluble solids, (c) titratable acidity, and (d) pH of tomatoes for samples collected in the first collection period made with predictive models based on spectral data acquired using the filament light source used without data pretreatment. The plots are showing datapoints for both calibration (blue) and cross validation (red) and the corresponding regression lines.

Figure 99 and Figure 100 show the plots of predicted versus measured values of DM, TSS, TA, pH, and firmness obtained using calibration models based on spectral data acquired using the in-house spectrometer prototype equipped with the filament light source.

As can be seen in Table 33, the results indicate that the R^2 values for calibration and cross-validation (in brackets) for models developed using spectral data acquired using the spectrometer equipped with filament light source without pretreatment for DM, TSS, TA, pH, Firmness, Firmness1, Firmness2, Firmness3, Firmness4, and Firmness5 were 0.56 (0.33), 0.35 (0.21), 0.50 (0.37), 0.46 (0.40), 0.90 (0.80), 0.85 (0.65), 0.90 (0.82), 0.91 (0.83), 0.85 (0.67), and 0.88 (0.73), respectively. The RMSE values for DM, TSS, TA, pH, Firmness, Firmness1, Firmness2, Firmness3, Firmness4, and Firmness5 were 0.43% (0.54%), 0.39 °Brix (0.43 °Brix), 0.14% (0.16%), 0.13 (0.14), and 0.56N (0.79N), 3.33N (5.05N), 0.82N (1.11N), 1.63N (2.25N), 0.26N/mm (0.39N/mm), 0.24N/mm (0.35N/mm), respectively.

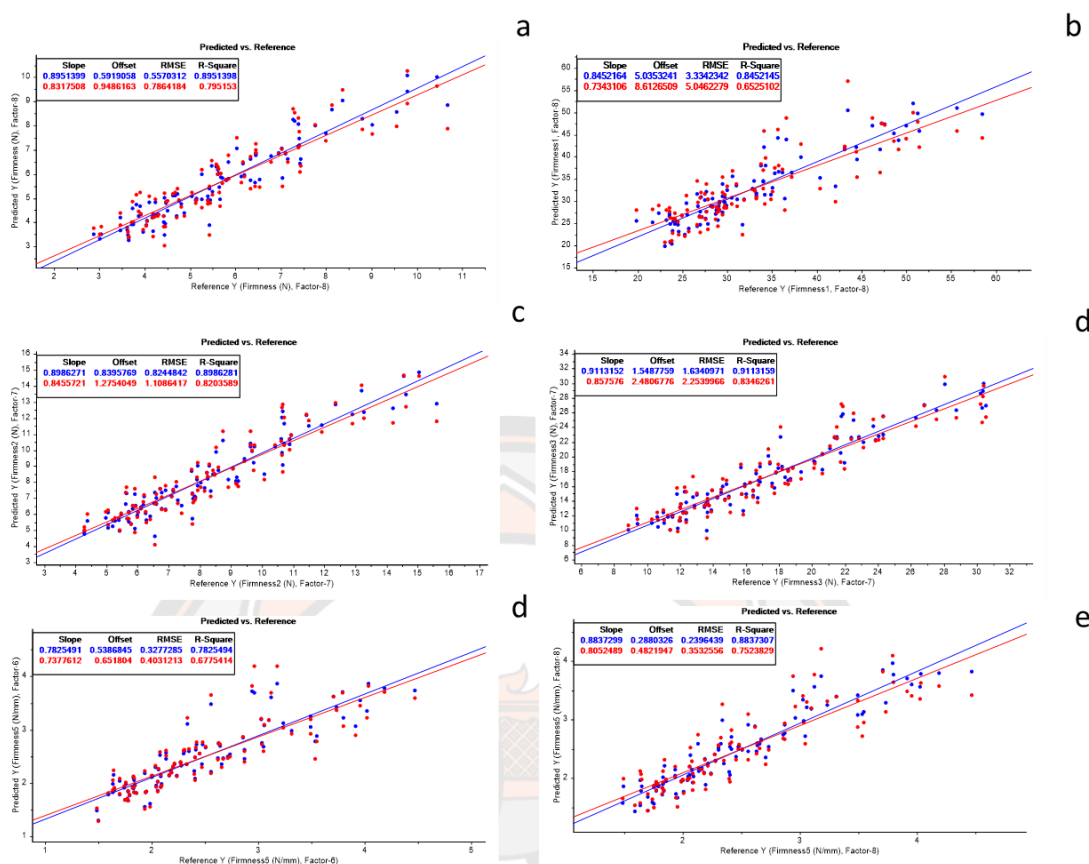


Figure 10 Plot of predicted versus measured values of (a) Firmness, (b) Firmness1, (c) Firmness2 (d) Firmness3, (e) Firmness4, and (f) Firmness5 of tomatoes for samples collected in the first collection period made with predictive models based on spectral data acquired using the filament light source used without data pretreatment. The plots are showing datapoints for both calibration (blue) and cross validation (red) and the corresponding regression lines.

The best R^2 values for models developed using tomato samples collected in the first sampling period are shown in Table 33. The R^2 values for calibration and cross-validation (in brackets) for models developed with spectral data acquired using the filament light source for DM, TSS, TA, pH, Firmness, Firmness1, Firmness2, Firmness3, Firmness4, and Firmness5 were 0.77 (0.54), 0.51 (0.28), 0.52 (0.40), 0.54 (0.35), 0.88 (0.73), 0.84 (0.63), 0.89 (0.77), 0.90

(0.80), 0.85 (0.67), and 0.88 (0.73), respectively. The RMSE values for DM, TSS, TA, pH, Firmness, Firmness1, Firmness2, Firmness3, Firmness4, and Firmness5 were 0.31% (0.45%), 0.33 °Brix (0.41 °Brix), 0.14% (0.16%), 0.12 (0.14), and 0.60N (0.89N), 3.43N (5.24N), 0.84N (1.25N), 1.69N (2.50N), 0.26N/mm (0.39N/mm), 0.25N/mm (0.37N/mm), respectively. The best model for DM has been obtained after 1st derivative pretreatment procedure. The best model for TSS was obtained after SNV pretreatment procedure. The best models for TA, firmness, firmness1, firmness2, firmness3, and firmness5 were obtained after spectral data conversion to absorbance and SNV pretreatment procedure. The best model for pH was obtained after 2nd derivative pretreatment procedure with spectrum smoothing and a window 21 datapoints. The best model for firmness4 was obtained using spectral data without pretreatment.

Moreover, the best models obtained using samples from the first sampling period were used to predict values of quality parameters for samples collected in the second sampling period (Table 33). The results indicate that the R² values for prediction for samples from the second sampling period using spectral data acquired using filament light source for DM, TSS, TA, pH, Firmness, Firmness1, Firmness2, Firmness3, Firmness4, and Firmness5 for filament light source were non-detected, non-detected, non-detected, 0.11, 0.59, 0.38, 0.62, 0.64, 0.44, and 0.53, respectively. The RMSE values for DM, TSS, TA, pH, Firmness, Firmness1, Firmness2, Firmness3, Firmness4, and Firmness5 were 3.94%, 0.87 °Brix, 0.24%, 0.24, 0.27N, 8.70N, 2.21N, 4.55N, 0.61N/mm, and 0.62N/mm, respectively.

The predictions of the parameters of interest for tomato samples from the second collection period made with models calibrated on data acquired with tomato samples in the first collection period resulting in R² values below 0.50. The moderate predictive performance of the models based on tomato samples collected in the first collection period is likely due to lack robustness given the number of samples and limited sampling time frame. To address the issue, a new sample set was created by combining the samples from the first and the second collection periods. The descriptive statistics for quality parameters of combined sample set can be found in Table 34

Table 33 Summary of model parameters developed using NIR LED and filament bulb light source from tomato samples collected in the first sampling period and predictive model parameters for the second sampling period.

Parameter	Light source	Treatment	Calibration		Cross Validation		Prediction	
			R ²	RMSE	R ²	RMSE	R ²	RMSE
Dry Matter	NIR LED	None	0.39	0.51	0.18	0.59		
		Abs	0.66	0.38	0.33	0.54	NA	1.81
		Abs*	0.47	0.47	0.38	0.52		
TH	NIR LED	None	0.56	0.43	0.33	0.54		
		1 st SGD (21)	0.77	0.31	0.54	0.45	NA	3.94
		1 st SGD* (21)	0.74	0.33	0.61	0.41		
TSS	NIR LED	None	0.36	0.38	0.26	0.41		
		Abs and 2 nd SGD (21)	0.60	0.30	0.29	0.41	NA	3.39
		Abs and 2 nd SGD* (21)	0.32	0.39	0.24	0.42		
TH	NIR LED	None	0.35	0.39	0.21	0.43		
		SNV	0.51	0.33	0.28	0.41	NA	0.87
		SNV*	0.19	0.43	0.16	0.44		

Parameter	Light source	Treatment	Calibration		Cross Validation		Prediction	
			R ²	RMSE	R ²	RMSE	R ²	RMSE
TA	NIR LED	None	0.55	0.13	0.37	0.16		
		Abs and 2 nd SGD (21)	0.62	0.12	0.47	0.15	NA	0.81
		Abs and 2 nd SGD* (21)	0.60	0.12	0.52	0.14		
	TH	None	0.50	0.14	0.37	0.16		
		Abs and SNV	0.52	0.14	0.40	0.16	NA	0.24
		Abs and SNV*	0.56	0.13	0.45	0.15		
pH	NIR LED	None	0.58	0.11	0.43	0.14		
		Abs	0.60	0.11	0.40	0.14	NA	1.30
		Abs*	0.62	0.11	0.51	0.13		
	TH	None	0.46	0.13	0.40	0.14		
		2 nd SGD (21)	0.54	0.12	0.35	0.14	0.11	0.27
		2 nd SGD* (21)	0.51	0.12	0.40	0.14		

Parameter	Light source	Treatment	Calibration			Cross Validation			Prediction		
			R ²	RMSE		R ²	RMSE		R ²	RMSE	
Firmness	NIR LED	None	0.83	0.70	0.76	0.85					
		Abs	0.84	0.68	0.78	0.82		0.68	1.36		
		Abs*	0.83	0.70	0.79	0.79					
TH		None	0.90	0.56	0.80	0.79		0.59	1.53		
		Abs and SNV	0.88	0.60	0.73	0.89		0.59	1.53		
		Abs and SNV*	0.82	0.72	0.78	0.81					
Firmness1	NIR LED	None	0.69	4.73	0.57	5.60					
		Abs and SNV	0.72	4.48	0.59	5.50		NA	26.36		
		Abs and SNV*	0.77	4.03	0.68	4.85					
TH		None	0.85	3.33	0.65	5.05		0.34	8.95		
		Abs and SNV	0.84	3.43	0.63	5.24		0.38	8.70		
		Abs and SNV*	0.70	4.67	0.64	5.12					
Firmness2	NIR LED	None	0.83	1.05	0.78	1.22					
		Abs	0.86	0.96	0.81	1.15		0.65	2.12		
		Abs*	0.85	0.99	0.82	1.12					

Parameter	Light source	Treatment	Calibration		Cross Validation		Prediction	
			R ²	RMSE	R ²	RMSE	R ²	RMSE
Firmness3	TH	None	0.90	0.82	0.82	1.11		
		Abs and SNV	0.89	0.84	0.77	1.25	0.62	2.21
		Abs and SNV*	0.85	1.02	0.80	1.18		
Firmness3	NIR LED	None	0.83	2.26	0.78	2.63		
		SGD (3)	0.85	2.14	0.80	2.50	NA	10.61
		SGD* (3)	0.85	2.15	0.80	2.47		
Firmness4	TH	None	0.91	1.63	0.83	2.25		
		Abs and SNV	0.90	1.69	0.80	2.50	0.64	4.55
		Abs and SNV*	0.87	1.99	0.82	2.33		
Firmness4	NIR LED	None	0.79	0.31	0.61	0.42		
		SNV	0.78	0.31	0.63	0.41	NA	4.57
		SNV*	0.80	0.30	0.73	0.36		
Firmness5	TH	None	0.85	0.26	0.67	0.39	0.44	0.61
		None*	0.79	0.31	0.73	0.36		
		None	0.78	0.33	0.68	0.40		
Firmness5	NIR LED	None	0.84	0.28	0.70	0.39	NA	2.68
		Abs and SNV	0.84	0.28	0.79	0.33		
		Abs and SNV*	0.84	0.28	0.79	0.33		

Parameter	Light source	Treatment	Calibration		Cross Validation		Prediction	
			R ²	RMSE	R ²	RMSE	R ²	RMSE
	TH	None	0.88	0.24	0.75	0.35	NA	7.61
		Abs and SNV	0.88	0.25	0.73	0.37	0.53	0.62
		Abs and SNV*	0.78	0.33	0.73	0.37		

*Model made after selection of significantly contributing variables

SGD – Savitzky-Golay derivative

Table 34 Descriptive statistics for quality parameters analyzed in tomato sample for combine period time.

Parameter	N	Average	Min	Max	Std
DM	200	5.1756	3.6823	7.8026	0.68
TSS	200	4.3	3.0	6.0	0.58
TA	200	0.682	0.299	1.659	0.23
pH	200	4.19	3.63	4.80	0.24
Firmness (N)	200	5.71	2.47	12.35	2.09
Firmness1 (N)	200	32.88	14.56	59.47	9.86
Firmness2 (N)	200	8.45	3.72	18.60	3.15
Firmness3 (N)	200	18.19	8.33	40.13	6.67
Firmness4 (N/mm)	200	2.45	0.97	4.66	0.75
Firmness5 (N/mm)	200	2.54	1.03	5.10	0.81

Table 34 shows the range of measurement values (minimum and maximum values), average, and standard deviation of the quality parameters in the tomato sample from both collection periods.

The Dry matter, TSS, TA, pH, Firmness, Firmness1, Firmness2, Firmness3, Firmness4, and Firmness5 values were in the range from 3.6823-7.8026 %, 3.0-6.0 °Brix, 0.299-1.659 %, 3.63-4.80, and 2.47-12.35 N, 14.56-59.47 N, 3.72-18.60 N, 8.33-40.13 N, 0.97-4.66 N/mm, and 1.03-5.10 N/mm, respectively.

Figure 101 and Figure 102 show the plots of predicted versus measured values of DM, TSS, TA, pH, and firmness obtained using calibration models based on spectral data acquired using the in-house spectrometer prototype equipped with the NIR LED light source.

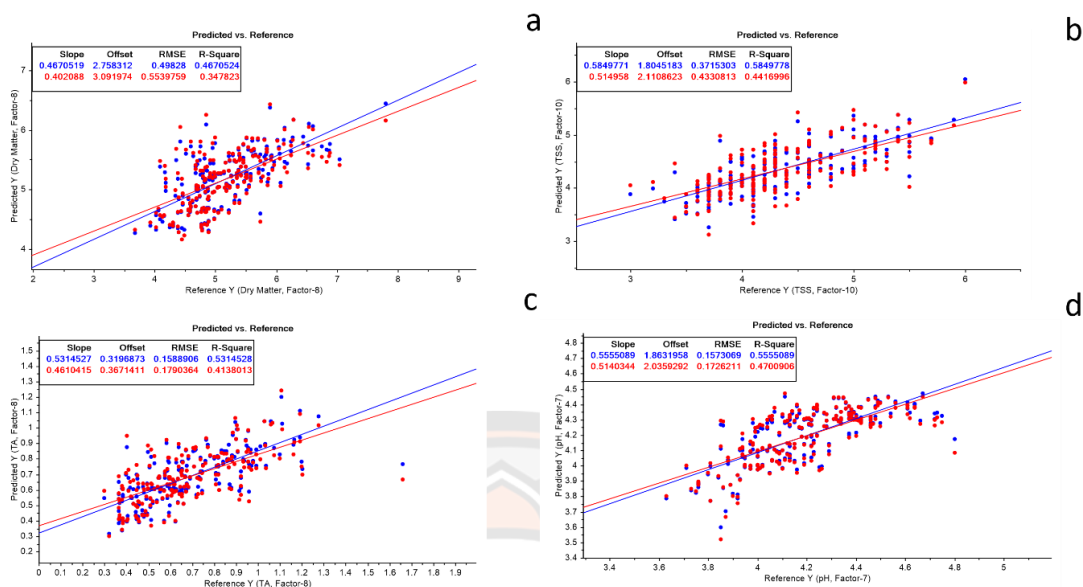


Figure 101 Plot of predicted versus measured values of (a) dry matter, (b) total soluble solids, (c) titratable acidity, and (d) pH of tomatoes for samples collected in both collection periods made with predictive models based on spectral data acquired using the NIR LED light source used without data pretreatment. The plots are showing datapoints for both calibration (blue) and cross validation (red) and the corresponding regression lines.

As can be seen in Table 35, the results indicate that the R^2 values for calibration and cross-validation (in brackets) for models developed from tomato samples from both sampling periods using spectral data acquired using the spectrometer equipped with NIR LED light source without pretreatment for DM, TSS, TA, pH, Firmness, Firmness1, Firmness2, Firmness3, Firmness4, and Firmness5 for NIR LED were 0.47 (0.35), 0.58 (0.44), 0.53 (0.41), 0.56 (0.47), 0.75 (0.70), 0.57 (0.51), 0.76 (0.71), 0.75 (0.69), 0.61 (0.50), and 0.68 (0.59) respectively. The RMSE values for DM, TSS, TA, pH, Firmness, Firmness1, Firmness2, Firmness3, Firmness4, and Firmness5 were 0.50% (0.55%), 0.37 °Brix (0.43 °Brix), 0.16% (0.18%), 0.16 (0.17), and 1.03N (1.13N), 6.24N (6.68N), 1.52N (1.68N), 3.28N (3.67N), 0.46N/mm (0.52N/mm), 0.45N/mm (0.51N/mm), respectively.

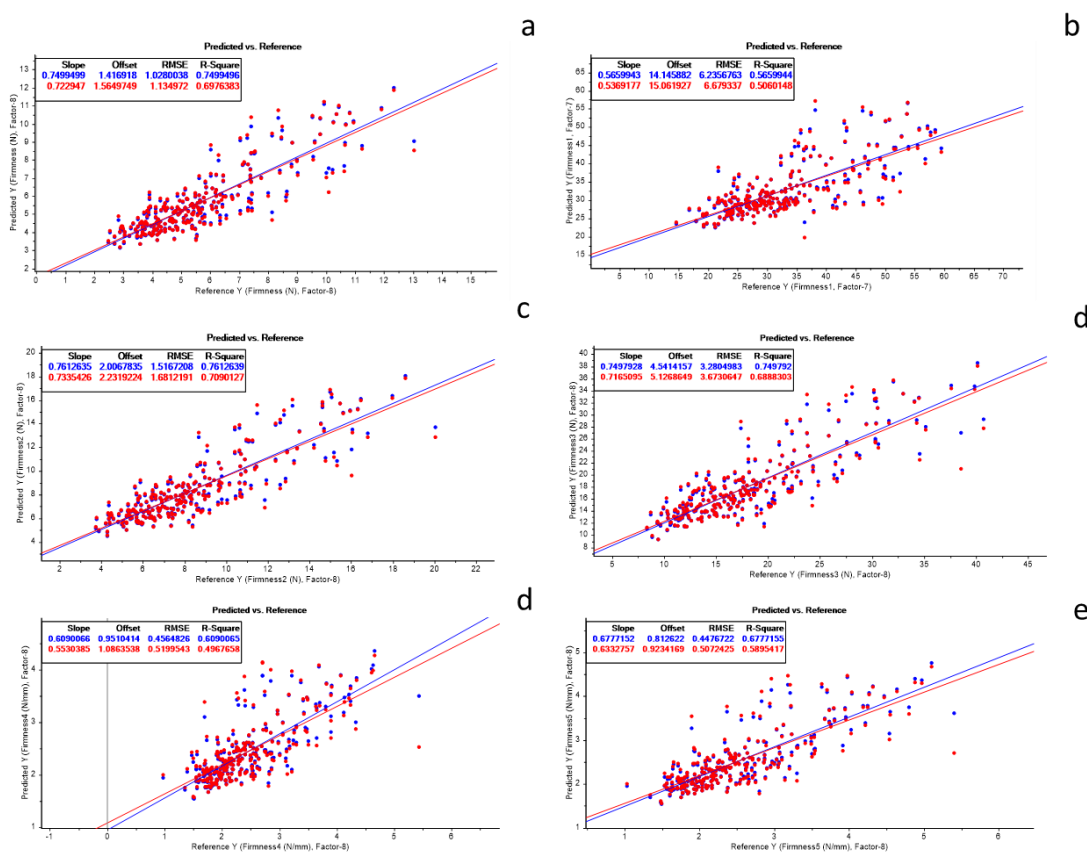


Figure 102 Plot of predicted versus measured values without pretreatment of (a) firmness, (b) firmness1, (c) firmness2 (d) firmness3, (e) firmness4, and (f) firmness5 of tomatoes using NIR LED light source from samples collected in the combine period time showing both datapoints for both calibration (blue) and cross validation (red) and the corresponding regression lines

The best R^2 values for models developed using tomato samples collected in both sampling periods are shown in Figure 105, Figure 105, and Table 35. The R^2 values for calibration and cross-validation (in brackets) for models developed with spectral data acquired using the NIR LED light source for DM, TSS, TA, pH, Firmness, Firmness1, Firmness2, Firmness3, Firmness4, and Firmness5 for NIR LED light source were 0.55 (0.42), 0.63 (0.41), 0.53 (0.41), 0.67 (0.49), 0.77 (0.68), 0.54 (0.45), 0.82 (0.54), 0.79 (0.56), 0.65 (0.54), and 0.72 (0.59) respectively. The RMSE values for DM, TSS, TA, pH, Firmness,

Firmness1, Firmness2, Firmness3, Firmness4, and Firmness5 were 0.46% (0.52%), 0.35 °Brix (0.45 °Brix), 0.16% (0.18%), 0.14 (0.17), and 0.99N (1.17N), 6.42N (7.03N), 1.30N (2.12N), 3.01N (4.34N), 0.43N/mm (0.50N/mm), 0.42N/mm (0.52N/mm), respectively. The best models for DM and Firmness1 were obtained after spectral data conversion to absorbance and 1st derivative pretreatment procedure. The best model for TSS was obtained after 1st derivative pretreatment procedure with spectral smoothing and a window of 3 datapoints. The best models for pH and Firmness2 were obtained after spectral data conversion to absorbance and 2nd derivative pretreatment procedure with spectral smoothing and a window of 3 datapoints. The best models for Firmness, Firmness3, Firmness4, and Firmness5 were obtained after spectral data conversion to absorbance and 2nd derivative pretreatment procedure with spectral smoothing and a window of 21 datapoints. The best model for TA was obtained with spectral data without pretreatment.

Moreover, the best models developed from data from both sampling periods were applied the data to investigate the possibility of predictions of the quality parameters. The combined data set was divided into calibration and test sets. The results of the predictions made for samples in the test set using models made with samples in the calibration set are shown in Figure 109-110

Figure 103 and Figure 104 show the plots of predicted versus measured values of DM, TSS, TA, pH, and firmness obtained using calibration models based on spectral data acquired using the in-house spectrometer prototype equipped with the filament light source.

As can be seen in Table 35, the results indicate that the R^2 values for calibration and cross-validation (in brackets) for models developed from tomato samples from both sampling periods using spectral data acquired using the spectrometer equipped with filament light source without pretreatment for DM, TSS, TA, pH, Firmness, Firmness1, Firmness2, Firmness3, Firmness4, and Firmness5 0.52 (0.43), 0.48 (0.42), 0.61 (0.55), 0.67 (0.66), 0.49 (0.46), 0.68 (0.66), 0.67 (0.65), 0.53 (0.47), and 0.68 (0.59), respectively. The RMSE values for DM, TSS, TA, pH, Firmness, Firmness1, firmness2, Firmness3, Firmness4, and Firmness5 were 0.47% (0.52%), 0.41 °Brix (0.46 °Brix), 0.17% (0.18%), 0.15 (0.16), and 1.17N

(1.21N), 6.79N (6.99N), 1.75N (1.81N), 3.78N (3.92N), 0.50N/mm (0.53N/mm), 0.45N/mm (0.51N/mm), respectively.

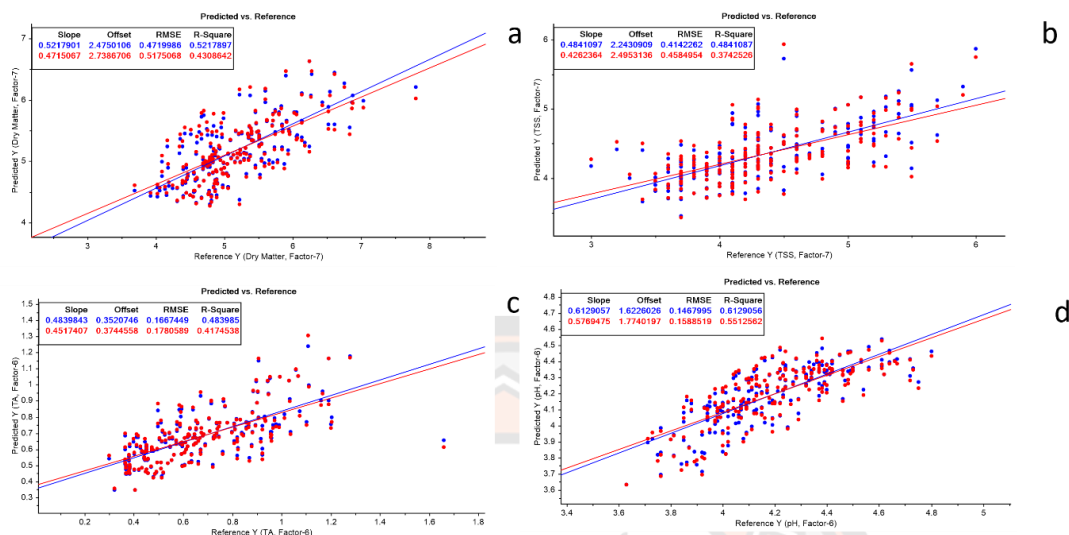


Figure 103 Plot of predicted versus measured values without pretreatment of (a) dry matter, (b) total soluble solids, (c) titratable acidity, and (d) pH of tomatoes using filament bulb light source from samples collected in the combine period time showing both datapoints for both calibration (blue) and cross validation (red) and the corresponding regression lines

The best R^2 values for models developed using tomato samples collected in both sampling period are shown in Figure 107, Figure 108, and Table 35. The R^2 values for calibration and cross-validation (in brackets) for models developed with spectral data acquired using the filament light source for DM, TSS, TA, pH, Firmness, Firmness1, Firmness2, Firmness3, Firmness4, and Firmness5 were 0.68 (0.58), 0.64 (0.43), 0.53 (0.42), 0.66 (0.56), 0.72 (0.69), 0.60 (0.44), 0.72 (0.69), 0.72 (0.67), 0.59 (0.40), and 0.65 (0.47) respectively. The RMSE values for DM, TSS, TA, pH, Firmness, Firmness1, Firmness2, Firmness3, Firmness4, and Firmness5 were 0.38% (0.45%), 0.35 °Brix (0.44 °Brix), 0.16% (0.18%), 0.14 (0.16), and 1.08N (1.15N), 5.97N (7.11N), 1.63N (1.75N), 3.49N (3.78N), 0.47N/mm (0.57N/mm), 0.47N/mm (0.58N/mm), respectively.

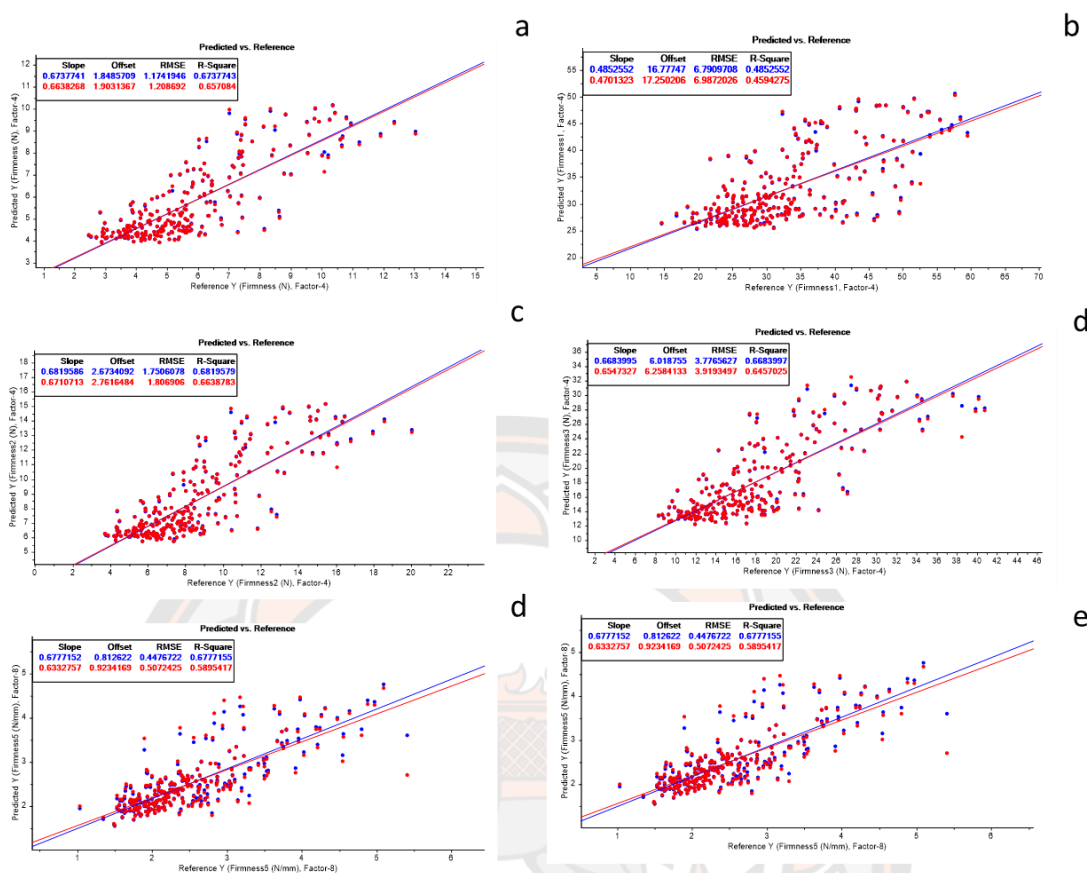


Figure 104 Plot of predicted versus measured without pretreatment of (a) Firmness, (b) Firmness1, (c) Firmness2 (d) Firmness3, (e) Firmness4, and (f) Firmness5 of tomatoes using filament bulb light source from samples collected in the combine period time showing both datapoints for both calibration (blue) and cross validation (red) and the corresponding regression lines

These best models for DM and pH were obtained after 1st derivative pretreatment procedure with spectral smoothing and a window of 3 datapoints. The best model for TSS was obtained after 2nd derivative and spectral smoothing and a window of 3 datapoints as a pretreatment procedure. The best model for TA was obtained after SNV pretreatment procedure. The best models for Firmness, Firmness2, Firmness4, and Firmness5 were obtained after spectral data conversion to absorbance and 2nd derivative pretreatment procedure with

spectral smoothing and a window of 3 datapoints. The best model for firmness1 was obtained after 2nd derivative pretreatment procedure with spectral smoothing and a window of 3 datapoints. The best model for firmness3 was obtained after spectral data conversion to absorbance and 2nd derivative pretreatment procedure with spectral smoothing and a window of 21 datapoints.

Moreover, the best models developed from data from both sampling periods were applied the data to investigate the possibility of predictions of the quality parameters. The combined data set was divided into calibration and test sets. The results of the predictions made for samples in the test set using models made with samples in the calibration set are shown in Figure 111 and Figure 112.

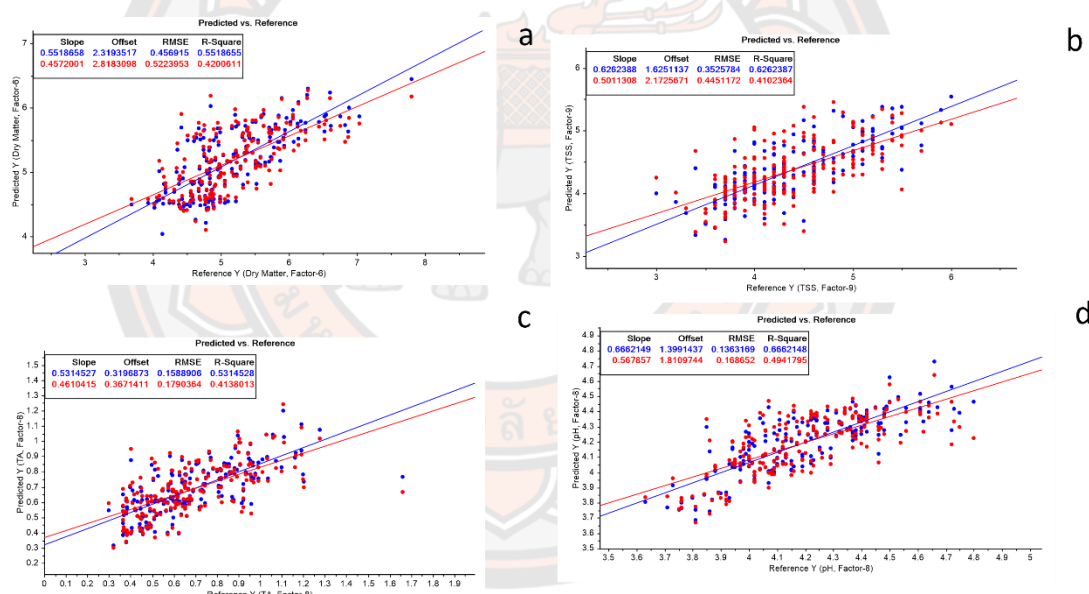


Figure 105 Plot of best cases of predicted versus measured values of (a) dry matter, (b) total soluble solids, (c) titratable acidity, and (d) pH of tomatoes for samples collected in both collection periods made with predictive models based on spectral data acquired using the NIR LED light source. The plots are showing datapoints for both calibration (blue) and cross validation (red) and the corresponding regression lines.

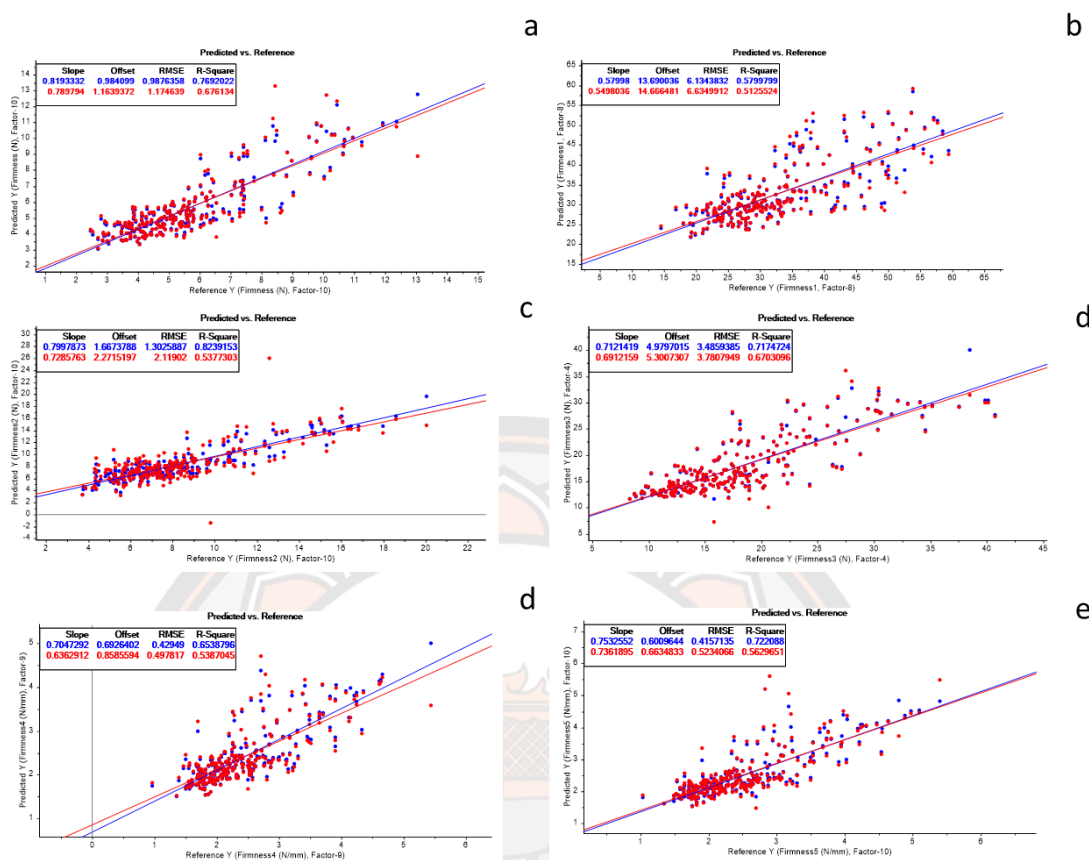


Figure 106 Plot of best cases of predicted versus measured values of (a) Firmness, (b) Firmness1, (c) Firmness2 (d) Firmness3, (e) Firmness4, and (f) Firmness5 of tomatoes for samples collected in both collection periods made with predictive models based on spectral data acquired using the NIR LED light source. The plots are showing datapoints for both calibration (blue) and cross validation (red) and the corresponding regression lines.

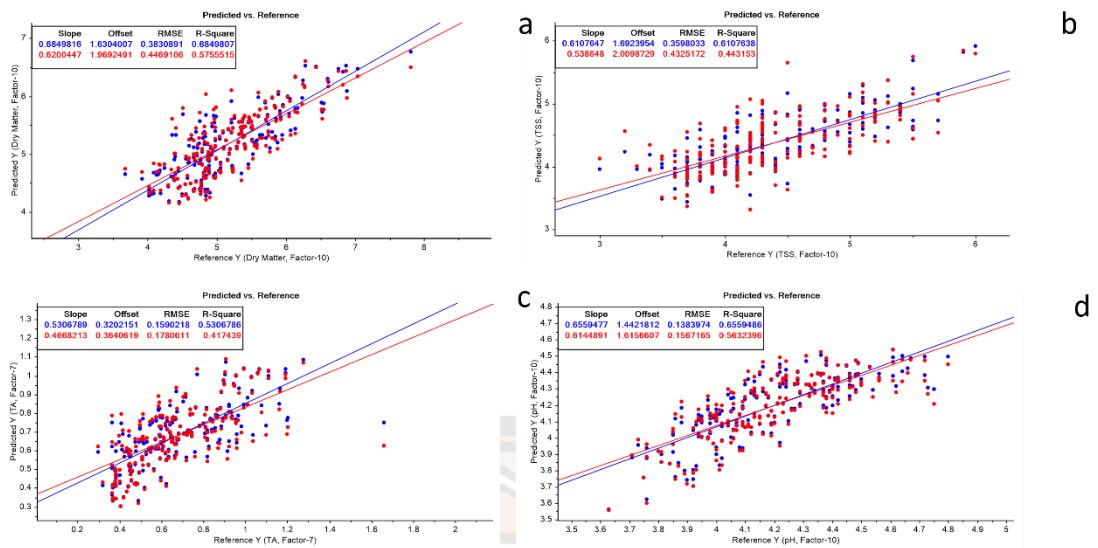


Figure 107 Plot of best cases of predicted versus measured values of (a) dry matter, (b) total soluble solids, (c) titratable acidity, and (d) pH of tomatoes for samples collected in both collection periods made with predictive models based on spectral data acquired using the filament light. The plots are showing datapoints for both calibration (blue) and cross validation (red) and the corresponding regression lines.

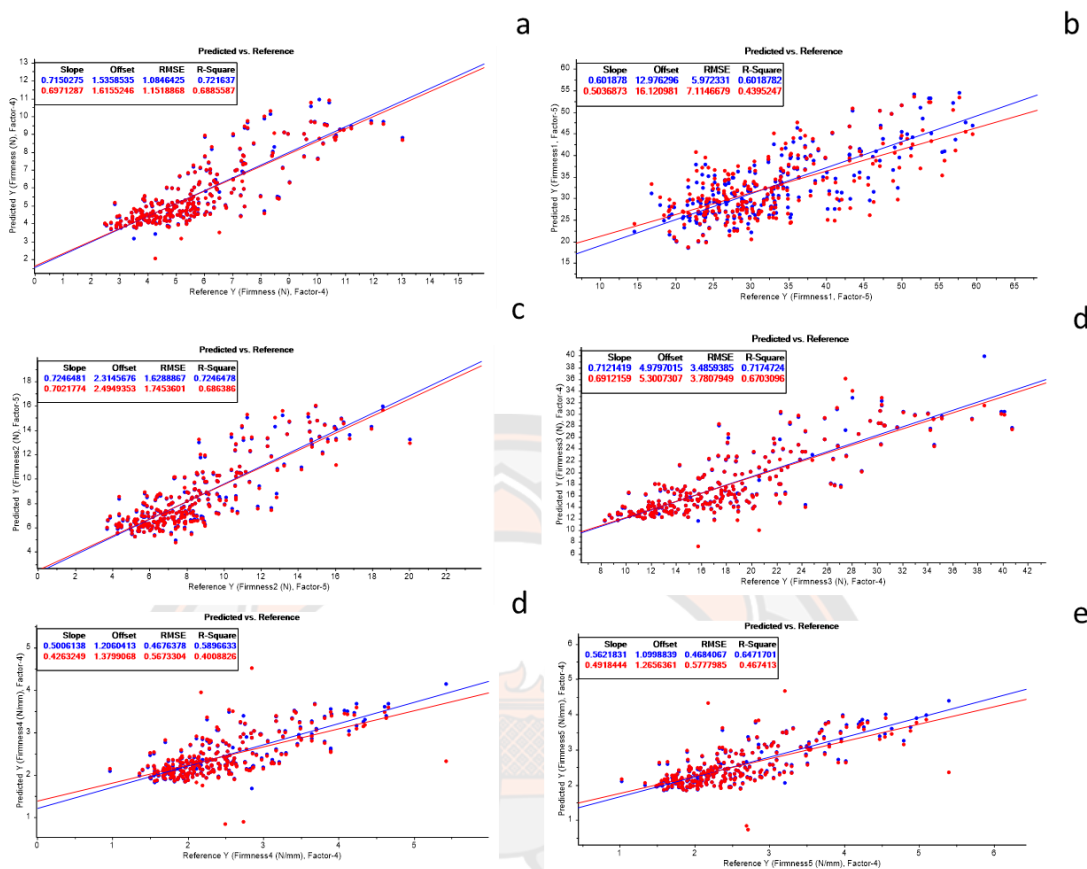


Figure 108 Plot of best cases of predicted versus measured values of (a) Firmness, (b) Firmness1, (c) Firmness2 (d) Firmness3, (e) Firmness4, and (f) Firmness5 of tomatoes for samples collected in both collection periods made with predictive models based on spectral data acquired using the filament light source. The plots are showing datapoints for both calibration (blue) and cross validation (red) and the corresponding regression lines.

Table 35 Summary of model parameters developed using NIR LED and filament bulb light source from tomato samples collected in combine sampling periods

Parameter	Light source	Treatment	Calibration		Cross validation	
			R ²	RMSE	R ²	RMSE
DM	NIR	None	0.47	0.50	0.35	0.55
	LED	Abs and 1 st SGD (3)	0.55	0.46	0.42	0.52
		Abs and 1 st SGD* (3)	0.51	0.48	0.45	0.51
	TH	None	0.52	0.47	0.43	0.52
		1 st SGD (21)	0.68	0.38	0.58	0.45
		1 st SGD* (21)	0.71	0.37	0.64	0.41
TSS	NIR	None	0.58	0.37	0.44	0.43
	LED	1 st SGD (3)	0.63	0.35	0.41	0.45
		1 st SGD* (3)	0.49	0.41	0.40	0.45
	TH	None	0.48	0.41	0.37	0.46
		2 nd SGD (21)	0.64	0.35	0.43	0.44
		2 nd SGD* (21)	0.60	0.37	0.53	0.40
TA	NIR	None	0.53	0.16	0.41	0.18
	LED	None*	0.52	0.16	0.45	0.17
	TH	None	0.48	0.17	0.42	0.18
		SNV	0.53	0.16	0.42	0.18
		SNV*	0.52	0.16	0.46	0.17
	pH	NIR	None	0.56	0.16	0.47
LED		Abs and 2 nd SGD (21)	0.67	0.14	0.49	0.17
		Abs and 2 nd SGD* (21)	0.37	0.19	0.29	0.20
TH		None	0.61	0.15	0.55	0.16
		1 st SGD (21)	0.66	0.14	0.56	0.16

Parameter	Light source	Treatment	Calibration		Cross validation	
			R ²	RMSE	R ²	RMSE
			1 st SGD (21)		0.60	0.15
Firmness	NIR	None	0.75	1.03	0.70	1.13
	LED	Abs and 2 nd SGD (21)	0.77	0.99	0.68	1.17
		Abs and 2 nd SGD* (21)	0.60	1.31	0.58	1.34
	TH	None	0.67	1.17	0.66	1.21
		Abs and 2 nd SGD (21)	0.72	1.08	0.69	1.15
		Abs and 2 nd SGD* (21)	0.39	1.61	0.29	1.73
Firmness1	NIR	None	0.57	6.24	0.51	6.68
	LED	Abs and 1 st SGD (3)	0.54	6.42	0.45	7.03
		Abs and 1 st SGD* (3)	0.54	6.41	0.49	6.78
	TH	None	0.49	6.79	0.46	6.99
		2 nd SGD (3)	0.60	5.97	0.44	7.11
		2 nd SGD* (3)	0.56	6.25	0.52	6.61
Firmness2	NIR	None	0.76	1.52	0.71	1.68
	LED	Abs and 2 nd SGD (3)	0.82	1.30	0.54	2.12
		Ans and 2 nd SGD* (3)	0.70	1.70	0.66	1.81
	TH	None	0.68	1.75	0.66	1.81
		2 nd SGD (21)	0.72	1.63	0.69	1.75
		2 nd SGD* (21)	0.71	1.68	0.69	1.74
Firmness3	NIR	None	0.75	3.28	0.69	3.67
	LED	Abs and 2 nd SGD (21)	0.79	3.01	0.56	4.34
		Abs and 2 nd SGD* (21)	0.63	4.00	0.61	4.12
	TH	None	0.67	3.78	0.65	3.92
		Abs and 2 nd SGD (21)	0.72	3.49	0.67	3.78
		Abs and 2 nd SGD* (21)	0.41	5.03	0.39	5.14

Parameter	Light source	Treatment	Calibration		Cross validation	
			R ²	RMSE	R ²	RMSE
		(21)				
Firmness4	NIR	None	0.61	0.46	0.50	0.52
	LED	Abs and 2 nd SGD (21)	0.65	0.43	0.54	0.50
		Abs and 2 nd SGD* (21)	0.43	0.55	0.39	0.57
	TH	None	0.53	0.50	0.47	0.53
		Abs and 2 nd SGD (3)	0.59	0.47	0.40	0.57
		Abs and 2 nd SGD* (3)	0.54	0.50	0.52	0.51
Firmness5	NIR	None	0.68	0.45	0.59	0.51
	LED	Abs and 2 nd SGD (21)	0.72	0.42	0.56	0.52
		Abs and 2 nd SGD* (21)	0.56	0.52	0.53	0.54
	TH	None	0.68	0.45	0.59	0.51
		Abs and 2 nd SGD (3)	0.65	0.47	0.47	0.58
		Abs and 2 nd SGD* (3)	0.61	0.49	0.60	0.50

*Model made after selection of significantly contributing variables
 SGD – Savitzky-Golay derivative

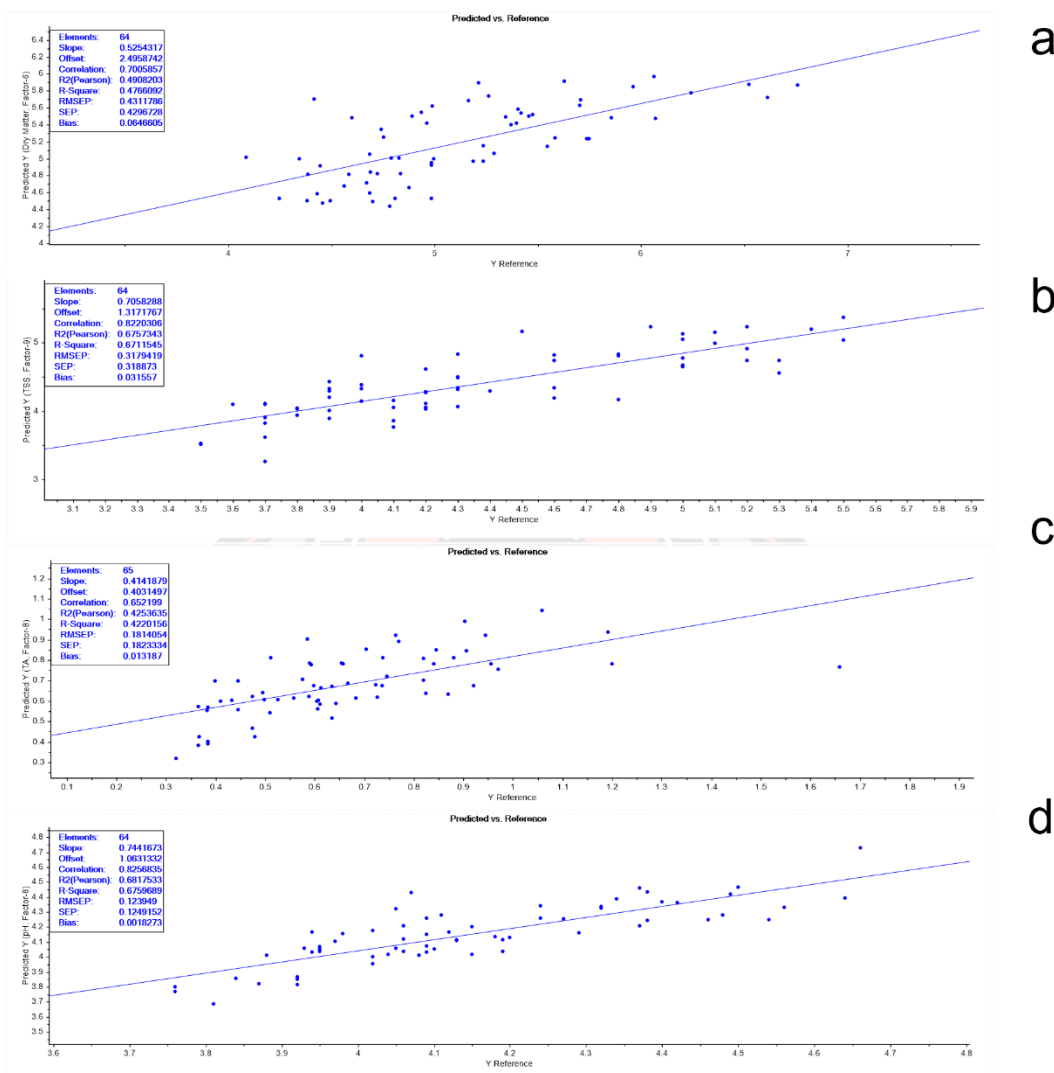


Figure 109 Plot of predicted versus measured values of dry matter (a), total soluble solids (b), titratable acidity (c), and pH (d) of tomatoes obtained using spectral data measured with NIR LED light source based on data from testing set of samples collected in both collection periods

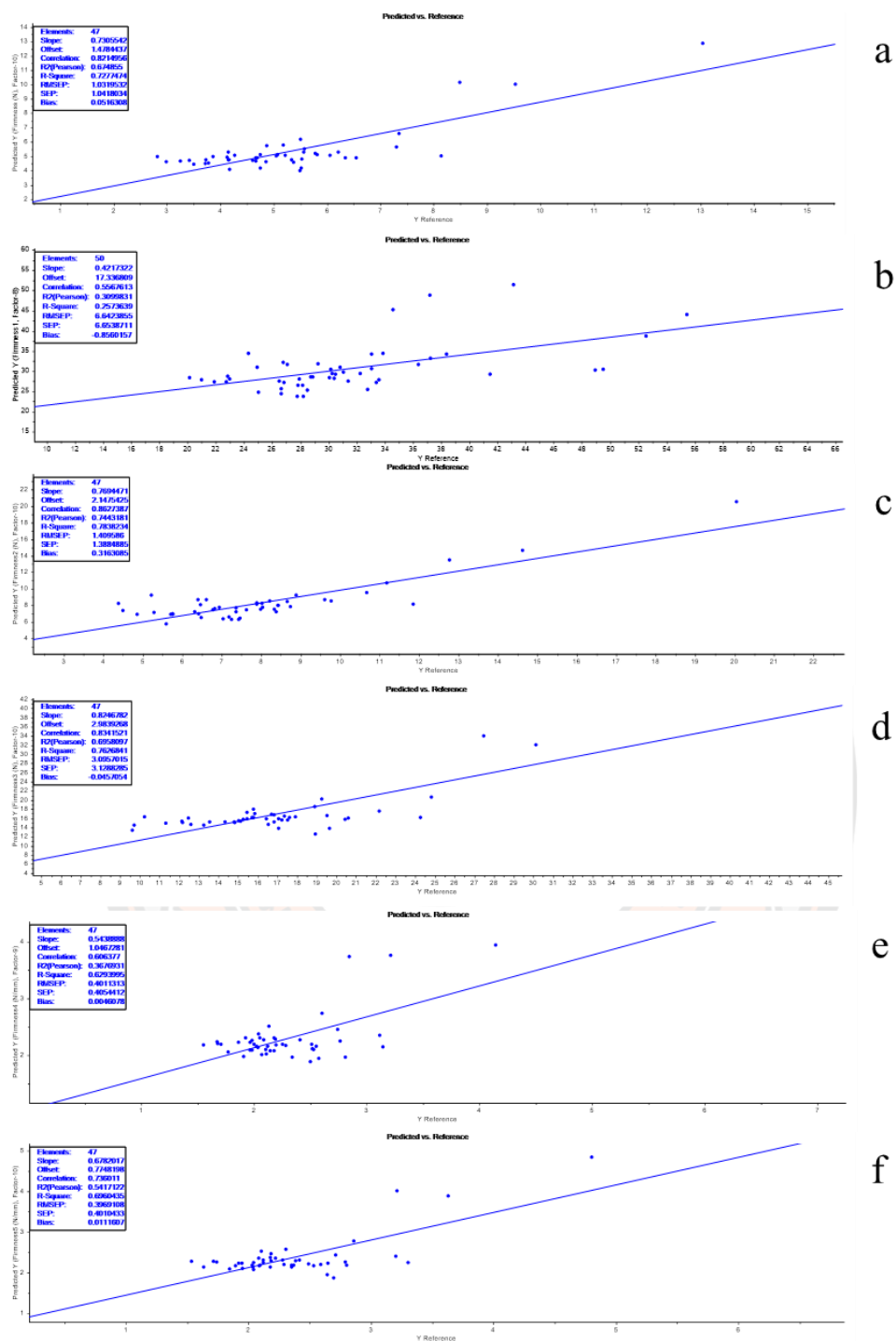


Figure 110 Plot of predicted versus measured values of (a) Firmness, (b) Firmness1, (c) Firmness2 (d) Firmness3, (e) Firmness4, and (f) Firmness5 of tomatoes obtained using spectral data measured with NIR LED light source

based on data from testing set of samples collected in both collection periods

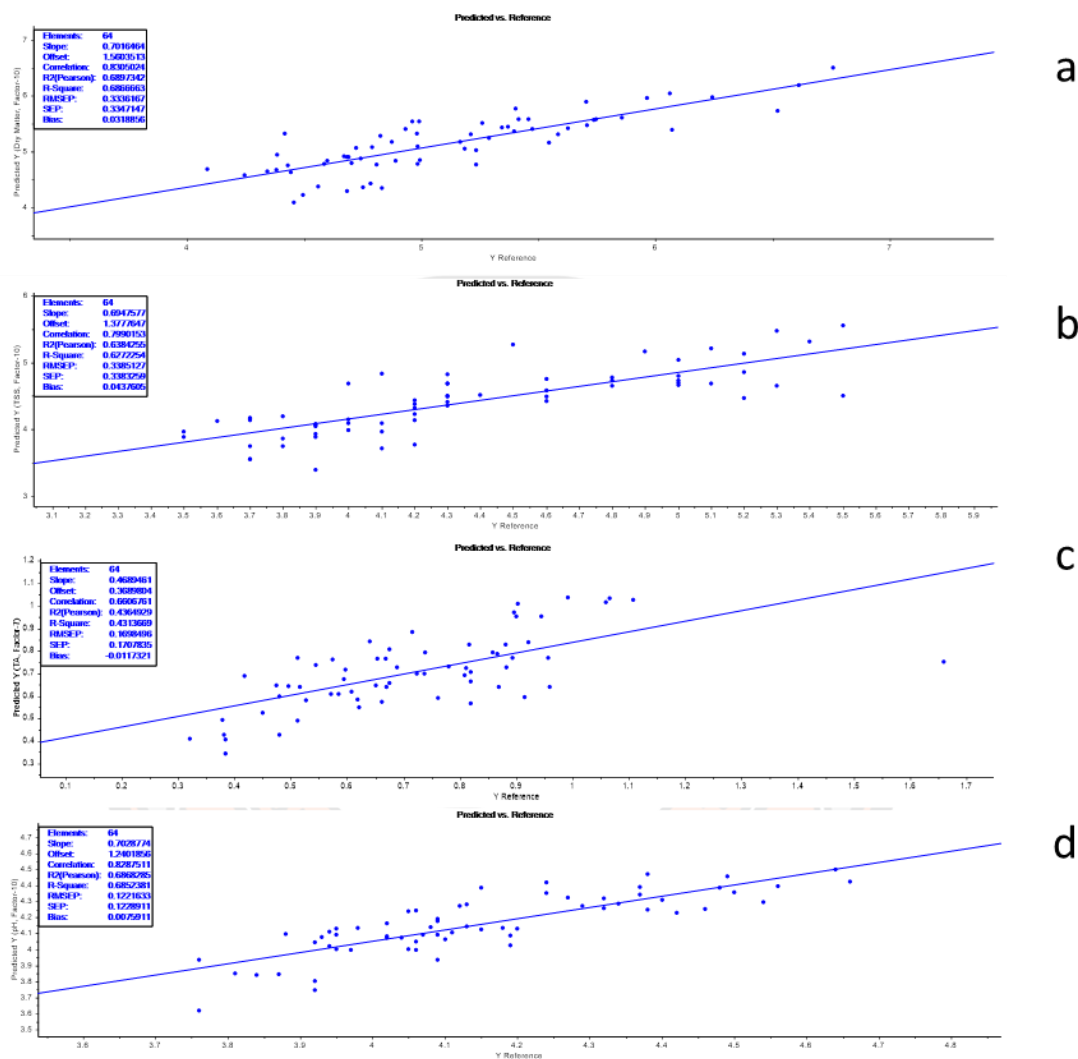


Figure 111 Plot of predicted versus measured values of dry matter (a), total soluble solids (b), titratable acidity (c), pH (d), and firmness (e) of tomatoes obtained using spectral data measured with filament light source based on data from testing set of samples collected in both collection periods

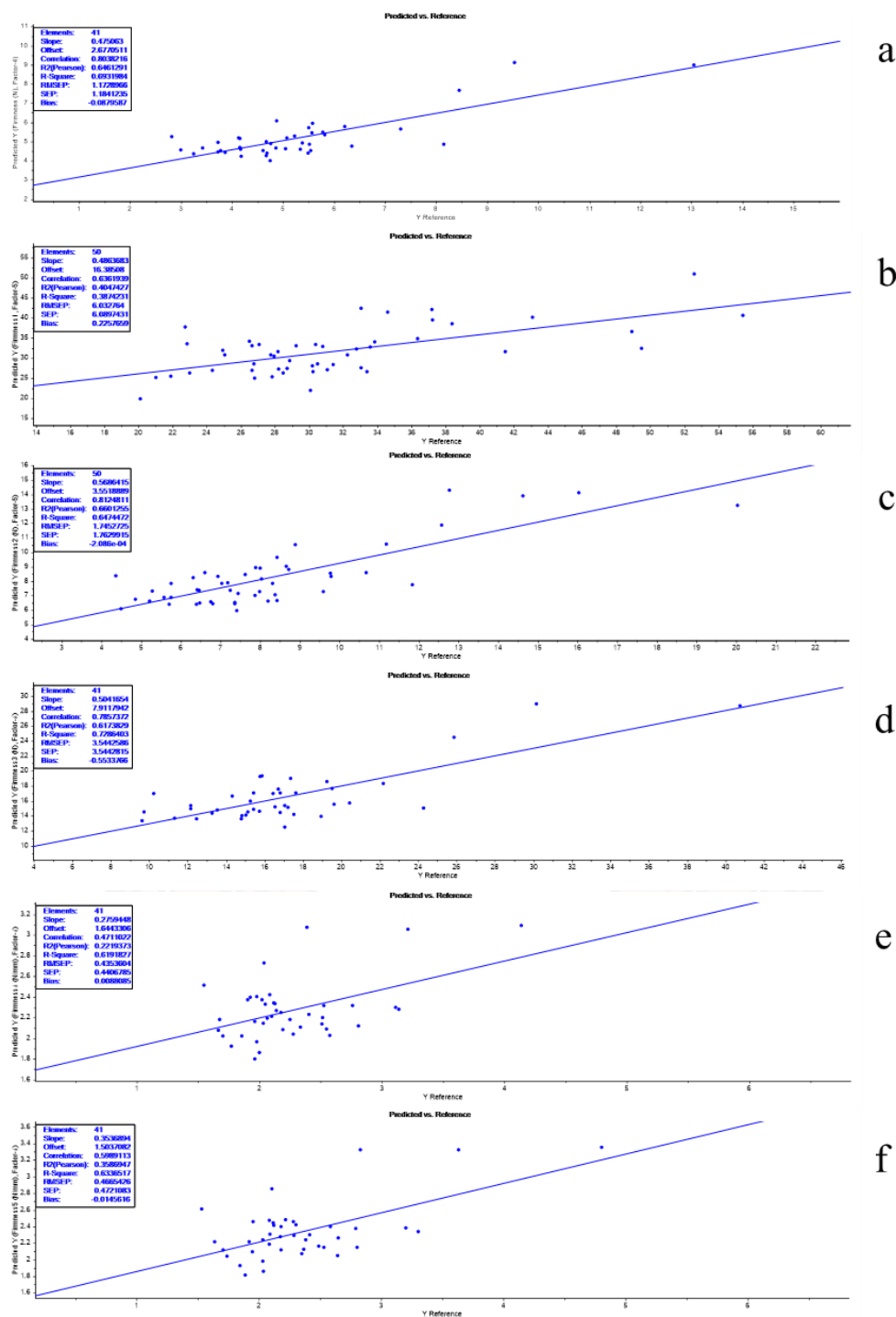


Figure 112 Plot of predicted versus measured values of (a) Firmness, (b) Firmness1, (c) Firmness2 (d) Firmness3, (e) Firmness4, and (f) Firmness5 of tomatoes obtained using spectral data measured with filament light source based on data from testing set of samples collected in both collection periods



Table 36 Summary of model parameters developed using NIR LED and filament bulb light source from tomato samples collected in both sampling periods and split into calibration and prediction sets

Parameter	Light source	Analyte mode	Treatment	Calibration		Cross Validation		Test set	
				R ²	RMSE	R ²	RMSE	R ²	RMSE
DM	NIR LED	Absorbance	1 st SGD (3)	0.55	0.46	0.42	0.52	0.48	0.43
	TH	Reflectance	1 st SGD (21)	0.68	0.38	0.58	0.45	0.67	0.33
TSS	NIR LED	Reflectance	1 st SGD (3)	0.63	0.35	0.41	0.45	0.67	0.32
	TH	Reflectance	2 nd SGD (21)	0.63	0.35	0.43	0.44	0.63	0.34
TA	NIR LED	Reflectance	None	0.53	0.16	0.41	0.18	0.42	0.18
	TH	Reflectance	SNV	0.53	0.16	0.42	0.18	0.43	0.17
pH	NIR LED	Absorbance	2 nd SGD (3)	0.67	0.14	0.49	0.17	0.68	0.12
	TH	Reflectance	1 st SGD (21)	0.66	0.14	0.56	0.16	0.69	0.12
Firmness	NIR LED	Absorbance	2 nd SGD (21)	0.77	0.99	0.68	1.17	0.73	1.03
	TH	Absorbance	2 nd SGD (21)	0.72	1.08	0.69	1.15	0.69	1.17
Firmness1	NIR LED	Absorbance	1 st SGD (3)	0.54	6.42	0.45	7.03	0.46	5.86
	TH	Reflectance	2 nd SGD (3)	0.60	5.97	0.44	7.11	0.39	6.03

Parameter	Light source	Analyte mode	Treatment	Calibration		Cross Validation		Test set	
				R ²	RMSE	R ²	RMSE	R ²	RMSE
Firmness2	NIR LED	Absorbance	2 nd SGD (3)	0.82	1.30	0.54	2.12	0.78	1.41
	TH	Reflectance	2 nd SGD (21)	0.72	1.63	0.69	1.75	0.65	1.75
Firmness3	NIR LED	Absorbance	2 nd SGD (21)	0.79	3.01	0.56	4.34	0.76	3.10
	TH	Absorbance	2 nd SGD (21)	0.72	3.49	0.67	3.78	0.73	3.54
Firmness4	NIR LED	Absorbance	2 nd SGD (21)	0.65	0.43	0.54	0.50	0.63	0.40
	TH	Absorbance	2 nd SGD (3)	0.59	0.47	0.40	0.57	0.62	0.44
Firmness5	NIR LED	Absorbance	2 nd SGD (21)	0.72	0.42	0.56	0.52	0.70	0.40
	TH	Absorbance	2 nd SGD (3)	0.65	0.47	0.47	0.58	0.63	0.47

*Model made after selection of significantly contributing variables

SGD – Savitzky-Golay derivative

Table 37 Summary of model parameters developed using NIR LED and filament bulb light source from mango samples collected in both sampling periods and split into calibration and prediction sets

Parameter	Light source	Treatment	Test set	
			R ²	RMSE
DM	TH	1 st SGD (21)	0.67	0.33
TSS	NIR LED	1 st SGD (3)	0.67	0.32
TA	NIR LED	None	0.42	0.18
pH	TH	1 st SGD (21)	0.69	0.12
Firmness	NIR LED	Abs and 2 nd SGD (21)	0.73	1.03
Firmness1	NIR LED	Abs and 1 st SGD (3)	0.46	5.86
Firmness2	NIR LED	Abs and 2 nd SGD (3)	0.78	1.41
Firmness3	NIR LED	Abs and 2 nd SGD (21)	0.76	3.10
Firmness4	NIR LED	Abs and 2 nd SGD (21)	0.63	0.40
Firmness5	NIR LED	Abs and 2 nd SGD (21)	0.70	0.40

*Model made after selection of significantly contributing variables
SGD – Savitzky-Golay derivative

Furthermore, the figures of merit for the models used in the separate prediction set are summarized in Table 36. The results indicate that the R² values of the test set for DM, TSS, TA, pH, Firmness, Firmness1, Firmness2, Firmness3, Firmness4, and Firmness5 obtained using spectral data measured with NIR LED light source were 0.48, 0.67, 0.42, 0.68, 0.73, 0.46, 0.78, 0.76, 0.63, and 0.70, respectively. The RMSE values of NIR LED for DM, TSS, TA, pH, Firmness, Firmness1, Firmness2, Firmness3, Firmness4, and Firmness5 were 0.43%, 0.32 °Brix, 0.18%, 0.12, and 1.03N, 5.86N, 1.41N, 3.10N, 0.40N/mm, and 0.40N/mm, respectively.

The R² value of the test set for DM, TSS, TA, pH, Firmness, Firmness1, Firmness2, Firmness3, Firmness4, and Firmness5 of filament bulb light source were 0.67, 0.63, 0.43, 0.69, 0.69, 0.39, 0.65, 0.73, 0.62, and 0.63, respectively. The RMSE values of filament bulb light source for DM, TSS, TA, pH, Firmness, Firmness1,

Firmness2, Firmness3, Firmness4, and Firmness5 were 0.33%, 0.34 °Brix, 0.17%, 0.12, and 1.17N, 6.03N, 1.75N, 3.54N, 0.44N/mm, and 0.47N/mm, respectively.

The best models developed for predicting DM, TSS, TA, pH, Firmness, Firmness1, Firmness2, Firmness3, Firmness4, and Firmness5 were developed using filament light bulb, NIR LED, NIR LED, filament light bulb, NIR LED, NIR LED, NIR LED, NIR LED, NIR LED, and NIR LED, respectively.

Spectral characteristics of tomato and reference measurements

Figure 113a shows the important absorbance spectra for the tomato samples recorded by the spectrometer equipped with the NIR LED light source. The spectral data clearly show the water signal around 970 nm. The spectra also show strong pronounced variability at 670, 710, and 750 nm for chlorophyll content, O-H str of starches and sugars, and C-H str of starches and sugars, respectively.

Figure 113b shows the important absorbance spectra for the tomato samples recorded by the spectrometer equipped with the TH light source spectrometer. The spectral data clearly show the chlorophyll and water signals around 670 and 970 nm, respectively.

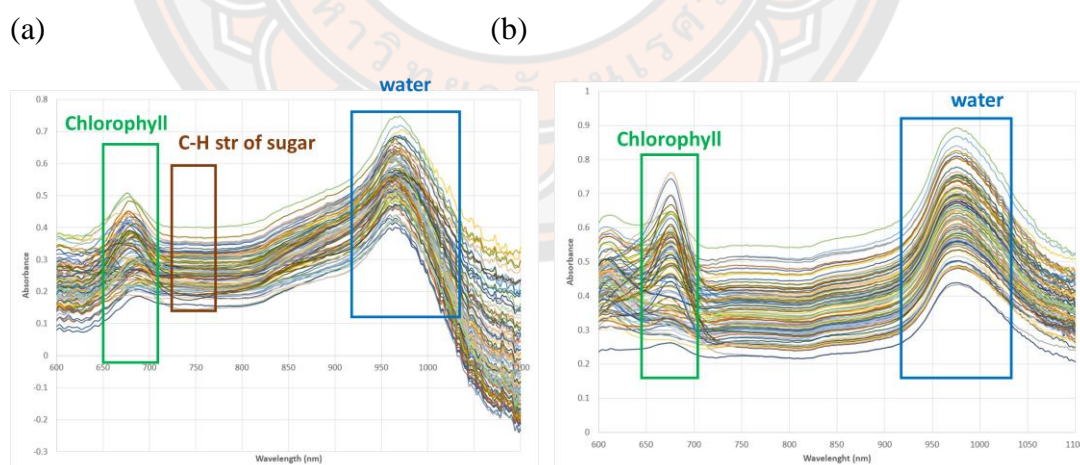


Figure 113 Plot of absorbance versus wavelength for important spectra acquired using in-house spectrometer equipped with the (a) NIR LED (b) Filament light sources used for tomato samples

In the case of tomatoes, the developed models show moderate performance for all of quality parameters. The R^2 values of calibration, cross-validation, and prediction for the test set were below 0.80. However, the performance to predict DM, TSS, TA, pH and firmness using NIR LED and TH are significantly worse than predictive models obtained in previous publication reports. In recent years the performance for determination of DM, TSS, TA, pH and firmness in tomatoes was studied using the F-750 produce quality meter.

Four publication papers report the predictive models of quality parameters for tomato samples were shown in Table 38. The first publication was published by Mekheled M. and co-workers in 2020. This work was conducted by the F-750 Produce Quality Meter at the wavelength range from 285 to 1200 nm. The models for prediction flesh firmness were obtained with R^2 of calibration and cross-validation (bracket) of 0.919 (0.679), which is significantly better than the results obtained in this work.

The second work was reported by Amanjot K. and co-workers in 2020. They studied the F-750 Produce Quality Meter at the wavelength range from 402 to 1137 nm. The models for prediction pH and %Brix were obtained the R^2 of prediction for 0.23 and 0.55. which is significantly worse than the results obtained in this work.

The third work was studied by Annelisa A. and co-workers in 2021. They determined the performance of F-750 Produce Quality Meter for predicting SSC at 840-1050 nm. The R^2 values of calibration, cross-validation, and prediction for SSC were 0.65, 0.63, and 0.65, respectively, which is significantly worse than the results obtained in this work.

Finally, last publication was published by Annelisa A and co-workers in 2021. In this work, they studied the performance for predicting TA and DM using the same spectrometer. The R^2 values of calibration and prediction (bracket) for TA and DM were 0.26 (0.25) and 0.62 and 0.59, respectively, which is comparable to the results obtained in this work.

The results above, show the possibility to utilize in-house built spectrometers (NIR and TH) as the new generation of new series of micro-opto-electro-mechanical-systems (MOEMS) technology. These spectrometers show better performance for the prediction TSS, DM, TA and pH for tomato samples. This work indicated that the

feasibility of using the new generation of MOEMS technology (C14383MA-01) to determine quality parameters of tomato samples.



Table 38 Comparison of performance models for the quality parameters of tomato reported in previous literature using F-750 Produce Quality Mater and describe in this work

Reference	Instrument	Wavelength (nm)	DM	TSS/SSC	TA	pH	Firmness
			$R_c^2 (R_p^2)$	$R_c^2 (R_p^2)$	$R_c^2 (R_p^2)$	$R_c^2 (R_p^2)$	$R_c^2 (R_p^2)$
Mekheled M. and co-workers in 2020	F-750	285-1200	N.D.	N.D.	N.D.	N.D.	0.919 (0.679)
Amanjot K. and co-workers in 2020	F-750	402-1137	N.D.	0.55*	N.D.	0.23*	N.D.
Annelisa A. and co-workers in 2021	F-750	840-1050	N.D.	0.65 (0.63)	N.D.	N.D.	N.D.
Annelisa A. and co-workers in 2022	F-750	729-975	0.62, 0.59*	N.D.	0.26, 0.25*	N.D.	N.D.
This work	NIR LED	640-1050	0.55 (0.42)	0.63 (0.41)	0.53 (0.41)	0.67 (0.49)	0.54-0.82 (0.45-0.68)
	TH	640-1050	0.68 (0.58)	0.63 (0.43)	0.53 (0.42)	0.66 (0.56)	0.59-0.72 (0.40-0.69)

CHAPTER V

CONCLUSION

Near-infrared (NIR) spectroscopy is a powerful tool for non-destructive measurements of various quality parameters. Moreover, the performance of NIR spectroscopy for predicting quality parameters is dependent on two key components: 1) suitable spectrometers and 2) appropriate calibration models.

The aim of this study was: 1) to develop predictive models for quality parameters of mangoes and tomatoes using different commercial spectrometers and 2) to construct an in-house built NIR spectrometer prototype and investigate the possibility to use it as a source of spectral data for the development of predictive models for quality parameters of mangoes and tomatoes. The quality key parameters that were investigated in this work are dry matter (DM), total soluble solids (TSS), titratable acidity (TA), pH, and firmness.

The possibility to perform the prediction of quality parameters for mango and tomato samples was investigated using different commercial spectrometers (SCIO, Linksure, Texas Instruments NIRscan Nano, Neospectra). In case of mango samples, good predictive models were developed for predicting DM, TSS, TA, and pH using spectroscopic measurements carried out with the SCIO and Linksure, operating in both visible and NIR modes, spectrometers. The best model for DM was obtained using data acquired with the SCIO spectrometer. It exhibited a cross-validation values of 0.92 and 0.739% for R^2 and RMSE, respectively. The best calibration models for TSS, TA, and pH were developed using data acquired with the Linksure instrument operated in the visible mode. The R^2 values of calibration and cross-validation (brackets) for TSS, TA, and pH were 0.91 (0.75), 0.91 (0.79), and 0.93 (0.81), respectively. The RMSE values of calibration and cross-validation (brackets) for TSS, TA, and pH were 1.03 °Brix (1.76 °Brix), 0.38% (0.58%), and 0.21 (0.35), respectively. The performance of models for predicting quality parameters using data from Texas Instruments NIRscan Nano and Neospectra were poor with modest R^2 values.

For the work with tomatoes, cherry tomato was chosen for test of quality parameters. Only three commercial spectrometers (SCIO, Linksure and Texas Instruments NIRscan Nano) were utilized in this part because of the sampling window of Neospectra is too large to allow the spectroscopic measurements. Good predictive models were developed for DM, and firmness using the spectroscopic measurements from SCIO and Linksure operating in visible and NIR modes. The best model for DM was obtained using data from the SCIO spectrometer and exhibited a cross validation values of 0.89 and 0.27% for R^2 and RMSE, respectively. For the firmness, the best results were obtained using data from Linksure operating in the visible mode. The R^2 values for calibration and cross-validation (brackets) were 0.91 (0.87). The RMSE values for calibration and cross-validation (brackets) for firmness were 0.91 N (0.87 N). The performance of models based on spectral data acquired using the Texas Instruments NIRscan Nano were poor with modest R^2 values as for the work carried out with mangoes. In summary, two of the tested commercial spectrometers exhibited good performance for predicting quality parameters in mango and, to a lesser extent, in tomato. These instruments were the SCIO spectrometer and the Linksure spectrometer operating in the visible mode. The important wavelength in the spectral range of these spectrometers are at the regions around 950, nm 750 nm, and 800 nm. The region around 950 nm is related to water stretching. 750 nm are related to the 4th overtone of C-H stretching. The band around 800 nm is related to the first overtone with O-H stretching of organic acids. These regions are this suitable to be used for characterization of TSS, TA, and pH contents.

In the second part of this work an in-house NIR spectrometer prototype was constructed and tested. The performance of an NIR spectrometer depends on three key components: light source, wavelength selector, and detector. This choice of the wavelength selector was inspired by the F-751 mango Quality Meter, which is a commercial portable spectrometer for predicting mango quality parameters TSS and DM. This spectrometer has shown strong performance in a validation study with very high accuracy for the prediction of dry matter and %brix. The photovoltaic silicon (Si) diodes have suitable sensitivity in the wavelength range of 700-1100 nm and they are suitable for compact and inexpensive instruments operating in the Visible and Visible to short wavelength NIR regions. It features lower S/N. In case of light source, two

different types of NIR light sources are commonly used in commercially available spectrometers: 1) light emitting diodes (LED) and 2) tungsten halogen (TH) filament light source. Both types of the light source were used in this work.

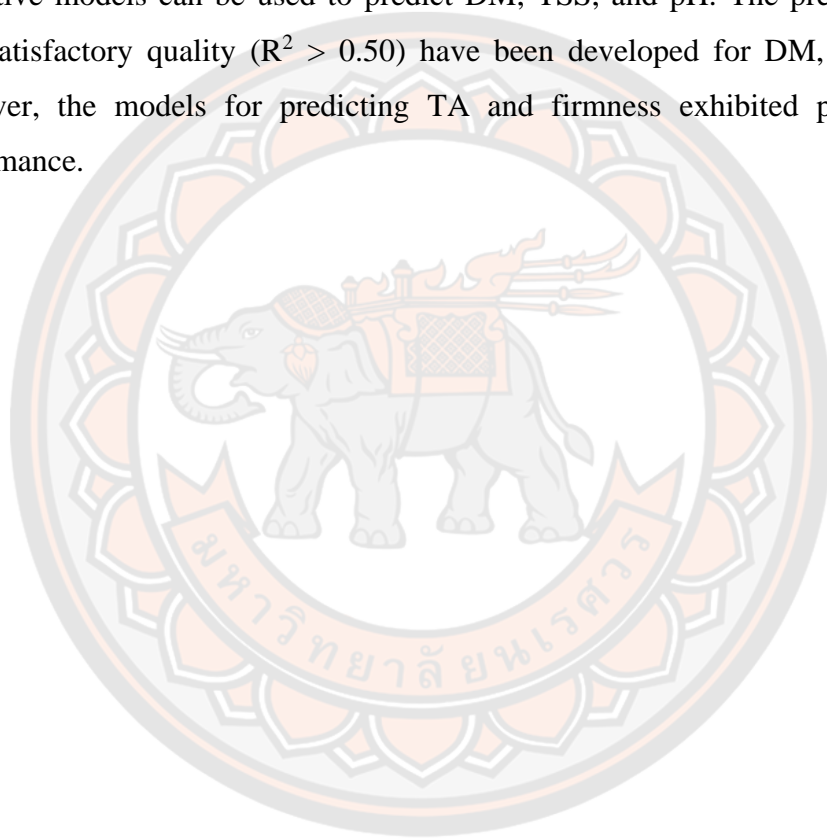
Based on the reasons outlined above the prototype of the potentially low cost portable NIR spectrometer has been constructed around the Hamamatsu C14384MA-01 sensor, which combines the functions of both the wavelength selector and detector. The cost of this sensor, at modest order volumes should be below \$300 In addition, the in-house spectrometer prototype has been made in two versions using an NIR LED (SFH 4376, OSRAM) and a tungsten halogen filament bulb (TH) light sources. Both spectrometer versions operate in the 650 to 1050 nm range. The repeatability and reproducibility of the measurements carried out with the instrument are below RSD of 5%, which indicates good performance of the developed instrument.

In case of mango samples, good predictive models were developed for predicting DM, TSS, TA, and pH using both NIR LED and TH filament light sources. The best models for predicting DM were obtained using the spectrometer version with the TH filament light source. The R^2 value for the test set was 0.82. For the best models for TSS, TA, and pH were developed using the spectrometer version with NIR LED light source. The R^2 values of the test sets for TSS, TA, and pH were 0.86, 0.92, and 0.86, respectively. Poor models were obtained for firmness analysis exhibiting modest R^2 for both versions of the spectrometer prototype. In summary the spectrometer prototype has been used to collect spectroscopic data from Nam Dok Mai mangoes, which were collected in two different harvesting seasons. Predictive models for mango quality parameters (DM, TSS, TA, pH, firmness) were developed from this spectroscopic data. Models with satisfactory quality ($R^2 > 0.80$ in the test set) were developed for DM, TSS, TA, and pH. The results indicate that the constructed instrument can collect usable spectroscopic data from produce samples. Further iterations of the instrument, which should include in house control board, battery power source, and wireless data transfer capability, will be constructed and tested in the future.

For tomato work, models with moderate performance were developed for all of the quality parameters. The R^2 values of the test sets were below 0.70. The predictive performance for DM, TSS, TA, pH, and firmness using both NIR LED and

TH filament are significantly worse than prediction models in previous publications. On the other hand, the predictive models of in-house spectrometers show better performance in comparison with previous prototypes (MOEMS technology) for predicting, TSS, DM, TA, and pH in tomato samples.

The potential of low cost NIR spectrometer using new generation of MOEMS technology (C14383MA-01) was evaluated for rapid and non-destructive measurement of quality parameters of tomato samples. The results showed that the predictive models can be used to predict DM, TSS, and pH. The predictive models with satisfactory quality ($R^2 > 0.50$) have been developed for DM, TSS, and pH. However, the models for predicting TA and firmness exhibited poor prediction performance.



REFERENCES

- [1] Golic M.; Walsh K.B., Robustness of calibration models based on near infrared spectroscopy for the in-line grading of stonefruit for total soluble solids content. *Analytica Chimica Acta*, **2006**. 555, 286-291.
- [2] DW J., Near-infrared spectroscopy. **2021**.
- [3] Marques E.J.N.; de Freitas S.T.; Pimentel M.F.; Pasquini C., Rapid and non-destructive determination of quality parameters in the 'Tommy Atkins' mango using a novel handheld near infrared spectrometer. *Food Chemistry*, **2016**. 197, 1207-1214.
- [4] dos Santos Neto J.P.; de Assis M.W.D.; Casagrande I.P.; Cunha Júnior L.C.; de Almeida Teixeira G.H., Determination of 'Palmer' mango maturity indices using portable near infrared (VIS-NIR) spectrometer. *Postharvest Biology and Technology*, **2017**. 130, 75-80.
- [5] Sun X.; Subedi P.; Walsh K.B., Achieving robustness to temperature change of a NIRS-PLSR model for intact mango fruit dry matter content. *Postharvest Biology and Technology*, **2020**. 162, 111117.
- [6] Chiong W.L.; Omar A.F., White light emitting diode as potential replacement of tungsten-halogen lamp for visible spectroscopy system: a case study in the measurement of mango qualities. *Journal of Instrumentation*, **2017**. 12, P07002.
- [7] DW J., Tomato. **2021**.
- [8] Cortés V.; Ortiz C.; Aleixos N.; Blasco J.; Cubero S.; Talens P., A new internal quality index for mango and its prediction by external visible and near-infrared reflection spectroscopy. *Postharvest Biology and Technology*, **2016**. 118, 148-158.
- [9] Schmilovitch Z.e.; Mizrach A.; Hoffman A.; Egozi H.; Fuchs Y., Determination of mango physiological indices by near-infrared spectrometry. *Postharvest Biology and Technology*, **2000**. 19, 245-252.
- [10] Jha S.N.; Chopra S.; Kingsly A.R.P., Determination of Sweetness of Intact Mango using Visual Spectral Analysis. *Biosystems Engineering*, **2005**. 91, 157-161.
- [11] Kasim N M.P., Schouten RE, Woltering EJ, Assessing firmness in mango

- comparing broadband and miniature spectrophotometers. *Infrared Phys. Technol.*, **2021**. 115.
- [12] wikipedia_new, mango. **2021**.
- [13] Bergougnoux V., The history of tomato: From domestication to biopharming. *Biotechnology Advances*, **2014**. 32, 170-189.
- [14] Ding X.; Guo Y.; Ni Y.; Kokot S., A novel NIR spectroscopic method for rapid analyses of lycopene, total acid, sugar, phenols and antioxidant activity in dehydrated tomato samples. *Vibrational Spectroscopy*, **2016**. 82, 1-9.
- [15] Clément A.; Dorais M.; Vernon M., Nondestructive Measurement of Fresh Tomato Lycopene Content and Other Physicochemical Characteristics Using Visible–NIR Spectroscopy. *Journal of Agricultural and Food Chemistry*, **2008**. 56, 9813-9818.
- [16] Flores K.; Sánchez M.-T.; Pérez-Marín D.; Guerrero J.-E.; Garrido-Varo A., Feasibility in NIRS instruments for predicting internal quality in intact tomato. *Journal of Food Engineering*, **2009**. 91, 311-318.
- [17] Pedro A.M.K.; Ferreira M.M.C., Nondestructive Determination of Solids and Carotenoids in Tomato Products by Near-Infrared Spectroscopy and Multivariate Calibration. *Analytical Chemistry*, **2005**. 77, 2505-2511.
- [18] Tilahun S P.D., Seo M, Hwang IG, Kim S, Prediction of lycopene and β -carotene in tomatoes by portable chromameter and VIS/NIR spectra. *Postharvest Biol. Technol.*, **2018**. 136, 50-56.
- [19] Sheng R.; Cheng W.; Li H.; Ali S.; Akomeah Agyekum A.; Chen Q., Model development for soluble solids and lycopene contents of cherry tomato at different temperatures using near-infrared spectroscopy. *Postharvest Biology and Technology*, **2019**. 156, 110952.
- [20] Lin H.; Ying Y., Theory and application of near infrared spectroscopy in assessment of fruit quality: a review. *Sensing and Instrumentation for Food Quality and Safety*, **2009**. 3, 130-141.
- [21] Jha S.N.; Narsaiah K.; Sharma A.D.; Singh M.; Bansal S.; Kumar R., Quality parameters of mango and potential of non-destructive techniques for their measurement - a review. *J Food Sci Technol*, **2010**. 47, 1-14.

- [22] Blanco M.; Coello J.; Iturriaga H.; Maspoch S.; de la Pezuela C., Near-infrared spectroscopy in the pharmaceutical industry . Critical Review. *Analyst*, **1998**. *123*, 135R-150R.
- [23] Nicolai B.M.; Beullens K.; Bobelyn E.; Peirs A.; Saeys W.; Theron K.I.; Lammertyn J., Nondestructive measurement of fruit and vegetable quality by means of NIR spectroscopy: A review. *Postharvest Biology and Technology*, **2007**. *46*, 99-118.
- [24] Manley M., Near-infrared spectroscopy and hyperspectral imaging: non-destructive analysis of biological materials. *Chem Soc Rev*, **2014**. *43*, 8200-14.
- [25] Wang H.; Peng J.; Xie C.; Bao Y.; He Y., Fruit quality evaluation using spectroscopy technology: a review. *Sensors (Basel)*, **2015**. *15*, 11889-927.
- [26] Maldonado-Celis M.E.; Yahia E.M.; Bedoya R.; Landázuri P.; Loango N.; Aguillón J.; Restrepo B.; Guerrero Ospina J.C., Chemical Composition of Mango (*Mangifera indica* L.) Fruit: Nutritional and Phytochemical Compounds. *Front Plant Sci*, **2019**. *10*, 1073.
- [27] Jha S.N.; Kingsly A.R.P.; Chopra S., Non-destructive Determination of Firmness and Yellowness of Mango during Growth and Storage using Visual Spectroscopy. *Biosystems Engineering*, **2006**. *94*, 397-402.
- [28] Jha S.N.; Jaiswal P.; Narsaiah K.; Gupta M.; Bhardwaj R.; Singh A.K., Non-destructive prediction of sweetness of intact mango using near infrared spectroscopy. *Scientia Horticulturae*, **2012**. *138*, 171-175.
- [29] Rungpichayapichet P.; Mahayothee B.; Nagle M.; Khuwijitjaru P.; Müller J., Robust NIRS models for non-destructive prediction of postharvest fruit ripeness and quality in mango. *Postharvest Biology and Technology*, **2016**. *111*, 31-40.
- [30] Phuangsombut K P.A., Terdwongworakul A, Empirical approach to improve the prediction of soluble solids content in mango using near-infrared spectroscopy. *Int. Food Res. J.*, **2020**. *27*, 217-223.
- [31] Hernández Suárez M.; Rodríguez Rodríguez E.M.; Díaz Romero C., Chemical composition of tomato (*Lycopersicon esculentum*) from Tenerife, the Canary Islands. *Food Chemistry*, **2008**. *106*, 1046-1056.
- [32] Xie L.; Ying Y.; Ying T., Rapid determination of ethylene content in tomatoes

- using visible and short-wave near-infrared spectroscopy and wavelength selection. *Chemometrics and Intelligent Laboratory Systems*, **2009**. 97, 141-145.
- [33] Radzevičius A V.J., Karklennine R, Juskeviciene D, Viskelis P, Determination of tomato quality attributes using near infrared spectroscopy and reference analysis. *Zemdirbyste*, **2016**. 103, 91-98.
- [34] Huang Y.; Lu R.; Chen K., Assessment of tomato soluble solids content and pH by spatially-resolved and conventional Vis/NIR spectroscopy. *Journal of Food Engineering*, **2018**. 236, 19-28.
- [35] Beć K.B.; Grabska J.; Huck C.W., Principles and Applications of Miniaturized Near-Infrared (NIR) Spectrometers. *Chemistry – A European Journal*, **2021**. 27, 1514-1532.
- [36] Yan H.; Siesler H.W., Quantitative analysis of a pharmaceutical formulation: Performance comparison of different handheld near-infrared spectrometers. *Journal of Pharmaceutical and Biomedical Analysis*, **2018**. 160, 179-186.
- [37] Puig-Bertotto J.; Coello J.; MasPOCH S., Evaluation of a handheld near-infrared spectrophotometer for quantitative determination of two APIs in a solid pharmaceutical preparation. *Analytical Methods*, **2019**. 11, 327-335.
- [38] Guillemain A.; Dégardin K.; Roggo Y., Performance of NIR handheld spectrometers for the detection of counterfeit tablets. *Talanta*, **2017**. 165, 632-640.
- [39] Wiedemair V.; Mair D.; Held C.; Huck C.W., Investigations into the use of handheld near-infrared spectrometer and novel semi-automated data analysis for the determination of protein content in different cultivars of *Panicum miliaceum*L. *Talanta*, **2019**. 205, 120115.
- [40] Zeiss, Light source. **2021**.
- [41] Ferrara G.; Melle A.; Marcotuli V.; Botturi D.; Fawole O.; Mazzeo A., The prediction of ripening parameters in Primitivo wine grape cultivar using a portable NIR device. *Journal of Food Composition and Analysis*, **2022**. 114, 104836.
- [42] Dashti A.; Müller-Maatsch J.; WeesePoel Y.; Parastar H.; Kobarfard F.; Daraei B.; AliAbadi M.H.S.; Yazdanpanah H., The Feasibility of Two Handheld

- Spectrometers for Meat Speciation Combined with Chemometric Methods and Its Application for Halal Certification. *Foods*, **2021**. 11.
- [43] Gelabert P.; Pruett E.; Perrella G.; Subramanian S.; Lakshminarayanan A., *DLP NIRscan Nano: an ultra-mobile DLP-based near-infrared Bluetooth spectrometer*. 2016. 97610B.
- [44] Sharififar A.; Singh K.; Jones E.; Ginting F.I.; Minasny B., Evaluating a low-cost portable NIR spectrometer for the prediction of soil organic and total carbon using different calibration models. *Soil Use and Management*, **2019**. 35, 607-616.
- [45] Golic M.; Walsh K.; Lawson P., Short-wavelength near-infrared spectra of sucrose, glucose, and fructose with respect to sugar concentration and temperature. *Appl Spectrosc*, **2003**. 57, 139-45.
- [46] Subedi P.P.; Walsh K.B., Assessment of sugar and starch in intact banana and mango fruit by SWNIR spectroscopy. *Postharvest Biology and Technology*, **2011**. 62, 238-245.
- [47] Goddu R.F.; Delker D.A., Spectra-Structure Correlations for Near-Infrared Region. *Analytical Chemistry*, **1960**. 32, 140-141.
- [48] Baloch M.K.; Bibi F., Effect of harvesting and storage conditions on the post harvest quality and shelf life of mango (*Mangifera indica* L.) fruit. *South African Journal of Botany*, **2012**. 83, 109-116.
- [49] Paixão dos Santos Neto J.; Carvalho L.C.; Leite G.W.P.; Cunha Junior L.; Grato P.; De Freitas S.; Almeida D.P.F.; Teixeira G., Postharvest behavior of mangoes nondestructively sorted based on dry matter content during and after storage under controlled atmosphere. *Fruits*, **2019**, 294-302.
- [50] Rungpichayapichet P.; Nagle M.; Yuwanbun P.; Khuwijitjaru P.; Mahayothee B.; Müller J., Prediction mapping of physicochemical properties in mango by hyperspectral imaging. *Biosystems Engineering*, **2017**. 159, 109-120.
- [51] Mishra P.; Woltering E.; El Harchioui N., Improved prediction of 'Kent' mango firmness during ripening by near-infrared spectroscopy supported by interval partial least square regression. *Infrared Physics & Technology*, **2020**. 110, 103459.



1. Plots of sample absorbances or reflectances versus wavelength acquired for the purpose of development of models for quality parameters of mangoes and tomatoes acquired using commercial spectrometers.

1.1 Plots of spectra of mango samples acquired using commercial spectrometers.

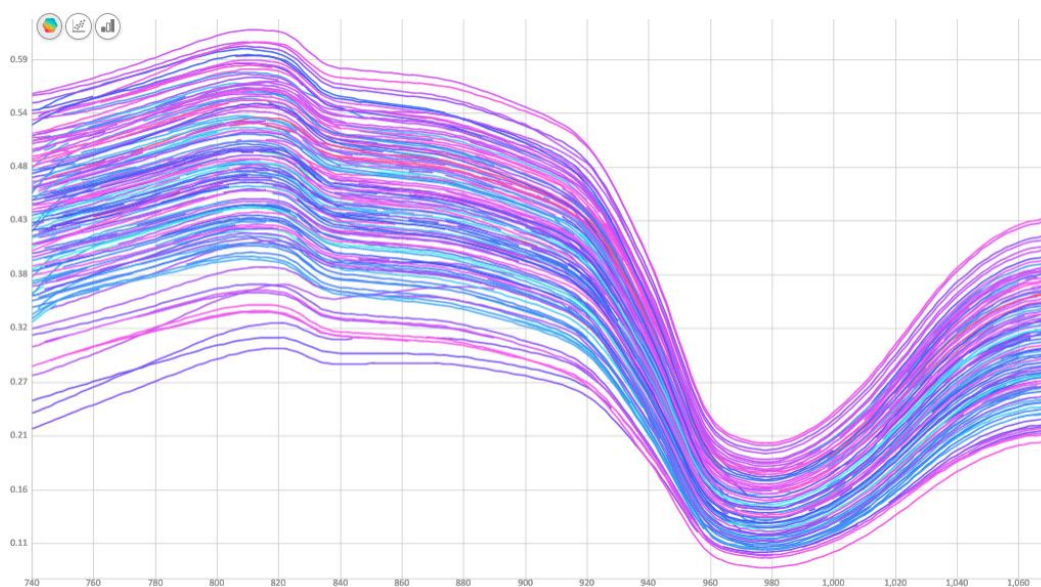
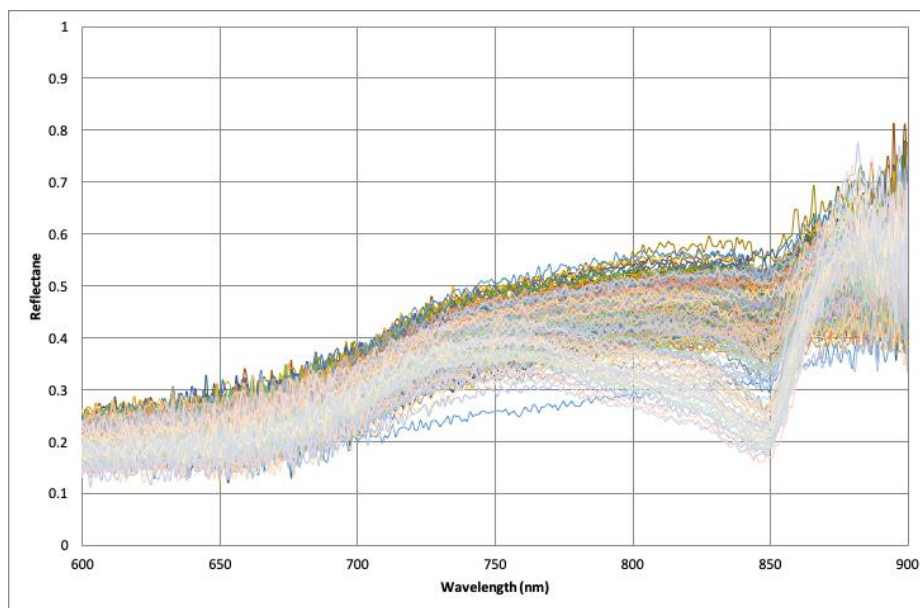


Figure 114 Plot of reflectance versus wavelength acquired using the SCiO spectrometer for samples used to develop predictive model for dry matter

(a)



(b)

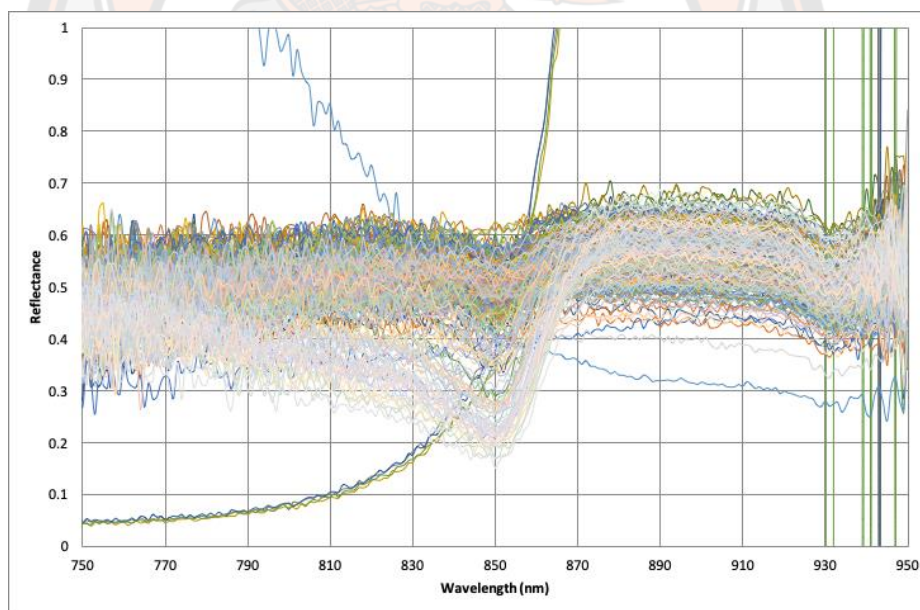


Figure 115 Plots of reflectance versus wavelength acquired using the Linksquare spectrometer operated in the (a) visible (b) NIR modes for mango samples used to develop predictive model for dry matter

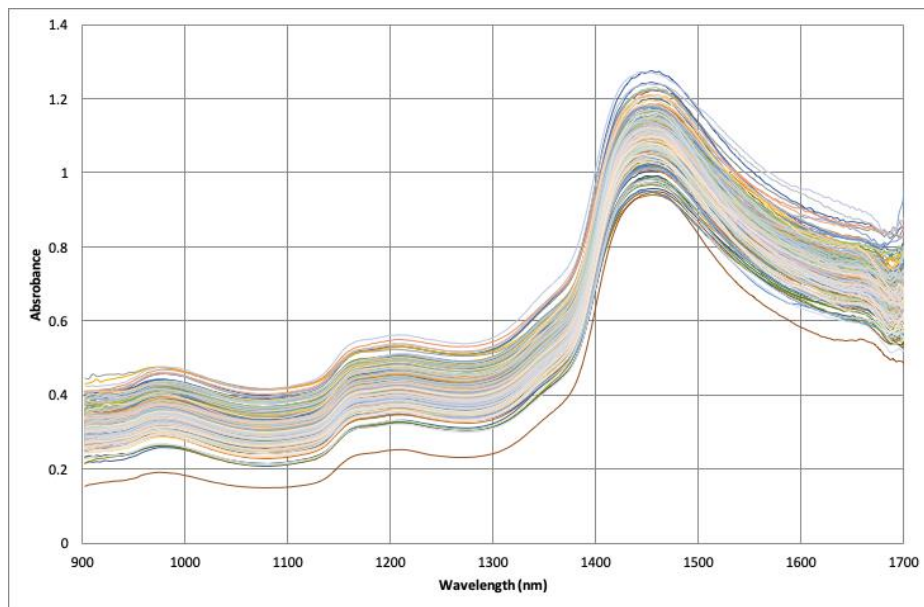


Figure 116 Plot of absorbance versus wavelength acquired using the NIRScan Nano spectrometer for mango samples used to develop predictive model for dry matter

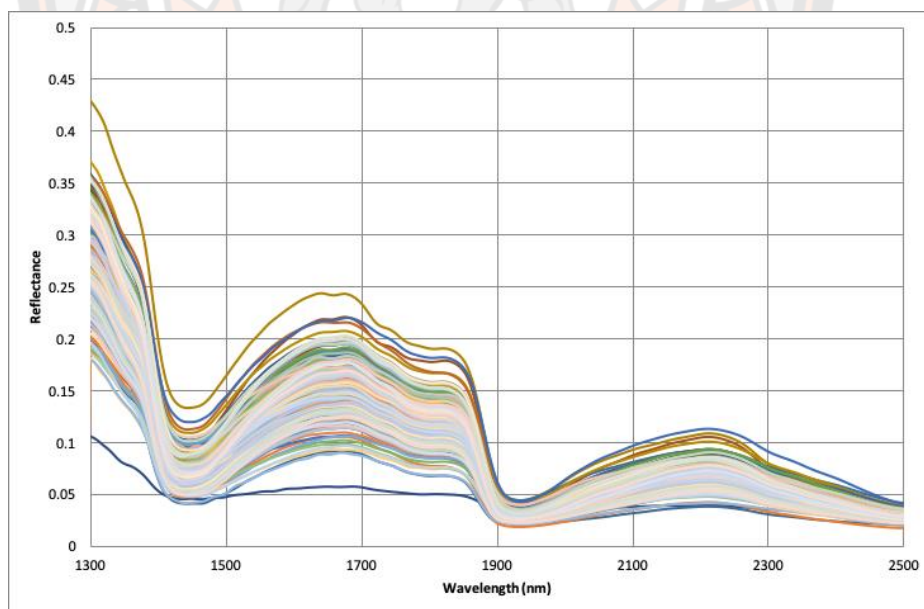


Figure 117 Plot of reflectance versus wavelength acquired using the Neospectra spectrometer for mango samples used to develop predictive model for dry matter

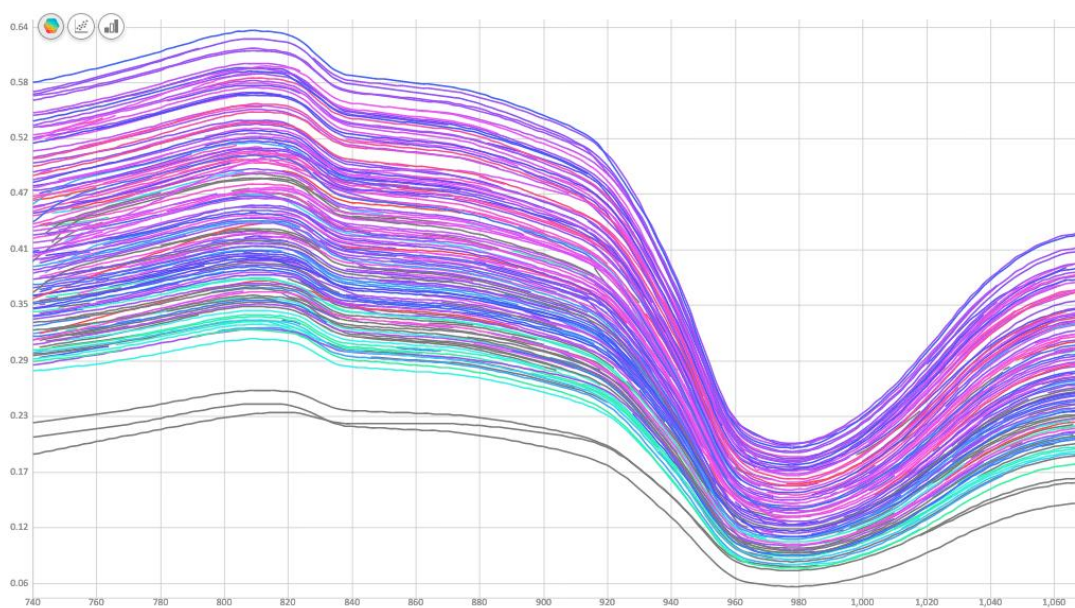
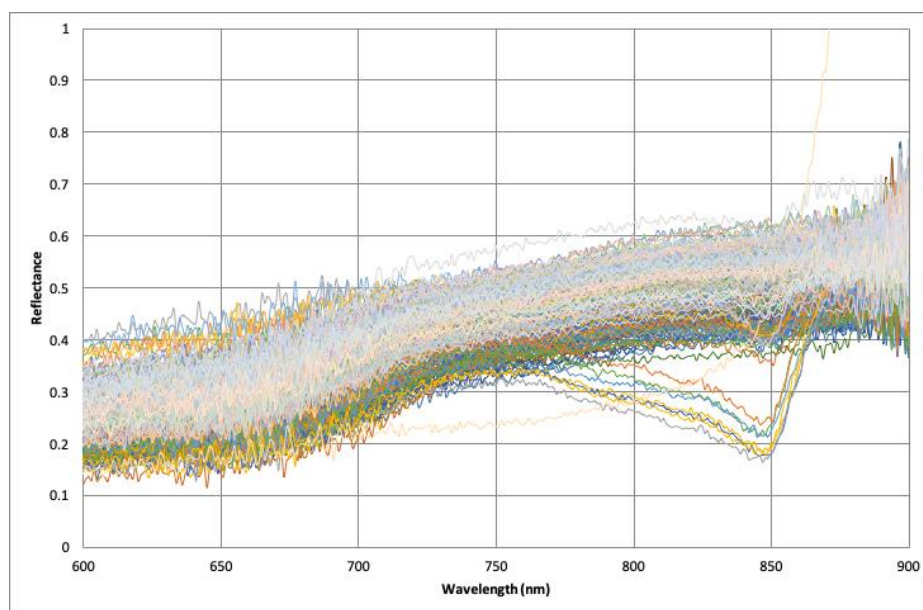


Figure 118 Plot of reflectance versus wavelength acquired using the SCiO spectrometer for mango samples used to develop predictive model for total soluble solids, titratable acidity, and pH

(a)



(b)

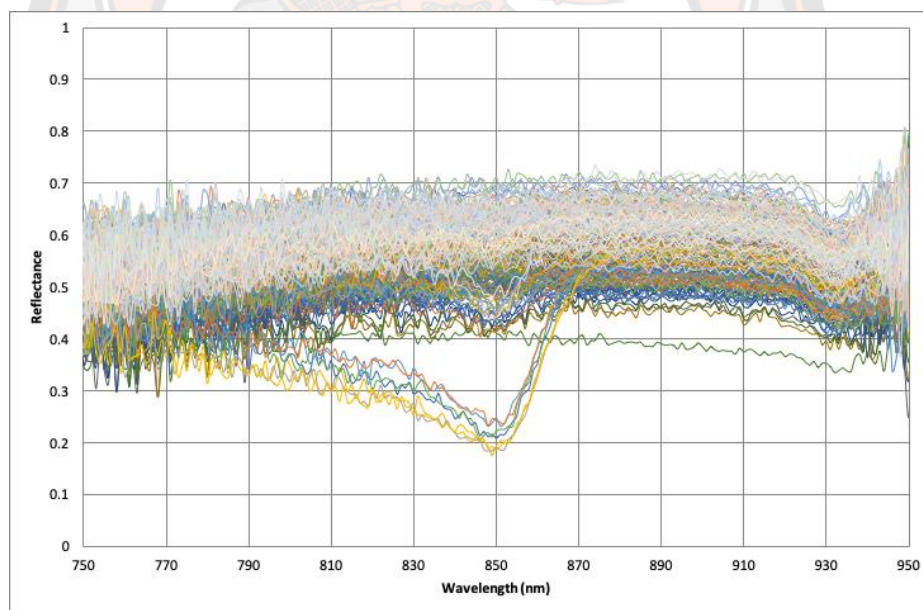


Figure 119 Plots of reflectance versus wavelength acquired using the Linksquare spectrometer operated in the (a) visible and (b) NIR modes for mango samples used to develop predictive model for total soluble solids, tirtratable acidity, and pH

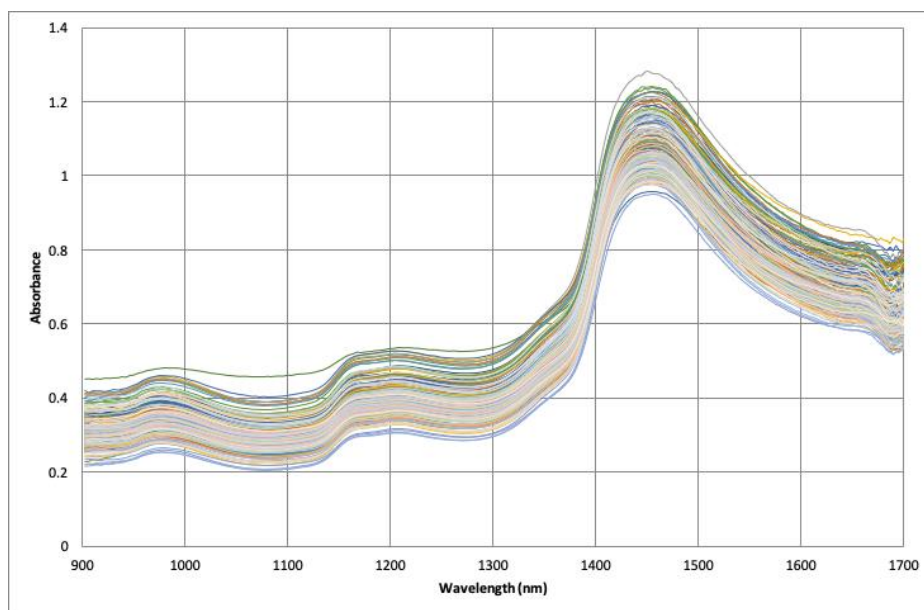


Figure 120 Plot of absorbance versus wavelength acquired using the NIRScan Naon spectrometer for mango samples used to develop predictive model for total soluble solids, tirtatable acidity, and pH

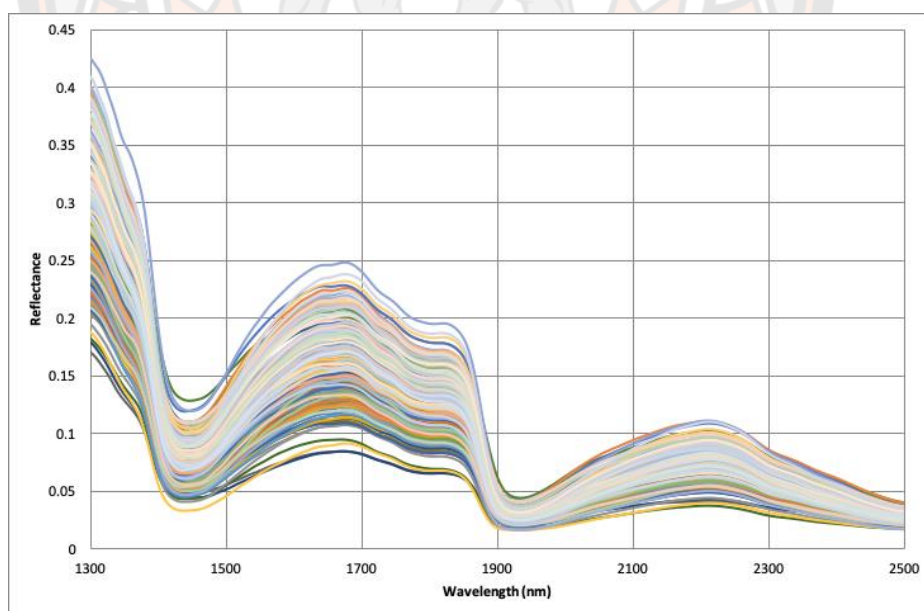


Figure 121 Plot of reflectance versus wavelength acquired using the Neospectra spectrometer for mango samples used to develop predictive model for total soluble solids, tirtatable acidity, and pH

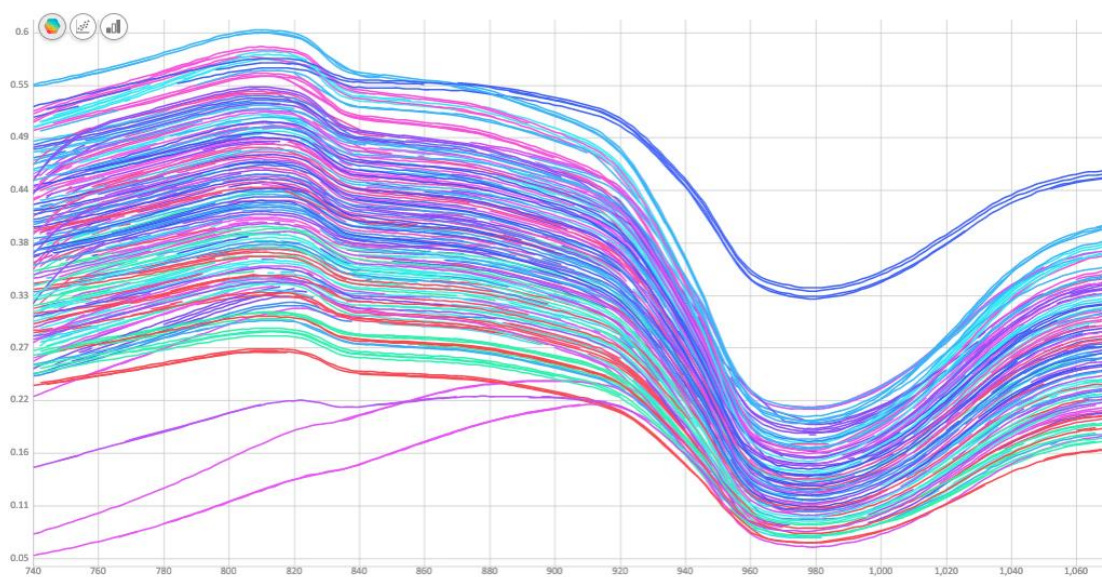
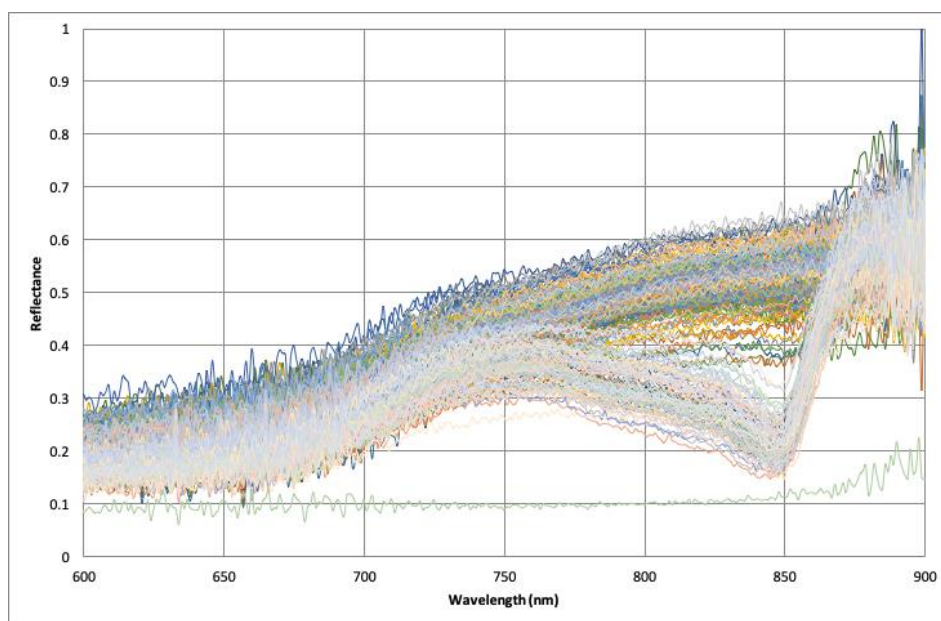


Figure 122 Plot of reflectance versus wavelength acquired using the SCiO spectrometer for mango samples used to develop predictive model for firmness

(a)



(b)

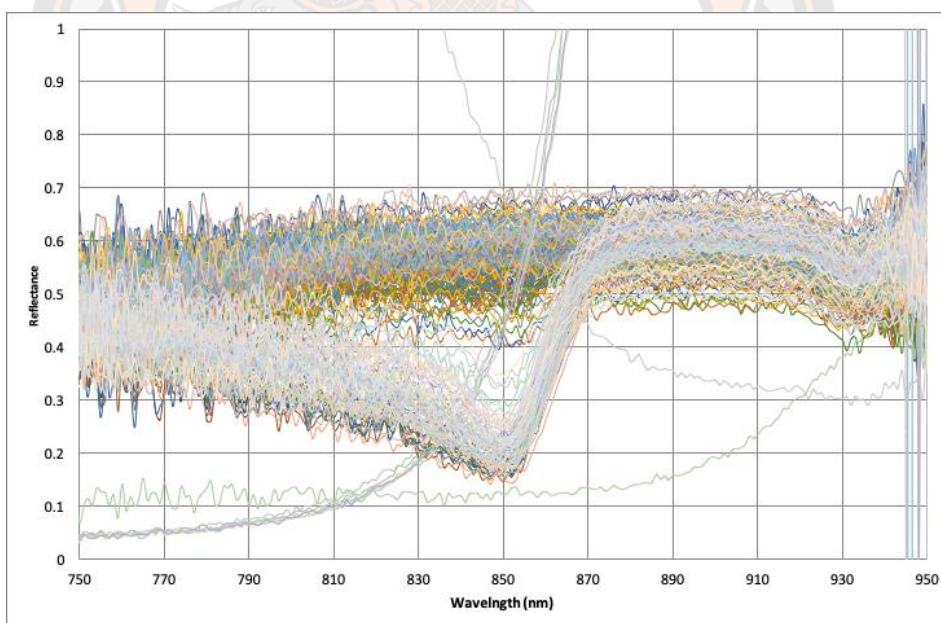


Figure 123 Plots of reflectance versus wavelength spectra acquired using the Linksquare spectrometer operated in the (a) visible and (b) NIR modes for mango samples used to develop predictive model for firmness

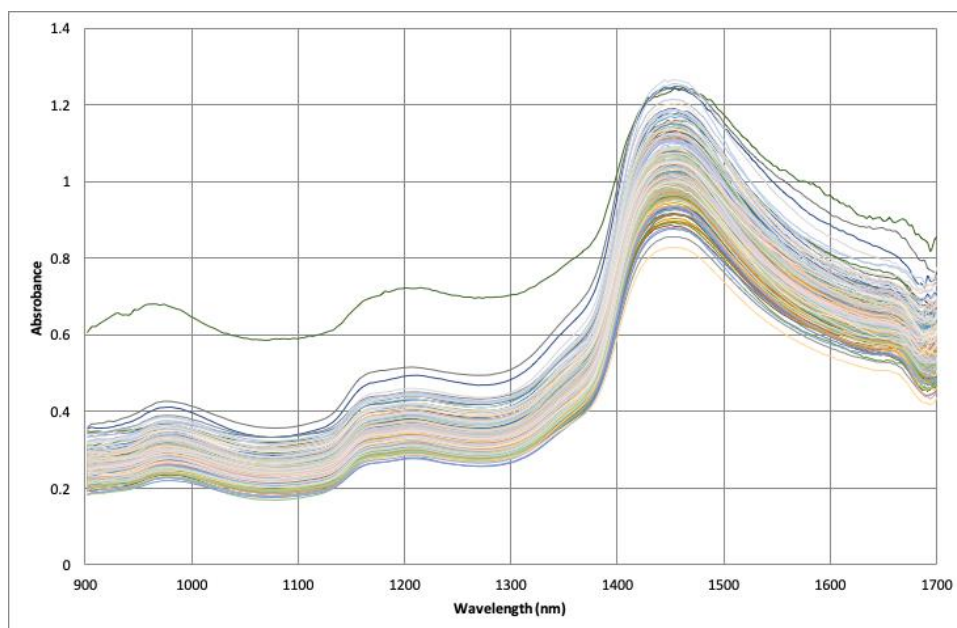


Figure 124 Plot of absorbance versus wavelength acquired using the NIRScan Nano spectrometer for mango samples used to develop predictive model for firmness

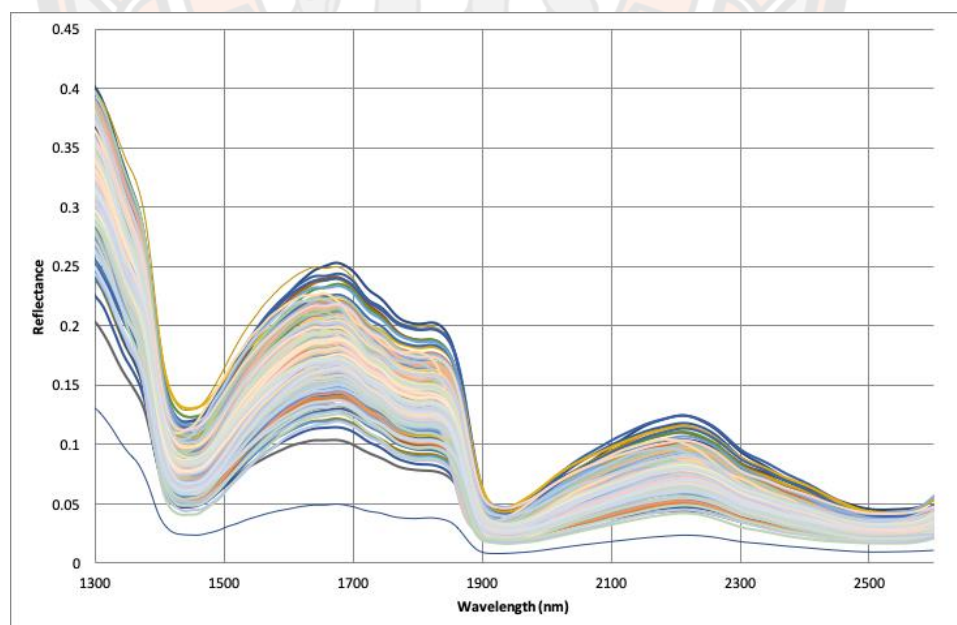


Figure 125 Plot of reflectance versus wavelength spectra acquired using the Neospectra spectrometer for samples used to develop predictive model for firmness

1.1 Spectra of tomato samples acquired using commercial spectrometers.

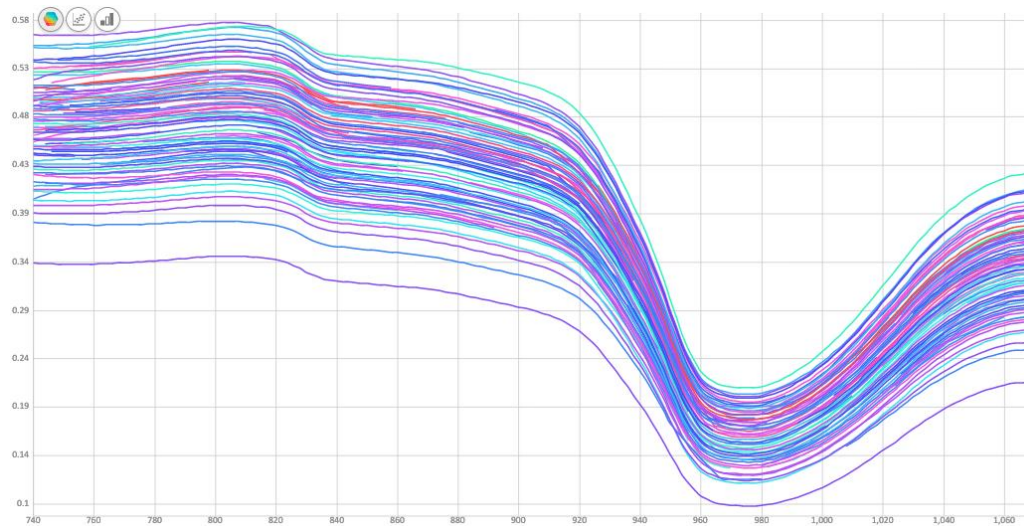
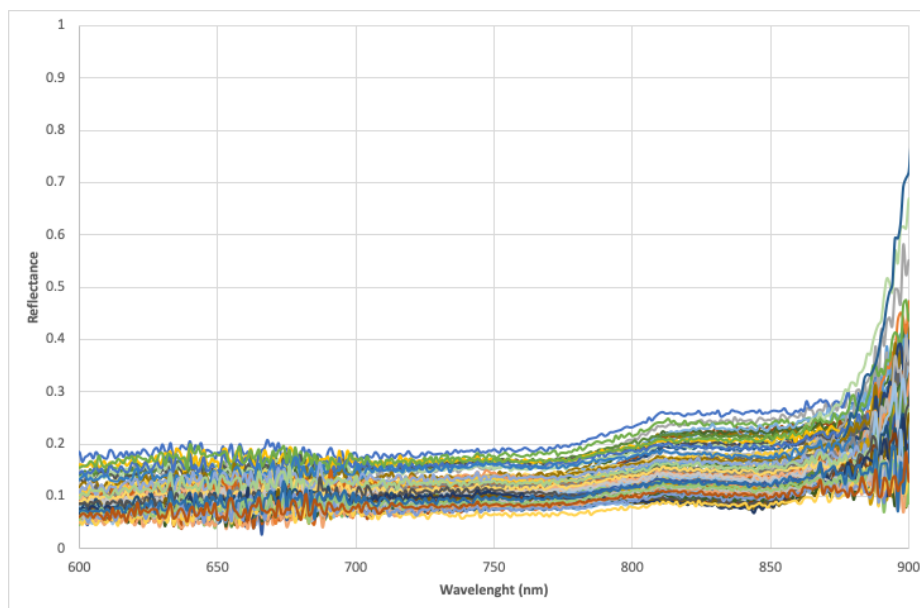


Figure 126 Plot of reflectance versus wavelength acquired using the SCiO spectrometer for tomato samples used to develop predictive model for dry matter

(a)



(b)

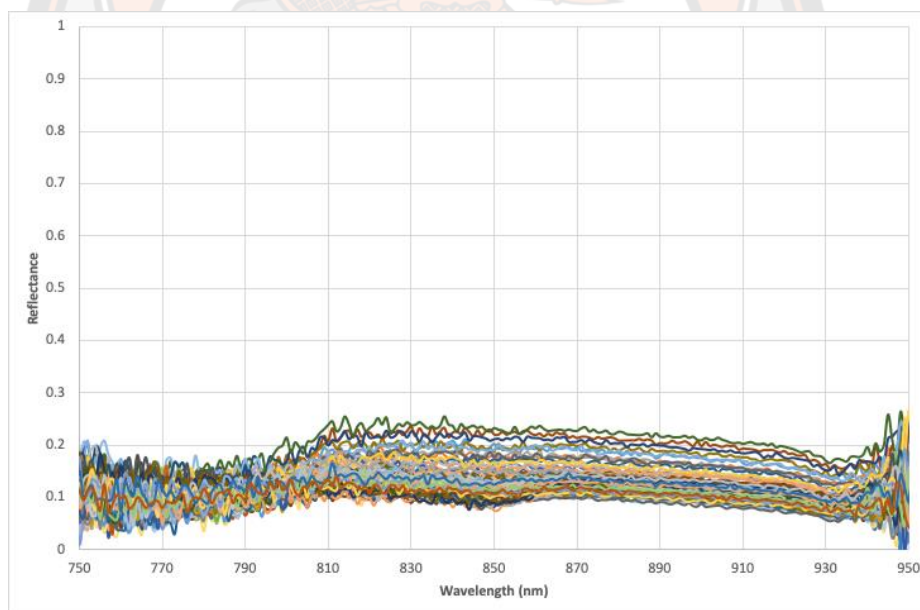


Figure 127 Plots of reflectance versus wavelength acquired using the Linksquare spectrometer operating in (a) visible and (b) NIR modes for tomato samples used to develop predictive model for dry matter

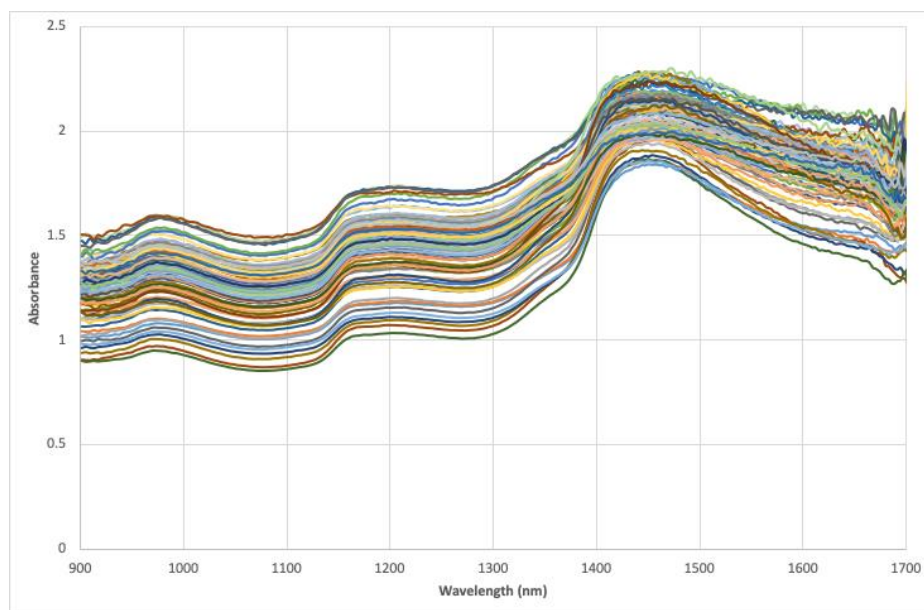


Figure 128 Plot of reflectance versus wavelength spectra acquired using the NIRScan Nano spectrometer for tomato samples used to develop predictive model for dry matter

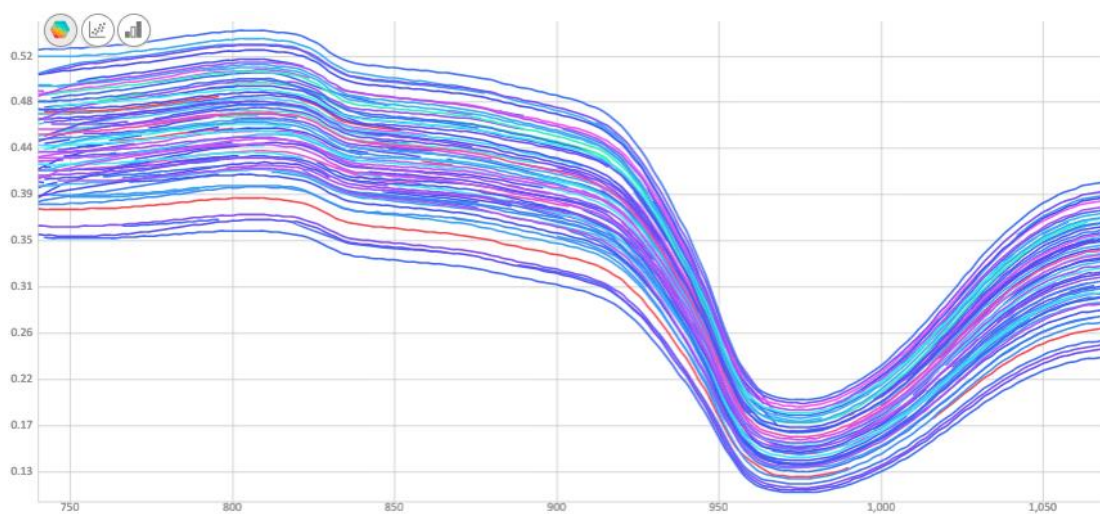
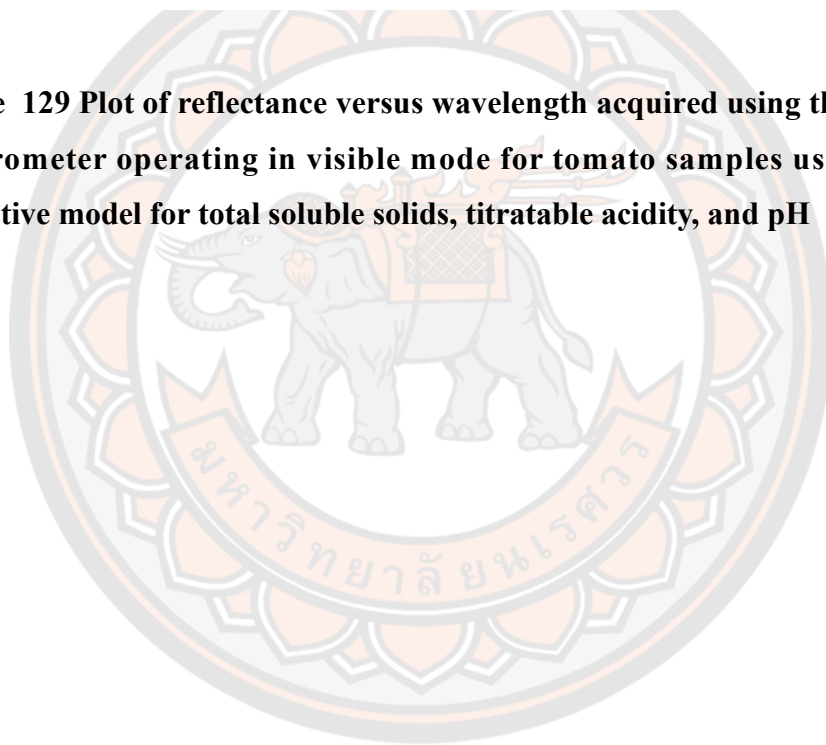
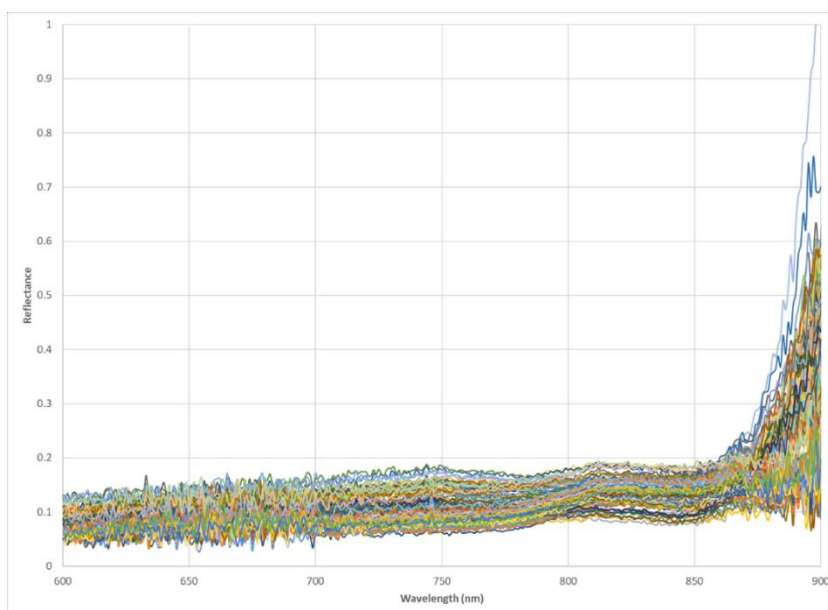


Figure 129 Plot of reflectance versus wavelength acquired using the Linksquare spectrometer operating in visible mode for tomato samples used to develop predictive model for total soluble solids, titratable acidity, and pH



(a)



(b)

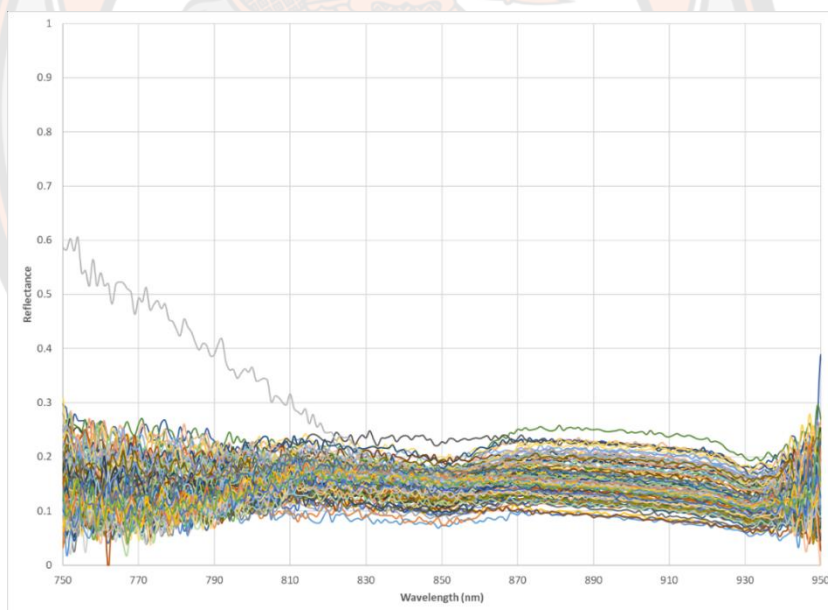


Figure 130 Plot of reflectance versus wavelength spectra acquired using the Linksquare spectrometer operating in (a) visible (b) NIR modes for tomato samples used to develop predictive model for total soluble solids, titratable acidity, and pH

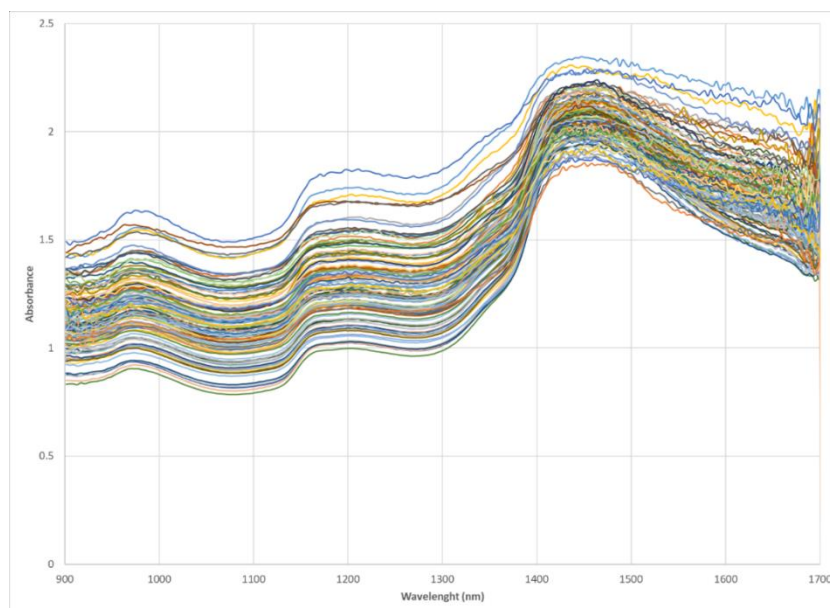


Figure 131 Plot of reflectance versus wavelength spectra acquired using the NIRscan Nano spectrometer for tomato samples used to develop predictive model for total soluble solids, titratable acidity, and pH

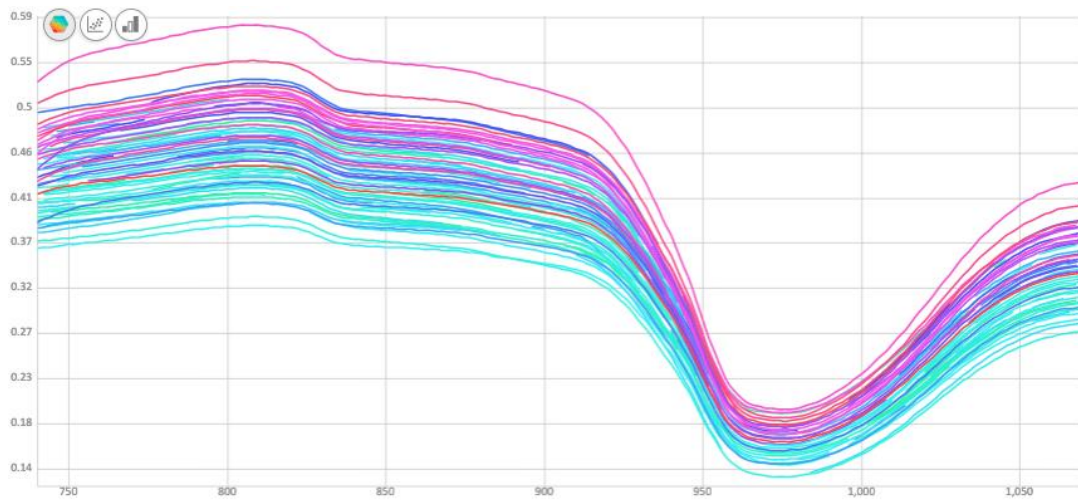
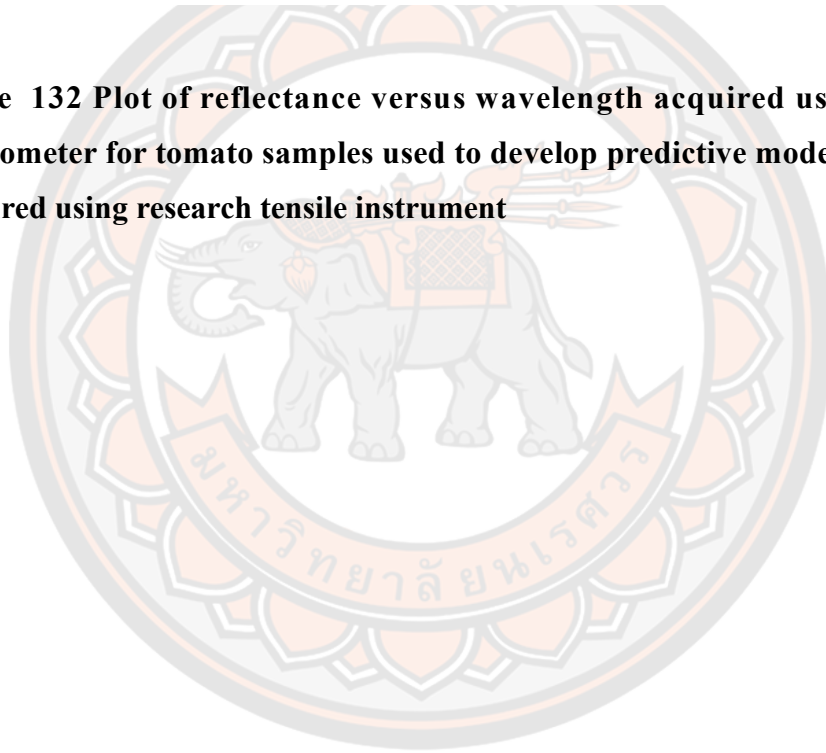
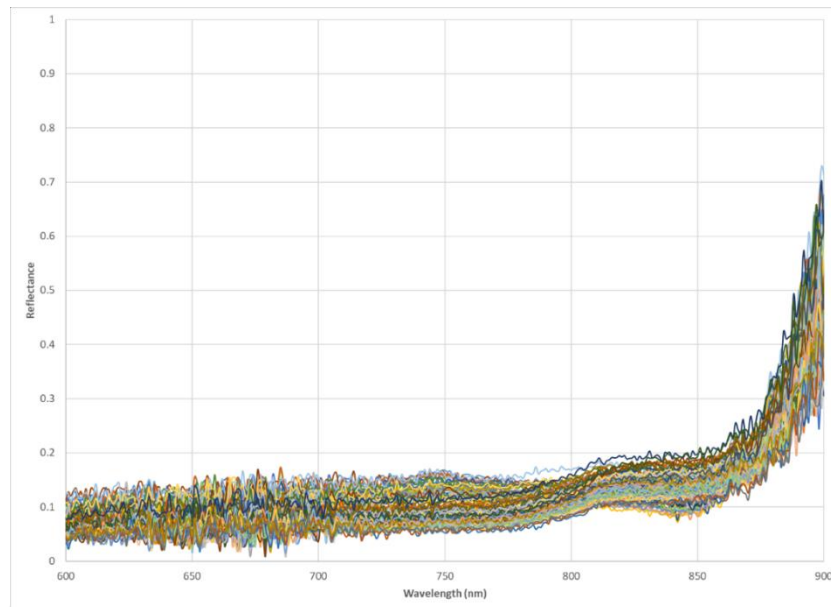


Figure 132 Plot of reflectance versus wavelength acquired using the SCiO spectrometer for tomato samples used to develop predictive model for firmness measured using research tensile instrument



(a)



(b)

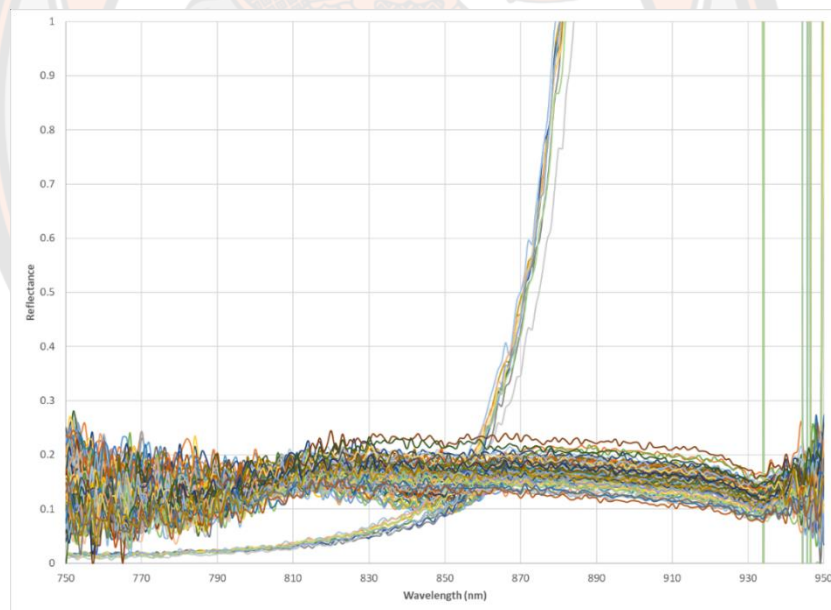


Figure 133 Plots of reflectance versus wavelength for spectra acquired using the Linksquare spectrometer operating in (a) visible (b) NIR modes for tomato samples used to develop predictive model for firmness measured using research tensile instrument

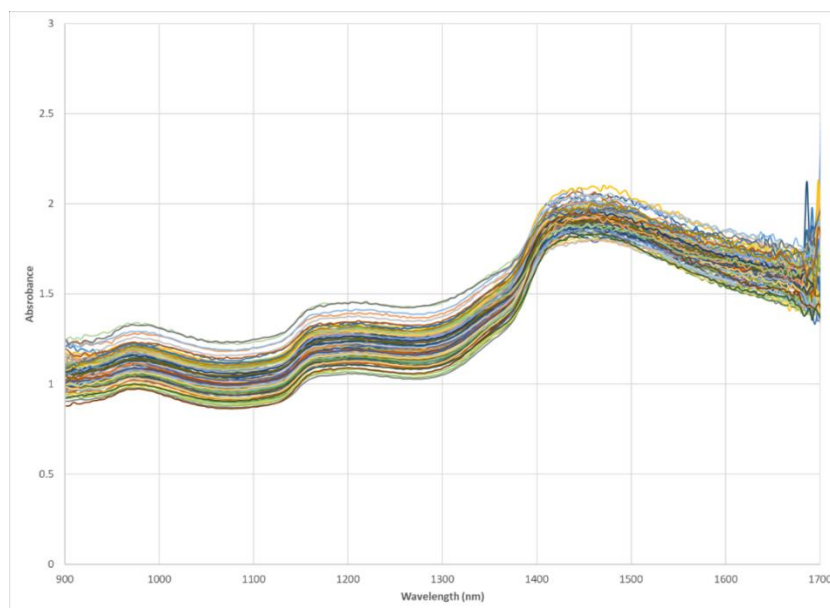
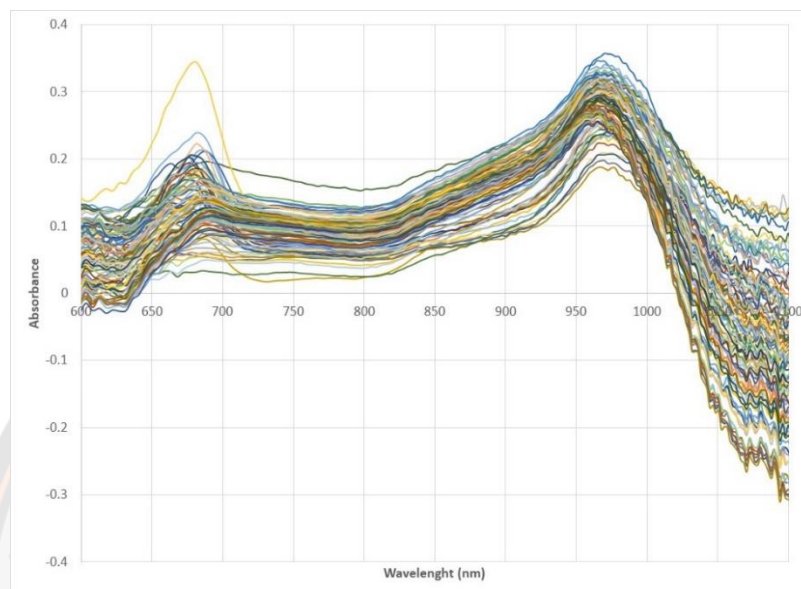


Figure 134 Plot of reflectance versus wavelength acquired using the TI NIRScan Nano spectrometer for tomato samples used to develop predictive model for firmness measured using research tensile instrument

2. Spectra of mango and tomato samples acquired with the in-house spectrometer used to develop predictive models for quality parameters.

2.1 Spectra of mango samples acquired using the in-house spectrometer.

(a)



(b)

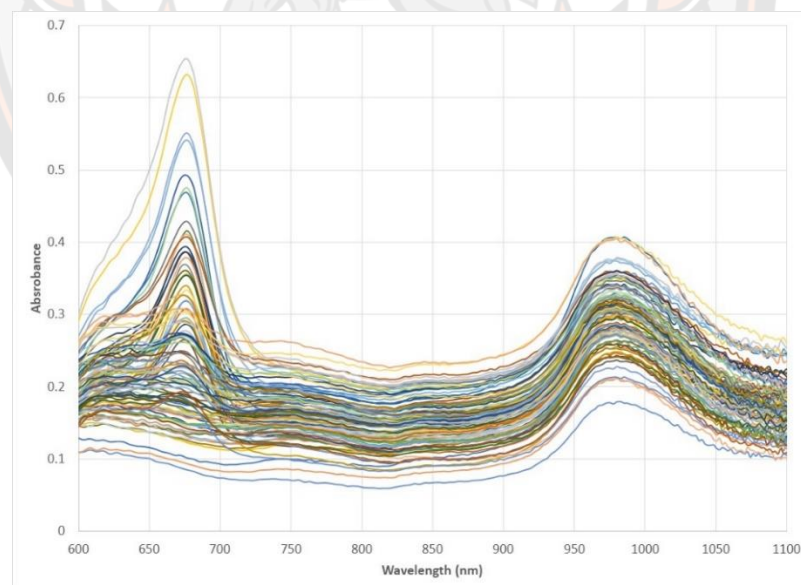
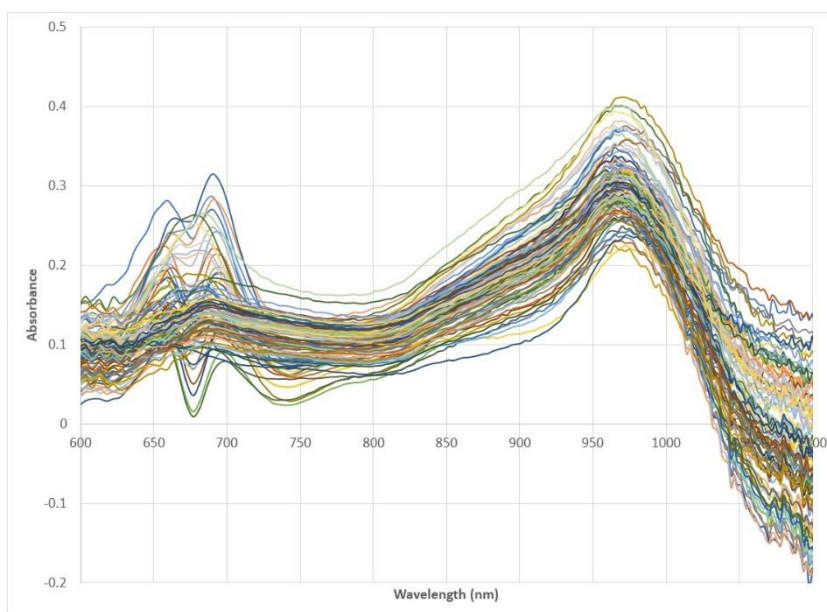


Figure 135 Plots of absorbance versus wavelength acquired using the in-house spectrometer equipped with the (a) LED light source and (b) tungsten light source for mango samples used to develop predictive models for dry matter

(a)



(b)

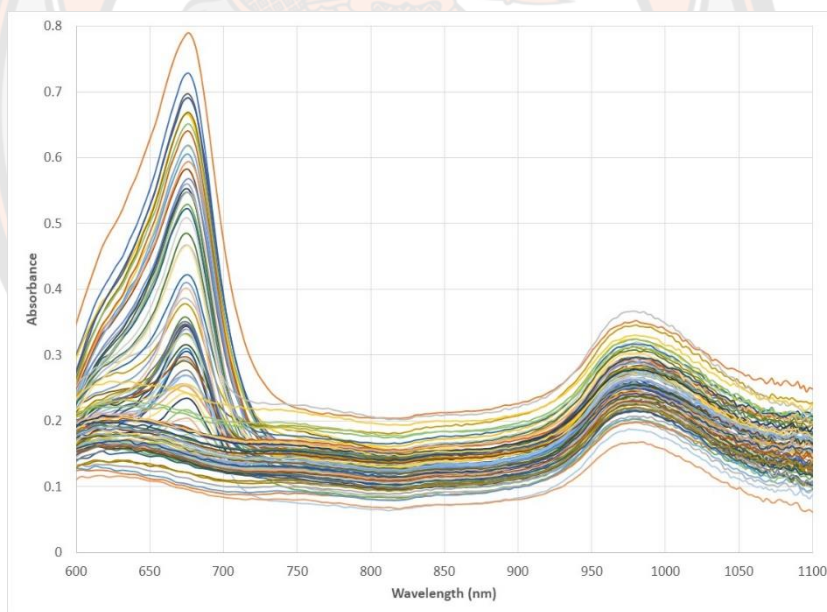
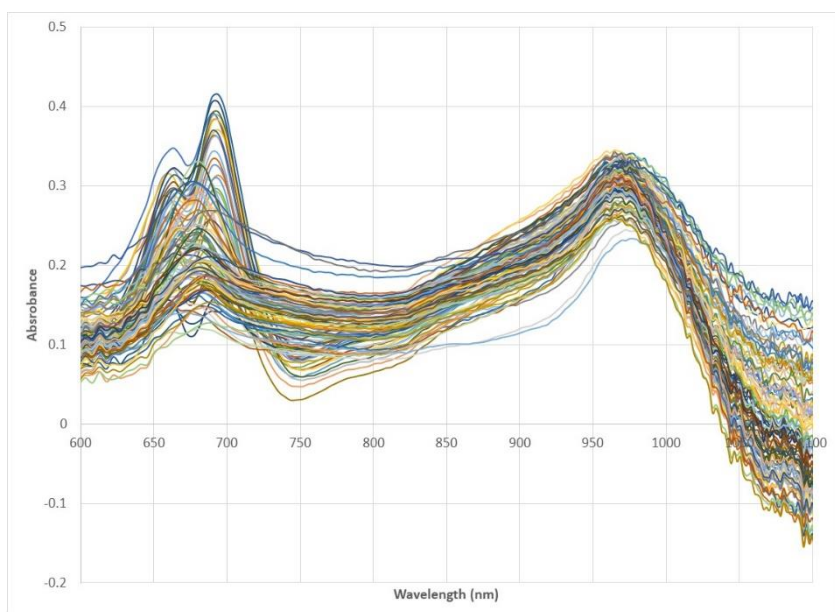


Figure 136 Plots of absorbance versus wavelength acquired using in-house spectrometer equipped with the (a) LED light source and (b) tungsten light source for mango samples used to develop predictive models for total soluble solids, titratable acidity, and pH

(a)



(b)

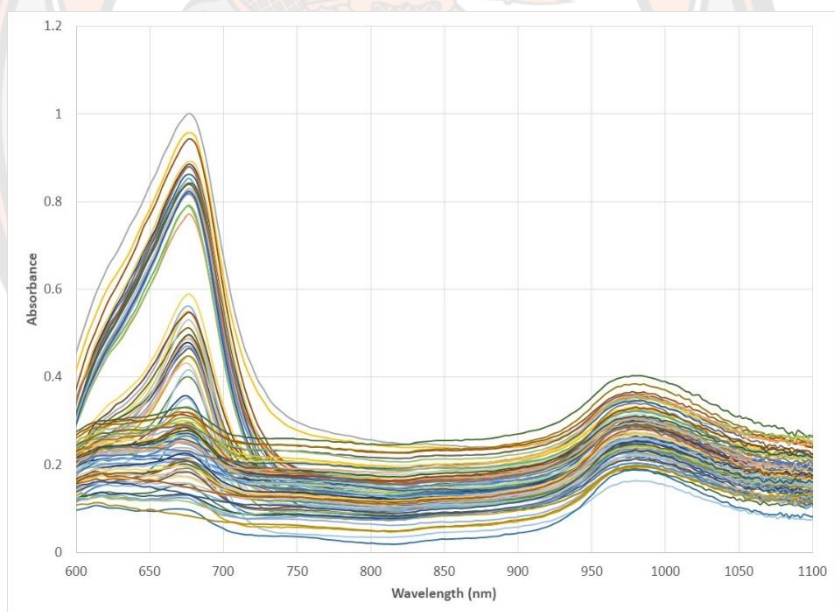
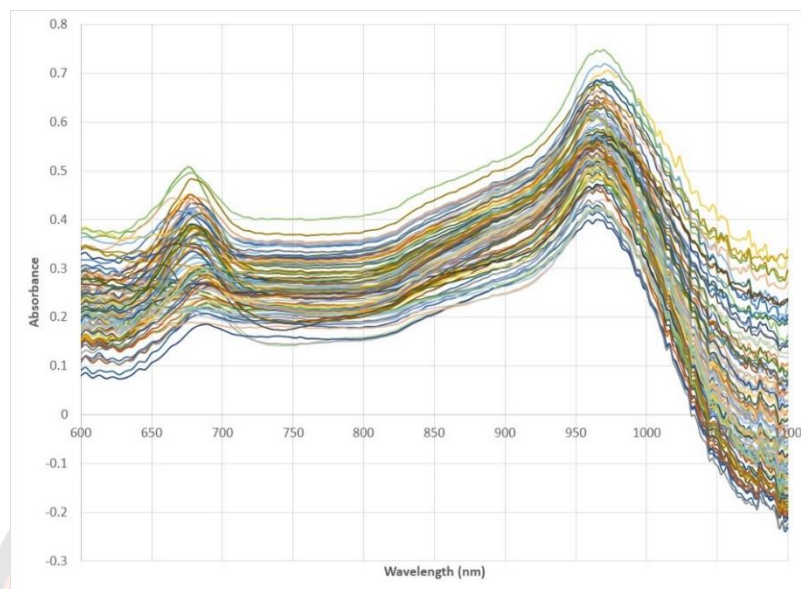


Figure 137 Plots of absorbance versus wavelength acquired using in-house spectrometer equipped with the (a) LED light source and (b) tungsten light source for mango samples used to develop predictive models for firmness

2.2 Spectra of tomato samples acquired using in-house spectrometer.

(a)



(b)

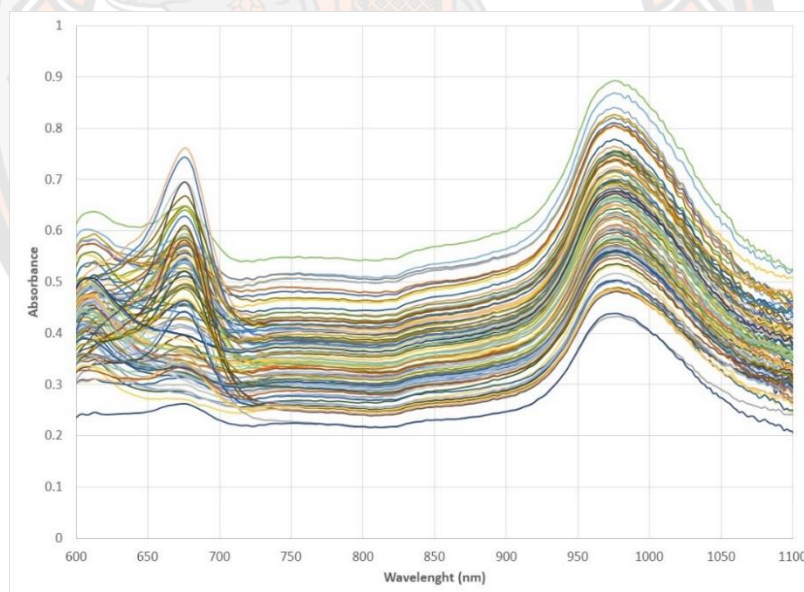
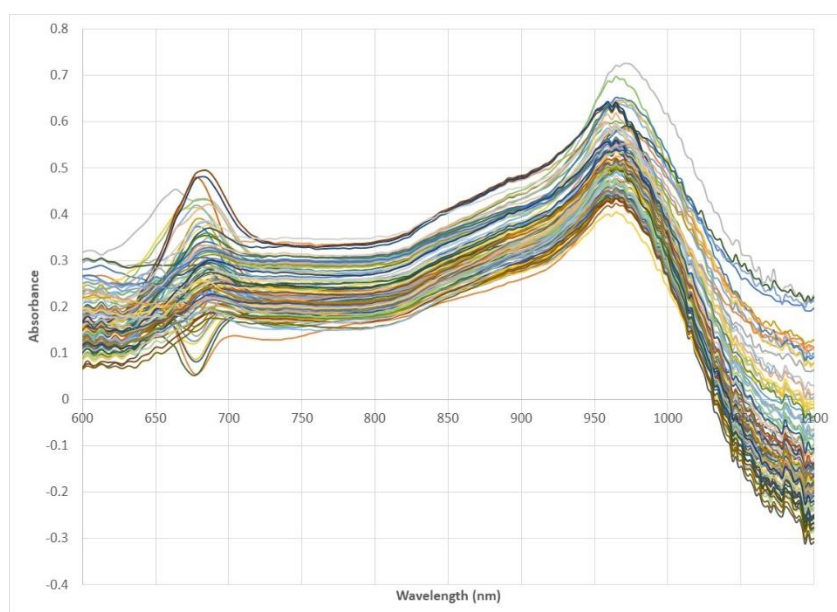


Figure 138 Plots of absorbance versus wavelength for spectra acquired using in-house spectrometer equipped with the (a) LED light source and (b) tungsten light source for tomato samples used to develop predictive models for dry matter

(a)



(b)

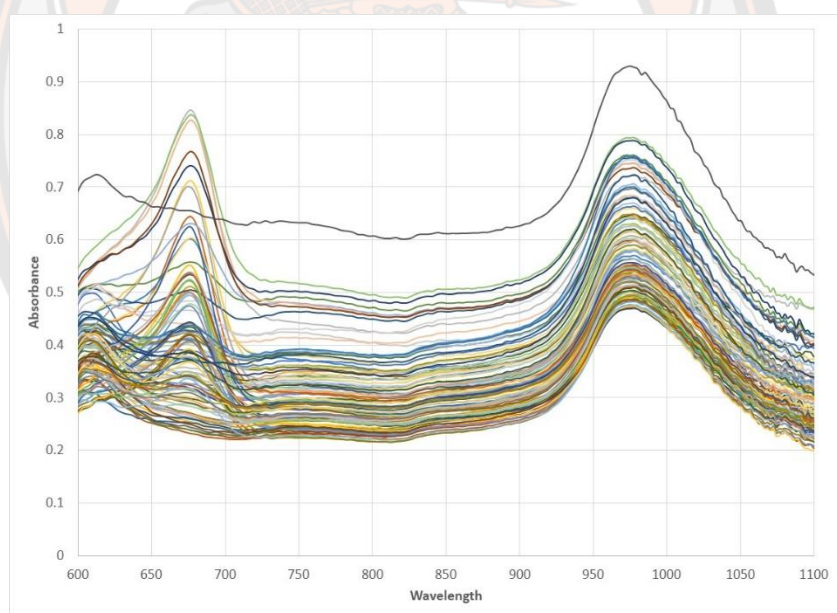
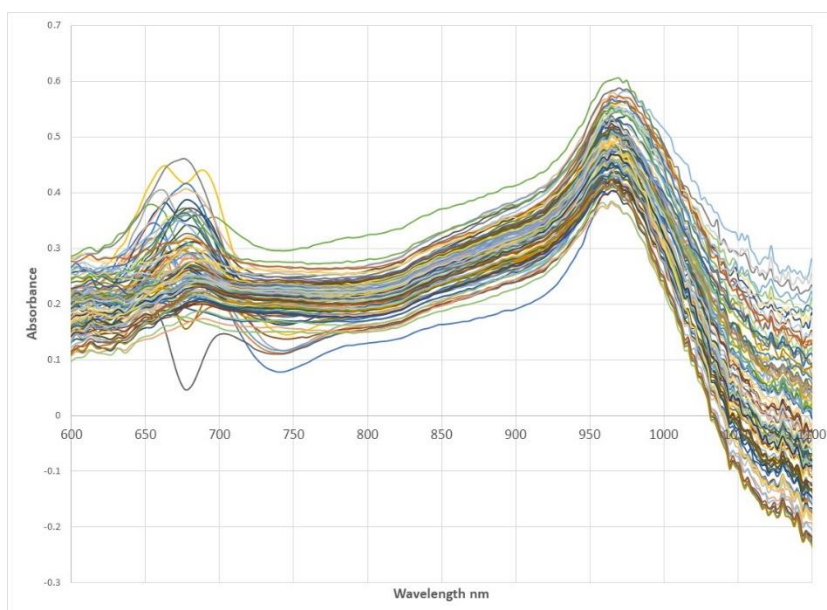


Figure 139 Plots of absorbance versus wavelength acquired using in-house spectrometer equipped with the (a) LED light source and (b) tungsten light source for tomato samples used to develop predictive models for total soluble solids, titratable acidity, and pH

(a)



(b)

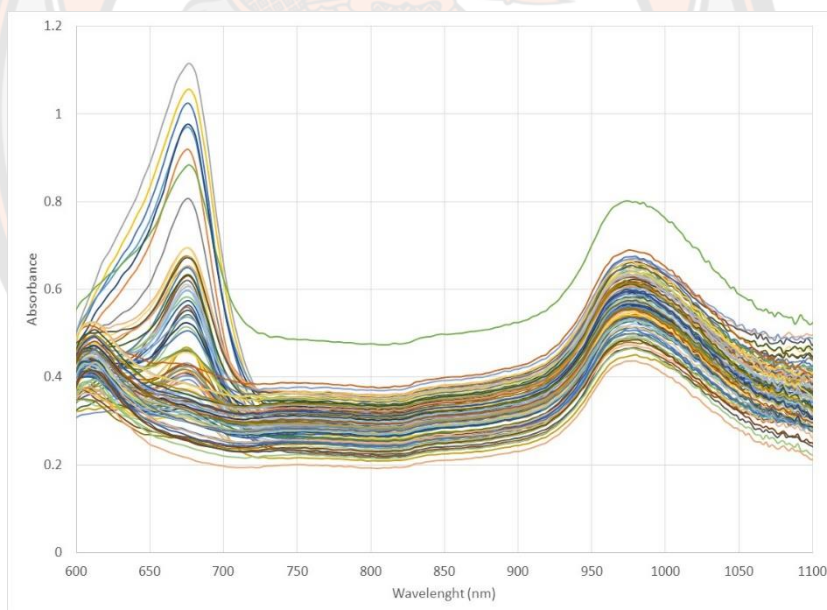


Figure 140 Plots of absorbance versus wavelength acquired using in-house spectrometer equipped with the (a) LED light source and (b) tungsten light source for tomato samples used to develop predictive models for firmness